SIDI MOHAMED BEN ABDELLAH UNIVERSITY
&
PAU AND PAYS ADOUR UNIVERSITY

CO-SUPERVISED DOCTORAL THESIS

Solar hot water production and thermal energy storage using phase change materials (PCMs) for solar air-conditioning applications in Morocco

---

Presented on May 02, 2019 by

Tarik BOUHAL

A thesis submitted in fulfillment of the requirements for the degree of PhD

in

Energy

In front of the jury composed of:

M.	R. Benelmir	Pr. - Lorraine University (FST, Vandoeuvre-Les-Nancy) - France	President
	L. Royon	Pr. - Paris Denis-Diderot University (LIED, Paris)- France	Reviewer
	R. Saadani	Pr. - Moulay Ismaîl University (EST, Meknes) - Morocco	Reviewer
	J.A. Ehmimed	Pr. - Abdelmalek Essaâdi University (FS, Tetouan) - Morocco	Reviewer
	A. Benbassou	Pr. - Sidi Mohamed Ben Abdellah University (EST, Fez) - Morocco	Examiner
	A. Jamil	Pr. - Sidi Mohamed Ben Abdellah University (EST, Fez) - Morocco	Superviser
	T. Kousksou	Pr. - Pau and Pays Adour University (SIAME, Pau) - France	Superviser
	Y. Zeraouli	Pr. - Pau and Pays Adour University (SIAME, Pau) - France	Co-Superviser

Declaration of Authorship

I, Tarik BOUHAL, declare that this thesis titled, "Solar hot water production and thermal energy storage using phase change materials (PCMs) for solar air-conditioning applications in Morocco" and the work presented in it are my own. I confirm that:

- This work was done wholly or mainly while in candidature for a research degree at these universities.
- Where any part of this thesis has previously been submitted for a degree or any other qualification at this University or any other institution, this has been clearly stated.
- Where I have consulted the published work of others, this is always clearly attributed.
- Where I have quoted from the work of others, the source is always given. With the exception of such quotations, this thesis is entirely my own work.
- I have acknowledged all main sources of help.
- Where the thesis is based on work done by myself jointly with others, I have made clear exactly what was done by others and what I have contributed myself.

Signed: _____

Date: _____

Sidi Mohamed Ben Abdellah University
&
Pau and Pays Adour University

Abstract

Centre d'Etudes Doctorales: Sciences et Techniques de l'Ingénieur (LPEDD, EST, Fez, Morocco)
Ecole Doctorale Sciences Exactes et de leurs Applications (SIAME, IUT/GTE, Pau, France)

PhD

Solar hot water production and thermal energy storage using phase change materials (PCMs) for solar air-conditioning applications in Morocco

by Tarik BOUHAL

This thesis reports the results of research into the modeling and simulation of a solar air-conditioning system for Morocco in the framework of the project "**Solar Cooling Process in Morocco (SCPM)**" funded by the *Research Institute for Solar Energy and New Energies (IRESEN)*. The aim is to investigate the factors concerning the optimization of a LiBr-H_2O solar absorption chiller under Moroccan conditions. Further, a number of design criteria, which can be used by designers of solar cooling and heating systems, have been established using energy and economic considerations. Accordingly, this thesis covers four aspects. The first overviews, through Chapter 2, the literature survey on solar technologies with a focus on solar cooling systems which reports the relevant processes, summarizes the market status, presents the recent developments of the most promising technologies and describes the main performance indicators figuring in the literature. Chapter 2 describes also the experimental aspect of the solar air-conditioning installation adopted in the **SCPM** project to identify the important technical characteristics of the installation and the difficulties encountered during the realization of the prototype.

The second dimension concerns the technical feasibility of solar air-conditioning system and its integration in Moroccan building sector. Therefore, Chapter 3 focuses on the modeling, design and performance optimization of solar absorption cooling systems using energy and economic indicators taking into account the combined effects of climates, building categories and cooling demands under Moroccan conditions.

The third aspect presents the latent thermal energy storage using Phase Change Materials (PCMs). In this way, Chapter 4 concerns the investigation of numerical methods used in the modeling of phase change phenomena. To this end, a numerical comparative approach and optimization of thermal energy storage by means of PCM integration within solar hot water production system operating in dynamic mode is presented. Besides, Chapter 5 focuses on PCMs addition in the solar cooling process integrated inside solar storage tank connected to the generator of the absorption chiller to evaluate the possible enhancement in the system efficiency.

The fourth aspect of this thesis outlines the technico-economic and sensitivity analysis applied to the development of a combined processes of solar DHW, heating and air-conditioning in Morocco. Thus, Chapter 6 presents a technico-economic assessment of a complete solar DHW, heating and air-conditioning plant using an absorption chiller operating under Moroccan climates based on adequate indicators. The overall analysis via a generalization of the results to the national level was carried out in addition to a sensitivity analysis related to the investment in these systems in order to assess the potential of replacing traditional technologies with the solar systems and the possible earnings related to their implementation in Morocco.

Finally, in Chapter 7, several recommendations and relevant policy directions are suggested in order to improve the adoption of solar cooling/heating technologies and remove different barriers facing their implementation in Moroccan building sector. Accordingly, appropriate prospects and relevant future research issues have been pointed out in order to extend the knowledge in the field of solar cooling systems for possible improvement of their performance in terms of cost and efficiency.

Keywords: Solar energy; Solar water heating; Solar air-conditioning; Absorption chiller; Thermal energy storage; PCM; Numerical modeling; Optimization; Morocco.

Acknowledgements

Firstly, I would like to thank God for immensely blessing and providing me with everything needed to achieve all that I have accomplished. My thesis is prepared in the framework of the project "**Solar Cooling Process in Morocco (SCPM)**" funded by the *Research Institute for Solar Energy and New Energies (IRESEN)*. This thesis is supervised jointly between Sidi Mohammed Ben Abdellah University (USMBA, Fez-Morocco) and University of Pau & Pays de l'Adour (UPPA, Pau-France) in collaboration with Moulay-Ismaïl University (UMI, Meknes-Morocco). Accordingly, I would like to express my gratitude to my Directors, Dr A. Jamil (EST, Fez-Morocco), Dr T. Kousksou (SIAME, Pau-France) and my co-Director Dr Y. Zeraouli (SIAME, Pau-France), for their constructive criticism and guidance. I am also indebted to Dr T. El Rhafiki (ENSAM, Meknes-Morocco), who originally acted as local advisor, for his support, enthusiasm and encouragement. My appreciation is also due to our research member's team, for their discussion, stimulating interest and valuable advice throughout the work.

Special thanks to my colleague Saïf ed-Dîn Fertahi with whom I worked a lot of nights and nights also for the excellent works we have done together. My thanks are also extended to my colleague Younes Agrouaz and all my colleagues who have assisted me, for their encouragement and support.

I am glad to place on record my gratitude to the IRESEN (Rabat, Morocco) for logistic, technical and funds assistance and its Director, Mr B. Ikken, for the financial supprt, provision of research and other facilities.

I am also indebted to the staff of the Laboratoire de Productique, Energie et Développement Durable (LPEDD) at Ecole Suéprieure de Technologie of Fez (EST, USMBA) for valuable discussions on energy matters and also to the Ecole Nationale Supérieure d'Arts et Métiers of Meknes (ENSAM, UMI) for hosting me in the premises of the school during the preparation of my thesis. I gratefully acknowledge the industrial company Energypoles (Rabat, Morocco) for the supply of the absorption machine, solar equipment and and other accessories.

My appreciation is also extended to the Laboratoire des Sciences pour l'Ingénieur Appliquées à la Mécanique et au Génie Electrique (SIAME) at the Institut Universitaire de Technologie, Génie Thermique et Energie des Pays de l'Adour (IUT/GTE, UPPA) and particularly to all professors and administrative staff for the facilities provided to me during my study visits to the University. The technical assistance and the course vacation proposal to me in thermal engineering at the IUT/GTE are also gratefully acknowledged.

I am grateful to all of those with whom I have had the pleasure to work during this and other related projects. Each of the members of my Dissertation Committee has provided me extensive personal and professional guidance and taught me a great deal about both scientific research and life in general.

Most importantly, I wish to thank my loving and supportive parents: my mother Amina and my father Ahmed, my sisters and my brothers, without whose prayers, love, understanding, patience and for their almost unbelievable support throughout my life, this work might never have been completed. I would like to dedicate also this work to all my compatriots in Zagora.

Contents

List of Figures

List of Tables

List of Abbreviations

DNI	Direct Normal Irradiance
SWH	Solar Water Heater
DSWH	Domestic Solar Water Heating
DHW	Domestic Hot Water
SWHS	Solar Water Heating Systems
HTF	Heat Transfer Fluid
HWC	Hot Water Consumption
FPC	Flat Plat Collector
ETC	Evacuated Tube Collector
CPC	Compound Parabolic Collector
CSP	Concentrated Solar Power
PTC	Parabolic Trough Collector
LFR	Linear Fresnel Reflector
PCM	Phase Change Material
CFD	Computational Fluid Dynamics
CFL	Courant–Friedrichs–Lewy
NPV	Net Present Value
IRR	Intern Rate of Return
COP	Coefficient of Performance
CF_t	Cash flow at time t
amb	ambient
avg	average
aux	auxiliary
u	useful
loss	losses
col	collector
sol	solar
adv	advection
cd	conduction
cv	convection
cw	cold water
hw	hot water
c	center monitor
b	bottom monitor
l	left monitor
r	right monitor
t	top monitor
Lv	vertical line monitor

List of Symbols

g	gravitational acceleration	$9.81\,\mathrm{m\,s^{-2}}$
T	temperature	K
T_{amb}	ambient temperature	K
T_{ini}	initial temperature	K
T_{in}	inlet temperature	K
T_{out}	outlet temperature	K
T_i	temperature of the ith tank segment	K
T_{ref}	reference temperature	K
T_{top}	tank top temperature	K
T_{bottom}	tank bottom temperature	K
T_{avg}	average temperature	K
T_m	melting temperature of the PCM	K
T_m	mean temperature	K
A	collector area	$\mathrm{m^2}$
A_c	collector area	$\mathrm{m^2}$
I_{rad}	solar radiation	$\mathrm{W\,m^{-2}}$
I_c	solar radiation	$\mathrm{W\,m^{-2}}$
C_p	specific heat at constant pressure	$\mathrm{J\,kg^{-1}\,K^{-1}}$
C_{pf}	specific heat of the tank fluid	$\mathrm{J\,kg^{-1}\,K^{-1}}$
k	thermal conductivity	$\mathrm{W\,m^{-1}\,K^{-1}}$
f	liquid fraction	$-$
N	number of fully mixed tank layers	$-$
L_f	latent heat capacity	$\mathrm{J\,kg^{-1}}$
h_a	ambient heat transfer coefficient	$\mathrm{W\,m^{-2}\,K^{-1}}$
h_g	global heat transfer through shell of capsule	$\mathrm{W\,m^{-2}\,K^{-1}}$
U	tank heat loss coefficient	$\mathrm{W\,m^{-2}\,K^{-1}}$
k_1	first order heat loss coeffcient	$\mathrm{W\,m^{-2}\,K^{-1}}$
k_2	second order heat loss coeffcient	$\mathrm{W\,m^{-2}\,K^{-2}}$
V	tank volume	$\mathrm{m^3}$
V_t	tank volume	$\mathrm{m^3}$
H	enthalpy	J
L	length of the tank	m
h	location of the plate	m
h	inlet and outlet apertures of the tank	m
D	diameter of the tank	m
u_{in}	water inlet velocity	$\mathrm{m\,s^{-1}}$
Q_{in}	inlet mass flow rate	$\mathrm{kg\,s^{-1}}$
Q_{out}	outlet mass flow rate	$\mathrm{kg\,s^{-1}}$
C_{es}	cost of energy saving	€
$C_{prod.energy}$	cost of produced energy	€/kW h
$\dot{m}_{load}$	mass load flow rate	$\mathrm{kg\,s^{-1}}$
$\dot{m}$	flow rate	$\mathrm{kg\,s^{-1}}$

$\dot{m}_{coll}$	collector mass flow rate	$\mathrm{kg\,s^{-1}}$
Q	heat	J
Q_u	useful energy	$\mathrm{W\,m^{-2}}$
Q_{load}	energy to load	J
Q_{aux}	auxiliary energy of the booster system	J
$\dot{Q}_i$	rate of energy input of the i^{th} tank's segment	J
ΔE	internal energy change of the tank	J
S	momentum sink	$\mathrm{N\,m^{-3}}$
q	thermal heat	$\mathrm{W\,m^{-2}}$
Re	Reynolds number	$-$
Ra	Rayleigh number	$-$
Pr	Prandlt number	$-$
Nu	Nusselt number	$-$
Ri	Richardson number	$-$
Str	Stratification number	$-$
θ	tilt angle	$^\circ$
α	thermal diffusivity	$\mathrm{m^2\,s^{-1}}$
ρ	density	$\mathrm{kg\,m^{-3}}$
ρ_f	fluid density	$\mathrm{kg\,m^{-3}}$
η_c	collector efficiency	$-$
η_0	zero loss efficiency	$-$
β	thermal expansion coeffcient	$\mathrm{K^{-1}}$
μ	dynamic viscosity	$\mathrm{Pa\,s}$
λ	thermal conductivity	$\mathrm{W\,m^{-1}\,K^{-1}}$
ϵ	amount of the PCM	$-$
ω	under relaxation factor	$-$
γ_f	control function if the auxiliary heater is off or on (1 is off, 0 is on)	$-$
Δt	time step	s
Δz	space step	m

Chapter 1

General introduction

1.1 Background

In recent years, the public has become increasingly concerned about the rapid depletion and escalating costs of fuels. The increases in the oil prices and the rising demand for energy, have made people conscious of the wisdom of reducing the energy consumption through conservation of conventional sources of energy and exploitation of renewable energy sources. Solar energy is one such energy source that can probably make a vital contribution to our energy needs. According to 2015 statistics, global energy consumption is likely to increase by 27% by 2030 (Petroleum, 2014). In 2017, the global energy consumption reached more than 2.6% as shown in Fig. 1.1.

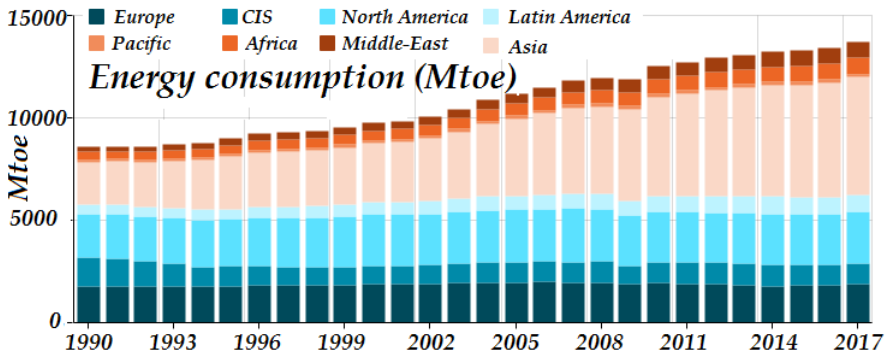

FIGURE 1.1: Global energy consumption (*Global Energy Statistical Yearbook 2018 (GESY)*)

On the other hand, fossil sources dominate the energy supply chain with a share that exceeds 80% of global energy demand (McGlade and Ekins, 2015, see Fig. 1.2).

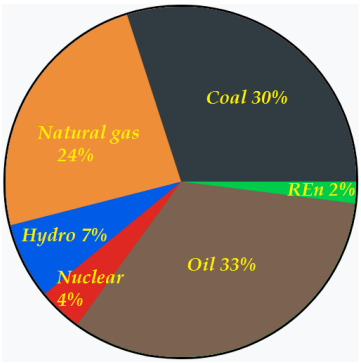

FIGURE 1.2: Share of fossil sources for global energy supply (adapted from McGlade and Ekins, 2015)

The situation is further complicated by the inevitable depletion of fossil resources (Shafiee and Topal, 2009). To these considerations, it should be added that one-third of the world's population today does not have access to electricity (Vujić, Antić, and Vukmirović, 2012). We are therefore faced with an unsustainable energy system on which we must act quickly and efficiently.

Moreover, the current environmental context is notably marked by a growing increase in greenhouse gas emissions which was 2.2% between 2000-2010 (Climate Change, 2015). Fig. 1.3 shows greenhouse gas emissions between 1990 and 2017 according to *Global Energy Statistical Yearbook 2018 (GESY)*.

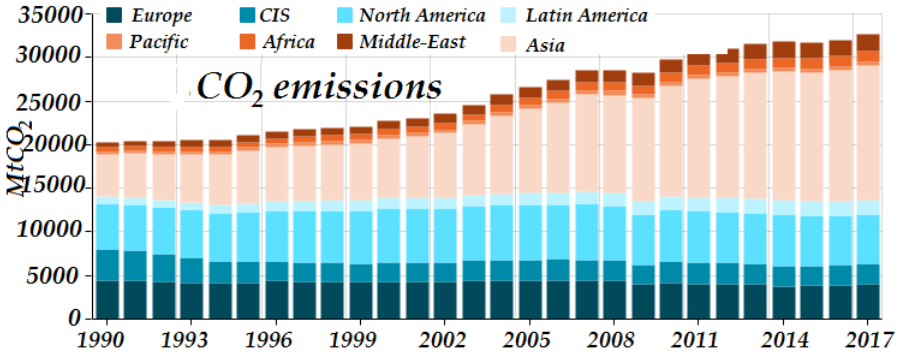

FIGURE 1.3: Greenhouse gas emissions (*Global Energy Statistical Yearbook 2018 (GESY)*)

Due to global warming, the temperature of the atmosphere and the ocean increased by 0.85 °C between 1880-2012 (Alves, Duarte, and Gonçalves, 2016). This resulted in massive melting of the ice and rising sea levels (see Fig. 1.4).

FIGURE 1.4: Massive melting of ice and rising sea levels (Alves, Duarte, and Gonçalves, 2016)

These changes can have serious consequences for the structure and function of ecosystems and the ecological interactions of different species and their distribution. Otherwise, the problem of energy and the environment arises in all sectors of activity such as: building, transport, industry, etc.

This thesis deals in particular with the problem related to the application of DHW, heating and cooling in the building, and this for the following reasons: Firstly, because cold applications have a very important part of building energy consumption (between 18% and 22%, Book, 2010) and use about 15% of the electricity produced in worldwide (*Institut international du froid (IIF)*). Secondly, the high use of

these applications during the summer period causes peaks in consumption, putting pressure on the energy supply chain. On the other hand, the refrigerants used by conventional systems contribute to the destruction of the ozone layer, the increase of the greenhouse effect and accentuate the vicious circle of climate change. Thus, it has become essential to seek alternatives to conventional systems by proposing innovative cooling technologies based on renewable energies. In this vision, this thesis introduces a new concept that can replace conventional cooling systems which is solar cooling.

Basically, solar cooling allows the exploitation of an abundant and renewable energy resource. In fact, according to a study conducted in 2009 (Perez and Perez, 2009), the theoretical potential of solar is 1400 times greater than global energy demand (see Fig. 1.5-(a)).

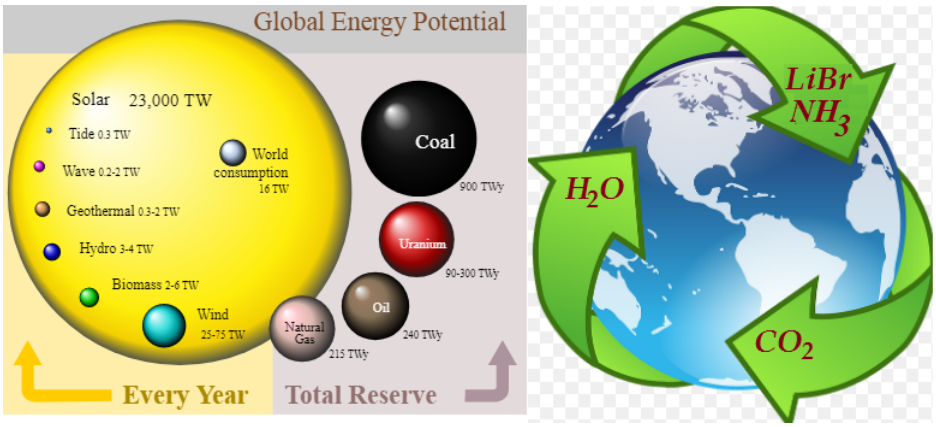

FIGURE 1.5: (a)- Solar energy as an abundant and renewable resource (Perez and Perez, 2009) and (b)- Refrigerants used in solar cooling process

Furthermore, solar cooling uses refrigerants with low environmental impact such as water, lithium bromide (LiBr), ammonia and CO_2 (see Fig. 1.5-(b)). Finally, as shown in Fig. 1.6, cooling demand usually coincides in time and space with the availability of the solar resource compared to DHW and heating requirements.

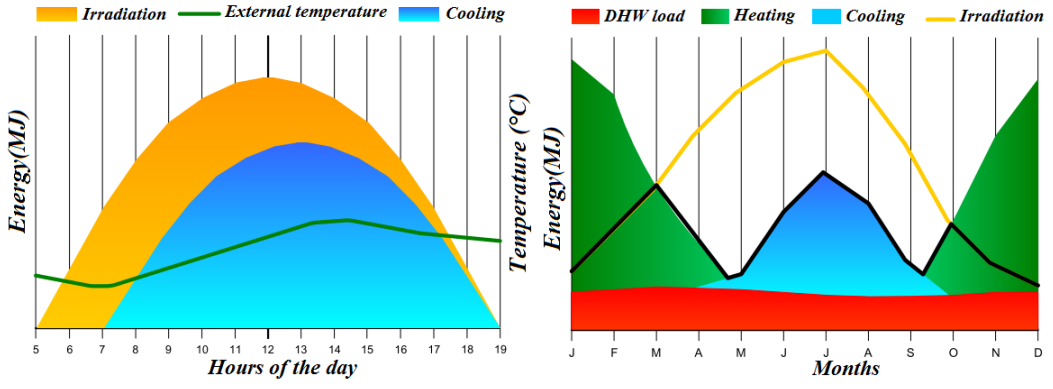

FIGURE 1.6: Solar irradiation, DHW, heating and cooling requirements (*Institut international du froid (IIF)*)

The sizing of a solar cooling or heating system is a complex problem involving a number of interrelated factors which include collector area and performance, storage

size, heating and cooling purposes, solar radiation, mechanical equipment sizing and system control, as well as an economic evaluation of the entire proposed system.

In Morocco, the climatic weather conditions are such that the country can be classified as one of the countries where the potential of solar energy utilization is very high (*Moroccan Agency for Energy Efficiency (AMEE)*). During the past 10 years, the solar water heaters installation in building has been increased and it is estimated that more than $220,000m^2$ are being implemented. Nowadays, the use of solar energy is not only used for domestic hot water applications but also extended to electricity generation using CSP technologies (Bouhal et al., 2018c) implemented by *Moroccan Agency for Sustainable Energy (MASEN)*.

To enhance the utilization of solar energy, a wider range of applications must be considered through careful design of cost effective solar-based energy systems which can be applied not only to domestic dwellings but also to large building complexes such as apartment blocks, hotels, sports centers, mosques, etc. In order, thus, to produce effective designs of such systems, it is necessary to optimize their performance in relation to various design parameters on the basis of Moroccan climatic and socioeconomic conditions.

This can be achieved through numerical modeling and simulation of solar heating and cooling systems which will enable the synthesis of optimum design criteria for such systems. It is, therefore, very useful if a design tool is available which will take into consideration both the technical and economic aspects of the problem. This will help the designer to evaluate the cost effectiveness of a solar heating and cooling system and at the same time serve as a tool for sizing the system components.

The purpose of this research is two-fold. First, to develop suitable models for solar water heating and cooling systems for Morocco. Second, to carry out computer simulations of the performance of such systems over a wide range of operating conditions and for various design parameters in order to investigate some of the factors concerning the optimisation of the system. This will assist in the synthesis of design criteria which can be used by consulting engineers and designers of solar heating and cooling systems in Morocco.

In order to support the national energy strategy by supporting applied R&D in the field of renewables energies, the *Research Institute for Solar Energy and New Energies (IRESEN)* (**IRESEN** for "**Institut de Recherche en Energie Solaire et Energies Nouvelles**") was created in 2011 by the *Ministry of Energy, Mines and Sustainable Development (MEMSD), Morocco*, and several key players in the energy sector in Morocco. Therefore, the research institute **IRESEN** operates in the field of R&D through its resources agency and research centre as the *Green Energy Park*, offering several opportunities for creating synergy between the socio-economic world and the scientific world around collaborative R&D projects.

In this framework, the project of **Solar Cooling Process in Morocco (SCPM)** was retained and financially supported by **IRESEN**. The value and the background of the **SCPM** project will be explained in the next section.

1.2 Scope of the thesis: Project of Solar Cooling Process in Morocco (SCPM)

The problem of energy and the environment arises in all sectors of activity (building, transport and industry) and at the level of most of the essential applications for man. This thesis deals in particular with the problem related to the application and use of air-conditioning in the building. Indeed, cooling applications are a very important

part of building energy consumption as shown in Fig. 1.7 which consume between 18% and 22% (Reddy et al., 2016).

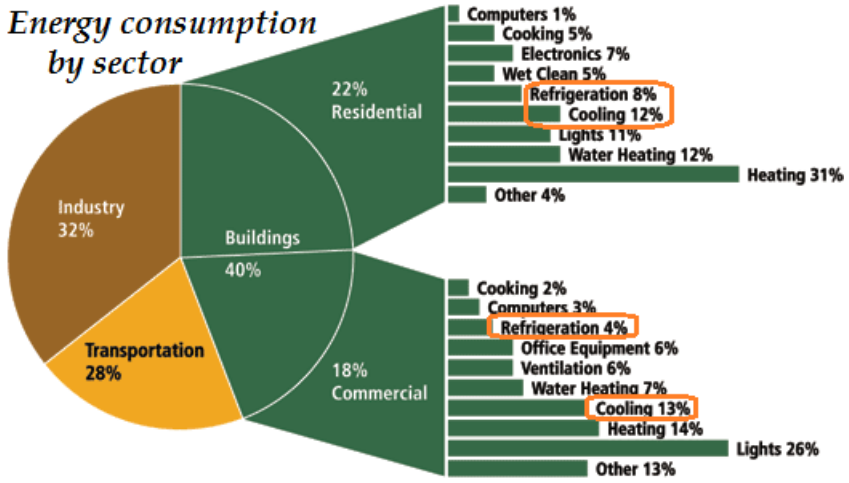

FIGURE 1.7: Share of electricity consumption for cooling in building sector (Reddy et al., 2016)

At Moroccan level, the electricity consumption in the residential sector has considerably increased throughout the last decades. At the global level, the current level of dioxide carbon emissions resulting from human activity might cause serious repercussions on the environment and ecosystems. In Morocco, this issue is extremely relevant since most of the power generation is issued from fossil fuels with high global warming potential. Air-conditioning is responsible for a significant part of this energy consumption principally because of the high thermal loads in buildings and the wide use of vapor compression chillers. Thus, the use of air conditioning systems in the summer periods causes energy consumption which creates problems of production and routing of electrical energy. In Morocco, the *Office National d'Electricité et de l'Eau Potable (ONEE)* is often forced to import electricity from Spain at a very high price. Solar air-conditioning from thermal origin can therefore contribute to:

- Replace the demand for fossil fuels by the use of solar thermal energy;
- Reduce greenhouse emissions through primary energy savings and non-use of refrigerants dangerous for the environment;
- Stabilize power grids through lower peak power consumption in summer;
- Optimize the use of solar thermal systems through the combination of solar heat for space heating, air-conditioning and domestic hot water production. This installation consists of a solar absorption chiller coupled to the evacuated tube collector's field which will be implemented in *Green Energy Park*.

Accordingly, the present work is directed towards a very small subject area in the field of solar energy. It is an attempt to investigate the possibility of utilizing solar energy for water heating and cooling for domestic and commercial requirements, and in particular to consider this in relation to the conditions of Morocco. Solar DHW, heating and air-conditioning applications offer interesting opportunities for Morocco in building sector. For this reason, the government encourages the

development of new projects related to solar energy technologies through the promotion of R&D research works. In this vision, this thesis belongs to the project of **Solar Cooling Process in Morocco (SCPM)** funded by the *Research Institute for Solar Energy and New Energies (IRESEN)*. The general view of solar central for DHW, heating and air-conditioning adopted in SCPM project is shown in Fig. 1.8.

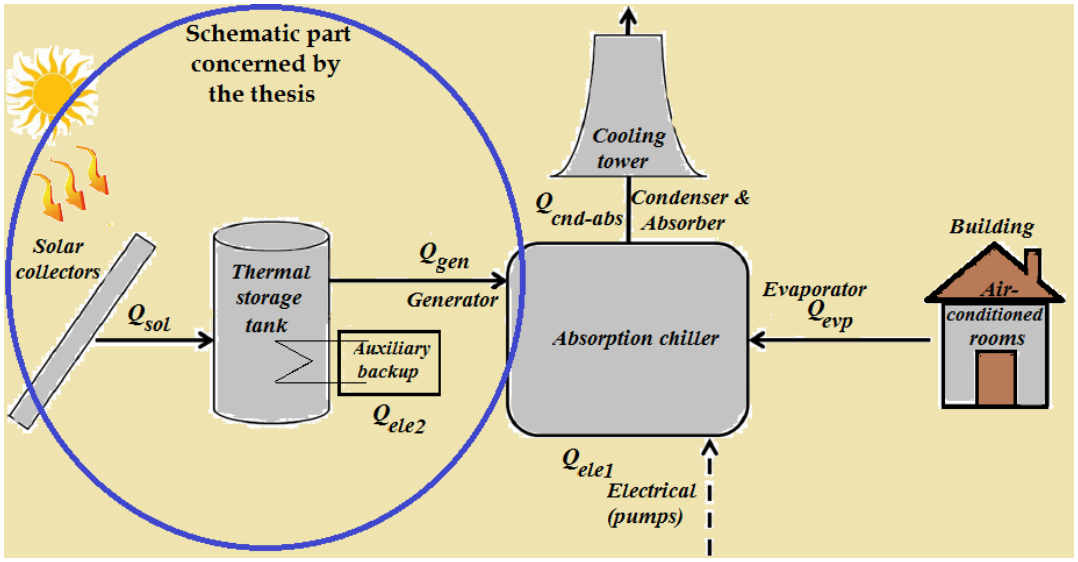

FIGURE 1.8: Solar central for air-conditioning process

The **SCPM** project focuses on the study of the processes of solar air-conditioning, heating and DHW in Morocco and more particularly on the refrigeration systems with low power ($11.5kW$) i.e. a generating station of air-conditioning with absorption chiller supplied with solar collectors for solar hot water production at temperature range 80-90 °C.

The scientific problems subjacent with the optimization of solar air-conditioning systems reside in the difficulty to predict the non-stationary behaviour of the system, itself induces by the operation transitory character of each subsystems and of the sources to which they are connected. The energy and technico-economic assessment of the system are all crucial steps to optimize the energetic "performance/cost" ratio.

The main objective of this thesis is to improve the performance of the solar hot water production including the collector's field and the storage tank to continuously feed the absorption machine (see Fig. 1.8). In this context, the aim is to conduct dynamic numerical simulations to optimize the field of solar evacuated tube collectors and the storage volume necessary to operate the absorption chiller operating by the interaction between H2O and LiBr agents. A special focus will be done on thermal energy storage by integrating phase change materials (PCMs) into the storage tank connected to the generator of the absorption machine. The study of numerical methods used in the modeling of phase change phenomena will be performed to evaluate the possible improvements in the system performance.

1.3 Organization of the thesis

This thesis consists of the final phase of the project of **Solar Cooling Process in Morocco (SCPM)** funded by the *Research Institute for Solar Energy and New Energies (IRESEN)* which will be implemented in *Green Energy Park* in Ben Guerir (Morocco). **IRESEN** reflects the Moroccan national research and development strategy in the field

of solar energy and new energies trough supporting, financing and managing innovative projects carried out by research institutions and by industrialists. The SCPM project combines the efforts of four institutions: (i) Sidi Mohamed Ben Abdellah University (presented by the High School of Technology which is the first institution where the thesis was conducted) as the piloting institution (Fez, Morocco), (ii) Moulay Ismail University (Meknes, Morocco), (iii) Pau and Pays de l'Adour University (Pau, France), and the Moroccan industrial company Energypoles (Rabat, Morocco) specialized in solar energy and their applications. The objective of this collaboration is to implement the first solar cooling system in Morocco serving as a prototype model for a future integration in the Moroccan building sector (see Fig. 1.9).

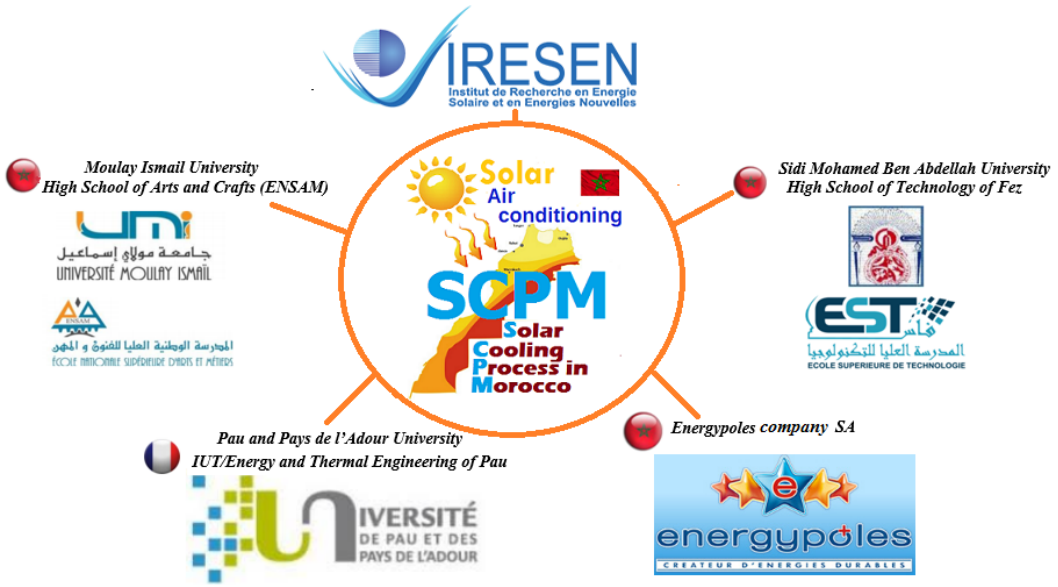

FIGURE 1.9: Key partners of the project of Solar Cooling Process in Morocco (SCPM)

This thesis reports the results of research into the modeling and simulation of solar air-conditioning system for Morocco, and the investigation of the factors concerning the optimisation of such systems. Further, a number of design criteria, which can be used by designers of solar cooling and heating systems, have been established. From the literature survey (Ge et al., 2018), it is seen that the great majority of researchers followed the approach of modeling and simulation of solar systems to predict the performance of a system and investigate its optimum design parameters. Since the present work is essentially based on modeling and simulation of solar cooling systems, it would be appropriate to explain the value and the background of modeling and simulation of solar systems currently in use.

Accordingly, this thesis covers four aspects. The first overviews, through Chapter 2, the literature survey on solar technologies with a focus on solar cooling systems which reports the relevant processes, summarizes the market status, presents the recent developments of the most promising technologies and describes the main performance indicators figuring in the literature. Chapter 2 describes also the experimental aspect of the solar air-conditioning installation adopted in the project of **Solar Cooling Process in Morocco (SCPM)** funded by the *Research Institute for Solar Energy and New Energies (IRESEN)*. The aim of this section is to identify the important technical characteristics of the installation, the sensitive points and to consider

avenues for improvement with a view to future implementation and industrialization of the solar absorption cooling process in Morocco. In this part, the difficulties encountered during the realization of the project are as well discussed. The second dimension concerns the technical feasibility of solar air-conditioning system and its integration in Moroccan building sector. Therefore, Chapter 3 focuses on the modeling, design and performance optimization of solar absorption cooling systems using energy and economic indicators taking into account the combined effects of climates, building categories and cooling demands under Moroccan conditions.

The third aspect presents the latent thermal energy storage using Phase Change Materials (PCMs). In this way, Chapter 4 concerns the investigation of numerical methods used in the modeling of phase change phenomena. To this end, a numerical comparative approach and optimization of thermal energy storage by means of PCM integration within solar hot water production system operating in dynamic mode is presented. Besides, Chapter 5 focuses on PCMs addition in the solar cooling process integrated inside solar storage tank connected to the generator of the absorption chiller to evaluate the possible enhancement in the system efficiency.

The fourth aspect of this thesis outlines the technico-economic and sensitivity analysis applied to the development of a combined processes of solar DHW, heating and air-conditioning in Morocco. In fact, the economic aspect is a determinant parameter deciding on the adoption of solar cooling technologies for air-conditioning requirements in residential buildings (Chapter 6). A technico-economic assessment of a complete solar DHW, heating and air-conditioning plant using an absorption chiller and operating under Moroccan climates was carried out based on adequate indicators. Thus, annual dynamic simulations of the optimal configuration were lunched for various Moroccan climatic regions. A scenario evaluation was conducted based on economic, social and Moroccan policy attributes. The overall analysis via a generalization of the results to the national level was carried out in addition to a risk analysis related to the investment in these systems in order to assess the potential of replacing traditional technologies with the solar systems and the possible earnings related to their implementation in Morocco.

Finally, in Chapter 7, several recommendations and relevant policy directions are suggested in order to improve the adoption of solar technologies and remove different barriers facing their implementation especially the process of solar DHW, heating and air-conditioning systems in Moroccan building sector. Accordingly, appropriate prospects and relevant future research issues have been pointed out in order to extend the knowledge in the field of solar cooling systems for possible improvement of their performance in terms of cost and efficiency.

Chapter 2

Literature review on solar air-conditioning systems

2.1 Introduction

As presented in Chapter 1, the research project of **Solar Cooling Process in Morocco (SCPM)** was retained and funded by *Research Institute for Solar Energy and New Energies (IRESEN)*. Therefore, it is appropriate to give a clear picture of solar cooling options, the relevant cycles and the market status and report the recent developments of the most promising technologies and the main performance indicators figuring in the literature. Accordingly, Chapter 2 provides an overview of the developments in the field of solar DHW, heating and cooling for buildings. This will include a brief description of the types of solar heating and cooling systems that are available and in current use, and their basic functions and key components will be presented. The above will be followed by a review of research work carried out in the field of solar DHW, heating and cooling which seem to be relevant to the present work. Then, the energy profile of Morocco is presented with an overview of solar energy applications and their potential. Particular emphasis is given on solar cooling systems which is related to this work. Thus, the main experimental components of the installation adopted in the **SCPM** project using an absorption machine was thoroughly described and the problems encountered in the delivery and implementation of the solar cooling installation were also addressed.

2.2 Common components to solar thermal systems

Different technologies for capturing solar energy and storing thermal energy are available in the market, namely: Solar thermal collectors and storage tanks.

2.2.1 Solar thermal collectors

A solar collector is a device that collects the solar radiation incidents on it, converts it into thermal energy and transfers this energy to a working fluid (air or water). The heat picked up by working fluid can also be used to charge the thermal energy storage system to use in the night. For photovoltaic (PV) utilization: PV module converts solar radiation into electrical energy. In addition to it, it also produces abundant waste heat, which can be utilized by attaching PV board with recuperating tubes filled with carrier fluids (Tian and Zhao, 2013). The types of solar thermal collectors commonly used in solar thermal applications are shown in Fig. 2.1.

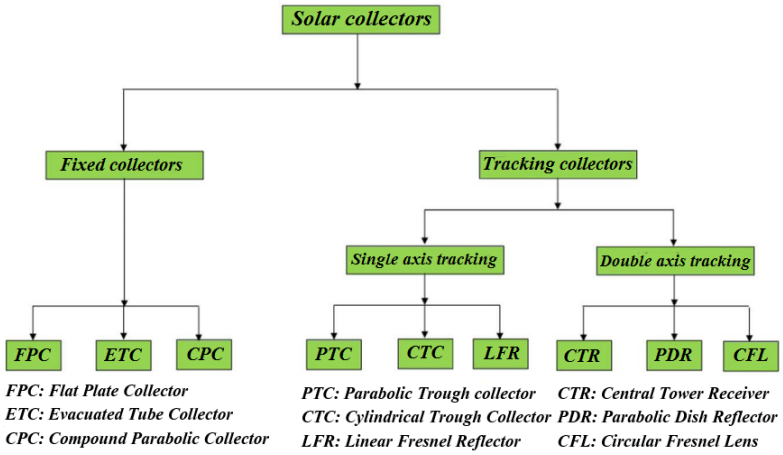

FIGURE 2.1: Types of solar thermal collector's technologies (Ghritlahre and Prasad, 2018)

Solar collectors are broadly classified into two categories, such as, fixed collectors and tracking collectors. The fixed collectors are kept at rest, whereas tracking collectors track as per the movement of sun such that the incoming solar radiations always incident perpendicular to them. The tracking solar collectors are subdivided into two categories: single and double axis tracking as shown in Fig. 2.2. The fixed collector is classified as flat plate collector, evacuated tube collector and compound parabolic collector. The single axis tracking collector is categorized into three types such as parabolic trough collector, cylindrical trough collector, and linear Fresnel reflector. Again, the double axis tracking collector is subcategorized as central tower receiver, parabolic dish reflector, and circular Fresnel lens (see Fig. 2.2). These solar collectors have their applications depending upon the feasibility and quantity of energy required (Khalifa and Al-Mutawalli, 1998).

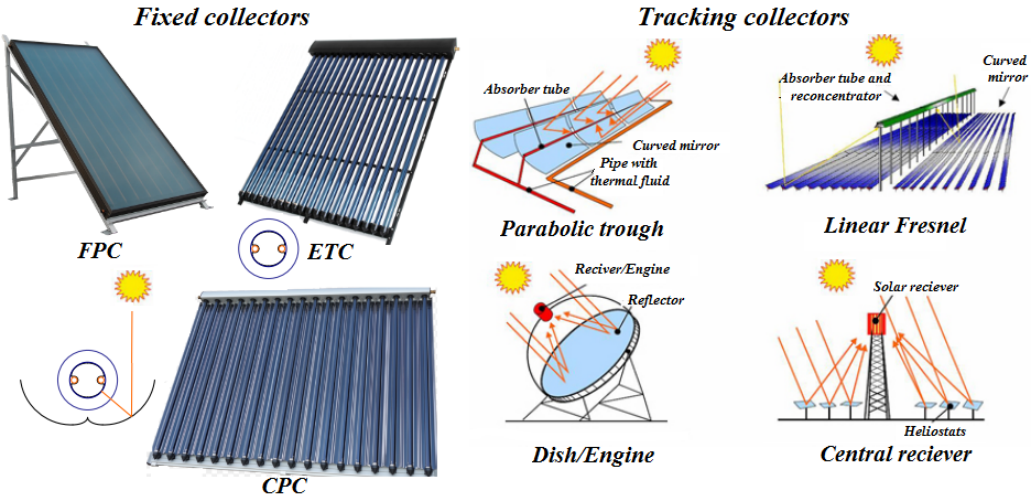

FIGURE 2.2: Solar collector's technology for different applications (Tyagi, Kaushik, and Tyagi, 2012)

2.2.2 Solar storage tanks

Storage is a key component of all solar thermal system. It overcomes the discontinuous nature of solar energy and non-simultaneity of production and needs. In practice, the solar thermal energy is stored via the water contained in one or more

tank(s) water accumulator(s) connected(s) in series. The domestic hot water storage tank is the most important device for domestic hot water production. There are several types of storage tank on the market. An example of storage tank used in solar DHW, heating and cooling systems is given in Fig. 2.3. The storage improvement in these tanks can be done by two different methods. We can act on the thermal insulation (an external factor to the tank), as we can act on parameters which affect thermal stratification (Weiss, 2003). The storage part is important, the more it is improved the more we are sure that the overall efficiency of the solar water heater is also improved.

FIGURE 2.3: Exemple of storage tanks used in solar DHW, heating and cooling systems (Bouhal et al., 2017b)

Thermal stratification is a performance parameter widely used in thermal applications so as to quantify the evolution of the thermal energy stored in a tank which is operating in a discharging/charging load cycles (see Chapter 4). The influence of the inlet mass flow rate on the degree of thermal stratification during an unloading process is analyzed. Yaïci et al., 2013 have conducted three-dimensional unsteady Computational Fluid Dynamics (CFD) simulations to study the effect of several design and operating parameters on the thermal stratification, the flow behaviour and the hot water storage tank performance that is used in solar thermal energy systems. They have used COMSOL as a CFD code to validate the experimental measurements of Zachár, Farkas, and Szlivka, 2003. They showed through their 3D transient CFD simulations that numerical simulations can be used at an early design stages to optimize the thermal storage tank parameters. Recently, Bouhal et al., 2017b used the 2D CFD simulations to study and optimize the stratification through the placing flat plates inside the storage tank.

The solar thermal applications by temperature range including DHW, heating, cooling and industrial processes are presented in Fig. 2.4.

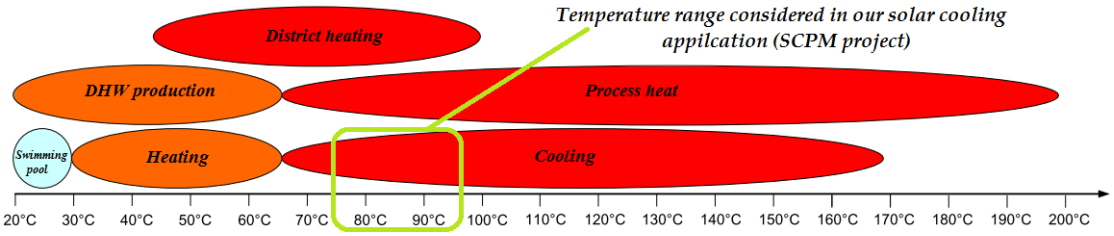

FIGURE 2.4: Solar thermal applications classified by temperature range (Tian and Zhao, 2013)

2.3 Solar DHW production systems

2.3.1 Solar water heaters

Solar energy is a clean, abundant and easily accessible form of renewable energy. Its intermittent and dynamic nature makes thermal energy storage (TES) systems highly valuable for many applications. The improvement in the solar water heating (SWH) have been identified as convincing solutions to reduce the high consumption and environmental impact in various building applications (Shirinbakhsh, Mirkhani, and Sajadi, 2018). The general structure of a solar DHW system is illustrated in Fig. 2.5.

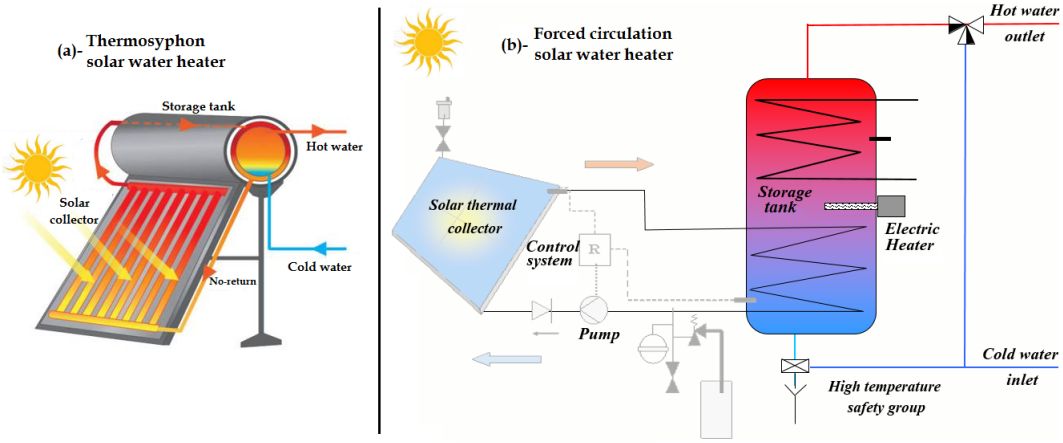

FIGURE 2.5: Layout of solar DHW production systems

The forced collective solar hot water production system are used for many years in residential buildings. There are variants of solar collective systems depending on the constraints of implementation or billing (see Fig. 2.6). It's interesting to derive a knowledgeable data base for the energetic performance parameters concerning the use and implementation of dynamic solar collective systems, because in general, the majority of the research reports focuses on hot water individual systems and uses simplified model in the simulations of the collective systems (Dîn Fertahi et al., 2018a).

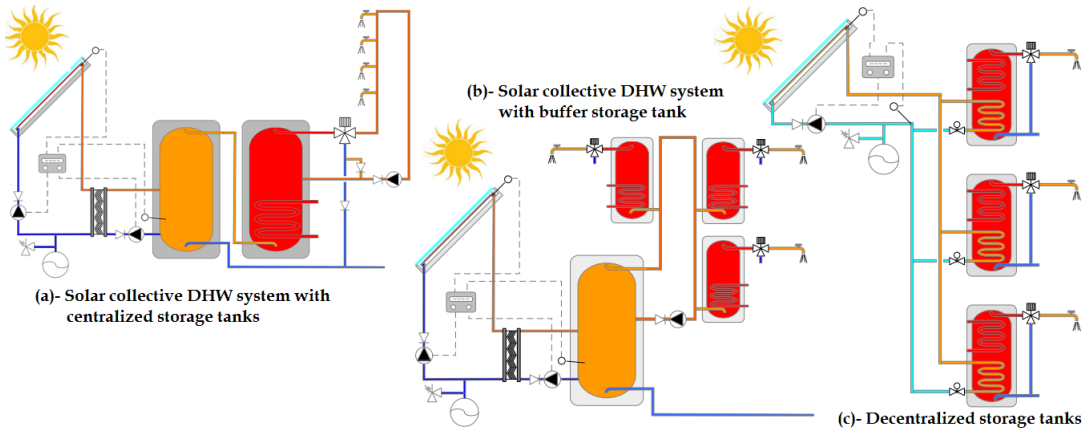

FIGURE 2.6: Variants of solar collective hot water generation systems

2.3.2 Solar DHW system with phase change materials (PCMs)

The use of phase change materials (PCMs) in solar DHW systems is a novel approach which in recent years gaining more and more ground thanks to their high storage density, high latent heat capacity and isothermal operation (Mazman et al., 2009). In the literature reports, there are several methods to integrate PCMs in solar DHW system either in solar collector or storage tank or in separate location (Haillot et al., 2013, Talmatsky and Kribus, 2008, Sharif et al., 2015) as shown in Fig. 2.7.

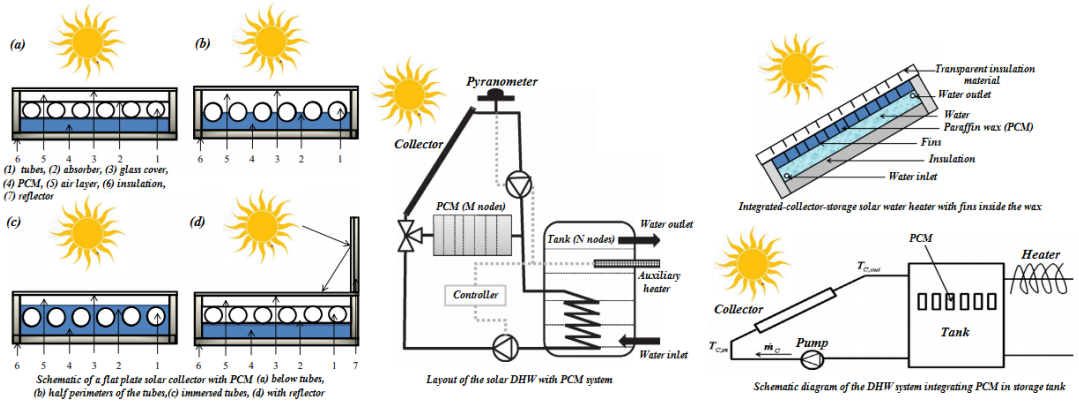

FIGURE 2.7: Different methods of PCM integration in solar DHW

Eames and Griffiths, 2006 studied the integration of PCM as a storage element for a solar collector. A transient finite volume model was used for capturing and conserving heat in a cross-sectional rectangular collector section filled once in water and other times with different concentrations of phase-change materials. Moreover, Summers, Antar, and Lienhard, 2012 presented the design and studied the optimization of a solar collector used for the humidification-dehumidification cycle, with the integration of a phase change material (paraffin wax) as a system of energy storage. Li et al., 2013 studied analytically latent heat storage by means of three phase-change materials (PCMs) named PCM1, PCM2 and PCM3 with different high melting temperatures and the heat transfer fluid (HTF: air) with resistance and viscous dissipation compared to the heat transfer method. The results showed that the PCM3 melting rates are the fastest and PCM1 is the slowest in both (x, r) directions. It was also found that the melting times of PCM1, PCM2 and PCM3 decrease with increase in air inlet temperatures.

Despite that solar water heating production systems with and without phase change materials (PCMs) are well used in widerange applications, solar heating options (for space heating and industrial process) are one of the privileged solar technologies applications.

2.4 Solar heating systems

The climatic conditions in winter are such that space heating is required for a period of 4 to 5 months and the average number of degree-days (base 18 °C) for winter is estimated to be 950 degree-days (see Fig. 2.8). For space heating, liquefied petroleum gas (LPG) and kerosene are the most widely used forms of energy, followed by oil and electricity. Solar energy has not been put into use for the heating of buildings except from very few cases where solar active systems have been combined with oil-fired central heating systems and floor heating in residential dwellings (Buker

and Riffat, 2016). However, performance data for these installations is not available and therefore no comprehensive conclusions as to their energy and economic performance can be drawn. Space heating consumes a great proportion of energy consumption in buildings. Non-renewable sources including electricity or natural gas are significant supply. Due to the roaring concerns on energy conservation and environmental protection, using electricity or fossil fuel driven heating devices in buildings is limited in many countries, solar energy are proposed instead to meet the legislation. Converting solar radiation into heat is the most simple and direct application of solar energy, with greater potential than other forms of renewable sources. Space heating also can be realized by solar energy. Solar space heating system, usually combined with solar water heating is starting to put in use. It also can be distinguished as passive solar space heating and active systems (Buonomano, Calise, and Palombo, 2018a; Monghasemi and Vadiee, 2017).

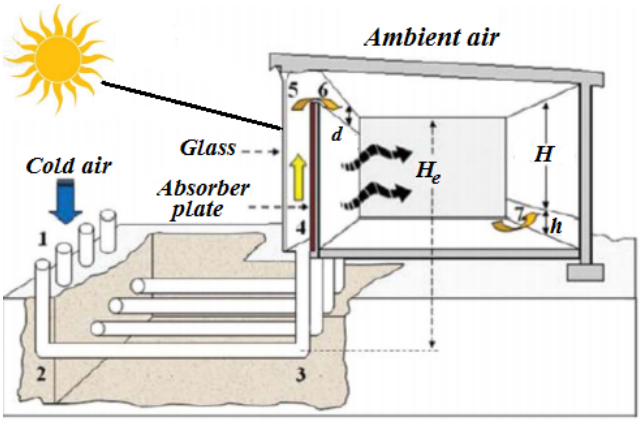

FIGURE 2.8: Schematic diagram of a solar passive heating system (Monghasemi and Vadiee, 2017)

2.5 Solar cooling systems

The climatic conditions are such that summer air-conditioning is essential and must in hot and humid areas and in some categories of buildings like hotels, apartments, public spaces, luxury houses etc. Generally, cooling is produced by electrically operated vapor compression refrigeration systems. For solar cooling, a large number of processes are possible thanks to the capacities of existing solar thermal collectors (Miranville, 2002). Among them, some innovative processes are still in development in order to evaluate experimentally or theoretically their real performances, for instance based on an ejector cycle (Kim and Ferreira, 2008; Balaras et al., 2007; Chunnanond and Aphornratana, 2004), (Abdulateef et al., 2009), magneto-thermal effect (Russek and Zimm, 2006) or thermo acoustic effect (Swift, 2002; Adeff and Hofler, 2000), (PERIER-MUZET et al., 2011). Fig. 2.9 shows a classification of solar cooling technologies and different processes utilizing solar energy for refrigeration applications including electric and thermal alternatives (Kalkan, Young, and Celiktas, 2012).

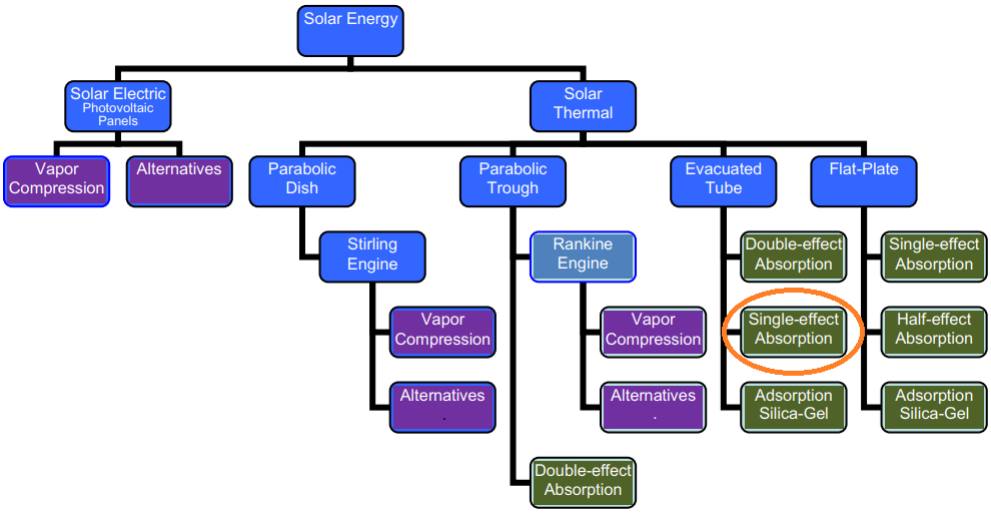

FIGURE 2.9: Classification of main solar air-conditioning technologies (Kalkan, Young, and Celiktas, 2012)

As shown in Fig. 2.9, the exploitation of solar energy can be done according to two types of energy conversion, namely the thermal process and the photovoltaic option. A multitude of cycles can be distinguished, such as thermo-mechanical, sorption, thermoelectric and conventional cycles. These cycles use a variety of technologies. Among these cycles, the absorption and adsorption systems occupy an increasingly important place (Allouhi et al., 2015b).

These innovative systems still have very little or no not at all of actual application in solar cooling, the following paragraph presents the main processes studied today. They are grouped into two broad categories: open cycle refrigeration systems and closed cycle refrigeration systems.

2.5.1 Open cycle refrigeration systems

Open systems are systems where the air is directly treated according to the desired comfort conditions. Refrigerant is always water, since it is in direct contact with air to cool. They are processes where exchanges of materials with the outside are made. The principle is to humidify the air in order to lower its dry temperature. Water is injected into the air, absorbing the heat of it to evaporate. This phenomenon is conceivable only if the initial air is dry enough. This preliminary dehumidification can be carried out by a hygroscopic material, which can be both liquid and solid (JOFFRE, 2005; Villa et al., 2009). The most common systems use a rotary desiccant wheel.

Solid desiccation

The most common technology uses spin adsorption wheels generally made of Silica gel, Zeolite or Lithium Chloride as sorbent materials. Fig. 2.10 shows the operating principle of such an installation, as well as an overview of the corresponding air handling unit.

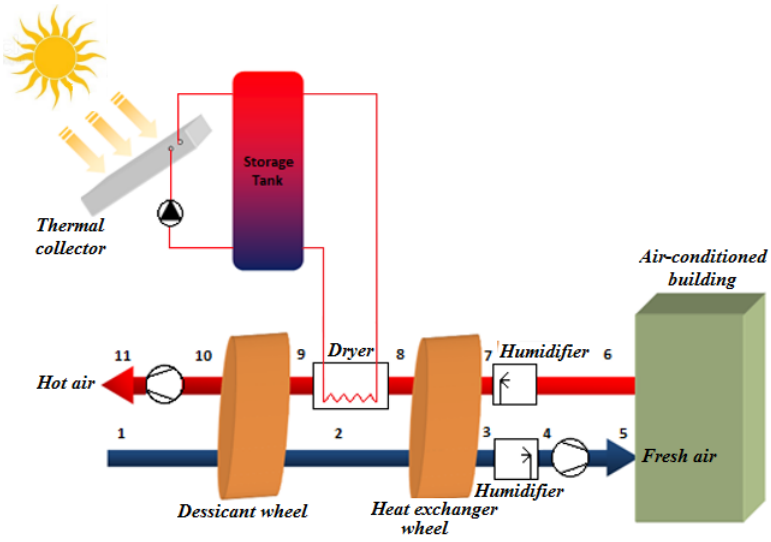

FIGURE 2.10: The principle of the solid desiccation cooling

The principle of the solid desiccation cooling in the building (see Fig. 2.10) is described as follows:

- The outside air (hot and humid) enters the system and passes through a rotating desiccant wheel to be dehumidified (path 1-2). The adsorption reaction being exothermic, the air is warmed up.
- The air then enters an exchanger, in order to be pre-cooled by the air extracted from the building (path 2-3). Several technologies are possible such as that of the rotary exchanger.
- The air is then humidified to obtain the desired cooling effect (path 3-4).
- The air extracted from the room is moistened again, in order to lower even further its dry temperature (path 6-7).
- This air then passes through the rotary exchanger, to cool the fresh air during phase 2-3. As a result, the air temperature increases between points 7 and 8. The air is then heated using heat at a temperature level compatible with solar generation between points 8 and 9. The heated air passes through the desiccant wheel in order to desorb the water contained in the adsorbent (regeneration step 9-10).

Such a system allows the use of a solar source that can be obtained by means of flat water or air sensors. In the case of water, the sensors can be associated with a storage tank, in order to partially cope with cloudy conditions. Studies have shown (Henning et al., 2001) that this process saves up to 50% primary energy compared to a conventional mechanical vapor compression solution. In addition, these facilities have very low operating costs and respect the environment.

Liquid desiccation

In the case of liquid desiccation (see Fig. 2.11), dehydration is carried out by absorption. The desiccant wheel is replaced by a dehumidifier and regenerator set. These elements allow cooling of the air blown through an absorbent solution, usually water/lithium chloride or water/calcium chloride (Oliveira et al., 2000). The operating principle is described in Fig. 2.11:

- Outside air (1) enters the absorber to be dehumidified. The heat of absorption (exothermic reaction) is evacuated to the outside by the cooling tower.
- The air (2) then passes through a humidifier, to be cooled to the desired temperature (3) and is then blown into the room to be cooled.
- The diluted solution created in the absorber is sprayed into the generator above the exchanger supplied by the solar hot source (endothermic reaction).
- The air extracted from the building (stale) is blown into the regenerator. The air thus heated and humidified is rejected outside. The concentrated solution obtained is sent back to the dehumidifier for a new cycle.

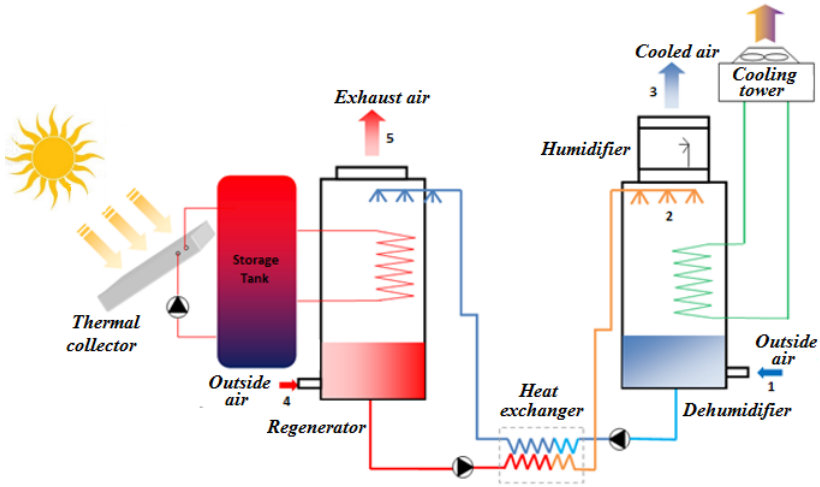

FIGURE 2.11: The principle of the liquid desiccation cooling

2.5.2 Closed cycle refrigeration systems (Sorption refrigeration)

Closed systems correspond to cold sorption production units (Allouhi et al., 2015b) (absorption and adsorption) and produce chilled water which can be used both in an air-handling unit and in a cooling network. Chilled water supplying decentralized facilities. The thermodynamic cycles of these systems are called tritherms because they work between a cold source, a hot source and an infinite well (Pons et al., 1999). The operating principles associated with each of the sorption systems are presented in the following with first adsorption, physical then chemical and then absorption. The principle of a closed sorption cooling system is described in Fig. 2.12.

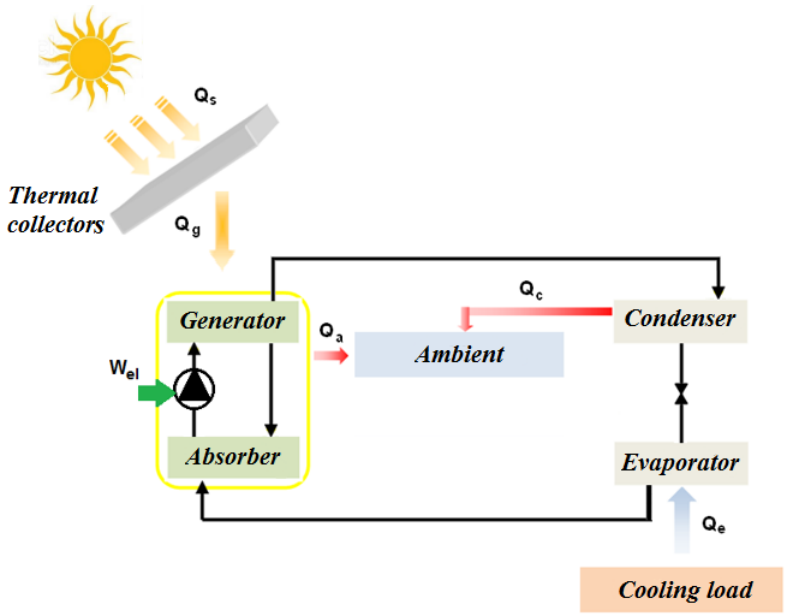

FIGURE 2.12: The principle of the sorption solar cooling system

The generator picks-up the heat Q_g from the solar collector to reactivate the sorbent which absorbed the refrigerant in the absorber. The refrigerant is then vaporized and subsequently condensed in the condenser with the release of the condensation heat Q_c to the ambient. The regenerated sorbent returns to the absorber, where the sorbent absorbs the refrigerant vapor coming from the evaporator. During this process, the sorption heat Q_a is pulled to ambient. In the evaporator, the liquefied refrigerant from the condenser evaporates and extract the heat Q_e from the refrigerated load. In an adsorption system, the sorbent is a porous medium having the ability of adsorbing and desorbing the refrigerant. The coefficient of performance (COP) in such systems can be written as:

$$COP = \frac{Q_e}{Q_g + W_{el}} \tag{2.1}$$

where W_{el} denotes the additional electrical work caused by the pump. The overall efficiency of solar sorption systems is given by:

$$\eta_{srp} = \frac{Q_e}{Q_s} \tag{2.2}$$

Q_s is the heat received by the solar collector from the sun. Q_s is expressed as:

$$Q_s = I_{rad} A_s \tag{2.3}$$

where A_s is the collector surface and I_{rad} is the solar radiation.

These systems also use a refrigerant and its phase changes (liquid/vapor). The refrigerant is in this case water added with a second component. If the latter is a liquid, then it is called absorbent and absorption machine; if it is a porous solid, then it is called adsorbent and adsorption machine.

Adsorption cooling systems

Two main categories of adsorption systems can be distinguished: continuous and intermittent, but depending on the use, these cycles are more or less adapted to the use of solar energy (Dieng and Wang, 2001). A longer use of the refrigerated product then involves its systematic storage in a phase change material for example (Wang, Wang, and Oliveira, 2009). On the other hand, when the goal is to refresh a building, a continuous system is better suited because if, for example, the previous day and the weather conditions were poor, the system would not be able to fulfill its purpose. In addition, these cycles can be operational without moving parts except a few solenoid valves. The result is low vibration, mechanical simplicity, reliability and long life. For adsorption machines, silicone gel is most often used as an adsorbent (Najeh et al., 2016). The machine is composed of two compartments. The hot water, whose temperature must be between 65 and 80 $^{\circ}\mathrm{C}$, allows the refrigerant to vaporize and separate from the adsorbent in the first compartment before entering the conventional cycle condenser/expander/evaporator and to adsorb in the second compartment. The adsorption refrigeration machines operate thanks to the ability of certain solids, to adsorb (exothermic reaction) and to desorb (endothermic reaction) a vapor on the surface of the material that constitutes them (up to several tens of m^2 per gram). Adsorption is a phenomenon that is widely known and widely used, particularly in gas capture (air treatment, depollution, chemical industry, etc.). The implementation of a refrigerating machine operating according to this principle requires the presence of two enclosures, one of which contains the adsorbent solid, the other constituting the refrigerant reservoir. The presence of a solid prevents any circulation between the elements, so that the operation is cyclic: a refrigeration production phase must succeed a regeneration phase to return the system to a state able to produce cold again (Critoph, 1999; Papadopoulos, Oxizidis, and Kyriakis, 2003). The sorbent/sorbate associations most known and used are: Zeolite/Water, Silicagel/Water, Activated Carbon/Methanol (Wang, Wang, and Oliveira, 2009).

Absorption cooling systems

Absorption refers to the process in which a substance penetrates and gets incorporated into another one of a different state. These two states create a special attraction to form a strong solution called mixture. This process is reversible and can occur by heating the mixture (Ayala, Heard, and Holland, 1998). In the absorption machine the energy transfer is carried out by means of a refrigerant continuously subjected to the succession of a thermodynamic cycle consisting of changes in vapor/liquid states (see Fig. 2.13). The cycle consists of the following four phases (Sun, 1998):

- Compression: the temperature and pressure of the fluid in gaseous form rises.
- Condensation: by passing through an exchanger located in contact with the outside environment (colder), the fluid passes to the liquid state and rejects calories to the outside.
- Detention: the fluid in liquid form sees its pressure lowered, as well as its temperature.
- Evaporation: by passing through an exchanger located in contact with the medium to be cooled, the fluid captures calories and vaporizes.

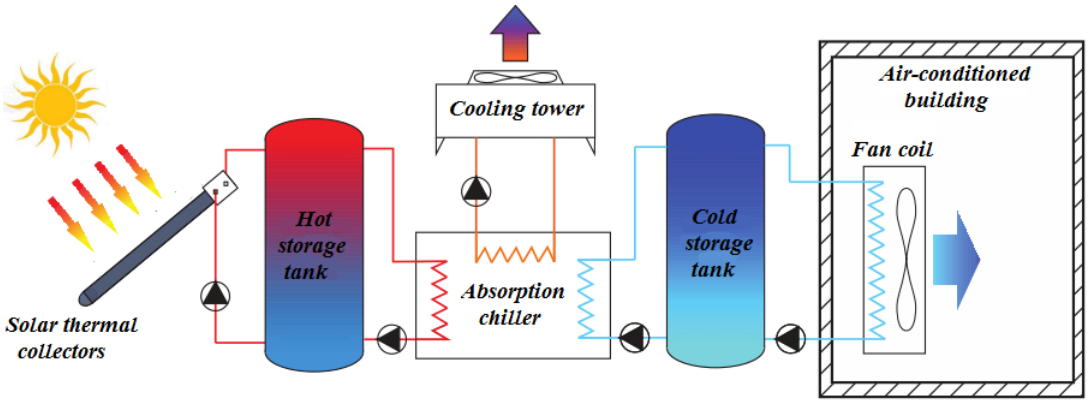

FIGURE 2.13: Schematic diagram of an absorption solar cooling plant

The absorption machines take advantage of two physical characteristics that guarantee a significant reduction in electrical consumption and an efficient production of cold (Lee et al., 2000). On the one hand, it is less expensive to circulate fluids rather than gases between two pressure levels. We use this specificity to achieve electricity savings. On the other hand, the fluids evaporate at different pressure levels and at different temperatures. In case of high pressure, the water evaporates only if the temperature itself is high. When the pressure is low, the temperature must also be low to allow the water to evaporate. We use this effect to produce cold (Şencan, 2007). In the high pressure zone (condenser and steam generator), when the temperature is high and the equivalent pressure, the refrigerant (water) is separated by expulsion of the lithium bromide (steam generator or boiler). For this, a source of motive heat necessary, for example, the heat produced by a solar water heater.

In the condenser, the refrigerant liquefies with the absorption of heat. This step aims to reuse the refrigerant, namely water, in its pure form. The fluid refrigerant then passes through pressure separation lines and is fed into the low pressure zone (evaporator, absorber). It evaporates at very low temperatures between 5 and 15 °C. In the evaporator, the refrigerant evaporates with the absorption of the ambient heat and cold is obtained. The vapor of the refrigerant generated is absorbed in the absorber by lithium bromide and dissolved in the salt by the release of heat pumped to the high pressure zone (boiler/condenser) consuming very little electrical energy. The operating cycle is maintained continuously.

The quality of the absorption process is regularly evaluated using the Coefficient of Performance COP (see Eq. 2.1), which indicates which cooling performance can be obtained depending on the transmission efficiency. The good absorption refrigeration machines get a value of 0.7 and the very good absorption refrigeration machines reach COPs close to 0.75 (Liao and Radermacher, 2007). This value cannot be compared to the figures of traditional refrigeration units. The COP is calculated using the ratio between electrical energy and the generated cold, the value of this ratio being between 2 and 3. If we calculate the ratio between the thermal efficiency and the electrical efficiency of the absorption refrigeration systems, values between 15 and 20 are obtained. Here again, this result shows that the absorption cold technique can lead to significant energy savings. Desiccation systems have not yet penetrated the market as absorption and adsorption do. As far as capture technologies are concerned, flat and vacuum collectors are the most used and there are very few systems requiring concentrated solar flux (Farshi, Mahmoudi, and Rosen, 2011).

To summary, absorption machines are the most important sorption refrigeration machines on the solar cooling market, whether large or small. Their combination

with flat and vacuum solar collectors is quite well known in the field of large installations. However, in the case of small systems, the unsteady behavior of these machines is not yet well known because of all the transient parameters influencing their operation, such as the solar resource, the environmental conditions and the cooling load of the equipment and building which is the aim of **Solar Cooling Process in Morocco (SCPM)**.

2.6 Solar energy profile in Morocco

The purpose of this part is to present the Moroccan energy profile with an overview of solar energy applications and their potential. Particular emphasis is given on solar DHW, heating and air-conditioning which is related to this PhD thesis.

2.6.1 Geography and economy in brief

Officially, the kingdom of Morocco ($32\mathrm{deg}00'\mathrm{N}\ 5\mathrm{deg}00'\mathrm{W}$) is a country in the Maghreb region of North Africa (see Fig. 2.14-(a)). Its eastern border is with Algeria and a relatively narrow body of water separates it from Spain to the north. Prediction of climatic change and global warming studies demonstrated that Morocco is among the countries that are more likely threatened by climatic change (Kousksou et al., 2015). Morocco imports about 96% of its required energy needs. Solar energy, as one of the most abundant and valuable renewable energy alternatives in the country, offers interesting opportunities for Morocco. In order to minimize its strong foreign energy dependence, Morocco hosts actually the largest Concentrated Solar Power (CSP) using parabolic trough collectors (PTC) as a technology for converting solar irradiation into thermal energy for electricity generation. The potential sites of CSP implementation concerned by Moroccan Solar Plan are presented in the map of Fig. 2.14-(b).

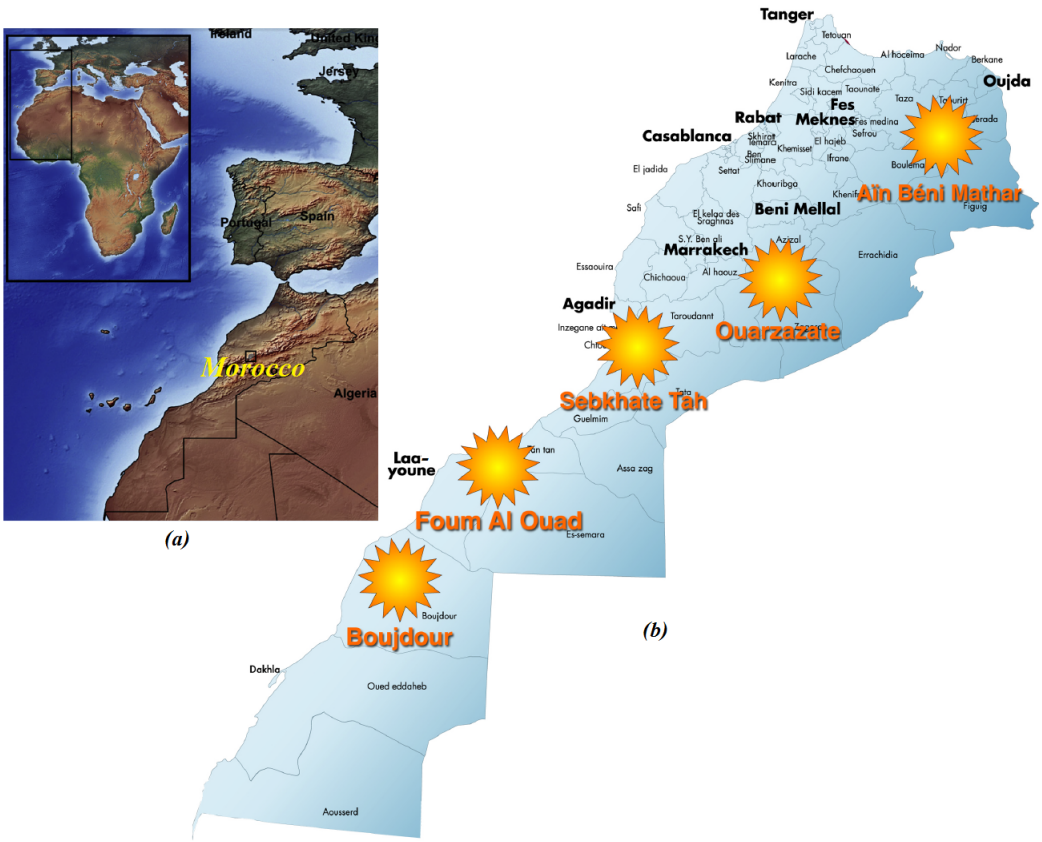

FIGURE 2.14: (a) Map of Morocco and (b) Selected CSP sites for electricity generation (*Moroccan Agency for Sustainable Energy (MASEN)*)

Global primary energy consumption has already reached 13.7 billion TEP in 2014. The International Energy Agency forecasts a 1.5% of annual increase in global energy demand to 2030, to reach 17.3 billion TEP by this horizon. Global energy consumption, as it stands today, cannot continue to keep pace and with the same structure. This consumption remains strongly dominated by fossil fuels, which represent more than 80% of primary energy sources. Oil continues to be the primary source of primary energy with a part of 31%, followed by coal with a part of 29% and natural gas with a part of 21% (Conti et al., 2016).

For the Kingdom of Morocco, in addition to its commitments to the climate change (Greenhouse reduction of 32% by 2030), the Moroccan energy transition faces many challenges. Particularly, it is a question of ensuring a match between supply and demand for primary energy, knowing that it increases by 5% per year, driven by electricity demand which follows a sustained annual growth rate exceeding 6% through the development of new power generation capacity which will have to increase the installed capacity to 25,000 MW in 2030 (*Ministry of Energy, Mines and Sustainable Development (MEMSD), Morocco*).

Security of supply also remains one of the major challenges of Moroccan energy model which is addressed through the diversification of energy sources and resources. Furthermore, the kingdom must reduce the energy dependence on fuel imports, which was 98% in 2009, through the ramp-up of renewable energies for which Morocco has a huge potential, including the cost of recovery which is increasingly competitive, strengthening energy efficiency in key sectors of the national economy including transport, building, industry, agriculture and street lighting (Bennouna and El Hebil, 2016).

2.6.2 Climatic conditions

The Moroccan climate is both Mediterranean and Atlantic, with a dry and hot season coupled with a cold and wet season, the end of the warm period being marked by October rains. The presence of the sea attenuates the differences in temperature, tempers the seasons and increases the humidity of the air (400 to 1000 mm of rains on the coast). In the interior, the climate varies according to the altitude. Summers are hot and dry, especially when blowing the hot sirocco or the chergui, summer wind coming from the Sahara. At this season, average temperatures are 22 °C to 24 °C. Winters are cold and rainy with frost and snow. The average temperature then varies from -2 °C to 14 °C and can go down to -26 °C. In the mountainous regions, the precipitation is very important (more than 2000 mm of rainfall in the Rif or 1800 mm in the Middle Atlas). Pre-Saharan and Saharan Morocco has a dry desert climate.

The kingdom suffers from a very high energy dependence rate of about 93% (Bouhal et al., 2018c). As shown in Fig. 2.15-(a), Morocco has a huge potential in solar energy with more than 3000 h/year of sunshine and an average solar irradiation of 5 kWh/m^2/day (*Moroccan Agency for Sustainable Energy (MASEN)*). Therefore, this potential can be exploited to ensure the comfort needs while reducing our energy bill and respecting the environment.

As shown in Fig. 2.15-(b), six Moroccan climate zones were defined by *Moroccan Agency for Energy Efficiency (AMEE)* where each zone is represented by a reference city in order to establish a new thermal building regulations.

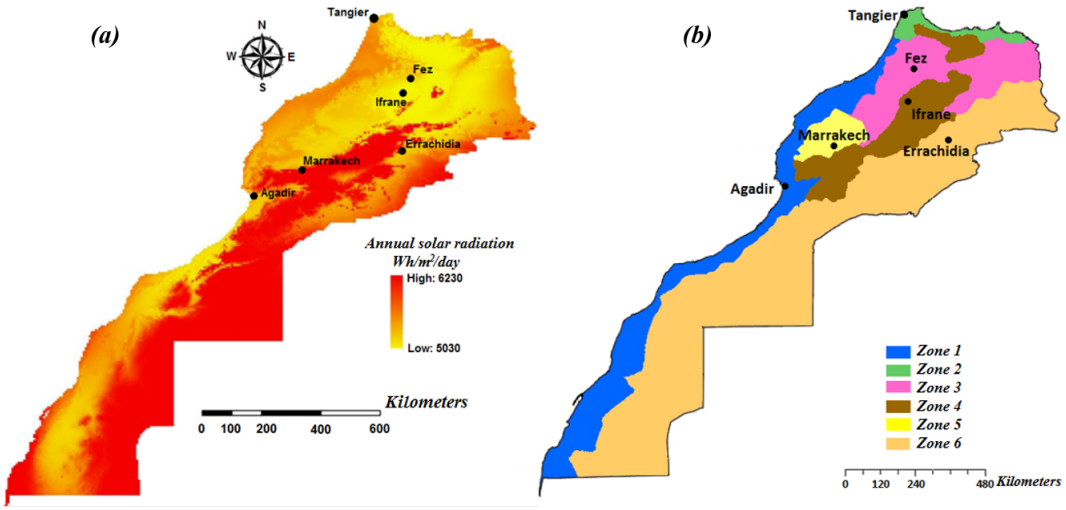

FIGURE 2.15: (a)- Solar energy potential and (b)- Moroccan climatic zoning in Morocco (*Moroccan Agency for Energy Efficiency (AMEE)*)

Fig. 2.16 shows the monthly average values of meteorological data referring to incident solar radiation and ambient temperature as generated by Meteonorm (*Meteonorm*) for the representative cities of Moroccan zones.

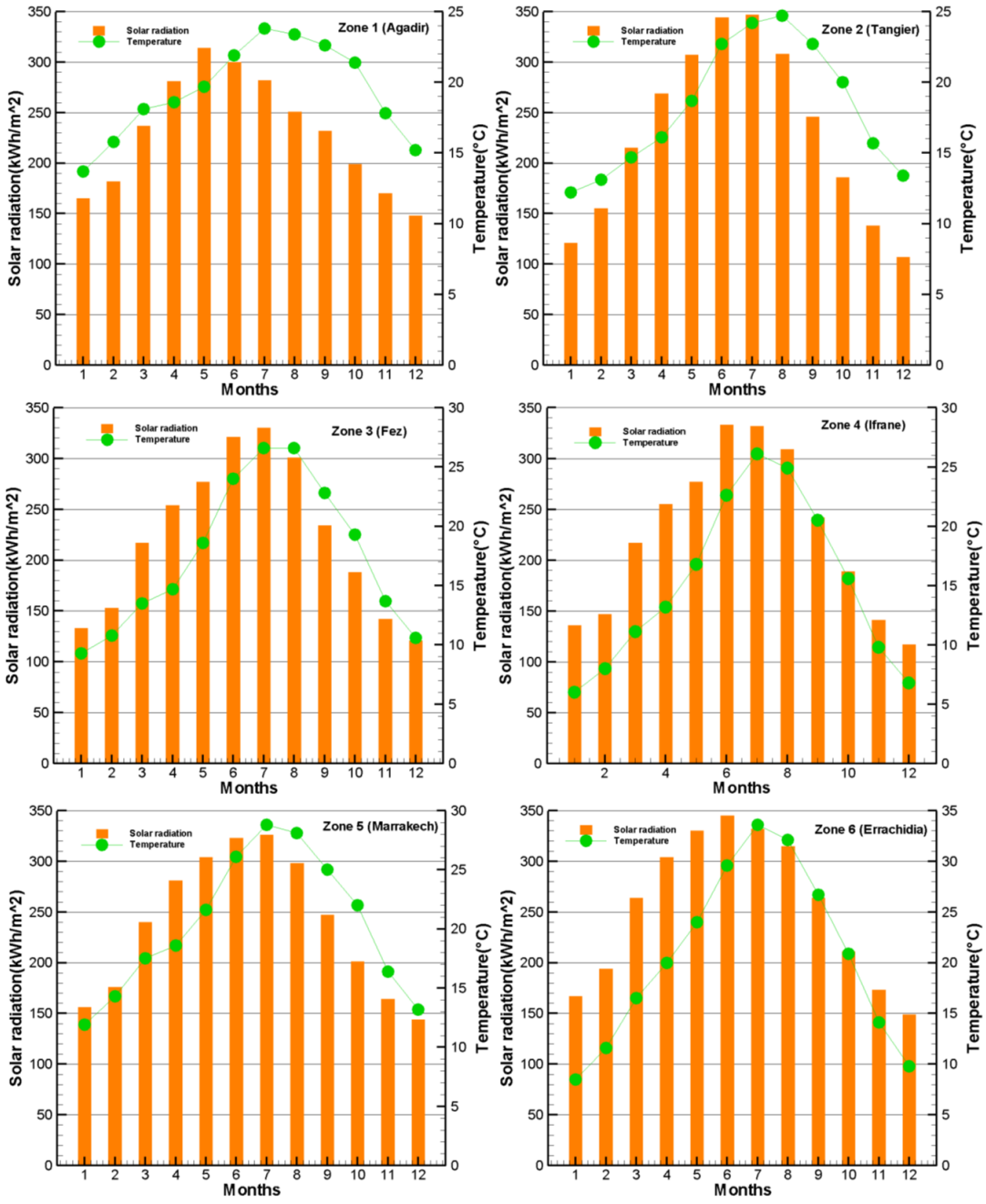

FIGURE 2.16: Mean monthly solar radiation and average air temperatures in different zones of Morocco (*Meteonorm*)

2.6.3 The energy scene

The energy sector plays a central role in the green growth policy of the Government of Morocco, and this on several levels. First, the success of the recently launched and ongoing sectoral strategies in key sectors (agriculture, fisheries, tourism, industry) is based on the country's ability to improve access to energy, which remains relatively low and to provide increase in additional demand linked to urbanization progressive country (*Haut Commissariat au Plan (HCP)*). In 2017, the country imported 93% of its commercial energy consumption, or 90.7 billion dirhams, instead of 19.1 billion dirhams in 2002. This dependence weighs heavily on the economic and financial equilibrium of the Kingdom and on its development opportunities (*Ministry of*

Energy, Mines and Sustainable Development (MEMSD), Morocco). Second, the energy challenge is also an environmental issue. The latest energy balance (2011) shows that the total consumption of 17.3 million TEP (oil equivalent tones) is made up of almost 61.9% of oil and 22.5% of coal. This has localized environmental effects (pollution) as well as global ones. Even though the Moroccan economy is not a major contributor to overall global CO_2 emissions, its relatively high dependence on fossil fuels could negatively impact the country's commitment to fighting climate change.

Indeed, the energy demand would reach 45 Million TEP by 2030 and the structure of energy consumption would not change much. By type of energy consumed (see Fig. 2.17), the structure of energy consumption remains dominated by coal, which by 2030 represents almost 26% of total energy consumption, followed by diesel fuel, which represents almost 22%. Natural gas would satisfy some 3.2% of total demand, followed by gasoline, whose consumption represents 3% of total energy demand. On the other hand, electricity consumption would be around 15% of total energy, of which 88% is thermal, 7.5% is hydro, 4% is wind and 0.8% is solar. The contribution of renewable energies (solar and wind) to the energy supply will not undergo a remarkable change because their yield would only grow between 1 and 2% per year (Kousksou et al., 2015). The impact on producer prices would be reflected in rising capital costs with low producer price growth between 0.6 and 0.4 percent per year. In this situation, there is little room for market penetration for solar and wind energy.

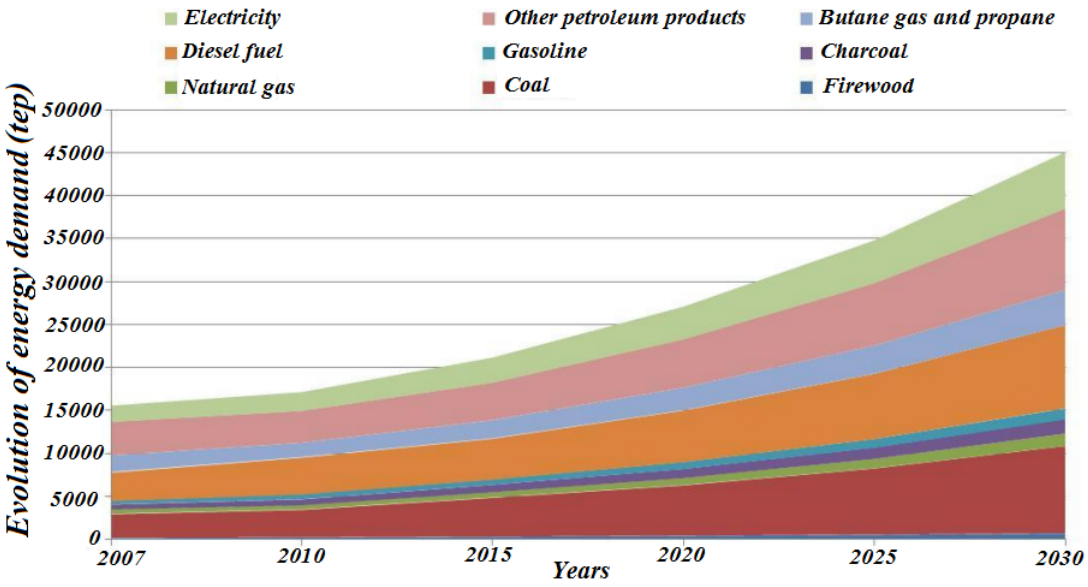

FIGURE 2.17: Evolution of energy demand in thousands of TEP in Morocco (*Ministry of Energy, Mines and Sustainable Development (MEMSD), Morocco*)

Renewable energy resources will play an important role in the world's future because they comes from natural sources that are constantly and sustainably replenished. Renewable energy sources like solar energy, wind energy, biomass energy, geothermal energy, etc are also often called alternative sources of energy. Renewable energy sources that meet domestic energy requirements have the potential to provide energy services with zero or almost zero emissions of both air pollutants and greenhouse gases (Bouhal et al., 2018c).

Among the Northern African countries, Morocco is the country which is extremely dependent on energy imports and fossil fuels. About 96% of Moroccan energy needs is met by the import. In the meanwhile, the country has abundant renewable energy resources such as wind and solar. Developing renewable energy is a main priority for the public authorities, which is projecting to achieve energy security, sustainable development and job creation by investing in renewable energy (Kousksou et al., 2015).

The Moroccan government has implemented an energy strategy aimed at diversifying the energy mix towards renewable energies, with the ambition of meeting the triple challenges of i) guaranteeing energy supply while reducing energy dependence on energy; ii) limit the environmental impacts of the Moroccan growth model and (iii) guarantee access to energy, especially for the poorest populations.

Thanks to its climate, Morocco benefits from a strong sunshine which it profits through, among others, photovoltaic installations for the pumping of the water, the rural electrification and the lighting. The average incident solar radiation oscillates between 4.7 and 5.6 $\mathrm{kW\,m^{-2}}day^{-1}$ with a number of sunshine hours which varies from 2700 hours/year in the North of Morocco to more than 3500 hours/year in the South (francophonie and d'Almeida, 2001; Brand and Zingerle, 2011), (Senhagi, 2003). Important potential in underserved networked areas and in electrical generating capacities. Particularly high cost (9% below reference cost).

For the 2020-2030 outlook, the resources of the future will be available from potential achievable not including export projects.

- 3,000,000 $\mathrm{m^2}$ for solar DHW as listed in Table 2.1;

	Cumulated surface feasible ($\mathrm{m^2}$)	Energy produced (GWh/year)	Energy saving (ktep/year)	CO_2 avoided (kt/year)	Power saved (MW)	Jobs creation
2020	1700000	1190	103	682	400	920
2030	3000000	2100	181	1204	700	1600

TABLE 2.1: Potential of solar DHW systems in Morocco and prospective 2020-2030

- 1000 MW for CSP;

  The *Moroccan Agency for Sustainable Energy (MASEN)* has launched the first phase of CSP central using a PTC (Parabolic Trough Collector), solar tower and PV technologies for electricity generation. Fig. 2.18 shows the CSP and PV installations in Ouarzazate city.

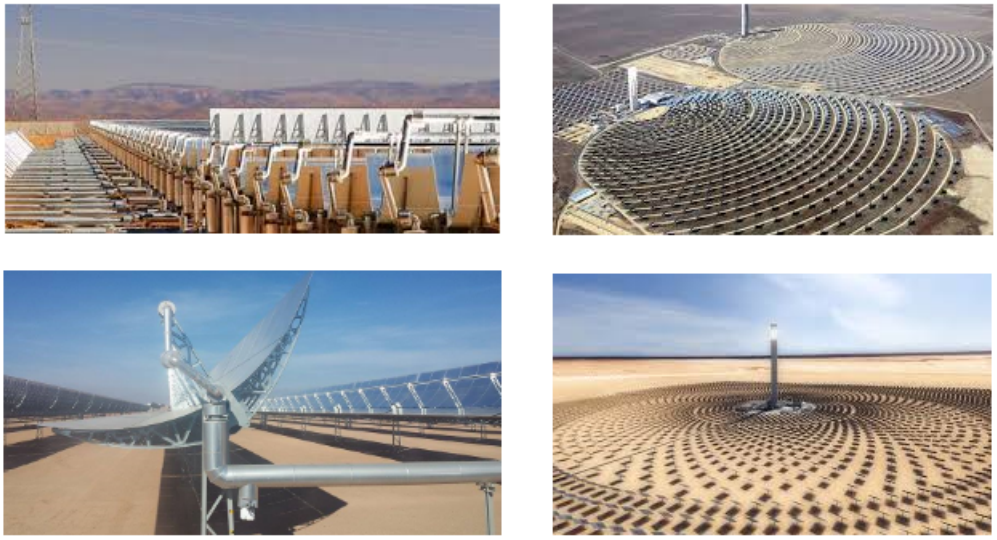

FIGURE 2.18: Concentrated solar power and solar power plant implemented in Ouarzazate solar complex, Morocco (Bouhal et al., 2018c)

The potential of Concentrated Solar Power (CSP) in Morocco within the Moroccan energy strategy is given in Table 2.2.

	Cumulated power feasible (MW)	Energy produced (GWh/year)	Energy saving (ktep/year)	CO_2 avoided (kt/year)	Jobs creation
2020	470	1880	161.7	1110.4	1500
2030	1040	4000	344	2362	3000

TABLE 2.2: Potential of Concentrated Solar power (CSP) in Morocco

- 4.2 million tonnes/year CO_2 avoided;
- 600 thousand tep/year saved;
- 15,000 jobs created.

The realization of this potential is conditioned by the profitability of the projects and in particular the reduction of the access costs to solar technologies. 2030 is a good goal for a foresight exercise, because on the one hand, we will perceive the reality of climate change much more than today, and on the other hand, we will have passed the "peak" of oil, which means that the energy of reference will be much more expensive, and that consequently the control of the energy and the use of the renewables will be essential for all. As a result, what appears today as a handicap (Morocco's strong dependence on imported fossil energy) can be turned into a chance if we know how to prepare in time for change, which is now (Bennouna and El Hebil, 2016).

For building applications, the possibility of integration of solar cooling process in Morocco occurs as a promising solution to save energy consumption in the building sector. Therefore, it is interesting to describe clearly the experimental aspect of the solar air-conditioning installation adopted in the framework of **SCPM** project.

2.7 Experimental description of solar cooling process

This part focuses on the experimental description of solar air-conditioning installation adopted in the project of **Solar Cooling Process in Morocco (SCPM)** funded by *Research Institute for Solar Energy and New Energies (IRESEN)*. The aim is to identify the important technical characteristics of the process, the sensitive points and to consider avenues for improvement with a view to future implementation and industrialization of the solar absorption cooling installation in Morocco.

2.7.1 Background: Solar cooling process in Morocco (SCPM)

In Morocco, energy efficiency, together with the development of renewable energies, is a major priority in the national energy strategy. It is the fastest and cheapest way to better use and save energy, while lowering our energy bills. The ambition of this strategy in terms of energy efficiency is to achieve 15% of energy savings by 2020 (Bouhal et al., 2018c).

It is interesting to note that energy consumption in buildings in Morocco has increased in recent years with the development of the national economy and accounts for 35% of the total energy used. Today, the building sector accounts for one-quarter of global greenhouse gas emissions (Bouhal et al., 2017a). Gradually, the contribution of renewable energies becomes essential in order to achieve the objectives of energy saving and reduction of greenhouse gas emissions set by the various authorities.

Over the past decade, demand for increased comfort and rising summer temperatures has led to a high use of conventional air-conditioning in Morocco. This development of air-conditioning is responsible for a significant peak of electricity consumption in summer. Associated with the possible leakage of refrigerants in conventional air conditioning systems, these peaks in electricity production lead to an increase in greenhouse gas emissions, accentuating the vicious cycle of climate change (Bouhal et al., 2017b). Furthermore, the use of air-conditioning systems in the summertime causes energy consumption which creates problems of production and routing of electrical energy. The *Office National d'Electricité et de l'Eau Potable (ONEE)* is often forced to import electricity from Spain at a very high price. Therefore, in the current context, the use of solar energy for air-conditioning in buildings is again an attractive concept. Kalkan, Young, and Celiktas, 2012 reported the classification of solar cooling technologies and different processes utilizing solar energy for refrigeration applications including electric and thermal alternatives.

The exploitation of solar energy can be done according to two types of energy conversion, namely the thermal process and the photovoltaic option. A multitude of cycles can be distinguished, such as thermo-mechanical, sorption, thermoelectric and conventional cycles. These cycles use a variety of technologies. Among these cycles, the absorption and adsorption systems occupy an increasingly important place (Allouhi et al., 2015b).

The advantages of solar absorption systems compared to solar adsorption machines are numerous. In fact, the absorption machines take advantage of two physical characteristics that guarantee a significant reduction in electrical consumption and an efficient production of cooling. On the one hand, it is less expensive to circulate fluids rather than gases between two pressure levels. We use this specificity to achieve electricity savings. In addition, the fluids used in absorption chiller evaporate at different pressure levels and at different temperatures. In case of high pressure, the water evaporates only if the temperature itself is high. When the pressure

is low, the temperature must also be low to allow the water to evaporate. We use this effect to produce cooling effect.

Accordingly, different technologies are available on the market in the power range of 50 kW and can be coupled with thermal solar collectors. The main obstacles to their large-scale development, even before their high cost, are the lack of practical knowledge on the design, control and operation of these systems. In the small power range, the lack of technology in the market has prevented their growth (Kim and Ferreira, 2008).

In response to the more favorable current situation, several companies have started to develop machines with nominal power ratings ranging from 5 kW to 200 kW. Then, turnkey kits appeared on the market (Balaras et al., 2007). The interest remains in the further development of small air-conditioning systems. The latter are the subject of both research and demonstration projects in many countries and also in the framework of international cooperation (for instance, the International Energy Agency (IEA) program, solar heating and cooling (Abdulateef et al., 2009)).

The global manufacturers of solar refrigeration technologies are summarized in the following Fig. 2.19:

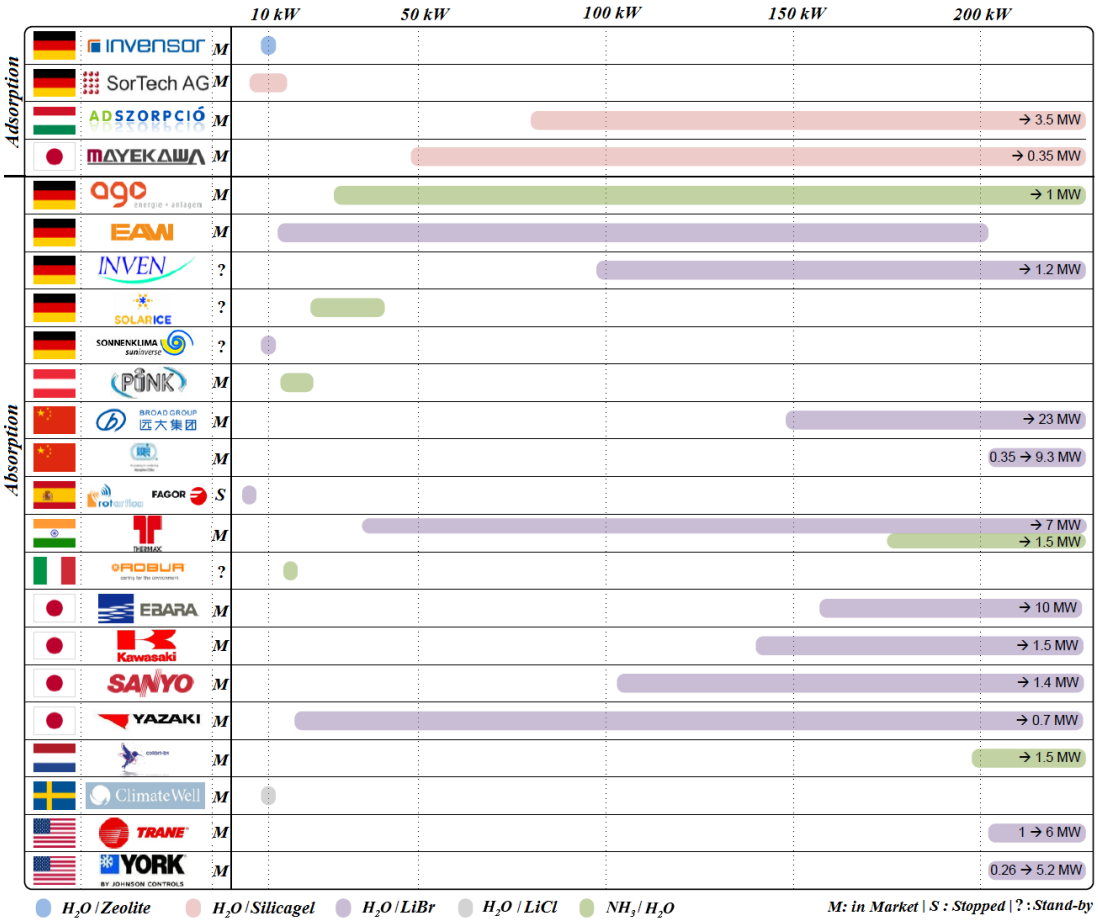

FIGURE 2.19: Global manufacturers of solar refrigeration technologies (Abdulateef et al., 2009, Kalkan, Young, and Celiktas, 2012)

It can be seen that most commercialized technologies have a power of less than 50 kW mainly belonging to the absorption technology and use LiBr/H_2O as operating fluid. The majority of these technologies are from Asian or German markets (*Etat des lieux de la climatisation solaire, INES, 2013*). Basically, the solar irradiance and cooling

requirements are approximately in phase (see Fig. 1.6), which makes solar cooling an attractive alternative to conventional (electric) cooling in modern buildings in Morocco.

The thermal pathway offers a certain advantage over the photovoltaic path, in particular from the point of view of conversion efficiency, environmental impact of the refrigerants used and from the point of view of the variety of the installation's size proposed (Wang et al., 2009). At the national level, the project of Solar Cooling Process in Morocco (SCPM) funded by *Research Institute for Solar Energy and New Energies (IRESEN)* focused on the study of the processes of solar air-conditioning under Moroccan conditions and more particularly on the refrigeration systems with a low power of 11.5 kW i.e. a solar air-conditioning production using an absorption chiller coupled to a solar evacuated tubes collector's field.

This section aims to derive a knowledgeable data base for the experimental description concerning the use and implementation of a dynamic solar air-conditioning installation in the framework of the project of Solar Cooling Process in Morocco supported by IRESEN. Indeed, this part aims to provide useful guidelines about the dynamic mode operation of solar air-conditioning systems under Moroccan conditions based on technical aspects. In this sense, the experimental solar cooling installation, which will be implemented in *Green Energy Park*, is described. Then, the most significate components and their technical characteristics are highlighted. Therefore, the installation is studied in the case of a typical type operation using a storage and having a start of the automatic machine according to the temperature and flow rate conditions at its inputs. Then, the thermal behavior of the installation is analyzed.

2.7.2 Numerical and experimental studies on solar absorption chillers

Various numerical studies have been published evaluating and predicting the performance of the solar cooling absorption chiller. Table 2.3 groups the relevant numerical studies previously published.

Numerical study	City/Country (Latitude)	Collector's area (m^2)	Storage volume (m^3)	Absorption chiller nominal size (kW)	Solar fraction (%)	Publication year
Florides et al., 2002a	Cyprus (35.1°N)	15	0.8	11	37	2002
Atmaca and Yigit, 2003	Antalya, Turkey (36.9°N)	50	3.75	10.5	55-100	2003
Joudi and Abdul-Ghafour, 2003	Baghdad, Iraq (33.3°N)	40-240	1-48	35-140	0-100	2003
Balghouthi, Chahbani, and Guizani, 2008	Tunisia (-33.9°N)	8-42	0.1-2	11	23-85	2008
Mazloumi, Naghashzadegan, and Javaherdeh, 2008	Ahwaz, Iran (31.3°N)	56.4-59.8	0.65-1.0	17.5	-	2008
Eicker and Pietruschka, 2009	-	440 to 1320	10 (Water)	106-229	50-80	2015
Mateus and Oliveira, 2009	Berlin (Germany), Lisbon (Portugal), Rome (Italy)	3-3000	0.2-90	10-1400	2-100	2009
Ortiz et al., 2010	Albuquerque, USA (35.1°N)	124 FP	35	70.3	-	2010
Cascales et al., 2011	Puerto Lumbreras, Spain (37.6°N)	-	1.5	8	-	2011
Fan, Ferreira, and Mosaffa, 2014	Netherlands (-52.1°N)	1000	8-16 (PCM)	100	88 to 100	2014
Shirazi et al., 2016a	Typical USA hotel	1023-5115	10-179 (Water)	1023-1163	20-90	2016
Shirazi et al., 2016b	Typical USA hotel	1023-5115	10-179 (Water)	1023	10 to 85	2016
Pintaldi et al., 2017	Sydney, Australia (33.9°S)	103-412	1-27 (Water, oil, PCM)	103	35-80	2017
Bouhal et al., 2018b	Ben Guerir, Morocco (32.243°S)	15-24	0.3-1	11.5	35-55	2018

TABLE 2.3: Summary of numerical solar absorption cooling system studies published in literature

Moreover, several experimental studies have been carried out for full scale solar absorption cooling systems provided by the literature community. Summary of system parameters for these studies are provided in Table 2.4.

Experimental study	City(Latitude)	Collector's area(m^2)	Water Size Tank (m^3)	Absorption chiller nominal size(kW)	Solar Fraction (%)	Generator Operating Temperature (°C)	Cooling Output (kW)	Period of Operation
Yeung et al., 1992	Hong Kong, China (22.4°N)	38.2 FPC	2.75	4.7	55	60–80	2.5	July 1987
Li and Sumathy, 2001	Hong Kong, China (22.4°N)	38 FPC	2.75	4.7	–	75–100	–	Jan. – Dec. 1999
Sumathy, Huang, and Li, 2002	Shenzhen, China (22.2 °N)	500 FPC	–	100	–	60–72	66.7–108.4	9 days Apr. 1999
Syed et al., 2005	Madrid, Spain (40.4°N)	49.9 FPC	2.0	35	–	58.7–90	5–7	20 days, Jul. Aug. 2003
Hidalgo et al., 2008	Madrid, Spain (40.4°N)	50 FPC	2.0	35	56	65–80	10–15	Jun – Oct. 2004
Izquierdo et al., 2008	Madrid, Spain (40.4°N)	–	–	4.5	–	80–107	5.5 MAX	Aug. 2005
Pongtornkulpanich et al., 2008	Phitsanulok, Thailand (16.8°N)	72 ETC	0.4	35	81	70–95		12 months, 2006. 8 h/day
Zhai et al., 2008	Shanghai, China (31.2°N)	150 ETC	2.5	2 x 8.5 (Adsorption Chillers)	71.7	60–80	15.3	Jun-Aug 2005. 8 h/day
Ali, Noeres, and Pollerberg, 2008	Oberhausen, Germany (51.5 °N)	108 ETC	6.8 (hot), 1.5 (cold)	35.2	25–70	75–85	–	Aug. 2002 - Nov. 2007
Balghouthi, Chahbani, and Guizani, 2008	Bordj-Cedria, Tunisia (36.7°N)	39 PTC	0.4	16	77	150–160	11.0	Summer 2010
Bermejo, Pino, and Rosa, 2010	Seville, Spain (37.4 °N)	352 LFR	–	174	44		135	2008–2009
Qu, Yin, and Archer, 2010	Pittsburgh, USA (40.4°N)	52 PTC	–	16	–	140–160	10.0	Summer, 2007
Agyenim, Knight, and Rhodes, 2010	Cardiff, UK (51.5°N)	12 ETC	1.0 (cold)	4.5	–	60–85	4.09	Summer/ Fall 2007
Mammoli et al., 2010	Albuquerque, USA (35.1°N)	124 FPC	34	70	–	75–88	–	Aug. 21 and 22, 2009
Praene et al., 2011	Reunion Island (21.1°S)	90 FPC	1.5	30	100	70–95	17 MAX	Jan. 2010
Darkwa, Fraser, and Chow, 2012	Ningbo, China (29.9°N)	220 ETC	16 (4 tanks)	55	–	82–96	–	7 days in Aug. 2010
Rossetti, Paci, and Alimonti, 2017	Milan, Spain (45.5°N)	50 PTC	0.75 (hot), 1.5 (cold)	23	–	165–185	22.8 MAX	Jul-Oct 2015
Zhou et al., 2017	Shanghai, China (31.2°N)	900–1100 LFR	5–8.5 (PCM)	102	13.2	85–180	93.4	N/A (Published 2017)

TABLE 2.4: Summary of experimental solar absorption cooling system installations published in literature

In the following section, the investigation of solar absorption cooling process, as one of the most promising solutions of solar thermal cooling cycles, will be conducted. Besides, the experimental description of the solar cooling installation is necessary.

2.7.3 Description of solar cooling process installation

As previously mentioned, the solar cooling process in Morocco is a research project funded by **IRESEN** to develop the first prototype of solar air-conditioning process in Morocco using an absorption chiller based on LiBr-H_2O as a driving fluid and coupled to solar evacuated tube collectors. Following pre-studies carried out by different partners of the SCPM project, design choices and materials have been made and the installation will be mounted by *Energypoles company SA, Rabat, Morocco* in the green town (*Green Energy Park*). Fig. 2.20 shows a simplified schematic of our installation with its main components composed of:

- Solar thermal collectors field of high performance with vacuum tubes manufactured by *Viessmann - Solar thermal systems*;
- RXZ solar absorption chiller with a nominal cooling power of 11.5 kW;
- Hot water storage tank of 300 l;
- Cooling tower system (aero-refrigerant);
- Set of hydraulic and safety equipment;
- Cold distribution circuit by fan coil;
- Regulation and control system.

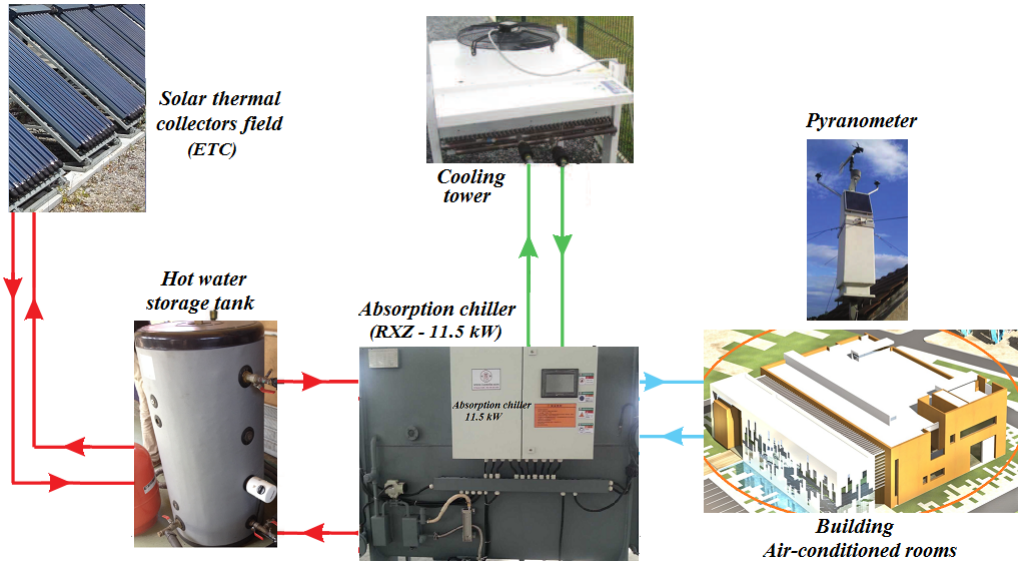

FIGURE 2.20: Synoptic of the solar cooling installation

Therefore, the project of Solar Cooling Process in Morocco (SCPM) aims to integrate the solar cooling applications in Moroccan building sector. The applied scientific research subjacent with the optimization of these cooling systems resides in the difficulty to predict the non-stationary behavior of the system induces by the transitory character of the operation of each subsystem and of the sources to which they are connected.

Fig. 2.21 represents a solar thermal integrated system for heating, air conditioning and DHW production with external exchanger, solar and auxiliary tank with indirect connection and supplement connected directly to the heating and indirectly to DHW.

The system consists of a set of solar collectors that supply energy to the solar storage tank through an external heat exchanger. The storage tank is connected by an immersed exchanger to the bottom of the auxiliary tank. The energy supplied to the auxiliary tank can also come from a hydraulic auxiliary heating through a heat exchanger situated in the upper zone of the tank. In the distribution loop, recirculation operates exclusively to obtain the set temperature of DHW.

The cold machine is directly connected to the solar storage tank, and operates when an air-conditioning need arises and if the temperature of the storage tank is higher than the set temperature. The flow through the generator is constant, so the fluid is mixed at the inlet to adjust the power of the machine. The cooling tower is controlled by a variable frequency drive. The return temperature to the tower is maintained above the set point by a valve which mixes with the inlet fluid. The flow of the cold distribution loop is always variable, with constant inlet and return temperatures.

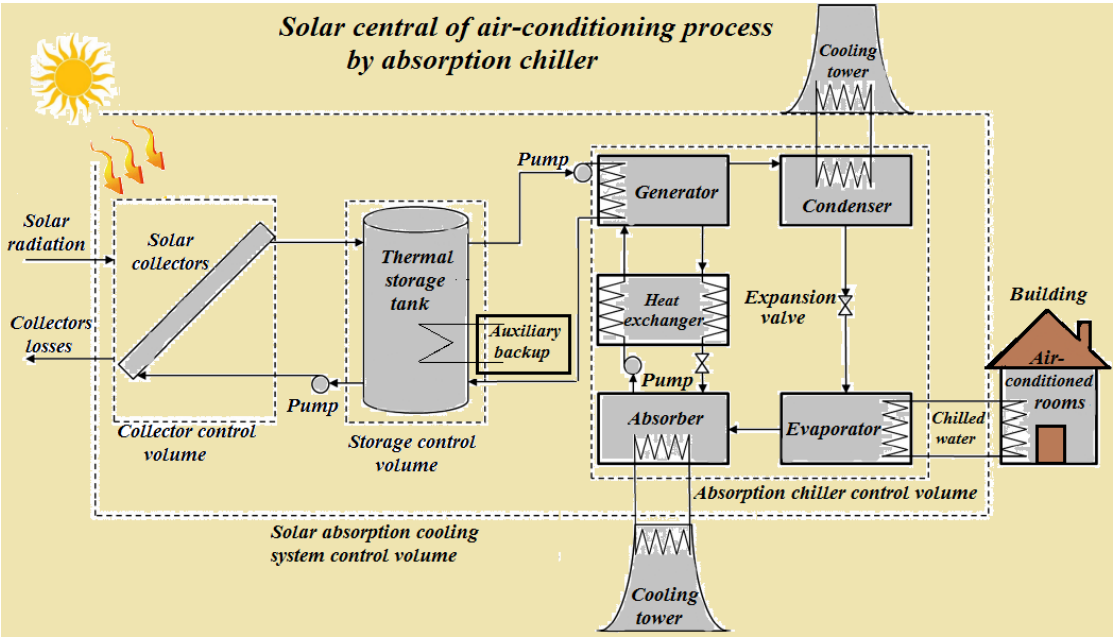

FIGURE 2.21: Schematic of integrated solar central heating and absorption cooling system for indoor space conditioning

As this installation (see Fig. 2.21) is intended to be integrated in building sector, it's appropriate to have a clear idea on the current situation of the residential building in Morocco. Accordingly, the building sector accounts for 35% of national energy consumption, with an average increase of 41% over the last 8 years, as previously mentioned. Demand for electricity peaks during the summer months due to the widespread use of vapor-controlled air-conditioning systems. In addition, these systems, because of the refrigerants used can negatively influence the environment. In this vision, this section aims to outline the integration of solar air-conditioning, heating and DHW production systems in the Moroccan residential sector according to the new climate zoning established by the *Moroccan Agency for Energy Efficiency (AMEE)*. It is interesting to draw the energy situation of our country. In fact, Morocco are facing increasingly significant electricity consumption (with an average rate of increase of 5.2%). Moreover, this electricity is largely of fossil origin. In addition, the kingdom suffer from a very high energy dependence rate of about 93% (Bouhal et al., 2018c). Although, Morocco has a huge solar energy potential with more than 3000 h/year of sunshine and an average solar irradiation of 5 kWh/m^2/day (*Moroccan Agency for Sustainable Energy (MASEN)*). Therefore, this potential can be exploited to ensure the comfort needs while reducing our energy bill and respecting the environment. In this framework, this study aims to carry out a technico-economic evaluation of solar air-conditioning, heating and DHW production systems at the national level and the potential for energy saving based on the socio-economic attributes of Morocco.

Geographical location and meteorological data

The solar cooling installation is intended to be implemented in the research platform of *Green Energy Park* in the green town Ben Guerir as shown in Fig. 2.22-(a)). The geographical coordinates of Ben Guerir city are as follows: Latitude: 32.23 ° and Longitude: -7.95 °. The building is oriented along the north axis. The reference building under investigation is a one floor building with a reference area of 300 m^2

including walls and windows. The building is oriented east west axis. The *Green Energy Park* was developed by IRESEN and the *Groupe Office Chérifien des Phosphates (OCP)* with the support of the *Ministry of Energy, Mines and Sustainable Development (MEMSD), Morocco*.

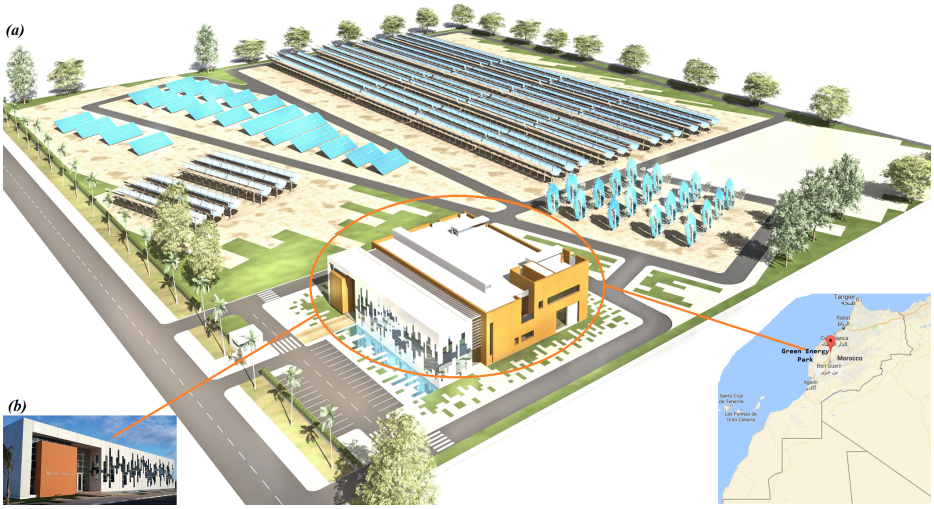

FIGURE 2.22: 3D view of the platform *Moroccan Agency for Energy Efficiency (AMEE)* (a) and building face adopted in the project of Solar Cooling Process (b), Benguerir, Morocco

The main building characteristics involved in the simulation procedure are given in Table 2.5.

Parameter description	Characteristics of the building
Walls	Cement mortar 2 cm, Hollow brick 10 cm, air cavity 10 cm, Hollow brick 10 cm, plaster 2 cm
U (W/m^2K)	1.25
The type of window	Clear, single
Floors number	1
Windows (%)	South 19, north 20, west 0 and east 0
Infiltration ($1/h$)	0.8
Specific gains (W/m^2)	15
Occupation rate (m^{-2})	0.06
Specific lighting (W/m^2)	10

TABLE 2.5: Parameters used for the reference building

Solar thermal collector's field

For the operation of absorption machine, the use of solar collectors allowing working at temperatures between 80 °C and 95 °C with good performance is necessary. The evacuated tube collector technology enables the best use of the solar resource, these levels of temperature and low sunlight, in comparison with flat plate collectors. We therefore selected the vacuum tube technology and opted for the Viessmann brand. In order to supply the hot storage tank and/or the generator of the absorption chiller, a solar thermal vacuum collector field of 22 m^2 intended to be installed on the ground in solar zone of *Green Energy Park*, as can be seen in Fig. 2.23.

FIGURE 2.23: Solar thermal collector's field using Evacuated Tubes Collectors (ETC) technology

The technical characteristics of the ETC technology used in our solar installation are listed in Table 2.6.

Parameter description	Value
Optical efficiency η_0	0.816
Loss coefficient k_1	2.735 W/m^2K
Loss coefficient k_2	0.0074 W/m^2K
Unitary area	1.51 m^2
Fan minimum capacity	30 %

TABLE 2.6: Technical parameters considered for solar thermal collectors (*Viessmann - Solar thermal systems*)

The solar collector's field will be mounted on variable tilt supports made internally. To have the lowest angle of incidence possible, in the case of an operation in summer (solar cooling), the supports will set to a minimum, i.e. 30 ° with respect to the horizontal. They will be oriented full south. All collectors are connected in series and can be covered with tarpaulins at any time, so as to interrupt any absorption of solar radiation and protect the collectors when the installation is stopped. Fig. 2.23 shows a schematic view of the collectors field allowing better understanding of its design. The water supplying this water is drawn from the bottom of a storage tank. Then, this water passes through a pipe to be transported to the circuit go from the collector's field, in which the coolant receives sunshine captured.

Hot water storage tank

A hot storage tank was installed between the solar collector's field and the generator of the absorption machine as shown in Fig. 2.24. This tank serves as a buffer tank to allow continuity of operation during cloudy periods for example. The storage volume must be able to allow the machine to maintain its operating condition for about 10 minutes. The regime will be considered maintained for a maximum decrease of 5 °C of the generator input temperature. The hot storage tank must therefore be capable of delivering a power of 9 kW (nominal desorption power) for 10 minutes (i.e. stored energy of 5000 kJ) with a temperature drop of 5 °C maximum. A 300 l of the storage tank would be enough, but the storage volumes available from different suppliers closest to each other are 200 and 300 liters. Finally, we chose to use a 300 l tank in order to obtain a autonomy of just over 12 minutes. It can be seen in Fig. 2.24 that the water feeding the generator is drawn from the top of the tank and reinjected

at the tank's bottom after passing through the machine. The water sent to collectors is drawn from the bottom of the tank (the coldest point) and the return of the collectors can be injected at different levels into the tank. This option has been made in order to test the influence of this position on the tank load its thermal behavior when the storage function is not used (bypass hot tank).

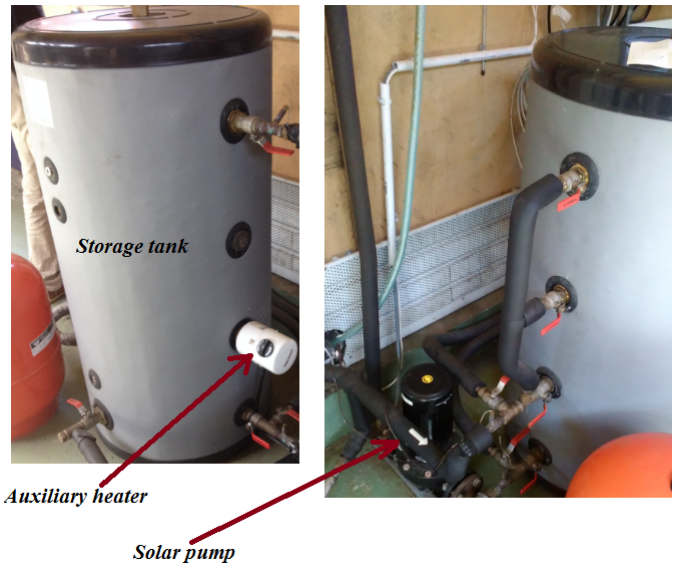

FIGURE 2.24: Hot water storage tank

Solar absorption chiller based LiBr-H_2O

The RXZ solar absorption machine is the main element of the solar cooling installation pilot shown in Fig. 2.25. It has been sized to provide, in its nominal conditions of temperature and flow, a power refrigeration of 11.5 kW with a COP of 0.7 (*Shandong Lucy New Energy Technology Co., Ltd.*). Fig. 2.25 shows the particularity of this machine consisting of a rotating system containing all the components that constitute it. The reason for this choice is the design hermetic obtained thanks to the drum which eliminates the risks of entry of air. Since the refrigerant is water, the whole is in depression. Low pressure (P_l) is included between 20 and 45 mbar, while the high pressure (P_h) is between 60 and 105 mbar.

FIGURE 2.25: Solar absorption chiller RXZ-11.5 kW implemented in Ben Guerir (*Green Energy Park*)

The technical parameters of the solar air-conditioning absorption chiller implemented in *Green Energy Park* are given in Table 2.7.

Model		RXZ–11.5	
Cooling capacity		11.5 kW	
	Hot water	Chilled water	Cooling water
Flow rate	2.8 m^3/h	2.0 m^3/h	4.8 m^3/h
Inlet/Outlet Temp.	90°C/85°C	15°C/10°C	30°C/35°C
Connection diameter	DN40	DN32	DN40
Pressure Loss	50 kPa	40 kPa	50 kPa
Power consumption		0.3 kW	
Cooling capacity adjusting range		20 - 100%	
Dimension	Length	1010 mm	
	Width	785 mm	
	Height	1622 mm	
Shipping weight		700 kg	

TABLE 2.7: Technical parameters of solar air-conditioning absorption chiller (*Shandong Lucy New Energy Technology Co., Ltd.*)

It's necessary to note that the fouling factor (which is a measure of the accumulation of unwanted material deposits on solid surfaces) and the standard gauge pressure limit for chilled water and cooling water are 0.086 m^2°C$/kW$ and $\leq 0.8MPa$, respectively.

The main technical characteristics of the absorption chiller are shown in Table 2.8 as it was given by the manufacturer *Shandong Lucy New Energy Technology Co., Ltd.*

Parameter description	Value
Thermal chiller	
Nominal cooling power	11.5 kW
Nominal COP	0.7
Electric power of auxiliaries	216 W
Electric chiller	
Nominal cooling power	7.5 kW
Nominal COP	3
Set point temperature	7 °C
Cooling tower	
Air flow rate	1900 m^3/h
Mass transfer constant	2.3
Mass transfer exponent	-0.72
Fan electric consumption	0.93 kW
Fan minimum capacity	30 %

TABLE 2.8: Main system input parameters (*Shandong Lucy New Energy Technology Co., Ltd.*)

Cooling tower (Dry cooler)

The cooling tower is a water/air heat exchanger (coolant outdoor air) located behind the building so that it is the most possible in the shade during the day and close to the machine so as to reduce the pressure losses of the circuit and the size of the circulation pump required. This component of the installation evacuates the heat

released by absorption and condensation in the outside air. The air is sucked from below and rejected from above with a flow of 5800 m^3/h (see Fig. 2.26).

FIGURE 2.26: Cooling tower used in the solar cooling installation

Fan coil and climatic cells

Fig. 2.27 shows the fan coil used to to refresh the typical rooms located in *Green Energy Park* where the refrigeration production is distributed in the building of Fig. 2.22. The fan coils operate with a flow rate of 1900 m^3/h, which allows them to achieve a cooling capacity of 5.6 kW per unit with a water inlet/outlet 10/15 °C and air at 25°C and 50% humidity. The climatic cells located in *Green Energy Park* (see Fig. 2.22) can be subjected to cooling load variations in order to analyze the behavior of the absorption machine for different temperature distribution levels.

FIGURE 2.27: Fan coil unit used in the solar cooling installation

Instrumentation and measurements

In order to study and analyze the behavior of the absorption chiller, the solar cooling installation will be instrumented. The measured quantities are the flows of circulating heat transfer fluids in each of the circuits and the input and output temperatures of components (absorption machine, solar collectors, hot storage tank, refrigerant, fan coils and building). The different measures will allow to control the adequate operation of the various components of the installation in order to perform the assessments of each of them and calculate different performance indicators required for the analysis of the system. Regarding the temperatures, the installation will be instrumented with thermocouples type T with watertight passages. Fig. 2.28 shows the instrumentation chain on a layout diagram of installation. Temperature measurements within the collector's field are performed by batteries.

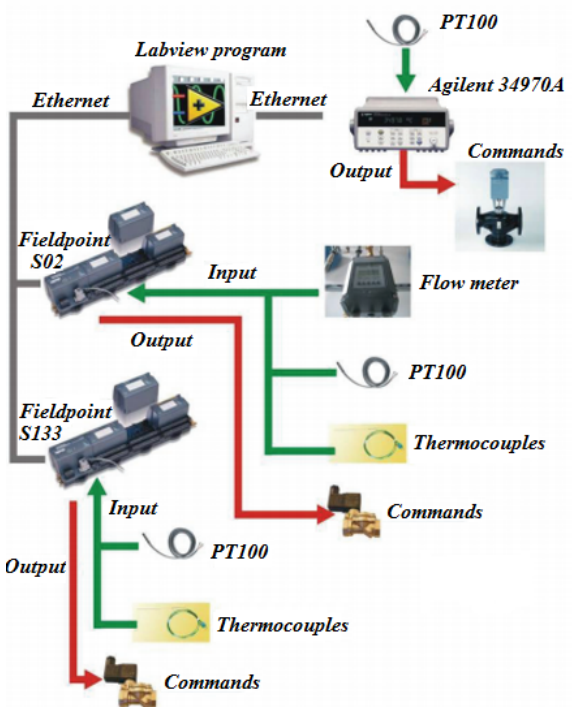

FIGURE 2.28: Acquisition central and regulation process of the solar cooling installation

Following the completion of several quotes from suppliers, *Energypoles company SA, Rabat, Morocco* may serves as instrumentation has been requested to supply Mac Naught oval wheel flow meters a precise measure adapted to our needs. 5 flowmeters were installed to measure the 5 following volumetric flow rates and balance the chilled water network including two fan coils mounted in parallel:

- Solar collector's circuit;
- Generator circuit;
- Cooling circuit (absorber/condenser and refrigerant);
- Fan coil circuit.

The measures will acquired using a computer and an acquisition central and all signals are recorded every 10 seconds with HP Bench Link Data Logger software as shown in Fig. 2.28.

Commissioning and problems encountered

At the beginning of this research project, we encountered a real problem in the purchase of the absorption chiller plant powered by solar hot water. This problem due essentially to the various developments and tests currently undergoing on this installation in the world. Recently, we have found a supplier who delivered the installation with the conditions and characteristics indicated in the specifications of the project of **Solar Cooling Process in Morocco (SCPM)**. The solar cooling process will be installed by *Energypoles company SA, Rabat, Morocco* and the supplier of the machine from China (*Shandong Lucy New Energy Technology Co., Ltd.*). Indeed, the first commissioning of the solar cooling system was carried out by our partner at the end

of September 2015 (following various supplies problems). To overcome these problems, we have made several journeys to *IUT/GTE des Pays de l'Adour, Pau, France*, because in this institute, a prototype of solar cooling system by absorption chiller has been already implemented with a cooling capacity of 4.5 kW. This installation required the control of the tightness of the circuits, the verification of the different flow rates, settings such as the adjustment of the balancing valves on the different hydraulic loops and control of the acquisition system. During the first commissioning, it will turn out that the chilled water circuit will generated too much losses and therefore, the pump will not able to provide the minimum flow required to start the machine. Similarly, for the solar circuit, in the case without storage tank the pump was undersized. Some modifications have been made to the installation in order to meet the nominal operating conditions of the machine. In june 30, 2016 a new problem has appeared because the machine could not get down to the required temperature. At best 27 °C were reached at the evaporator outlet, i.e. barely 2-3 °C below the outside temperature. After analyzing the machine, it was observed that the sealing valve of the machine was open and that this due to the vacuum inside the machine, in order to remove any inert gases introduced therein. Before the vacuum draw, the pressure in the drum was 19.5 mbar for 20 °C outside. The void could be pulled to a pressure of 14.5 mbar. After this maintenance operation carried out on the machine, the installation doesn't work properly again because of another problem related to the electricity. The evaporator outlet temperature is down below 9 °C without fan coil being turned on (virtually without charge therefore). Fig. 2.29 shows some pictures concerning the maintenance and commissioning tests carried out on the prototype of solar cooling installation implemented in *IUT/GTE des Pays de l'Adour, Pau, France*.

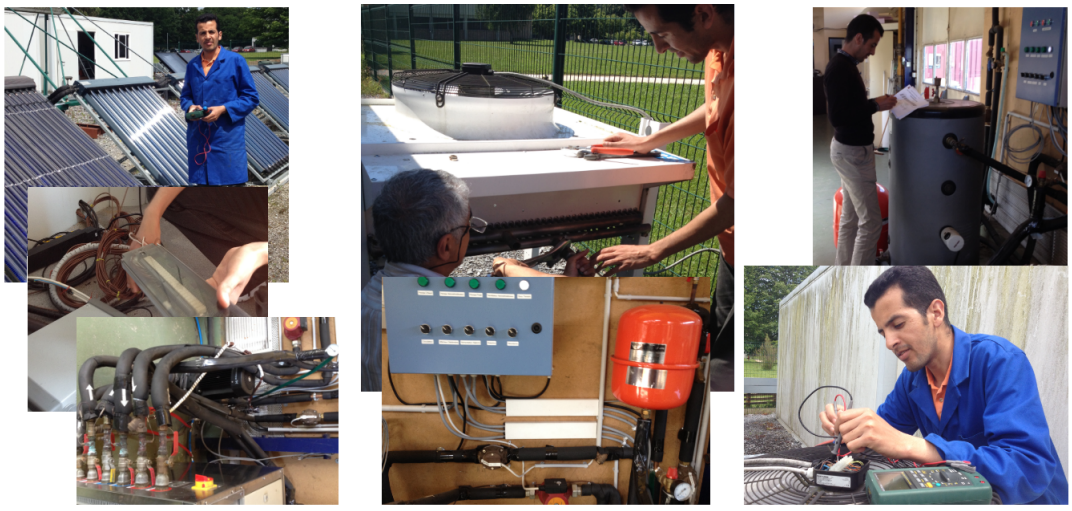

FIGURE 2.29: Pictures of maintenance and commissioning tests carried out on solar cooling installation on the period of 2016/2017 implemented in *IUT/GTE des Pays de l'Adour, Pau, France*

Due to several electrical problems (electric motor is down) and other technical issuses, the absorption machine could not work. Therefore, we were limited to carry out numerical simulations to evaluate the potential of solar air-conditioning in Morocco.

2.8 Conclusion

In this chapter (Chapter 2), we presented the state of the market for solar thermal systems worldwide and particularly in Morocco. In general, we have seen a significant evolution of the solar cooling systems in recent years. Solar air-conditioning still despite the fact that there are commercially available solar powered cooling systems, no application has so far been reported in Morocco. This is attributed to the high capital cost which yields very long payback periods and also to the lack of performance data of such systems operating under Moroccan climatic conditions. While the market is booming in some countries in the MENA region, for Morocco, efforts are still needed to facilitate the emergence and widespread diffusion of these technologies in the Kingdom. These technological, organizational and institutional efforts require close cooperation between all the players in the field. Particular emphasis was given on the experimental aspect of the absorption solar cooling installation adopted in the project of **Solar Cooling Process in Morocco (SCPM)**. It is well-known that experimental measurements are able to prove the validity of numerical simulations. Unfortunately, we did not have the chance to complete the implementation of the prototype of the installation due to enormous problems encountered previously described. However, Chapter 3 will focus on numerical modeling in order to test the different parameters influencing the thermal behaviour of LiBr-H_2O solar absorption air-conditioning system using energy and economic indicators based on technical and real operating characteristics of the absorption chiller prototype under Moroccan conditions.

Chapter 3

Design of solar air-conditioning systems: Effects of collector technology, cooling profiles and building category

3.1 Introduction

This chapter investigates the potential of LiBr-H_2O solar absorption air-conditioning system for Moroccan building applications. Hence, the combined effects of cooling demand profiles, building categories and collector's technology (Flat Plate FPC and Evacuated Tube ETC) on the performance of solar cooling systems operating under various climatic conditions were assessed in details. The *Transol* software, based on *Transient System Simulation Tool (TRNSYS)*, was used as a basis of dynamic simulations. Different cooling profiles were used (Morning, Day and Morning) and various building categories were evaluated: residential house, building office and hotel and different Moroccan zones and climates were considered: Fez (Zone 3), Marrakech (Zone 5) and Zagora (Zone 6) known as the hottest regions in Morocco. The results of both energy and economic assessment were presented for all configurations. The different Moroccan energy costs for auxiliary backups (electricity and gas) were taken into account and an optimization of storage tank volume and solar collector's size and other system indicators were also analyzed.

3.2 Background

The building sector represents a significant portion of electrical energy consumption and a major contributor to environmental problems (Pérez-Lombard, Ortiz, and Pout, 2008). Due to the high cost of fossil fuels and important CO_2 emissions caused by the extensive use of cooling systems for both industrial and residential buildings, the use of solar energy to drive cooling cycles becomes an attractive option since the cooling load is roughly in phase with solar energy availability (Henning, 2007). Solar air-conditioning is an attractive option since it has the advantage of removing the majority of harmful effects of conventional cooling machines and that the peaks of demands in refrigeration coincide most of the time with the availability of the solar insolation (Kim and Ferreira, 2008).

In this respect, research community is moving in two main directions. The first focuses on the building itself, aiming to minimize heat gains through the building envelope and to simultaneously maximize the use of natural heat sinks (Santamouris et al., 2007). While the second is dealing with the advancement of technologies

that can offer reductions in energy costs, energy consumption and peak electrical requirement and without decreasing the required level of comfort conditions. While this study is concerned with the solar cooling production, it is vital to consider the impact of solar hot water generation from a system perspective. Several numerical experimental investigations have shown the performance of fully integrated solar air-conditioning systems, and used the overall system performance as a metric of assessment (Sarbu and Sebarchievici, 2013).

Relevant studies have been identified dealing with the solar air-conditioning technologies used in building sector. Montagnino, 2017 presented the design, application and performance of solar cooling technologies and the existing projects. They have identified trends of innovation for both small and settlement scale applications, supporting the perspective of a more efficient exploitation of the solar cooling potential. Hirmiz, Lightstone, and Cotton, 2018 evaluated the performance enhancement of solar absorption cooling systems using thermal energy storage with phase change materials (PCMs). They have given an engineering approach for predicting the expected benefit from both PCMs and water based thermal storage for applications with limited temperature ranges. In addition, Xu and Wang, 2017 performed simulation of solar cooling system based on variable effect LiBr-water absorption chiller. They analyzed the effects of solar collector area, storage tank volume and cut-off driving temperature on the system performance and they obtained an average chiller COP of 0.88 and a solar COP of 0.35.

Solar thermal collectors used to produce hot water play a vital role since they feed the solar absorption machine with the required temperatures and water mass flow rates. In this sense, Tarsitano, Ciancio, and Coppi, 2017 examined the air-conditioning in residential buildings through absorption systems powered by solar collectors. They evaluated a small residential building and assessed the energy savings, reduction of CO_2 and the return on investment compared to a traditional solution. Moreover, Wang et al., 2016 studied various solar driven air conditioning and refrigeration systems corresponding to various heating source temperatures. They concluded that all the studied systems have improvements in comparison with existing systems and may offer good alternatives for high efficient solar cooling.

In various Maghreb countries, the technical feasibility of these machines has been evaluated according to literature reports. Balghouthi, Chahbani, and Guizani, 2008 studied the feasibility of solar absorption air-conditioning in Tunisia. They optimized a system for a typical building of 150 m^2 composed of a water lithium bromide absorption chiller of a capacity of 11 kW, a 30m^2 flat plate solar collector area and a 0.8 m^3 hot water storage tank. At Moroccan level, Allouhi et al., 2015a established annual simulations in six Moroccan climatic zones and an economic and environmental assessment of solar air-conditioning systems. The results show that these systems must be an attractive alternative to increase energy savings and mitigate CO_2 emissions especially in hot climates. Accordingly, Agrouaz et al., 2017 performed an energy and parametric analysis of solar absorption cooling systems in various Moroccan climates. They found that the coefficient of performance values in almost Moroccan regions have a significant variation from 0.12 to 0.33 all over the year due to variation of solar energy potential of each zone. Recently, Bouhal et al., 2018b conducted a technical assessment, economic viability and investment risk analysis of solar DHW production, heating and cooling systems in residential buildings in Morocco. The results show that solar contribution has increased from 605 kWh to 705 kWh in winter and summer periods, respectively, while the auxiliary consumption has achieved 1450 kWh, 1875 kWh and 2300 kWh for Agadir, Tangier and Ben Guerir, respectively.

One of the most affecting parameters on the viability of solar cooling systems is the daily cooling load profile. The demand cooling profile is impacted by various parameters such as climatic conditions, occupant behavior, desired hot water set temperatures and mass flow Fong et al., 2010. Determining the daily demand profile is considered as a key element on the solar air-conditioning designing. Consequently, the dynamic simulations presume repeating daily periodic working like that the system returns to its initial state at the end of each day therefore removing the impact of initial conditions while allowing the evaluation to be conducted for a specified 24 h period.

In general, the majority of research works uses simplified cooling load profiles in the simulations and considered relatively constant cooling rates during the night and day that often not accurately reflect the real demand and the availability of solar sunshine. Parametric studies concerning the effect of the cooling load profile on the fractional savings of solar cooling systems are less published despite their major importance.

This chapter investigates the combined effects of cooling load profiles, building categories and collector's technology (Flat Plate FPC and Evacuated Tube ETC) on the performance of solar cooling systems operating under various climatic conditions. The Transol software tool was used as a basis of simulations. Various building categories were evaluated: residential (residential house), building office and hotel and different Moroccan zones and climates were considered: Fez (Zone 3), Marrakech (Zone 5) and Zagora (Zone 6) known as the hottest regions in Morocco. The study also evidences the influence of the cooling load demand on the annual fractional savings of solar air-conditioning system using energy and economic indicators.

3.3 Simulation methodology

3.3.1 General considerations

Nowadays, the building sector represents one quarter of overall greenhouse gas emissions (Bouhal et al., 2017a). Progressively, the involvement of renewable energies becomes necessary in order to reduce greenhouse gas emissions and achieve the goals of energy saving set by the several authorities.

In the last few years, rising summer temperatures and needs for increased comfort have caused a huge use of conventional cooling in Morocco. This progress of cooling is responsible for an important peaks of electricity consumption especially in summer. Linked to the possible defection of refrigerants in conventional cooling technologies, these peaks in electricity production accentuate the brutal cycle of climate change and increase the greenhouse gas emissions (Bouhal et al., 2017b). In addition, the use of cooling technologies in the summer season leads to a high energy consumption which generates inevitable instabilities between the electricity production and the energy demand.

Therefore, the growth of renewable energies is an important preference in the Moroccan energy strategy. Indeed, it is the efficient way to optimize the energy use while decreasing our energy invoices. Thus, the objective of this strategy is to accomplish 15% of energy savings by 2020 in terms of energy efficiency (Bouhal et al., 2018c). Accordingly, the energy consumption in Moroccan building sector accounts for 35% of the total energy used which has been increased in recent years with the development of the national economy.

The *Office National d'Electricité et de l'Eau Potable (ONEE)* is usually coerced to import electricity from Spain expensively. Hence, the exploitation of solar energy for cooling in building sector is an attractive option. Solar energy potential could be exploited according to two categories of energy conversion either photovoltaic option or thermal process. Several cycles can be identified such as thermoelectric (Peltier effect), sorption, thermomechanical and conventional systems. These cycles utilize various types of technologies. The adsorption and absorption systems are among these cycles which occupy an important place in the market (Allouhi et al., 2015b).

The solar thermal option is advantageous compared to the photovoltaic solution especially in terms of the variety of the size of the installations proposed, conversion efficiency and environmental effect of the refrigerants used (Wang et al., 2009).

In this context, this part aims to carry out an energy and economic evaluation of solar air-conditioning systems at the national level. The potential for energy savings and the reduction of back-up energy are estimated on the basis of socio-economic attributes. The design methodology followed is presented in Fig. 3.1.

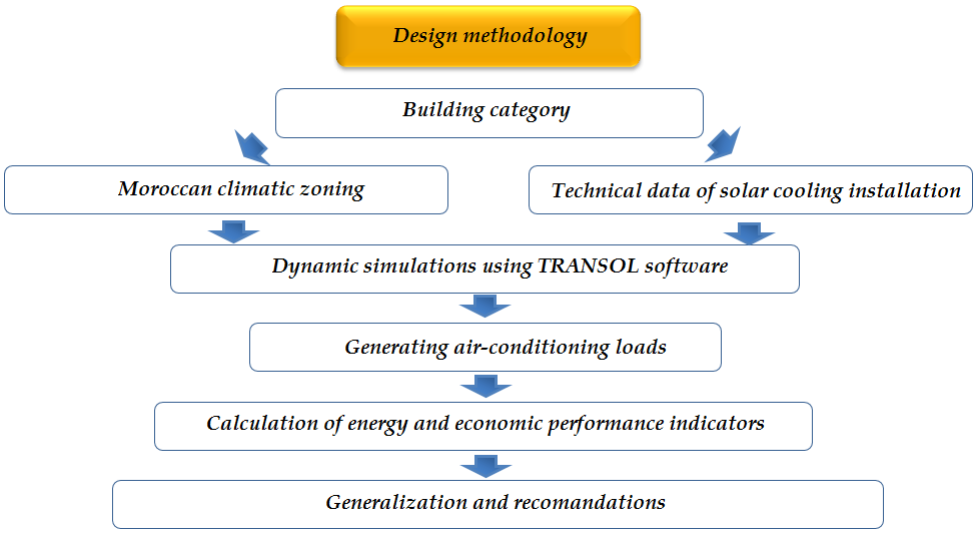

FIGURE 3.1: Design methodology followed for solar cooling system

The solar cooling system configuration consists of a solar air-conditioning absorption chiller with a distribution circuit of cold/hot water to the load using solar collectors and a hot water storage tank. When there is no insolation, an electric or a gas boiler backups were used to provide hot water which directly used to drive the absorption water chiller. The hot or cold water is circulated through fan-coils placed in the building's air-conditioned rooms as presented in Fig. 2.21. The thermal solar collectors provide solar energy contribution during the cooling period. An auxiliary electrical backup and a gas boiler were employed to deliver additional energy to the system for a larger buildings such as building offices or hotels. The auxiliary system operates if the tank temperature is below the set temperature or if there is a need for water heating when the tank temperature is not sufficient for the generator.

At the national level, the project of Solar Cooling Process in Morocco (SCPM) funded by *Research Institute for Solar Energy and New Energies (IRESEN)* focuses on the integration of solar cooling technologies in Moroccan building sector using refrigeration systems with low power in the range of $5 - 20$ kW i.e. a solar air-conditioning production using an absorption chiller coupled to evacuated tubes solar collector's field. Hence, the objective of this project is to implement the first solar

air-conditioning prototype in Morocco with a cooling capacity of 11.5 kW.

The solar air-conditioning installation implemented in the framework of Solar Cooling Process in Morocco (SCPM) is presented in Fig. 3.2.

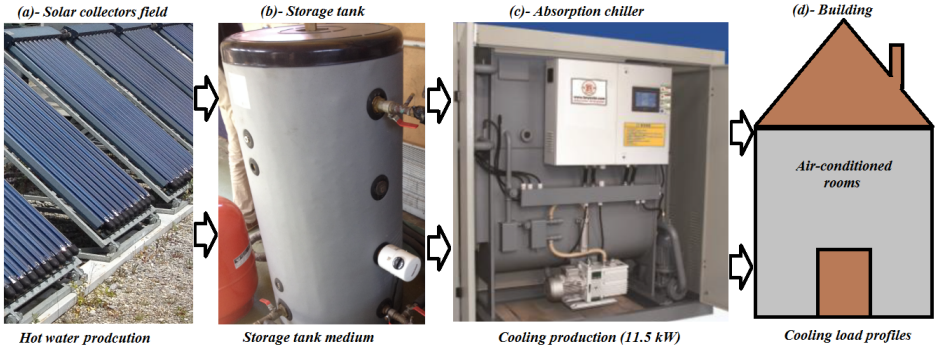

FIGURE 3.2: Solar installation: (a)- Solar thermal collector's field, (b)- Storage tank and (c)- Absorption chiller (RXZ-11.5 kW) and (d)- Building implemented in *Green Energy Park*; *IUT/GTE des Pays de l'Adour, Pau, France*

Transol software was used to carry out the dynamic simulations which uses the *Transient System Simulation Tool (TRNSYS)* to size the solar thermal systems connected to the building. Besides using Transol existing system components, technical parameters for absorption chiller using real COP values taken from the manufacturer data base (*Shandong Lucy New Energy Technology Co., Ltd.*) were introduced allowing the model to run for a whole year operating in cooling mode. For building simulation, the Transol model considers solar gains through the glazing area using a mono-zone building because it is less complex and the main objective of the simulation was to evaluate the cooling system and not the building itself. Transol allows the simulation of a Flat Plate Collector (FPC) as well as Evacuated Tubes Collector (ETC). A stratified tank with uniform heat losses is considered for the thermal storage tank. The energy interaction of the solar air-conditioning absorption chiller with linked components and their typical boundary temperatures with the absorption machine (RXZ-11.5 kW) implemented in *Green Energy Park* (Ben Guerir, Morocco) is presented in Fig. 2.21. The technical parameters of the solar air-conditioning absorption chiller implemented in *Green Energy Park* are given in Table 2.7.

For this absorption machine, the fouling factor is 0.086 $m^2°C/kW$ and the standard gauge pressure limit for chilled/cooling water is less than $0.8MPa$.

In the present work, the solar collector types investigated are Evacuated Tube Collectors (ETC) without concentration and Flat Plate Collectors (FPC) with selective coating. Table 3.1 gives the parameters used for both collector technologies in the simulations.

Parameters	Value		Unit
	FPC	ETC	
Collector absorber area	2.67	2.67	$[m^2]$
Optical efficiency η_0	0.735	0.821	[-]
Loss coefficient k_1	4.6	2.82	$[W/m^2.K]$
Loss coefficient k_2	0.0164	0.0047	$[W/m^2.K^2]$

TABLE 3.1: Technical characteristics of solar thermal collector's (*Viessmann - Solar thermal systems*)

The objective of this chapter is to carry out a technico-economic optimization based on dynamic simulations to optimize the energetic ratio "performance/cost" of a typical solar absorption chiller (see Fig. 3.2) of a power cooling of 11.5 kW implemented as a demonstration prototype for solar air-conditioning production in *Green Energy Park*, Ben Guerir, Morocco. Accordingly, the impacts of cooling demand profiles, collector's technology climatic data and the component's technical characteristics on the performance of the solar cooling system under Moroccan conditions were studied. The dynamic simulations were performed using Transol software which used to size thermal solar systems using the *Transient System Simulation Tool (TRNSYS)*.

3.3.2 Description of building categories

The Kingdom of Morocco is facing increasingly high electricity consumption which is largely of fossil origin with an average rate of increase of 5.3% (*Office National d'Electricité et de l'Eau Potable (ONEE)*). The country suffers from a very high energy dependence rate of about 93% (Bouhal et al., 2018c). However, Morocco has a huge solar energy potential represented by an average solar insolation of 5 kWh/m^2/day and more than 3000 h/year of sunshine. Hence, this potential can be exploited to ensure the air-conditioning comfort requirements by reducing the energy invoices and saving the environment. Accordingly, the integration of solar air-conditioning systems (absorption technology) in the Moroccan residential sector is an interesting alternative to reduce the energy consumption taking into account the new climates zoning and the thermal regulation established by *Moroccan Agency for Energy Efficiency (AMEE)*.

In this work, three categories of building were investigated in the simulations as they have different thermal output ranges: a residential house representing a lower power range, an office building and a hotel accounting for medium power range as shown in Fig. 3.3. The air-conditioning system was defined based on the climatic data of the considered cities namely; Marrakech (Z5), Fez (Z3) and Zagora (Z6).

(a)- Residential house *(b)- Office building* *(c)- Hotel*

FIGURE 3.3: The categories of building considered in the present work located in Morocco: (a)- Residential house, (b)- Office building and (c)- Hotel

The main characteristics of these building categories are listed below:

- **The residential house** has a global area of 200 m^2 with a floor's height of 2.3 m. The glazing area for the South and North façades accounts for 8% of façade area. In West and East walls don't contain any glazing.
- **The office building** is designed by one floor with a global area of 400 m^2 with a height of 2.54 m which has an East-West main axis. The glazing area accounts

for 35% of the South and North façades and 8% of the East façade and West façade is considered without glazing.

- The **hotel** is designed of two floors and each one with an area of 360 m^2 with a height 2.6 m and where the main building axis is North–South. The glazed area for the South and North façades accounts for 3% for the East and West façades and 20% of façade surface while the air-conditioned rooms represent 55% of the total area. Only one floor is considered for the thermal load for the air-conditioning system.

For all building categories, a common construction was adopted taking into account the thermal regulations in Morocco (*Moroccan Agency for Energy Efficiency (AMEE)*). Accordingly, the external walls are built with a double pane of brick where a thermal insulation is integrated in the middle while the floor and ceiling have also 3 cm of insulation and double glazing is used in all building types.

Furthermore, an air change per hour (acph) of 0.6 acph was considered for the residential house while 1.5 acph was used for both office building and hotel. Moreover, an inside air temperatures between 18 and 24 °C with a chilling water at 10 °C were adopted for all buildings. In this context, this study aims to carry out a technico-economic evaluation of solar air-conditioning process and the potential for energy preservation based on the socio-economic attributes under Moroccan conditions.

3.3.3 Weather data and cooling loads for simulations

Six climate regions were defined by *Moroccan Agency for Energy Efficiency (AMEE)* where each zone is referenced by a representative city in order to implement a new thermal building regulations for construction in Morocco. For an efficient investigation, three reference cities are considered in the present study which are Fez (Zone 3), Marrakech (Z5) and Zagora (Z6) because they have a very hot weather during summer which mean that the cooling requirements are important. The main climatic data are listed as follows:

- Fez (34°0.03′ N 4°0.58′ W) representing Zone 3, is located in the center of Morocco. Fez is an imperial city and the second most populous city in Morocco (1 782 256 inhabitants in 2015). It enjoys a Mediterranean climate, but has a touch of continentally. In summer, the average maximum temperatures can reach 38 °C.

- Marrakech (31°0.37′ N 8°0.00′ W) representing Zone 5, is located to the north of the foothills of the snowcapped Atlas Mountains. It is a touristic city and enjoys a semi-arid climate with mild damp winters and hot dry summers. Its population in 2013 was 914 000 inhabitants.

- Zagora (31°0.55′ N 4°0.25′ W) representing Zone 6, is a touristic city also and located in the south east of Morocco in the Daraa Valley and north of Tafilalet valley. A hot desert climate predominates in Zagora and the average maximum temperatures can reach 45 °C in summer.

The main meteorological data concerning the average values of the incident solar irradiation on the solar collector's field, the ambient temperature of the climate zones of Fez (Z3), Marrakech (Z5) and Zagora (Z6) are presented in Fig. 2.16 as they generated by *Meteonorm*. Concerning the climatic conditions for the investigated

locations, the highest temperature during summer period occurs in Zagora (Z6) followed by Marrakech (Z5) and Fez (Z3). Fez has the lowest temperatures throughout the year (see Fig. 2.16). In terms of solar radiation, Zagora receives the most solar energy potential compared to Marrakech and Fez cities.

The valuable solar potential of each region will be exploited in order to satisfy the cooling requirements of the studied buildings. The estimated cooling needs taking into account several factors such as external and internal gains, occupancy and climatic data are depicted in Fig. 3.4.

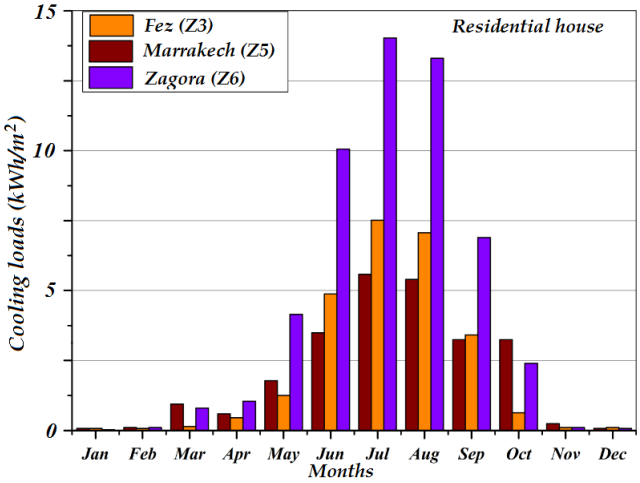

FIGURE 3.4: Monthly cooling requirements in the studied Moroccan zones

It can be seen from Fig. 3.4, the building instantaneous air-conditioning loads globally conformable to the season of maximum solar radiation especially in summer period for the hotter climates as Marrakech (Z5) and Zagora (Z6). The same comparison would put to the same conclusion for the residential house and the office building because of the various occupation styles where the instantaneous loads may be higher in evening and morning hours. Indeed, the cooling demand profile depends on user's behavior and the location where the simulation is performed. In fact, we have estimated the cooling consumption profiles for a typical residence (residential house). Our estimation is based on a simple user load profile that concentrates air-conditioning consumption during three periods per day (Morning, Evening and Day) as shown in Fig. 3.5. For this profile, the overall daily requirement was normalized to a power cooling of 10kW/day (for Morning and Evening profiles) and 5kW/day for Day profile. As the cooling loads are required in the simulations, Figs. 3.5 ((b), (c) and (d)) represent the daily cooling demand profiles. The advantage of thermal storage is affected by the consumption profiles due to the point of mismatch between the cooling demand and solar insolation. The simulation investigates the solar incident radiation profile for Marrakech city referring to Zone 5 with the other zones. Indeed, three different cooling demand profiles were considered to represent various degrees of mismatch to the solar radiation profile as shown in Figs. 3.5. For all configurations, the total available solar insolation is totally matched to provide 100% of solar fraction with 22 m^2 of collector's area delivered and sufficient storage volume existing. The effect of changing the volume of storage tank and the collector area and its technology was also examined to evaluate the advantage of thermal storage for conditions in which insufficient or excess in

solar radiation was available. Demand cooling profiles are a function of the temperature set points, the building and the cooling system. Solar air-conditioning systems reported in the literature used relatively constant cooling rates during the night and day (Syed et al., 2005) but several profiles are possible depending on the building function and the user needs. According to the solar radiation profile, the cooling demands are selected to be in phase simulating daytime cooling (Morning profile), On of phase cooling profile representing nighttime air-conditioning (Evening cooling) and flat demand profile simulating constant cooling (Day profile). All part models were performed in Transol and the full system models were integrated in time for an entire year.

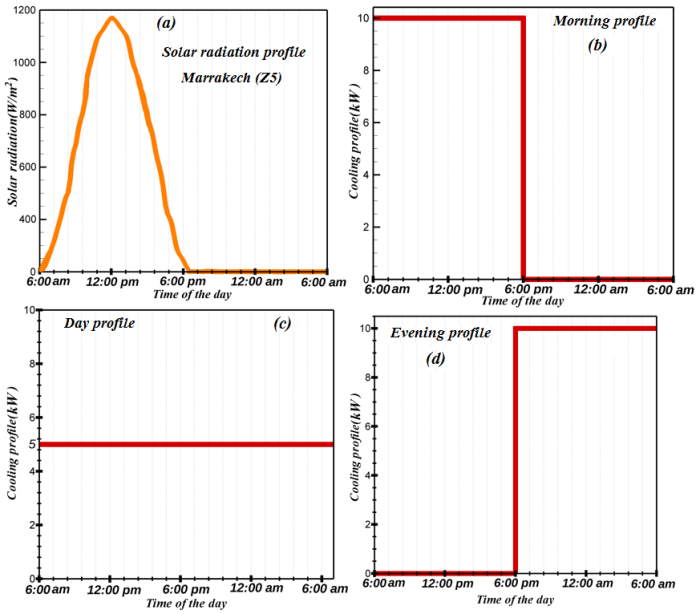

FIGURE 3.5: Solar radiation (a) and cooling loads profiles considered in the simulations: (b): Morning, (c)- Evening and (d)- Day

3.4 Mathematical formulation of solar air-conditioning system

3.4.1 Solar thermal collector's field

The thermal collector efficiency is usually used to assess the energy performance of the collector as described in Eq. 3.1.

$$\eta_c = \frac{\dot{m}C_p(T_{out} - T_{in})}{A_c I_{rad}} = \eta_0 - k_1 \frac{(T_m - T_a)}{I_{rad}} - k_2 \frac{(T_m - T_a)^2}{I_{rad}} \tag{3.1}$$

where $\dot{m}$ is the water mass flow entering the collectors field with T_{in} and outgoing with T_{out} temperature. A_c is the total collectors area and I_{rad} is the total solar irradiation on the titled surfaces of the thermal collectors. The second part of Eq. 3.1 represents the quadratic relation often used to define the efficiency of the thermal collectors. Indeed, η_0 shows the zero loss efficiency of the collector, k_1 and k_2 indicate the first and second order heat loss coefficients given by the manufacturer

Viessmann - Solar thermal systems (see Table 3.1), T_a is the ambient temperature and T_m is the average temperature expressed by the formula in Eq. 3.2.

$$T_m = \frac{T_{out} + T_{in}}{2} \tag{3.2}$$

3.4.2 Solar storage tank

The size of the storage tanks varied between about 0.5 m^3 to 4 m^3 depending on cooling needs and the cooling power capacity of the absorption chiller. For systems requiring night time cooling, the benefits of the storage unit can be considerable. The thermal model of the energy storage tank subjected to thermal stratification, can be modeled by assuming that the tank is divided into N fully mixed equal volume segments (Bouhal et al., 2017c), as presented in Fig. 3.6. The stratification degree is determined by the value of N.

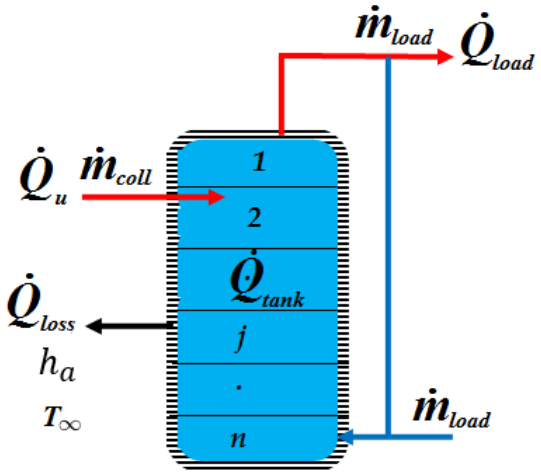

FIGURE 3.6: Configuration of a stratified fluid storage tank with a representative flow streams scheme between segments

As presented in Fig. 3.6. The energy balance for the storage tank can be formulated as the following:

$$\dot{Q}_{tank} = m_w C_w \frac{dT_j}{dt} = \dot{Q}_u - \dot{Q}_{load} - \dot{Q}_{loss} + \dot{Q}_{adv} \tag{3.3}$$

In Eq. 3.3, $\dot{Q}_{adv} = \chi_j C_w \Delta T_\chi$ where χ_j has the following form: $\chi_j = \dot{m}_u \sum_{k=1}^{j-1} \epsilon_k - \dot{m}_{load} \sum_{k=j+1}^{n} \delta_k$ and

$$\epsilon_k/\delta_k = \begin{cases} 1 & \text{fi } k^{th} \text{ layer} \in \text{top/bottom of the storage tank} \\ 0 & \text{ailleurs} \end{cases}$$

The other parameters defined in Eq. 3.3 are expressed as follow:

- Temperature difference: $\Delta T_\chi = \begin{cases} T_{j-1} - T_j & \chi_j > 0 \\ T_j - T_{j+1} & \chi_j < 0 \end{cases}$
- Useful energy provided by the collector's field : $\dot{Q}_u = \epsilon_k \dot{m}_{coll} C_w (T_{out} - T_j)$
- Energy delivred to the generator of the absorption chiller: $\dot{Q}_{load} = \delta_k \dot{m}_{load} C_w (T_j - T_{load})$

- Heat losses to the environnement: $\dot{Q}_{loss} = h_a A_j (T_j - T_\infty)$

3.4.3 Physical modeling of LiBr-H_2O solar absorption chiller

The operation of the absorption machine and the internal process of the absorption cycle is presented in Fig. 3.7. The absorption chiller operates with water (H2O) as refrigerant and the Lithium Bromide (LiBr) as sorbent. In the high pressure zone (steam generator and condenser), the refrigerant (H2O) is separated by expelling LiBr (boiler, steam generator) under the equivalent pressure when the temperature is high. For this reason, a source of motive heat is essential from the hot water produced by solar thermal collectors. In the condenser, the refrigerant liquefies with the absorption of heat. The objective of this step is to re-utilize the water (refrigerant) in its pure phase. Then, the fluid refrigerant passes through pressure separation lines and is brought into the low pressure zone (absorber, evaporator). Later, it evaporates at very low temperatures in the range of 5-15 °C. In the evaporator, the refrigerant evaporates with the absorption of the ambient heat and a cold is generated. The vapor of the refrigerant obtained is absorbed into the absorber by LiBr and dissolved in the salt by the release of heat pumped to the high pressure zone (condenser/ boiler) by consuming little of electricity. Finally, the dynamic cycle is maintained continuously.

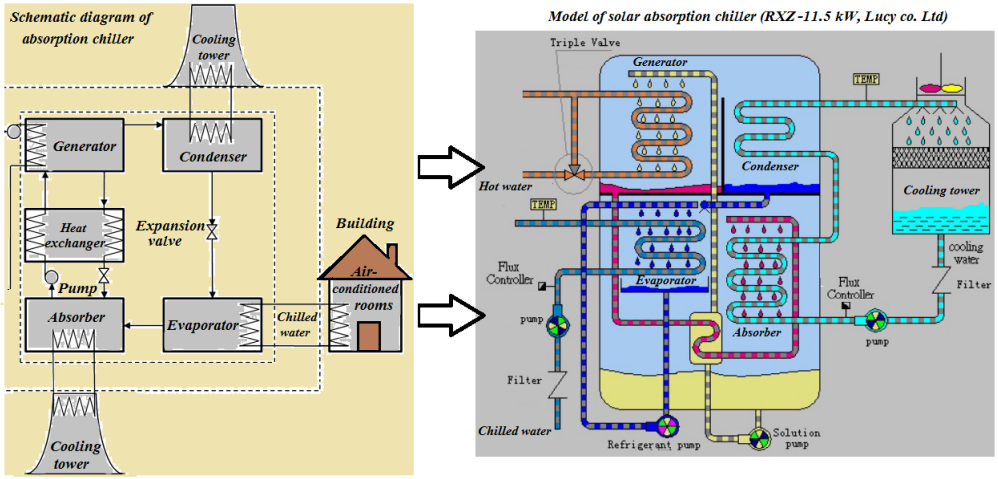

FIGURE 3.7: Model of the absorption chiller (*Shandong Lucy New Energy Technology Co., Ltd.*)

The main characteristics of the absorption chiller are given previously in Table 2.8.

The governing equations describing the physical model are formulated in the following:

- The generator power describing the heat exchanged from the solar hot water to the LiBr-H_2O solution inside the generator:

$$\dot{Q}_{gen} = \dot{m}_{gen}.C_p(T_{gen,i} - T_{gen,o}) \tag{3.4}$$

$T_{gen,o}$ and $T_{gen,i}$ are measured at the outlet and inlet entries of the generator, respectively.

- The chilling power expressing the heat exchanged from the chilling circuit to the evaporator:

$$\dot{Q}_{evp} = \dot{m}_{evp}.C_p(T_{evp,i} - T_{evp,o}) \tag{3.5}$$

$T_{evp,o}$ and $T_{evp,i}$are measured at the outlet and inlet entries of the evaporator, respectively.

- The cooling power representing the heat exchanged from the absorber and the condenser to the cooling circuit:

$$\dot{Q}_{cnd} = \dot{m}_{cnd}.C_p(T_{exh,i} - T_{exh,o}) \tag{3.6}$$

$T_{exh,o}$ and $T_{exh,i}$ are measured at the outlet and inlet entries of the absorber and condenser loop.

- The solar power describing the incident solar radiation on the solar thermal collector's field area of the installation:

$$\dot{Q}_{rad} = n \times I_{rad} \times A \tag{3.7}$$

where n is the number of collectors constituting the solar field and A the unitary area of the solar collector.

- The solar collecting power presenting the solar heat supplied by the solar thermal collectors:

$$\dot{Q}_{sc} = \dot{m}_{sc}.C_{sc}(T_{sc,o} - T_{sc,i}) \tag{3.8}$$

$T_{sc,o}$ and $T_{sc,i}$ are measured at the outlet and inlet entries of the solar field collectors, respectively.

- Coefficient of Performance of the absorption machine (COP):

  The performance of solar air-conditioning systems can be expressed through the concept of Coefficient of Performance (COP), defined as cooling capacity divided by solar input. It is calculated using the ratio between the electrical energy and the energy of cold generated and the value of this ratio is between 2 and 3.

$$COP = \frac{\dot{Q}_{evp}}{\dot{Q}_{gen} + \dot{Q}_{ele1}} \tag{3.9}$$

where $\dot{Q}_{ele1}$ is the electricity consumption of the absorption chiller (see Fig. 1.8).

3.4.4 Solar fraction S_f

Solar fraction S_f can be expressed as the total energy provided by the solar collectors to produce hot water. It is defined as the percentage of system energy requirements that is met by solar energy and the rest must be supplied through auxiliary energy. It is calculated using Eq. 3.10 (Buckles and Klein, 1980). The solar fraction is the most important indicator to characterize the thermal performance of the collective system

compared to the other parameters previously presented, since it takes into account the overall performance of the entire system and not only one single component.

$$S_f = 1 - \frac{\dot{Q}_{aux}}{\dot{Q}_{gain}} \tag{3.10}$$

where $\dot{Q}_{gain} = \dot{Q}_u - \dot{Q}_{loss}$ is the the total energy transferred by the collector field to satisfy the water heating requirements and $\dot{Q}_{aux} = \dot{Q}_{ele1} + \dot{Q}_{ele2}$ is the total auxiliary energy provided to the equipments to support the portion of the total solar energy load which is not sufficient (see Fig. 1.8).

3.5 Economic indicators

The absorption machines are the sorption refrigeration systems most present on the solar cooling market, whether they are small or large. Their combination with flat plat and evacuated tube solar thermal collectors is fairly well known in the field of large installations. In the case of small systems, the unsteady behavior of these machines is not yet well known due to all the transient factors affecting the operation of these machines like the refrigerating charge of the building, the environmental conditions and solar resource. In the other hand, desiccation systems have not yet penetrated the market as absorption and adsorption have done. In the following section, several economic indicators were defined to evaluate the economic viability of the solar cooling system.

3.5.1 Cost of energy saving K_{es}

The cost of energy saving K_{es} is considered as the first economic indicator. In our case, it compares economic gain when the solar absorption system replaces a conventional cooling unit (a vapor compression machine). The K_{es} is expressed as follows:

$$K_{es} = K_{cv} - K_{sol} \tag{3.11}$$

where K_{cv} is the cost of the consumed electric energy in the case of the conventional system and K_{sol} is the cost of the consumed electric energy in the case of solar cooling system. The cost of annual electricity consumption K_{el} can vary during the lifetime, so the inflation rate of electricity must be introduced, as in Eq. 3.12:

$$K_{el} = K_0(1 + r\%)^T \tag{3.12}$$

In Eq. 3.12, K_0 is the cost of annual electricity consumption at the first operation year, $r\%$ the inflation rate (%) which is the change in energy prices relative to general inflation or energy inflation in the country and T is the lifetime period.

3.5.2 Payback period P

The payback period P that refers to the required time of recovering the cost of the initial investment paid in the whole thermal installation. The payback period P is expressed as:

$$P = \frac{log(1 + \frac{I_0.r\%}{100.K_{es}})}{log(1 + \frac{r\%}{100})} \tag{3.13}$$

In Eq. 3.13, $r\%$ is the electricity inflation rate, and K_{es} is the cost of energy saving in (e/yr). The term I_0 presents the initial investment cost which is the sum of the separate costs including: the installation cost K_{inst}, the solar collectors (A_c, K_{coll}), the storage tanks volume (V_{st}, K_{tank}), the absorption chiller (Q_{abs}, K_{abs}) and the mechanical compression refrigerator (Q_{mec}, K_{mec}), are the main parts of the system that have to be taken into consideration in the cost calculation. The installation costs K_{inst} are assumed to be included in these quantities. Eq. 3.14 describes the way that the initial investment cost is calculated in every case:

$$I_0 = K_{inst} + K_{abs} \times Q_{abs} + K_{mec} \times Q_{mec} + K_{coll} \times A_c + K_{tank} \times V_{st} \tag{3.14}$$

The literature review indicates a wide difference on the costs of the thermal components. These costs vary according the country, the power range and the manufacturers. Accordingly, the following assumptions are justified through the literature reports and the market considerations (Tsoutsos et al., 2003). Consequently, the main economic input data of the solar cooling central under investigation are shown in Table 3.2.

Parameter description	Value
Average cost of absorption chiller	352-520 €/kW (Allouhi et al., 2015a)
Cost of the solar collectors	250 €/m^2 (ETC) and 200 €/m^2 (FPC) (Bellos, Tzivanidis, and Antonopoulos, 2016)
Cost of the heat storage tank	1200 €/m^3 (Allouhi et al., 2015a)
Cost of the cooling tower	150 €/kW (Allouhi et al., 2015a)
Installation costs	12% of the total equipment cost (Tsoutsos et al., 2003)
Maintenance cost of the solar system	1% of the initial investment cost (Allouhi et al., 2015a)
Maintenance cost of the conventional system	30 €/yr (Mateus and Oliveira, 2009)
Average Moroccan electricity cost	0.09 €/kWh (*Office National d'Electricité et de l'Eau Potable (ONEE)*)
Market discount rate	r =4 % (Year 2017) (*Haut Commissariat au Plan (HCP)*)
Moroccan energy inflation	$i\%$ =2.5 % (Year 2017) (*Haut Commissariat au Plan (HCP)*)

TABLE 3.2: Economic input data (Tsoutsos et al., 2003, Wang et al., 2016, Bellos, Tzivanidis, and Antonopoulos, 2016)

3.5.3 Cost of produced cooling energy $K_{prod.energy}$

Several simulations were carried out for the various buildings situated in Marrakech (Z5), to assess the variation of solar fraction and total costs with storage tank volume. Total costs K_{tot} were determined by summing initial costs (investment including installation costs), energy, maintenance and other running costs for a period of 25 years. As a result, the cost of produced energy $K_{prod.energy}$ was obtained by dividing those total costs by the total energy produced by the cooling system $Q_{prod.energy}$ (see Eq. 3.15).

$$K_{prod.energy} = \frac{K_{tot}}{Q_{prod.energy}} \tag{3.15}$$

The local electricity and natural gas costs were used taking into consideration their present value in Morocco and building sector, and using an estimate of inflation for energy prices (between 2% and 6%/year). Table 3.3 shows local costs used for 2017 according to *Haut Commissariat au Plan (HCP)*.

Auxiliary backup	Electricity		Gas	
	Residential	Professional	Residential	Professional
Cost (e/kWh)	0.09	0.1	0.06	0.08

TABLE 3.3: Energy costs in Morocco used in the economic analysis for the year of 2017 (*Haut Commissariat au Plan (HCP)*; *Ministry of Energy, Mines and Sustainable Development (MEMSD), Morocco*)

The results of financial costs of the solar cooling installation are listed in Table 3.4.

Components	Costs (€)
Thermal collector's field	6000
Absorption chiller	4050
Cooling tower	750
Back-up chiller	300
Cold storage tank	300
Hot storage tank	720
Pumps	600
Installation costs	1530
Initial investment I_0	14245
Maintenance cost of the solar system	142
Mean cost of energy saving	406
Payback period	25 years

TABLE 3.4: Financial costs of the solar cooling installation

3.6 Simulation results

Different parametric studies were conducted to optimize the thermal performance of the solar air-conditioning system under Moroccan conditions. The effect of the collector's field was assessed and the volume of the storage tank was varied and its influence on solar fraction was also evaluated. Indeed, the system performances were compared by adopting an evacuated tube collector (ETC), and a flat plate collector (FPC). The influence of cooling demand profiles was as well examined. Accordingly, a highlight of the main results is presented including an assessment of the impact of the system characteristics and their optimum values. The examined costs for the system and auxiliary supplement are compared and optimization values for system sizing are presented for various building categories and Moroccan climates zoning.

3.6.1 Impact of collector area and storage tank volume

Figs. 3.8-(a) and (b) show the solar fraction variation for cooling with storage volume and collector area for the residential house located in Marrakech (Z5). As shown in Figs. 3.8-(a) and (b), the optimal results occur for a storage capacity in the range of 400-1000 L of collector area but there is no important change of total cost or solar fraction above 600 L in the residential house.

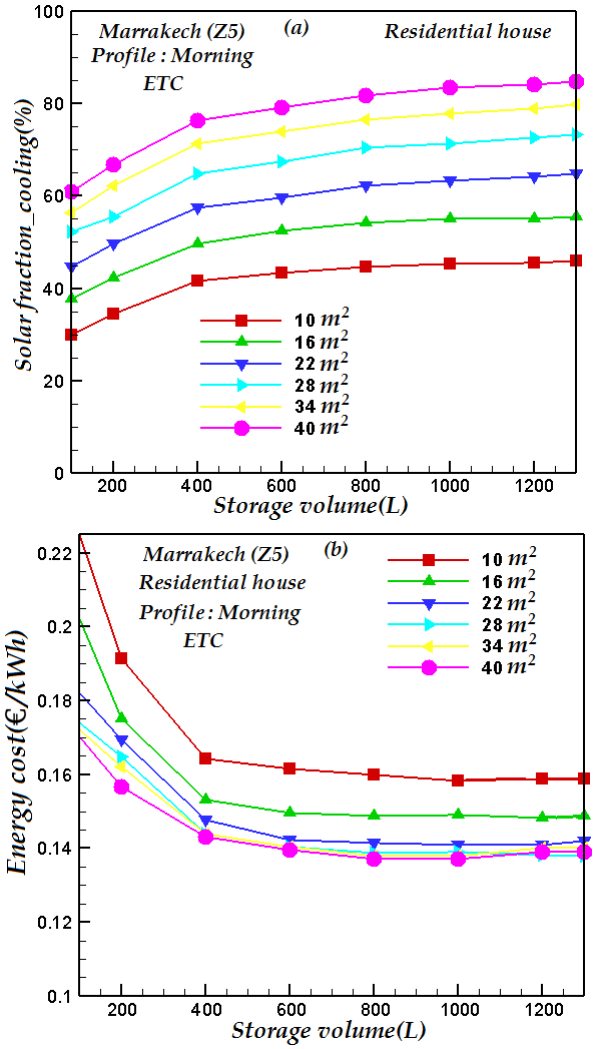

FIGURE 3.8: Solar fraction variation with storage volume and collector size for the residential house in Marrakech (Z5)

Figs. 3.9-(a), (b) and (c) represent the required collector area for a given annual solar fraction for both FPC and ETC solar technologies for residential house, office building and hotel, respectively. We note that for a given collector area, cooling loads in Marrakech city (Z5) are significant compared to Fez (Z3). As shown in Figs. 3.9-(a), (b) and (c), using FPC technology supplied either with electric or gas backups requires an important collector's area compared to ETC technology for different building categories. ETC technology shows the best performance, thanks to its efficiency, because low area is required using electric backup in Fez (Z3) and Marrakech (Z5). For a residential house under 70 % of solar cooling fraction, 24 m^2 is required for ETC technology while 32 m^2 for FPC technology is required (see Fig. 3.9-(a)). Concerning the office building, under 70 % of solar cooling fraction, 35 m^2 is required for ETC technology while 55 m^2 for FPC technology is required (see Fig. 3.9-(b)). Regarding the hotel, under 70 % of solar cooling fraction, 68 m^2 is required for ETC technology while 110 m^2 for FPC technology is required (see Fig. 3.9-(c)).

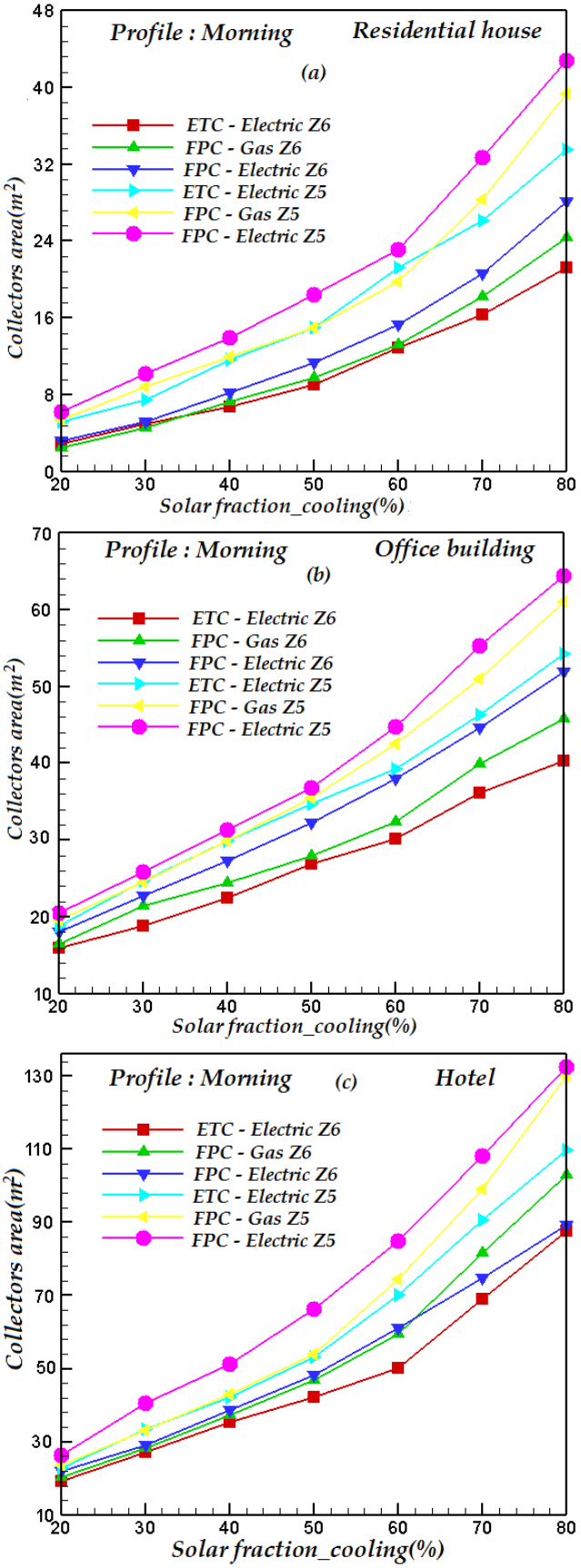

FIGURE 3.9: Required solar collector's area (FPC and ETC) for a given annual solar fraction for residential house (a), office building (b) and hotel (c) using electric and gas as auxiliary backup in Fez (Z3) and Marrakech (Z5)

Annual solar fraction values for cooling season are presented in Table 3.5. The energy performance results including solar fraction versus collector area (ETC), and also tank storage capacity and average collector efficiency for the three studied buildings with the three different climates are listed (see Table 3.5).

Building localisation		Fez (Z3)				Marrakech (Z5)				Zagora (Z6)			
Residential house													
Solar fraction	Cooling (%)	20	40	60	80	20	40	60	80	20	40	60	80
Size	A_c (m^2)	4	6	12	22	6	12	22	32	3	5	10	22
	Vol (m^3)	0.15	0.3	0.6	1.2	0.4	0.8	1	1.1	0.1	0.2	0.5	1
Efficiency	Collectors (%)	51	40	33	26	49	39	31	25	55	42	35	29
Office building													
Solar fraction	Cooling (%)	20	40	60	80	20	40	60	80	20	40	60	80
Size	A_c (m^2)	15	22	29	40	19	30	39	54	14	20	26	38
	Vol (m^3)	1.5	2	3.3	5.5	1.6	3.4	5.3	1.7	1.3	1.8	3.1	5.4
Efficiency	Collectors (%)	29	27	25	23	28	26	24	21	30	28	26	25
Hotel													
Solar fraction	Cooling (%)	20	40	60	80	20	40	60	80	20	40	60	80
Size	A_c (m^2)	20	38	50	88	25	40	70	110	18	37	48	87
	Vol (m^3)	1.6	3.6	5.8	6.7	1.7	3.8	5.9	6.8	1.4	3.4	5.6	6.6
Efficiency	Collectors (%)	35	29	26	22	33	28	25	20	26	30	27	25

TABLE 3.5: Optimization of system size, storage volume and efficiency of ETC technology for different solar fractions during cooling season

3.6.2 Impact of cooling load profiles

The solar cooling fraction is the performance indicator chosen, and storage volume is the key parameter being studied to evaluate the thermal performance of the solar air-conditioning system taking into account the cooling load profiles. The results are designed to test the optimal values by changing one main parameter at a time i.e. the degree of instantaneous mismatch of cooling load and solar availability, varying load profile (Morning, Day and Evening) and the effect of system temperature range. Fig. 3.10 shows the solar fraction versus storage tank volume under the various cooling demand profiles. As we can notice, the cooling profile has a strong impact on the system performance. Without any storage, the system is always at its minimum performance especially for Evening load profile (e.g. night time cooling), which can reach near zero cooling. Regardless of the amount of temporal mismatch between the loads cooling profiles and solar source there is a linear relationship between the storage volume and solar cooling fraction, with a near constant slope for all three cooling demand profiles examined. Note that in Fig. 3.10 the simulated system never reaches a solar fraction of 100 %. This is because the simulated system uses average values for collector efficiency which takes into account the nonlinear nature of collector efficiency and its changes with time. Indeed, Morning profile provides the higher solar cooling fraction thanks to the correspondence between the cooling requirements and the availability of solar sunshine. Day profile indicates solar cooling fraction values better than those of Evening profile.

From Figs. 3.10, the cooling load profiles directly affects the average efficiency of the solar air-conditioning system.

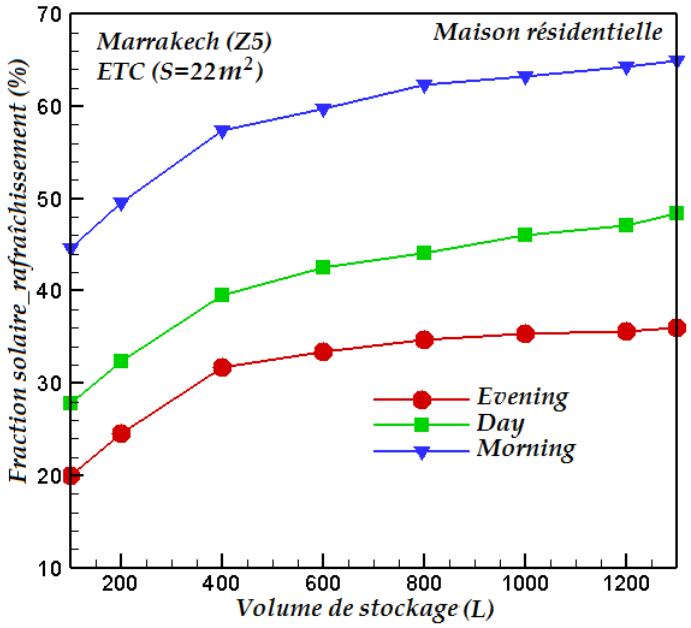

FIGURE 3.10: Solar cooling fraction vs. Storage volume at various cooling demand time requirements, Collector's area of 22 m^2, Absorption chiller capacity of 11.5 kW and average COP of 0.7

Figs. 3.11 show the contribution of the annual solar energy to produce air-conditioning for the studied Moroccan regions, namely: Fez (Z3) presented in Fig. 3.11-(a), Marrakech (Z5) shown in Fig. 3.11-(b) and the city of Zagora (Z6) presented in Fig. 3.11-(c) for different cooling demand profiles. The variation in the solar contribution observed with respect to each studied zone is due to the climate effect in terms of solar irradiation incident on the collector field. Concerning solar air-conditioning during June month, it was noticed that the solar contribution reaches 950 kWh, 690 kWh and 890 kWh respectively for the three zones of Fez, Marrakech and Zagora. It has been concluded that the field of solar collectors have to be sized according to the amount of incident solar radiation which is available per city, besides to the consumer needs in terms of cooling loads. In addition, it has been observed that the solar contribution of the absorption machine is zero during the summer season for Evening profile, but it is maximized for the Day cooling profile (Agrouaz et al., 2017).

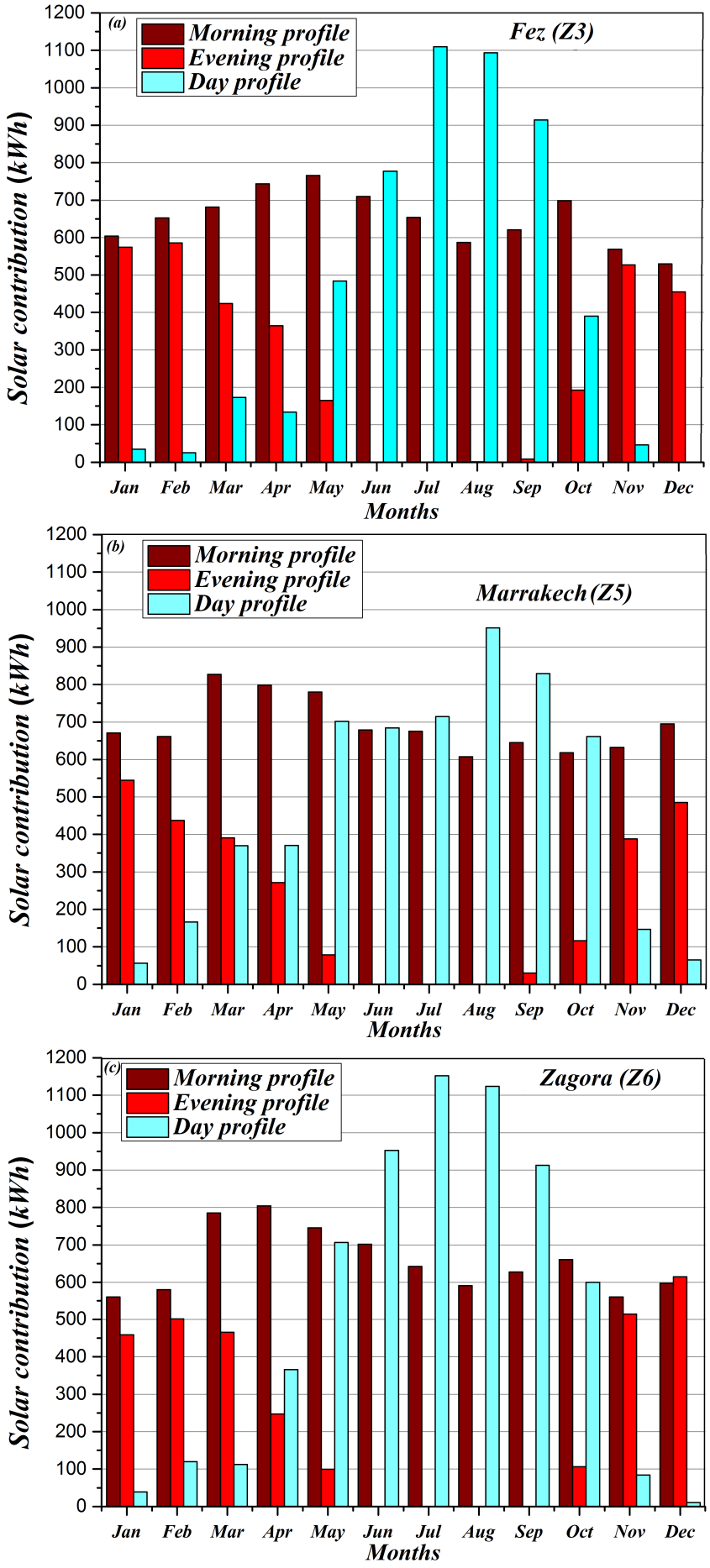

FIGURE 3.11: Solar contribution for various cooling demand time requirements in different regions

The annual solar cooling production for Fez (Z3), Marrakech (Z5) and Zagora (Z6) is presented in Fig. 3.12-(a). Concerning Fig. 3.12-(b), it allows to evaluate the amount of the annual auxiliary supplement consumption throughout the year. The results show that solar cooling production is maximized during the summer period thanks to important sunshine available (Agrouaz et al., 2017). For example, the cooling production reached 410 kWh for the city of Fez (Z3), 630 kWh for the city of Zagora (Z6) and 610 kWh for the city of Marrakech (Z6) during July month. An interest was brought to maximizing the cooling production in the summer months to ensure the comfort of the inhabitants and in the same time reducing the invoices for electricity/gas used to satisfy the requirements of the consumer when solar radiations are not sufficient. As shown in Fig. 3.12-(b), the electric auxiliary backup does not operate during the summer months namely: June, July, August and September caused by the availability of solar irradiation. However, it is maximized during the winter season. For instance for the month of January, it reaches 1255 kWh for the city of Fez, 1875 kWh for the city of Marrakech and 2230 kWh for the city of Zagora. Interesting studies have been carried out in other countries. In Europe for example, solar cooling systems were also investigated and validated. Accordingly, energy and economic aspects of an integrated solar absorption cooling and heating system in different building types were examined under various locations: Lisbon (Portugal), Berlin (Germany) and Rome (Italy) (Mateus and Oliveira, 2009).

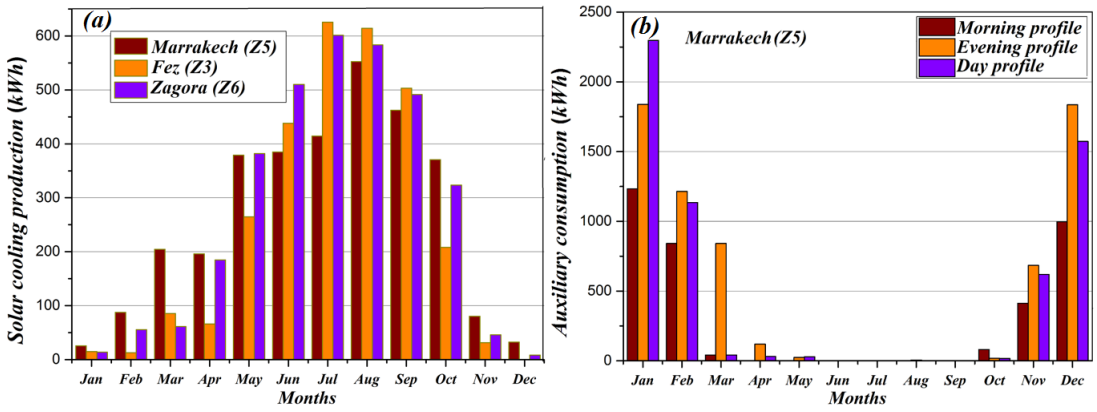

FIGURE 3.12: Solar cooling production and auxiliary consumption in different regions

3.6.3 Energy and economic optimization

In this section, the results of energy and economic approaches are presented under Moroccan conditions applied to the solar cooling installation of Fig. 2.21. A set of economic indicators were used to examine the economic viability of the solar air-conditioning system.

Accordingly, Table 3.6 presents the various costs calculated for each of the zones considered for a solar cooling system with an annual solar fraction of 70%. The initial investment (including installation cost), energy and maintenance and the different backup alternatives of electricity and gas have been identified. Thus, the ETC technology seems to be installed in Fez (Z3) and Marrakech (Z5) while FPC is seems to be implemented in Zagora (Z6) thanks to the high solar energy potential of this region.

Zone	Collector technology	Backup type	Investment solar (ke)	Investment backup (ke)	Electricity (1st year) ($ke/year$)	Gas (1st year) ($ke/year$)	Maintenance (1st year) ($ke/year$)
Fez (Z3)	ETC	Electric	16	5	0.414	0.022	0.324
	ETC	Gas	15	9	0.104	0.231	0.121
Marrakech (Z5)	ETC	Electric	15	6	0.423	0.026	0.365
	ETC	Gas	13	8	0.107	0.236	0.124
Zagora (Z6)	FPC	Electric	12	4	0.301	0.014	0.267
	FPC	Gas	10	6	0.095	0.187	0.105

TABLE 3.6: Costs generated of solar cooling system for the different Moroccan regions and backup systems by item for an annual solar fraction of 70%

Table 3.7 shows the results of the solar cooling system size (including the collector area and storage volume) for a residential house that leads to the minimum total cost of produced energy for the different locations, energy backup options and for an annual solar fraction of 70%. Table 3.7 also compares investment in a residential house and total costs for the solar cooling system and auxiliary system using electricity and gas backups for a period of 25 years.

Zone	Collector technology	Backup type	A_c (m^2)	Vol (m^3)	A_c per kW cool. (m^2/kWc)	Solar cooling system investment (ke)	System investment: sol vs. conventional (%)	Cost of produced energy: sol vs. conventional (%)
Fez (Z3)	ETC	Electric	16	0.6	1.2	18	+266	+12
	ETC	Gas	14	0.5	1	14	+165	+16
Marrakech (Z5)	ETC	Electric	15	0.5	1.1	17	+245	+13
	ETC	Gas	13	0.4	0.9	13	+137	+17
Zagora (Z6)	FPC	Electric	18	1.2	1.7	1.8	+315	+19
	FPC	Gas	20	1.4	1.8	2	+ 316	+20

TABLE 3.7: Solar cooling system scheme allowing minimum total cost for the residential house for an annual solar fraction of 70%

Table 3.8 presents the results of the solar cooling system size (including the collector area and storage volume) for the office building that leads to the minimum total cost of produced energy for the different locations, energy backup options and for an annual solar fraction of 70%. Table 3.8 also compares investment in an office building and total costs for the solar cooling system and auxiliary system using electricity and gas boiler backup for a period of 25 years.

Zone	Collector technology	Backup type	A_c (m^2)	Vol (m^3)	A_c per kW cool. (m^2/kWc)	Solar cooling system investment (ke)	System investment: sol vs. conventional (%)	Cost of produced energy: sol vs. conventional (%)
Fez (Z3)	ETC	Electric	35	6.5	1.2	35	+140	+20
	ETC	Gas	32	6.3	1.1	33	+135	+18
Marrakech (Z5)	ETC	Electric	40	6.8	1.4	38	+125	+17
	ETC	Gas	42	6.9	1.5	39	+128	+19
Zagora (Z6)	FPC	Electric	34	6.4	1.1	33	+165	+30
	FPC	Gas	33	6.3	1	32	+163	+28

TABLE 3.8: Solar cooling system scheme allowing minimum total cost for the office building for an annual solar fraction of 70%

Table 3.9 indicates the results of the solar cooling system size (including the collector area and storage volume) for the hotel that leads to the minimum total cost of produced energy for the different locations, energy backup options and for an annual solar fraction of 70%. Table 3.9 also compares investment in a hotel and total costs for the solar cooling system and auxiliary system using electricity and gas boiler backup for a period of 25 years.

Zone	Collector technology	Backup type	A_c (m^2)	Vol (m^3)	A_c per kW cool. (m^2/kWc)	Solar cooling system investment (ke)	System investment: sol vs. conventional (%)	Cost of produced energy: sol vs. conventional (%)
Fez (Z3)	ETC	Electric	72	5.7	1.3	65	+207	+14
	ETC	Gas	70	5.5	1.2	62	+115	+18
Marrakech (Z5)	ETC	Electric	71	5.8	1.2	72	+210	+15
	ETC	Gas	73	6	1.1	74	+208	+10
Zagora (Z6)	FPC	Electric	75	6.7	1.6	84	+400	+55
	FPC	Gas	78	6.9	1.8	86	+450	+60

TABLE 3.9: Solar cooling system scheme allowing minimum total cost for the hotel, for an annual solar fraction of 70%

3.7 Conclusion

In Chapter 3, the design and optimization of the solar air-conditioning process was investigated based on Moroccan energy and economic indicators using *Transol* software. Hence, the thermal performance of a LiBr-H_2O absorption chiller coupled to solar thermal collectors was numerically evaluated using annual dynamic simulations for various building categories and different Moroccan climates. This work evidences the influence of the cooling load profiles, collectors technology (ETC and FPC) and building categories: residential house, building office and hotel under the climates zones of Fez (Z3), Marrakech (Z5) and Zagora (Z6) known as the hottest regions in Morocco, on the annual fractional savings of solar air-conditioning system using economic considerations. It is found that minimum costs depend on climate zones and building category. Hence, it is possible to save in costs of produced cooling energy for the zones of Fez (Z3), Marrakech (Z5) and Zagora (Z6) when electricity is used as auxiliary backup for annual solar fractions between 40% and 70%. The residential house and the hotel are the buildings where the solar air-conditioning system has a larger economic viability especially for Marrakech (Z5) and Zagora (Z6). Moreover, ETC technology provides a reduction in collector's area between 20% and 45% compared to FPC one although, due to their initial costs, FPC allow a higher economic feasibility especially for Zagora (Z6). An annual solar fraction of 70% can only represent a reduction of exploitation costs between 25% and 50% due to significant maintenance and operation costs. Taking into account the present Moroccan costs of energy resources (electricity and gas), it is mandatory that initial costs of solar collectors and absorption chillers are more decreased for solar air-conditioning installations to become more competitive and accessible for domestic and professional users.

The integration of Phase Change Materials (PCMs), as thermal energy storage medium, has been shown to improve the efficiency of solar absorption cooling systems by capturing excess insolation during peak to meet cooling demand in low insolation periods. In this way, Chapter 4 is devoted to the investigation of numerical methods used in the modeling of phase change phenomena applied to the solar hot water production systems to show later their integration effect on the efficiency of solar absorption machine coupled to the water heating systems.

Chapter 4

Latent thermal energy storage by Phase Change Materials (PCMs): Numerical modeling and dynamic simulations applied to Solar Water Heaters

4.1 Introduction

After we have presented the modeling and design of absorption cooling machine powered by solar energy in Chapter 3, the next chapters (4 and 5) will focus particularly on studying the latent thermal energy storage by integrating Phase Change Materials (PCMs) inside solar cooling process. This objective cannot be achieved without the perfect understanding of the phase change phenomena. In this vision, Chapter 4 focuses on the use of two numerical methods to simulate the melting/solidification of PCMs integrated in solar hot water production systems operating in dynamic mode. The objective is to simulate working cycle of solar thermal energy storage systems with encapsulated PCM operating under realistic environmental conditions (Marrakech, Morocco) and typical consumption load profile. This research aims to compare two numerical procedures: The technique of apparent specific heat capacity (C_p^{app}) and the Enthalpy method, basically used to simulate the phase change phenomena for latent storage inside a solar tank integrating spherical PCM capsules. Effects, advantages and limits of these numerical methods were examined via various numerical observations as well as a set of system thermal performance indicators. The assumptions, equations used in numerical modeling, the temperature profiles and the PCM liquid fraction evolution are presented and discussed as well. Based on the design and parameter studies performed, various suggestions and several numerical model improvements for further studies are as well addressed.

4.2 Literature survey

Currently, solar heating/cooling intended to produce hot water or cooling charges are the subject of great interest, especially the assessment of their overall efficiency that depends not only on environmental climatic conditions, but also on the efficiency of other determinant devices such as the storage tank. The introduction of Phase Change Materials (PCMs) provides a solution by using latent heat instead of sensible heat to store thermal energy, as evidenced by the abundant literature in the

domain (Battisti and Corrado, 2005a, Thür, Furbo, and Shah, 2006). Moreover, in the last decades, one of the actual issues is the improvement of solar energy technologies (Battisti and Corrado, 2005b, Kylili et al., 2018), particularly solar water heater systems intended to store hot water whether for individual (Bouhal et al., 2017c, Dîn Fertahi et al., 2017) or collective applications (Dîn Fertahi et al., 2018a). Improving the energy performance of these hot water production systems could be reached using several ways (Dîn Fertahi et al., 2018b). In particular by improving the solar collector and heat exchanger efficiency (Bouhal et al., 2017a) or by improving the performance of the storage part (Bouhal et al., 2017b): thermal storage tank (horizontal/vertical), buffer tank, etc.

Nowadays, PCMs have become a potential contender used to improve the thermal inertia of the storage tank (Kousksou et al., 2011). In fact, miscellaneous CFD studies have been conducted to assess solidification and melting of PCMs through two-dimensional and three-dimensional numerical simulations. Relevant studies have been identified that are presented as follows. First, Sattari et al., 2017 investigated the melting process of phase change materials (PCMs) in a spherical capsule through CFD simulations. Their results showed that the surface temperature of the spherical capsule could have a significant effect on the heat flux and the melting rate, compared to other parameters such as geometrical parameters and other operational conditions. Moreover, the modeling and development of a novel heat exchanger with spiral-wired tubes which integrates phase change material (PCM) has been performed by Youssef, Ge, and Tassou, 2018 using a detailed 3D CFD simulations that were validated against experimental measurements. The energy performance of the exchanger with PCM has been improved and its integration with the solar system remains a possible option.

It was also reported that, the comparison between two numerical heat transfer models for phase change material namely: the effective heat capacity method and the enthalpy method were investigated by Jin et al., 2018, because they are considered as the two most common methods used to build the numerical heat transfer models for phase change material (PCM) board. The main results of Jin et al., 2018 have shown that the accuracy of those two models depends on the phase change temperature range. For instance, the capacity method could be efficient, if the phase change temperature range is small. However, the effective heat capacity method require less computing time than the model with the enthalpy method.

The scope of the PCMs is wide. Indeed, the aim of this part it to present recent studies which are interested in integrating PCMs in applications such as thermal energy storage systems, electronic cooling, batteries, etc. For instance, Wei et al., 2018 released a review to depict the multiple investigations on selection principles, innovation, and thermophysical properties of high temperature PCM used for thermal energy storage. In fact, this review could be considered as a helpful reference for the design of high temperature Thermal Energy Storage systems (TES). Besides, investigations of a horizontal PCM that assists a heat pipe system for electronic cooling incorporated in higher-power computer chips through CFD numerical simulations has been carried out by Behi, Ghanbarpour, and Behi, 2017. Indeed, they found that the PCM-assisted heat pipe could provide up to 86.7% of the required cooling load in the working power range of 50–80 W. This contribution has been assessed equal to 11.7%.

This chapter investigates numerically the working cycle of solar water heating systems and possible enhancement of thermal energy storage by means of PCM integration under typical consumption load requirements and realistic environmental conditions (Marrakech, Morocco). Thus, two numerical model characterizing

the transient phenomena of a phase change energy storage element were built to predict the temperature profile in a storage tank containing an amount (ϵ) of PCM. Comparison of these numerical methods used to simulate the heat transfer during melting of PCM integrated inside the solar storage tank for hot water production is less published despite its major importance. Therefore, working cycle of solar thermal energy storage systems was numerically investigated by applying the technique of apparent specific heat capacity (C_p^{app}) and the Enthalpy method to simulate the phase change phenomena. Accordingly, the objective is to compare the both numerical methods and highlight their superiorities and limitations. The effects of these numerical procedures on working cycle of solar water heating systems were analyzed via various numerical observations and results as well as a set of thermal performance indicators.

4.3 PCM selection

PCMs store energy as latent heat which is absorbed or released during the transition phase from the solid to liquid state or vice versa (Khudhair and Farid, 2004). Above a certain temperature which is characteristic of each material (solidification/melting point), the melting begins and absorbs heat at constant temperature. Many characteristic parameters should be taken into account for the choice of a PCM such as: cost, sensible and latent heat, melting point and heat conductivity in both solid and liquid phases (Barreneche et al., 2014) (see Fig. 4.1).

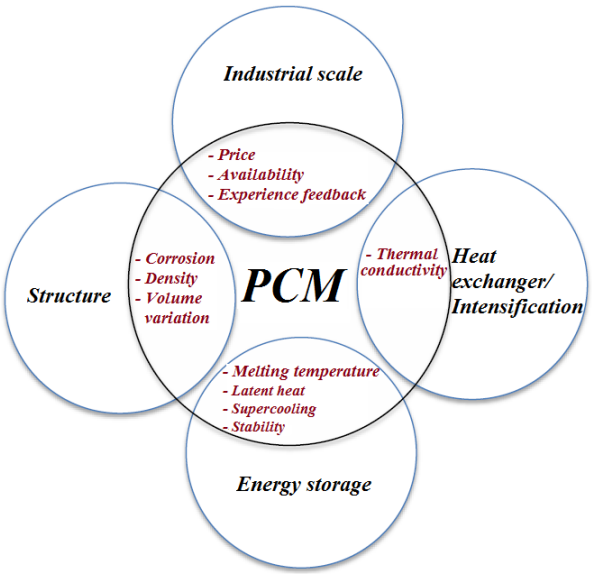

FIGURE 4.1: PCM's characteristics and barriers

The selection of an appropriate PCM for any application requires the PCM to have melting temperature within the practical range of application (between 40 °C and 60 °C corresponding to the set point temperature of the water tank). Fig. 4.2 illustrates the type of PCM versus the melting point temperature, this figure was inspired from the works of Zhou, Zhao, and Tian, 2012 and Farid et al., 2004. Numerous PCMs exist and can be used for thermal energy storage in solar thermal systems (Agyenim et al., 2010; Zalba et al., 2003). Several authors classified these PCMs (Agyenim et al., 2010) and determined the main properties they should have

for being a suitable PCM (Sharma et al., 2009). Some reviews were realized for listing all the available PCMs with their characteristics and presenting problems/issues such as stability, corrosion, containers and encapsulation (see Fig. 4.1) related with their utilization (Jamekhorshid, Sadrameli, and Farid, 2014).

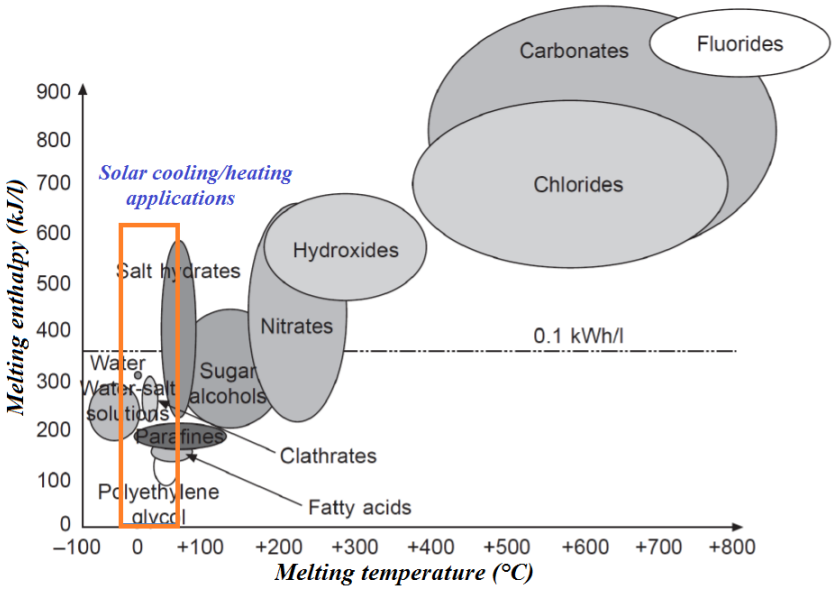

FIGURE 4.2: Applications and type of PCM versus the melting point temperature

One of the most affecting parameters on the viability of solar cooling systems is the load demand profile. The demand cooling profile is impacted by various parameters such as climatic conditions, occupant behavior, desired hot water set temperatures and mass flow (Fong et al., 2010). This chapter provides an analytical framework to quantify the benefit of the latent thermal energy storage. Using PCMs to enhance the performance of solar air-conditioning systems is not extensively discussed compared with separated solar heating/cooling systems. Further simulation works are thus required to identify best conditions of using latent heat storage for these systems. Selection of material, its position and how the thermal behavior of the PCM-based solar cooling applications is affected by operating conditions and weather data are tremendous aspects that should be decided judiciously for a better exploitation of latent energy for maximum performance and solar fraction. In that framework, the aim of the present chapter is to simulate working cycle of solar thermal energy storage systems with encapsulated PCM for solar hot water production intended for cooling applications under typical consumption load requirements and realistic environmental conditions (Marrakech, Morocco). Thus, a numerical model characterizing the transient phenomena of a phase change energy storage element is conducted to predict the temperature profile in a storage tank containing an amount (ϵ) of PCMs. Enthalpy method is used to simulate the phase change phenomena. Accordingly, numerical simulations were carried out to justify the benefits of using PCM in a low-cost and simple design to be in use by low income communities living. Optimizing melting/solidification processes are investigated and key operating conditions are evaluated under real fluctuating climatic conditions (Marrakech, Morocco). Three currently wide-spread solar collectors (i.e. FPC, ETC and CPC) were used and typical load cooling profiles were considered. Moreover, a new performance index is introduced to assess the benefit of using PCMs compared to basic

configurations in such particular solar thermal technologies.

4.4 Physical model

4.4.1 Problem specification

Hot water production is considered as one of solar energy's favored applications in the buildings sector due to the nature of the needs. For instance, the range of hot water temperature requirement is generally between 45 and 60 °C and the variation of needs during the year is weak. In addition to the solar collectors, the determinant equipment of a solar water heating system is the hot water storage tank. The energy stored inside the tank is increased, if the stratification is well improved Dîn Fertahi et al., 2018b. Consequently, the aim of the present study is to describe the thermal behaviour of the storage tank filled by PCM in its interior by performing a numerical parametric and comparative studies on a standard storage tank. Three typical solar collectors are considered in this work which consist of a Flat plate (FPC), Evacuated tube (ETC) and Compound parabolic (CPC), controller, a storage tank of $150l$ integrating layers of PCM inside the tank equipped with an auxiliary electric heater and a pump (see Fig. 4.3).

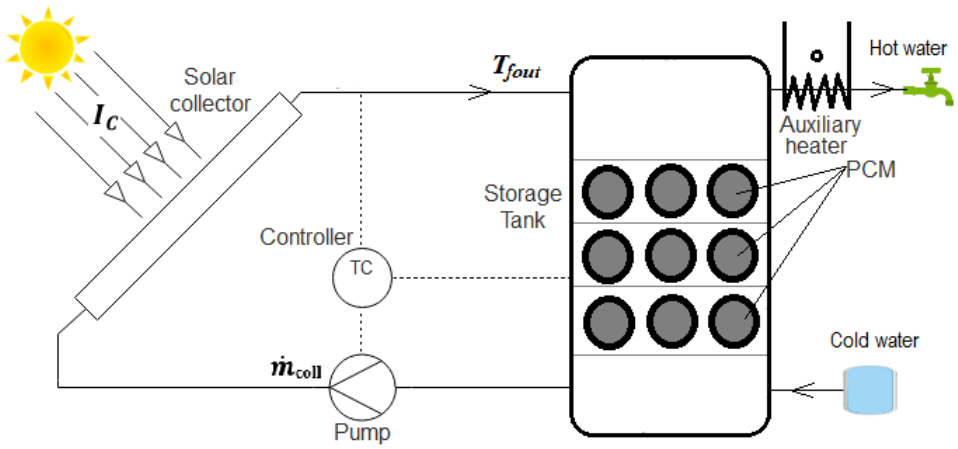

FIGURE 4.3: Layout of the studied hot water system integrating PCM

One of the determining points in this kind of modeling lies in the management of the phase change phenomena of the PCM, with overall problems that they cause (dissymmetry of the phase change, supercooling, etc.). For several years, numerous studies have been carried out on these phenomena (Yamagishi et al., 1996; Haillot et al., 2013,Zalba et al., 2003). Some parts of these studies focusing on the phase change modeling. There are now several numerical methods each having their advantages and disadvantages depending on the cases encountered. In particular, the Enthalpy method and the technique of monitoring the interface of phase change. The former are free from the evaluation of the evolution of the phase change front; the heat exchanges are represented by a variation of enthalpy and more precisely simulated by an apparent specific heat.

A numerical approach is used to compare two numerical procedures: a technique based on apparent specific heat called C_p^{app} in this study and the second considers the enthalpy method typically used to describe the PCM melting process integrated inside a storage tank. Therefore, the PCM with a reference proportion $\epsilon = 30\%$ is occupied a storage tank volume as schematically presented in Fig. 4.3.

The geometric characteristics of the studied storage tank are presented in the Table 4.1.

Volume (l)	150
Diameter (mm)	400
Length (mm)	1200
Environment temperature of the storage tank	20 [°C]
Initial temperature of the storage tank	25 [°C]
Tank heat loss coefficient	$0.57 - 1.133$ [W m^{-2} K^{-1}]
Insulation	40 mm cfc free Polyurethane

TABLE 4.1: Characteristics of the studied storage tank

The effect of the introduction of PCM on stratification is investigated inside the storage tanks and the temperature evolution of the solar hot water system operating in dynamic mode. A point not to be overlooked is in the packaging of PCM. It's a topic that has sparked a lot of research Marongiu, Berhe, and Fallon, 2000. The latest ones seem to agree on the merits of encapsulating PCMs in spherical nodules which is used in the current work. Indeed, it is a geometric configuration a priori optimal insofar as it allows to maximize the ratio between the volume of PCM in the tank (which directly impacts the storage capacity of the tank, so the amount of possible heat transfer) and the exchange surface between the water and the PCM (which affects the quality of thermal transfers occurring within the storage tank).

Accordingly, we have used the (NaOAc, 3H2O) as a working phase change material inside the storage tank which it's thermophysical properties are given in Table 4.2.

Density (liquid)	1300 [kg m^{-3}]
Density (solid)	1340 [kg m^{-3}]
Solidus temperature T_S	57.31 [°C]
Liquidus temperature T_L	60.75 [°C]
Thermal conductivity	5 [W m^{-1} K^{-1}]
Latent heat of fusion	173000 [J kg^{-1}]
Liquidus specific heat capacity C_L	3680 [J kg^{-1} K^{-1}]
Solidus specific heat capacity C_S	4020 [J kg^{-1} K^{-1}]
Dynamic viscosity	$1.81\ 10^{-3}$ [kg m^{-1} s]

TABLE 4.2: Physical properties of PCM-NaOAc, 3H2O (Talmatsky and Kribus, 2008)

As previously mentioned, the objective is to investigate numerically the effect of PCM integration on the water's temperature distributions inside the tank under various operating conditions. The investigation will also focus on the heat transfer during the melting process of PCM within the storage tank. A relevant consideration in such systems is the effective use of the storage tank filled by PCM in an optimal disposition, location and size. Consequently, the both numerical methods (Enthalpy method and C_p^{app} model) were used to simulate the PCM's melting inside the storage tank and were compared using a set of numerical results.

4.4.2 Mathematical model

Model description of the solar DWH with PCM

A number of phenomena are taken into account in terms of thermal processes that take place within the system. Each phenomenon is described in the code by a physical equation. The set of equations forms a system to describe the evolution of the temperature of the system as a function of time and along the storage tank's height. 1D unsteady flow models in dynamic mode were built in the **Fortran** programming code i.e the numerical code was accounting for one dimensional effects. Indeed, working on a 1D section was adopted for decreasing the computational time and it was a suitable approach to model the PCM melting process and water temperature inside the storage tank.

Fig. 4.4 shows a schematic of storage tank divided into N layers. The cold water comes in through the mains to solar collector by means of a pump. The temperature of water in each node varies and it decreases gradually from the top of the tank specified as node 1 to the bottom specified as node N. In order to maximize the amount of water above $45°C$ which is assumed to be the minimum water temperature for a comfortable use, it is important to control the mixing between the hot and cold water in the tank. In such modeling (see Fig. 4.4), 20 layers were used as required in the works of Kleinbach, Beckman, and Klein, 1993; Oliveski, Krenzinger, and Vielmo, 2003. The tank storing domestic hot water requires the stratification effect which means that there will be temperature gradient increasing from the bottom to the top. This stratification enables a better comfort for the user who will draw water from the top with a temperature higher than the bottom (Bouhal et al., 2017b). Furthermore, a low temperatures would also improve solar collector performance, maximizing collector output. To take advantage from the stratification, the storage tank is assumed to be divided into $N = 20$ separate, thoroughly mixed and isothermal layers of equal height as shown in Fig. 4.4.

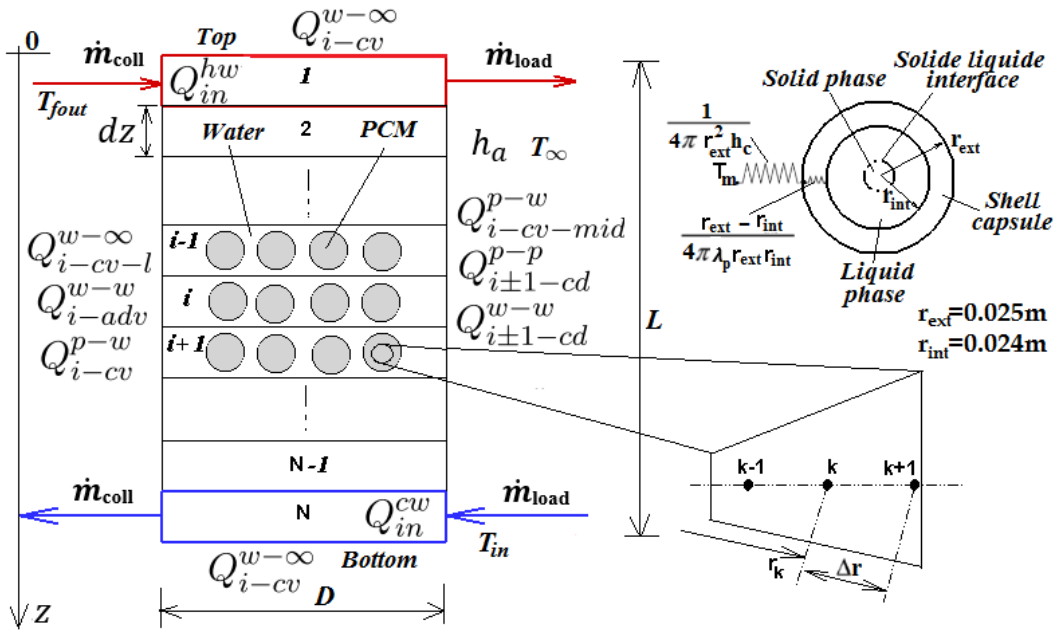

FIGURE 4.4: Discretization and scheme of the PCM capsules inside the storage tank

The following characteristics are considered during the design of the storage tank encapsulating PCM:

- The storage tank of 120 cm height and 40 cm diameter is divided into $N = 20$ fully mixed horizontal layers that contains both water and/or PCM in the interior;
- The top and bottom layers of the tank are PCM free in order to avoid direct losses from the PCM to surrounding;
- The height of the cold water inlet and the hot water outlet are at the bottom and the top of the tank respectively to take profit from the stratification;
- The heating system (electric booster) is placed outside the storage tank ;
- The PCMs are arranged in spherical capsules spaced apart in each layer, rather than a single unit (see Fig. 4.4) ;
- Uniform heat losses all around the tank;
- Ambient temperature of 20°C assuming that the storage is located in a heated space in the building.

Assumptions

An unsteady flow model of heat transfer during the melting process of PCM inside the storage tank were governed by the general following assumptions:

- *The fluid is incompressible and Newtonian ;*
- *The water flow is laminar as well as the melt zone ;*
- *The temperature of water is uniform in the same layer ;*
- *The thermophysical properties of the PCM are constant ;*
- *The viscous dissipation is negligible ;*
- *The top and bottom layers of the tank are PCM free in order to avoid direct losses from the PCM to surrounding ;*
- *For the i^{th} layer (Fig. 4.4), the internal energy variation of the fluid and PCM is due to energy fluxes exchanged at the top and the bottom of the layer, between PCM and water and the loss through the storage tank's wall ;*
- *The PCM is a composite type with high thermal conductivity, and thus the lumped system assumption can be used. The assumption that the PCM behaves like a lumped system is correct in case that the following condition holds: $Bi = \frac{hL_c}{\lambda} = \frac{h_c^{w-p} r_p}{2\lambda_p} < 0.1$. In this work the values of the heat transfer coefficient h_c^{w-p} between the PCM and the water ranges between 50 W/m^{2}K and 166 W/m^{2}K, thus the Biot number Bi is in the range from 0.05 to 0.166. It is concluded that even when using the highest value of heat transfer coefficient the assumption of the lumped system in case of PCM is reasonable;*
- *The melting and solidification of PCM are concentrics and take place at constant temperature (melting temperature).*

Model description of solar collector

The solar collector's efficiency η_c is a determinant indicator to evaluate the thermal performance of a solar water heater. The efficiency η_c is defined as the ratio of energy transferred from the collector to the heat transfer medium to the incident solar radiation. Three typical solar collectors were used in the current study, Flat Plate (FPC), Evacuated tube (ETC) and Compound Parabolic (CPC). In steady operating of the thermal collector, a mathematical modeling allows to express the overall energy balance based on the standard second-order collector performance Eq. 4.1:

$$\eta_c = k_0 - k_1 X^* - k_2 I_c X^{*2} \tag{4.1}$$

where η_c is the collector operating efficiency, X^* is the standardized temperature difference factor expressed as: $X^* = \frac{1}{I_c}(T_{avg} - T_\infty)$, $T_{avg} = \frac{1}{2}(T_N + T_{fout})$ is the average temperature within the collector, k_0 indicates the optical efficiency of the collector, and k_1 and k_2 present the first and second order heat loss coefficients, respectively, I_c is the solar incident radiation and T_∞ is the ambient temperature. The technical characteristics of the selected thermal collectors are listed in Table 4.3.

Parameters	Value			Unit
	FPC	ETC	CPC	
Collector absorber area A_c	2.67	2.67	2.67	[m^2]
k_0	0.735	0.821	0.660	[-]
k_1	4.6	2.82	0.82	[$W\,m^{-2}\,K^{-1}$]
k_2	0.0164	0.0047	0.0064	[$W\,m^{-2}\,K^{-2}$]

TABLE 4.3: Solar collector's characteristics (*Viessmann - Solar thermal systems*)

The rate of heat extraction from the collector may be measured by means of the amount of heat transferred to the fluid passed through it which is expressed in Eq. 4.2:

$$\eta_c I_c A_c = \dot{m}_{coll} C_w (T_{fout} - T_N) \tag{4.2}$$

Eqs. 5.1 and 5.2 were solved simultaneously to obtain the collector water outlet temperature. The pump with variable-speed sets in motion the heat transfer fluid when it is hotter than the water tank. Its operation is controlled by a regulating device acting on the temperature differences: if the temperature of storage tank is hotter than the solar collector temperature, the controller system stops the pump. Otherwise, the pump is restarted and the primary fluid heats the water inside the storage tank. Therefore, the operation logic of the studied solar water heater system requires a variable speed pump. The circuit includes two conditions for activating the pump based on the controllers in forced circulation systems. The hysteresis effect is considered in the differential controller that controls the solar pump. Typical values of ΔT between collectors outlet and bottom of the storage tank of positive 2 °C(switch off) and 7 °C (switch on) are recommended (Kalogirou, 2009). Accordingly, the pump controller activates the variable-speed pump when the collector water temperature exceeds 34 °C, or when the difference between inlet and outlet of the collector exceeds 4 °C. The detail of the pump operation logic is reported by Talmatsky et al. Talmatsky and Kribus, 2008. In our in-house code, the pump will be activated if:

- $T_{fout} > 34°C$

- $T_{fout} - T_N > 4°C$

In almost solar domestic hot water systems, an auxiliary electric heater is installed inside the storage tank. This may lead though to activation of the auxiliary heater in some situations when solar radiation is sufficient and there is no need for auxiliary heat. In our work, the electric heater is positioned outside the storage tank on the outlet pipe (Fig. 4.3). Indeed, the auxiliary heater is equipped with a thermostat that measures the temperature of the water delivered to the end-user: when this temperature falls below 45°C, the heater is activated at an average power sufficient to bring the temperature back to 45 °C. This setup enables a clear separation between solar derived heat and auxiliary heat, and definition of the minimum amount of backup electricity that is needed to satisfy the user's demands.

Thus, the electric supplement is triggered for two cases:

- if $T_1 < 45°C$, the backup electric energy is: $Q_{aux} = \dot{m}_{load} C_w (45 - T_1)$
- Otherwise, the water is cooled by water at 20°C with a flow rate of: $\dot{m}_{load} = \dot{m}_{max} \frac{45°C - 20°C}{T_1 - 20°C}$

The objective of this study is to analyze the thermal performance of a solar water heater enclosing a PCM by applying two physical models to describe the phase change process: the first model uses the apparent heat capacity C_p^{app} and the second one employs the Enthalpy method.

Energy equation for HTF (Water)

The global energy conservation for water is expressed as follow:

$$(1-\epsilon)\rho_w C_w \left(\frac{\partial T^w}{\partial t} + u\frac{\partial T^w}{\partial z}\right) = \lambda_w \frac{\partial^2 T_w}{\partial z^2} + h_c^{w-p} S_c (T^p(r = r_{ext}) - T^w) + h_a S_{ext} (T^w - T_\infty) \tag{4.3}$$

The coefficient h_a is estimated using the correlations reported by Ledesma et al. (Tores et al., 2013). Moreover, the value of the convection coefficient h_c^{w-p} was estimated during times when the fluid is stationary i.e. no flow through the tank using basic correlations for vertical and horizontal surfaces (Bergman and Incropera, 2011) and during times with net flow, using correlations for parallel flow around a sphere (Esen, Durmuş, and Durmuş, 1998; El-Wakil, 1971).

Using an explicit scheme, the energy balance for water in the i^{th} water layer can be written as:

$$(1-\epsilon)\rho_w C_w \frac{\partial T_i^w}{\partial t} = Q_{in}^{hw} + Q_{in}^{cw} + Q_{i-adv}^{w-w} + Q_{i\pm1-cd}^{w-w} + Q_{i-cv}^{w-\infty} + Q_{i-cv-l}^{w-\infty} + Q_{i-cv}^{w-p} + Q_{i-cv}^{w-p} \tag{4.4}$$

The expressions of different terms in Eq. 4.4 are the following:

- Energy transfered to water from collector: $Q_{in}^{hw} = \dot{m}_{coll} C_w (T_{fout}^w - T_1^w)$
- Energy injected to water from charging load: $Q_{in}^{cw} = \dot{m}_{load} C_w (T_{in}^w - T_N^w)$
- Advection between layers: $Q_{i-adv}^{w-w} = \mid \dot{m}_{coll} - \dot{m}_{load} \mid C_w (T_{i\pm1}^w - T_i^w)$
- Conduction (top/bottom layers): $Q_{i\pm1-cd}^{w-w} = \lambda_w S_b \frac{T_{i\pm1}^w - T_i^w}{dz}$ where $S_b = \frac{\pi D^2}{4}$, dz the space step.

- Convection heat loss (bottom and top layers, $i = 1$ and $i = N$): $Q_{i-cv}^{w-\infty} = h_a S_b (T_i^w - T_\infty)$
- Convection heat loss (lateral side): $Q_{i-cv-l}^{w-\infty} = h_a S_l (T_i^w - T_\infty)$ where $S_l = \pi D dz$.
- Convection (PCM/water in the same layer): $Q_{i-cv}^{w-p} = h_c^{w-p} S_c (T_i^p - T_i^w)$.
- Convection (PCM/water in top/bottom layers): $Q_{i-cv}^{w-p} = h_c^{w-p} S_c (T_{i\pm1}^p - T_i^w)$ S_c is the exchange area between water and PCM capsule.

Specific apparent heat capacity C_p^{app} model

The C_p^{app} method describes the melting/solidification processes through the specific heat capacity function. Most PCMs are not pure, as a result the phase change is not carried out at a constant temperature but over a range of temperature. In our case, (NaOAc, 3H2O) is selected as a PCM which its properties are given in Table 4.2. The apparent specific heat capacity function of this PCM is presented in Fig. 4.5.

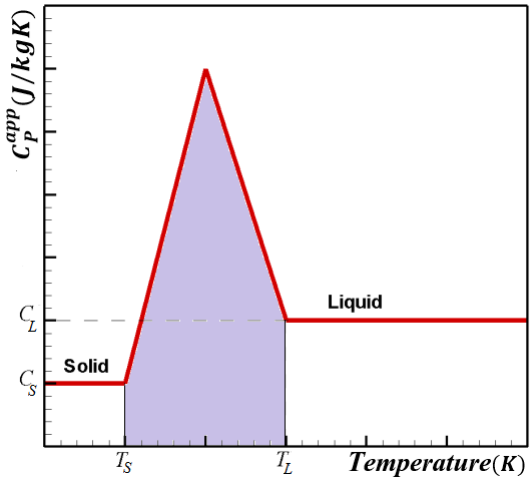

FIGURE 4.5: Evolution of the specific heat C_p^{app} model for the composite PCM (Talmatsky and Kribus, 2008)

The apparent specific heat capacity C_p^{app} is based on the monitoring of the phase change interface. The energy balance can be written explicitly for the i^{th} PCM layer as:

$$\rho_p C_p^{app} \frac{\partial T_i^p}{\partial t} = Q_{i\pm1-cd}^{p-p} + Q_{i-cv-mid}^{p-w} + Q_{i-cv}^{p-w} \tag{4.5}$$

The expressions of different terms in Eq. 4.5 are the following:

- Conduction (upper/bottom layers): $Q_{i\pm1-cd}^{p-p} = \lambda_p S_c \frac{T_{i\pm1}^p - T_i^p}{dz}$, where S_c is the contact area of PCM element, if it exists in the relevant layer, dz the space step.
- Convection (PCM/water in layer i): $Q_{i-cv-mid}^{p-w} = h_{i-cv}^{p-w} S_c (T_i^w - T_i^p)$
- Convection (PCM/water in top/bottom layers): $Q_{i-cv}^{p-w} = h_c^{p-w} S_c (T_{i\pm1}^w - T_i^p)$

During the phase change phenomena, the global heat transfer coefficient $h_g S_c = 1/(R_1 + R_2)$ through the shell of PCM capsule times the capsule area S_c can be obtained by applying thermal resistance method (see Fig. 4.4) where $R_1 = 1/(4\pi h_c r_{ext}^2)$

represents the thermal resistance by convection and $R_2 = (r_{ext} - r_{int})/(4\pi\lambda_p r_{ext} r_{int})$ is the thermal resistance by conduction. It's interesting to note that r_{int} and r_{ext} represent the interior and exterior radius, respectively, of the spherical capsules separating the PCM solid liquid interfaces during solidification and melting processes (see Fig.4.4). The external convective heat transfer coefficient $h_c = \lambda_w Nu/d_{ext}$ was obtained from an empirical correlation for Nusselt number proposed by Beek, 1962. This correlation is valid for big diameter, spherical particles layer of cubic arrangement suitable for energy storage applications and for $Re > 40$:

$$Nu = 2.42Re^{1/3}Pr^{1/3} + 0.129Re^{0.8}Pr^{0.4} + 1.4Re^{0.4} \tag{4.6}$$

where $Pr = \mu_w C_w/\lambda_w$ is the Prandtl number, $Re = \rho_w u d_{ext}/\mu$ is the Reynolds number and $u = \dot{m}_{load}/(\epsilon\rho S_b)$. The model adopted in this work is the result of an experimental study on a PCM (NaOAc, 3H2O) as reported by Zalba et al., 2003.

Even though it is not a question here of criticizing the type of modeling chosen, one can nevertheless specify that this method of apparent C_p^{app} is relevant when the whole phenomenon of melting (or solidification) is accomplished. The major problem of this method is encountered when the change of state is only partially realized, the approximation is then much larger.

Enthalpy method

This method introduces a source term in the energy equation to describe the progression of phase change in the PCM. Using this approach the liquid fraction of the PCM can be determined during the melting/solidification processes. In this work, the temperature and liquid fraction inside the PCM capsule were varying only in radial direction. The energy equation of the PCM can be expressed as:

$$\rho_p C_p \frac{\partial T^p}{\partial t} = \lambda_p\left(\frac{\partial^2 T^p}{\partial r_p^2} + \frac{1}{r_p}\frac{\partial T^p}{\partial r_p}\right) - \rho_p L_f \frac{\partial f}{\partial t} \tag{4.7}$$

where f and L_f represent the liquid fraction and the latent heat of melting of the PCM, respectively. The melting temperature T_m is chosen as the arithmetic mean between the solidus temperature T_S and the liquidus temperature T_L of the PCM. To determine the liquid fraction in the energy equation, the new source algorithm proposed by Voller et al. Voller, 1990 is used.

Initial and boundary conditions

The initial and boundary conditions were expressed as follows:

- Fluid: $T^w(z,0) = T_{ini},\ \forall z \in [0,L], T^w(0,t) = T_{in}\ and\ \lambda\frac{\partial T^w(L,t)}{\partial z} = h_a S_{ext}(T^w(r = R) - T_\infty),\ \forall t > 0$
- PCM : $T^p(r,0) = T_{ini},\ \forall r_p \in [0, r_{ext}], \frac{\partial T^p(r_p=0,t)}{\partial r_p} = 0\ and\ -\lambda_p\frac{\partial T(r_p=r_{int})}{\partial r} = h_g(T^p(r_p = r_{int}) - T^w),\ \forall t > 0$

As climatic conditions are required in the simulations, the average values of the incident solar irradiation on the solar collector system and the ambient temperature of the Moroccan climate zone 5 (Marrakech, 31°0.38′ N 7°0.59′ W) is presented in Fig. 4.6. Meteonorm platform (Version, 2010) was used to obtain the meteorological data which are intrinsic to the city of Marrakech in terms of ambient temperature and solar radiation flux.

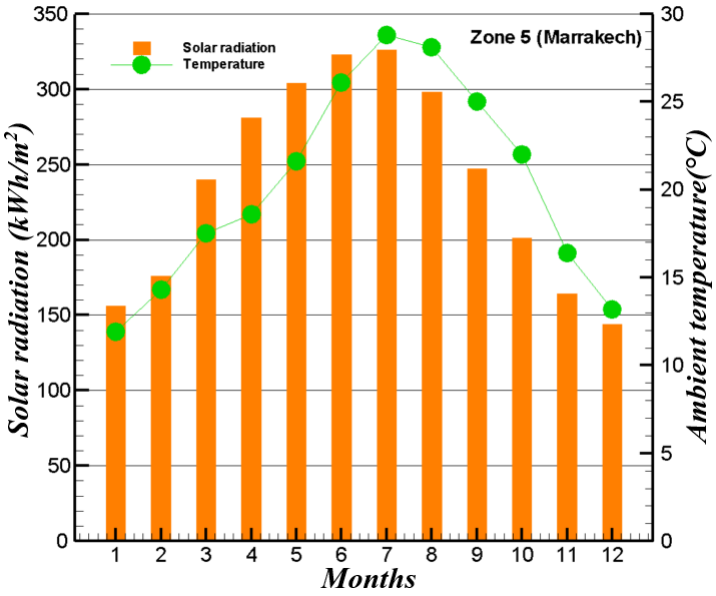

FIGURE 4.6: Marrakech's weather data considered in the simulations (Bouhal et al., 2018a)

We have estimated a domestic hot water consumption profile for a typical family of 5 occupants' residence. Our estimation is based on a simple user load profile that concentrates hot water consumption during three periods per day as shown in Fig. 4.7. For this profile, the overall daily requirement was normalized to 180l/day of water at a temperature of 45°C. The load profile corresponds to a consumption of 30 liters at 6 am for a 10 minutes of draw at a flow rate of 0.05 kg/s, 30 liters at 12 am for also 10 minutes of draw at a flow rate of 0.05 kg/s and 120 liters at 17 pm which represents 20 minutes of draw at a rate of 0.1 kg/s. The water from the tank is cooled with a cold water when its temperature is more than 45°C, and the auxiliary booster must be turn on whenever the opposite situation prevailed. All part models were performed in **Fortran** and the full system models were integrated in time for an entire year.

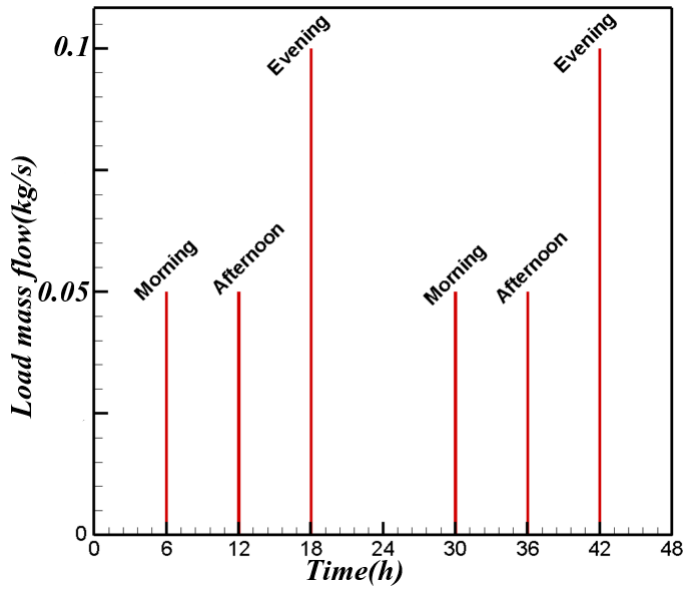

FIGURE 4.7: Hot water load profile

4.4.3 Numerical procedure

Basically, solidification and melting in the PCM transient phenomena, where the explicit schemes are too restrictive owing to stability limitations. Consequently, implicit schemes are usually privileged and the basic choice is the first order Euler scheme. The cell face values appearing in the convective fluxes were obtained by blending the central difference scheme and the upwind differencing scheme using the differed correction method. The sum of the fluxes through all the faces of a given control volume results in an algebraic equation which links the value of the dependent variable at the control volume center with the neighboring values. The energy equation may be expressed in a conventional manner as:

$$A_P\phi_P + A_E\phi_E + A_W\phi_W = B_\phi \tag{4.8}$$

The coefficients A_E and A_W consist of the contributions of the neighboring control volumes, arising out of diffusion fluxes and convection as defined in equations bellow. On the other hand, the central coefficient A_P includes the contributions from all the transient term and the neighbors. In some of the cases, where sources term linearization was applied, it also contained element of the source terms. B_ϕ contains all the terms those are treated as known (differed corrections, source terms and part of the unsteady term).

$$\begin{cases} A_E = \pi R^2\lambda_w/dz + \epsilon C_w(\dot{m}_{load} - \dot{m}_{coll}) \\ A_W = \pi R^2\lambda_w/dz + \epsilon C_w(\dot{m}_{coll} - \dot{m}_{load}) \\ A_P = \rho_w C_w V/dt + A_E + A_W + h_a(\pi R^2 + 2\pi RL) + h_g S_c \\ B_\phi = (\rho_w C_w V/dt)T_{ini} + h_a(\pi R^2 + 2\pi RL)T_\infty + h_g S_c T_p(r = r_{ext}) \end{cases} \tag{4.9}$$

In each control volumes, the values of the flow variables (liquid fraction, temperature,) at the outlet section of each control volume, are obtained by solving Eq. 4.8 from the known values at the inlet section and the boundary conditions. The solution method is carried out in this manner, moving forward by step in the flow direction. At each control volume, solutions for fluid flow and heat transfer in the PCM at particular time step were assumed converged if the relative errors between temperatures in two consecutive iterations for each layer of PCM capsule and for fluid were below convergence criterion given in Eq. 4.10:

$$\left|\frac{\phi^{k+1} - \phi^k}{\phi^k}\right| < 10^{-5} \tag{4.10}$$

where ϕ^{k+1} represents the dependent variables (temperature, liquid fraction) iteration $(k+1)$ and ϕ^k refers to their values at the previous iteration. The physical model was implemented based on **Fortran** platform. Environmental data for a typical meteorological year in selected Zone 5 (Marrakech, Morocco) were taken from the meteorological software Meteonorm. The overall solution procedure scheme is presented in Figs. 4.8.

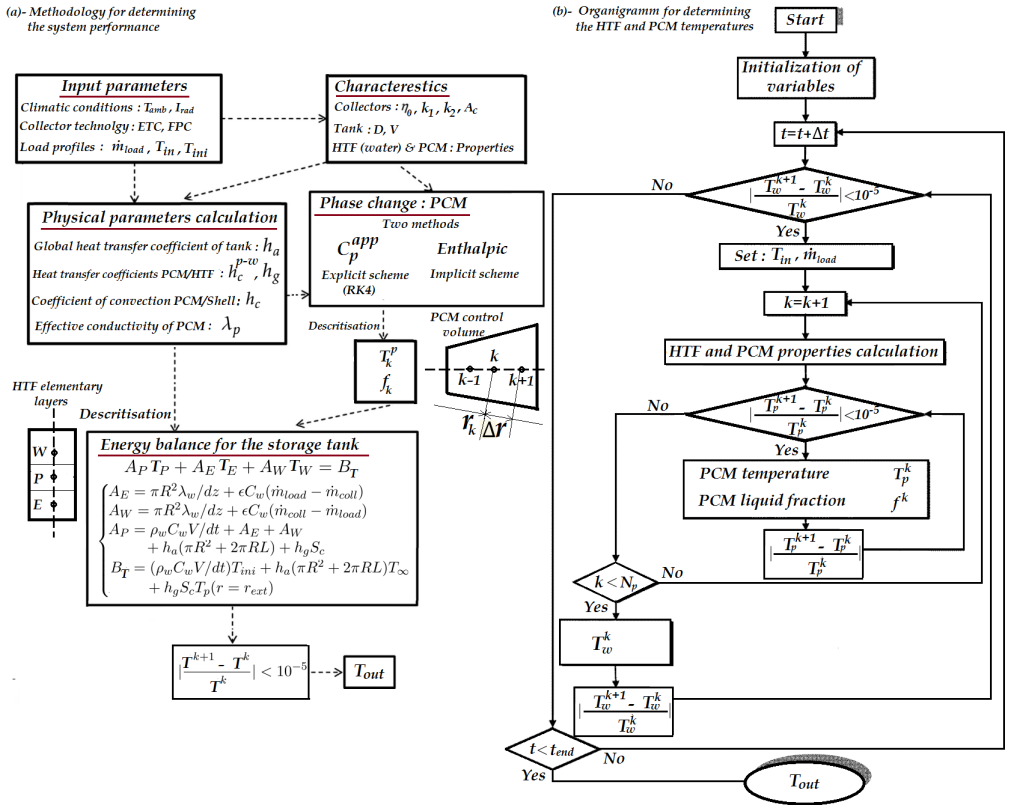

FIGURE 4.8: The overall solution procedure scheme for determining the HTF and PCM temperatures and liquid fraction

4.5 Mesh and time steps independence test

Transient numerical simulations were performed to compare the enthalpy method results against the technique of the specific apparent heat capacity to simulate the PCM melting process and its interactions with water inside the storage tank. The Runge Kutta 4 scheme is used for C_p^{app} method and the finite volume is employed in Enthalpy method for the discretization of the energy equation.

4.5.1 Grid independent test results for different grid sizes

A structured grid has been used to mesh the inside of the vertical thermal storage tank. The mesh independence test has been carried out to limit the number of the grid elements and thus the CPU calculation time (Almohammadi et al., 2013). In the multinode approach, the tank is modeled as N fully mixed volume layers (nodes) as it was used in the current implementation of *Transient System Simulation Tool (TRNSYS)*. The mesh topology of the discretized fields is presented in Fig. 4.9. The storage tank segments are enough small to catch the flow structure.

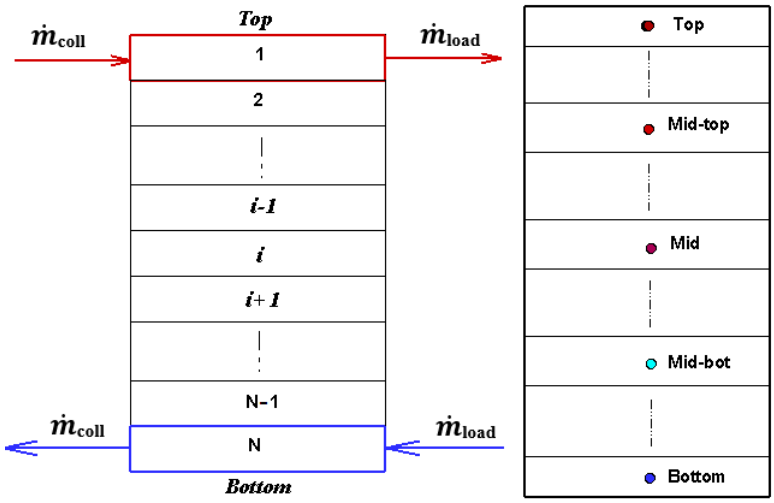

FIGURE 4.9: Structured mesh grid of the storage tank

A one-dimensional dynamic mode of solar water heating system with PCM was simulated which consists of a tank at an initial uniform cold temperature of 25°C. The hot water at 45°C and flow rate of 0.1 kg/s is delivered at the top of the tank as the discharging started according to load profile in Fig. 4.7. Thus, a thermocline formed along the hot and cold region interface and was advected downwards at the mean fluid flow rate within the tank. The tank height and diameter were set to 1.2 m and 0.4m respectively, and the heat losses through the tank were considered via the heat transfer coefficient h_a. The fluid properties used for the simulations were determined at the average water temperature, 25 °C. The results of the simulations for a varying number of nodes are shown in Fig. 4.10. The top layer temperature vs time for various number of nodes were plotted for 48 hours. The temperature profiles indicate that the number of elements has a large effect on the numerical results and on divergence of temperatures values especially when $N = 20$ segments while for $N \leq 15$ we can observe a good trend in temperature values (a difference less than 1 °C especially during night). A maximum number of 15 nodes can be chosen in the current implementation of *Transient System Simulation Tool (TRNSYS)*. Indeed, Kleinbach, Beckman, and Klein, 1993 have investigated several one-dimensional storage tank models. Relationships for determining the recommended number of nodes regarding the respect of stratification condition were determined from comparison with experimental data for a wide range of conditions. The tank was divided into 20 equal-height layers which is enough to obtain a rational accuracy.

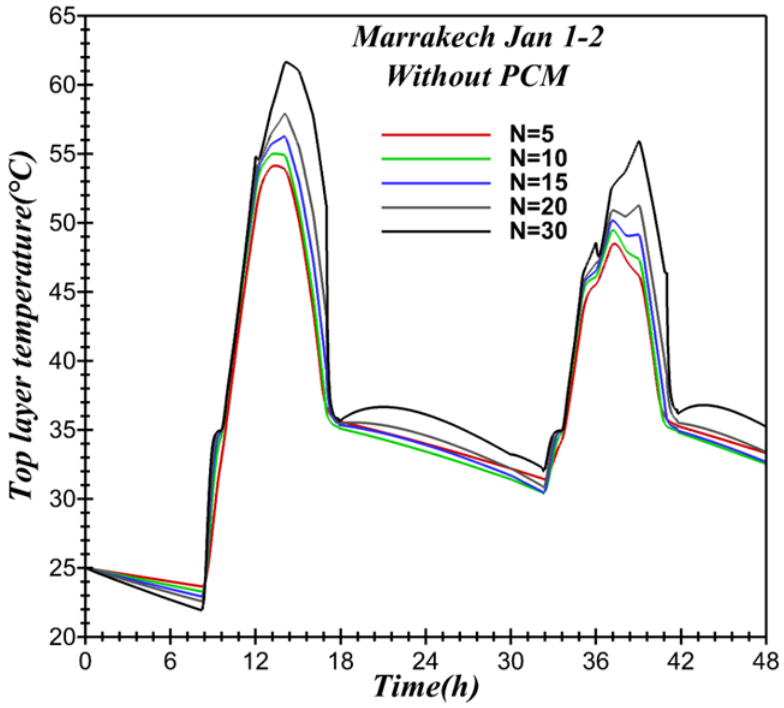

FIGURE 4.10: Effect of nodes number on the temperature evolution inside the storage tank without PCM

According to the literature reports, the degree of stratification is determined by the choice of the number of elements N. Higher values of N ($N > 20$) result to a non respect of thermal stratification where the temperature values increase from bottom to top of the storage tank. In the current investigation, a maximum number of 20 layers ($N = 20$) is chosen to respect the condition of stratification inside the storage tank as recommended by Kleinbach, Beckman, and Klein, 1993.

4.5.2 Time independent test results for different time steps

To conduct a rationally precise statement of the time step condition, it is required to define a time step which describes the evolution of the PCM liquid fraction and the temperature evolution inside the storage tank for 24 hours in dynamic mode. In all the simulations that were carried out, the storage tank was divided into 15 equal-height layers. According to a relevant opinion a great number of stratified segments required in order to get high accuracy. Thus, unsteady simulations were conducted to model the heat transfer phenomena inside the vertical storage tank filled with PCM and its melting process. However, before starting the numerical investigations, a time step sensitivity analysis was performed in order to provide its independency from the simulation results. To conduct this independence test, five time steps were used: Δt = 15s, Δt = 30s, Δt = 45s, Δt = 60s and Δt = 75s.

In order to check the influence of the time step on the accuracy of simulation results, simulations with several time steps were carried out. The setup of $\epsilon = 30\%$ PCM was used to perform a complete annual simulation with 15, 30, 45, 60 and 75 s. The top layer temperatures were plotted in 48 hours for C_p^{app} and Enthalpy methods for different time steps. Comparison is shown using the tank's top layer temperature and two days results for top layer storage tank with PCM (including both C_p^{app} and Enthalpy methods) are shown in Fig. 4.11.

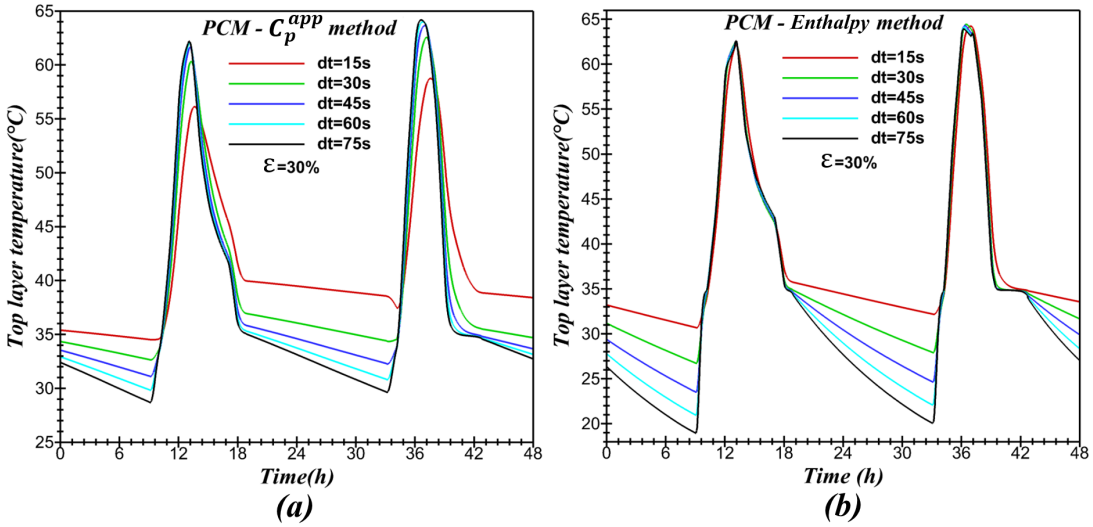

FIGURE 4.11: Time step independence test for both Enthalpy and C_p^{app} methods

The temperature profiles indicate that the time step size has a large impact on the simulation accuracy especially during the night when there is no insolation. For each simulation, the integrals of energy transport were computed to yield the total amounts of energy delivered from the collector, delivered to the load, lost to a surrounding and provided by the auxiliary heater. It was assumed that the temperature values obtained in the case of 60 s are the most suitable because this time step allows to simulate the behavior of full system over taking into account the meteorological data and the interaction between water and PCM inside the storage tank. The number of numerical iterations per physical time step was 60 (Balduzzi et al., 2016). All subroutine models were performed in **Fortran** and the global system model was combined with time for an entire year.

4.5.3 Numerical model validation

As previously mentioned, two numerical methods (Enthalpy method and C_p^{app}) were developed and compared to show their superiorities and limits when simulating the phase change phenomena of PCM inside solar storage tank. Talmatsky and Kribus, 2008 have performed a physical model to describe the heat storage tank with and without PCM. Annual simulations were done to compare the performance of a storage tank with PCM to a standard tank without PCM. Fig. 4.12 illustrates the schematic layout of the physical model adopted by Talmatsky and Kribus, 2008 that consists of a storage tank with PCM, collector, pump, controller and auxiliary heater. The aim is to compare our developed numerical code with that one constructed by Talmatsky and Kribus, 2008 to validate our numerical simulations. Thus, the mathematical model based on the one reported in the work of Talmatsky and Kribus, 2008 is considered and the same realistic meteorological data and the typical end-user needs are imposed.

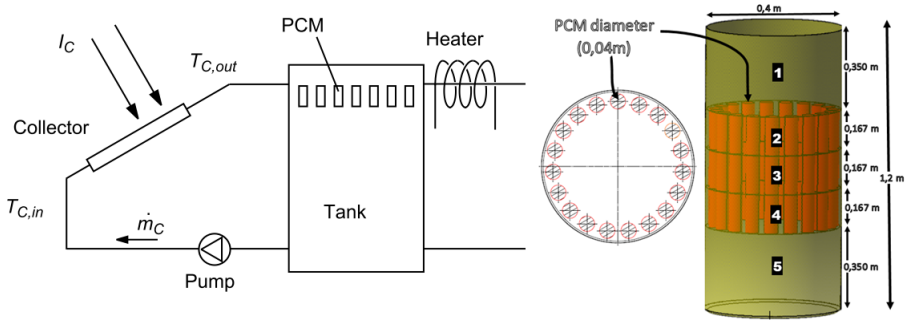

FIGURE 4.12: Layout of the solar hot water system with PCM adopted by Talmatsky and Kribus, 2008

The specific apparent heat capacity C_p^{app} technique has been successfully validated with the work of Talmatsky and Kribus, 2008 who have performed a physical model to describe the heat storage tank with and without PCM. They carried out annual simulations to compare the performance of a storage tank with PCM to a standard tank without PCM. Annual simulations were carried out to validate our numerical results against the achieved results of Talmatsky and Kribus, 2008. The physical model of Fig. 4.12 is reproduced and the transient simulations are launched. In order to illustrate the temperature evolution inside the storage tank, Fig. 4.13 presents the 2-days (January 30-31) temperature history of the top layer of the tank filled with PCM (NaOAc-H2O). The temperature drops seen in that figure at 6 am, 12 am and 5 pm are due to the hot water consumption profile load. As expected, during the afternoon, when there is no insolation, there is a reheating of water resulting from heat transfer from the PCM to the water. A slight relative errors are observed and a qualitative accordance is noticed which proves that our results are in a good agreement with the numerical simulations carried out by Talmatsky and Kribus, 2008.

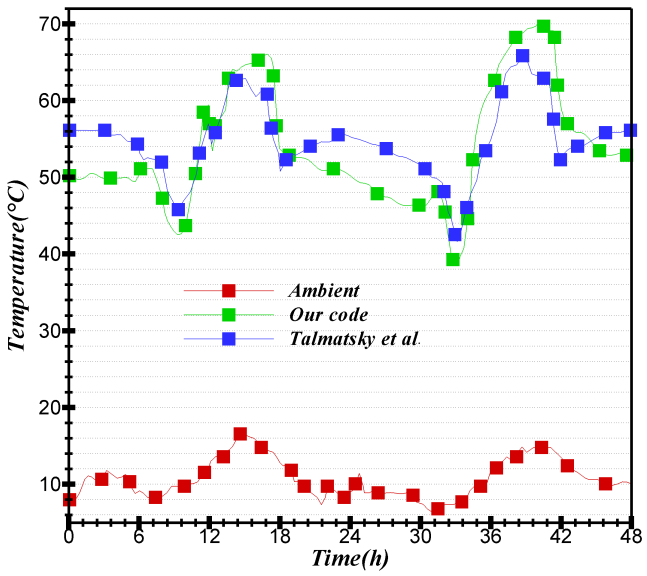

FIGURE 4.13: Validation curve: Solar water heating system with PCM (NaOAc, 3H2O, see properties Table 4.2), 2-day temperature evolution of the top layer in the tank

In another hand, the Enthalpy method has been used by Kousksou and Bruel, 2010 when they evaluated numerically the encapsulation of phase change material

under cyclic pulsed heat load. We focus here on the comparison of the both numerical methods (Enthalpy method and C_p^{app}) under realistic boundary conditions involving the simulation of PCM integration inside the solar water heating systems for solar cooling applications.

4.6 Results and discussion

In this section, the results of two numerical methods (C_p^{app} technique and Enthalpy method) described previously are presented. These methods were used to simulate the PCM melting and the temperature evolutions inside the storage tank. Thus, a set of important parameters such as temperature profiles and liquid fraction were drawn as indicators to numerically compare these two methods and the predicted enhancement of the energy storage tank and the possible increase in its thermal performance.

4.6.1 Temperature evolutions

To examine the thermal behavior of the system, Figs. 4.14 present the temperature evolutions inside the storage tank. Indeed, Figs. 4.14-(a) and (b) depict the temperature inside the storage tank filled with PCM using C_p^{app} and Enthalpy methods and Fig. 4.14-(c) show the temperature history inside the storage tank without PCM. For a rational analysis, two successive days of winter (January 1-2) relative to the Moroccan city Marrakech are considered. Representative numerical tank temperatures plotted in these figures show very definite stratification for all configurations.

Indeed, Figs. 4.14 present the 48-hours evolution of the ambient temperature, top, bottom and other layers temperatures of the solar tank and outlet temperature from the collector for FPC technology. During these two days, it is interesting to mention that the ambient temperature has a low annual values. During the night, the ambient temperature decreases from 20°C to 10°C while during the morning it goes up gradually to reach its maximum daily value of 23°C and decreases during the evening. In addition, the collector outlet temperature follows the trend of the ambient temperature and the incident solar radiation. As illustrated in Figs. 4.14, it is important to note that the solar water tank temperatures, i.e. outlet collector and different tank layers, drops when the consumption profile load are present at 6h, 12h and 17h. This phenomena is clearly apparent in the case of C_p^{app} and Enthalpy methods at 12h. During the afternoon, the temperature of the top layers in the tank with PCM (C_p^{app} and Enthalpy methods) has approximately the same profile than that observed without PCM (see Figs. 4.14-(a), (b) and (c)). After 17h, i.e. overnight when there is no solar radiation, we observe that the top layer temperature in case without PCM decrease roughly while there is an opposite situation in the both cases with PCM as a result of heat transfer from the PCM to the water and the values of temperature in the collector in the storage tank with PCM (C_p^{app} and Enthalpy methods) become slightly higher than in the case without PCM. A such situation is in qualitative accordance with that reported by Kleinbach, Beckman, and Klein, 1993.

It is interesting to note that the introduction of PCM in solar domestic hot water systems and their beneficial fact has to be considered with great attention. Indeed, the PCM (NaOAc, 3H2O), used in the current work, has a melting point in a small temperature range around 60 °C. During January 1-2 when the insolation and ambient temperature are low, the temperatures in the storage tank are often below the

phase change temperature level and most of the time both systems (without and with PCM) store energy as sensible heat only. Consequently, the PCM is far from being completely utilized. It's necessary to find a suitable PCM melting point taking into account the specific weather climate of the site over the year.

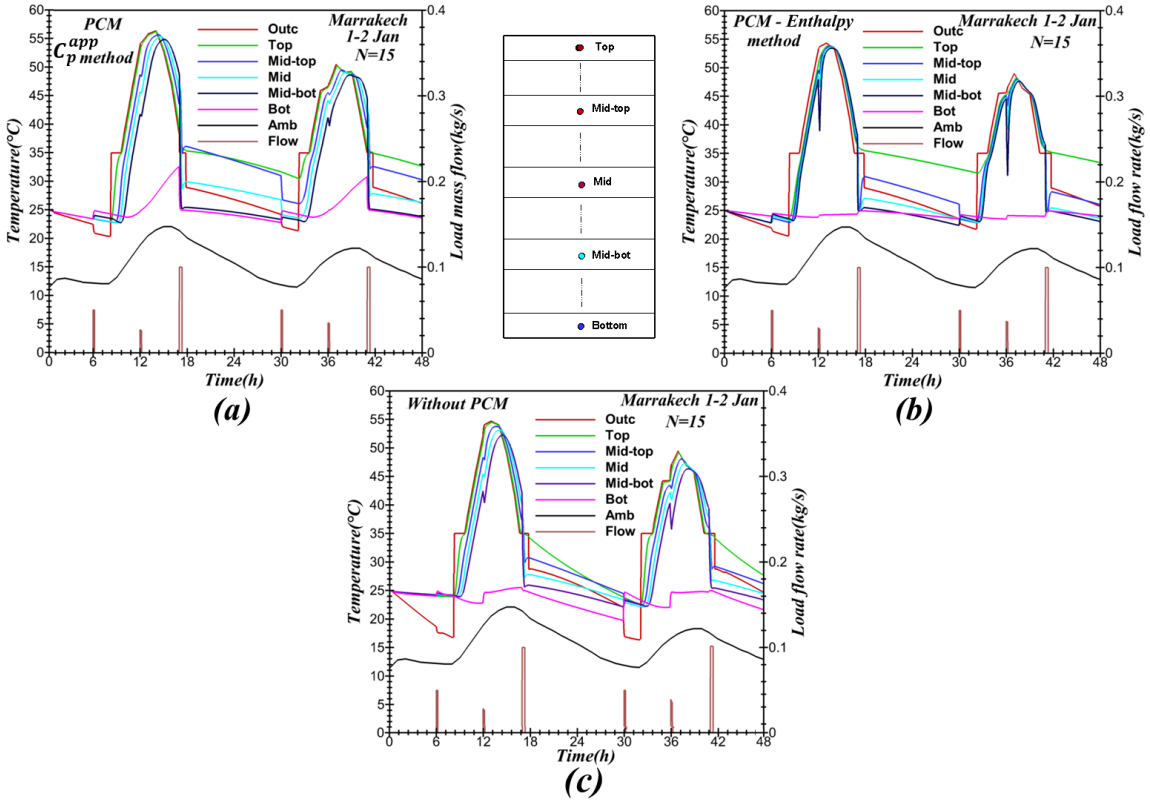

FIGURE 4.14: Temporal evolution of temperatures inside the storage tank for different cases

In order to examine the influence of meteorological data on the system performances, another day of the year (July 1) is evaluated. Fig. 4.15 shows the evolution of water outlet collector, top layer and PCM temperatures during the first day of July in the same location (Marrakech-Morocco). Accordingly, simulations were carried out with the same type of PCM whose melting temperature around 60 °C and the Enthalpy method is used. The effect of PCM is well observed, which limits the water temperature drop. It should be noted in this case that all of the PCM is melted during the heating period and then again solidified over the high night period, the changes of state corresponding to the temperature step presents at the melting temperature of the PCM 60 °C. Fig. 4.15 indicates a reheating of water overnight even if there is no solar radiation as a result of heat transfer from the PCM to the water and the temperatures in the storage tank with PCM become higher than in the case without PCM. As can be seen in Fig. 4.15, the top layer temperature is characterized by a higher and a quasi-constant temperature level which is apparently due to the stationary reheating of the water because of the solidification process follow up by the PCM.

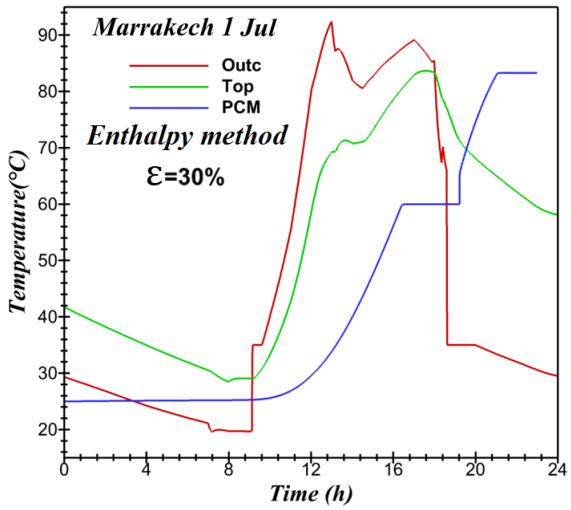

FIGURE 4.15: Temporal evolution of collector, PCM (middle of the tank in PCM center) and tank top layer temperatures

The results of the water temperature along the tank height for the studied cases at $t = 25$ h under different heat losses coefficients (The reference value is $h_a = 1.133$ W/m^2K) are presented in Fig. 4.16. These figures (Figs. 4.16-(a), (b) and (c)) describe the temperature variation along the longitudinal direction for three heat loss coefficients ($1/2 \times h_a$, h_a and $1/2 \times h_a$) for two cases of the tank filled by PCM using C_p^{app} and Enthalpy methods in addition to the case without PCM. For all configurations, we can observe that the tank bottom temperature is lower than the top layer thanks stratification effect. Moreover, the temperature decreases when the h_a is increased due to heat losses to the surrounding. Similar behaviour of internal temperature maps is observed in both cases i.e. C_p^{app} and Enthalpy methods even if we note a slight difference in temperature values which is due to numerical scheme used in the both methods. However, the temperature level inside the storage tank using PCM is higher than the case without PCM which is due to reheating by the PCM during the solidification process.

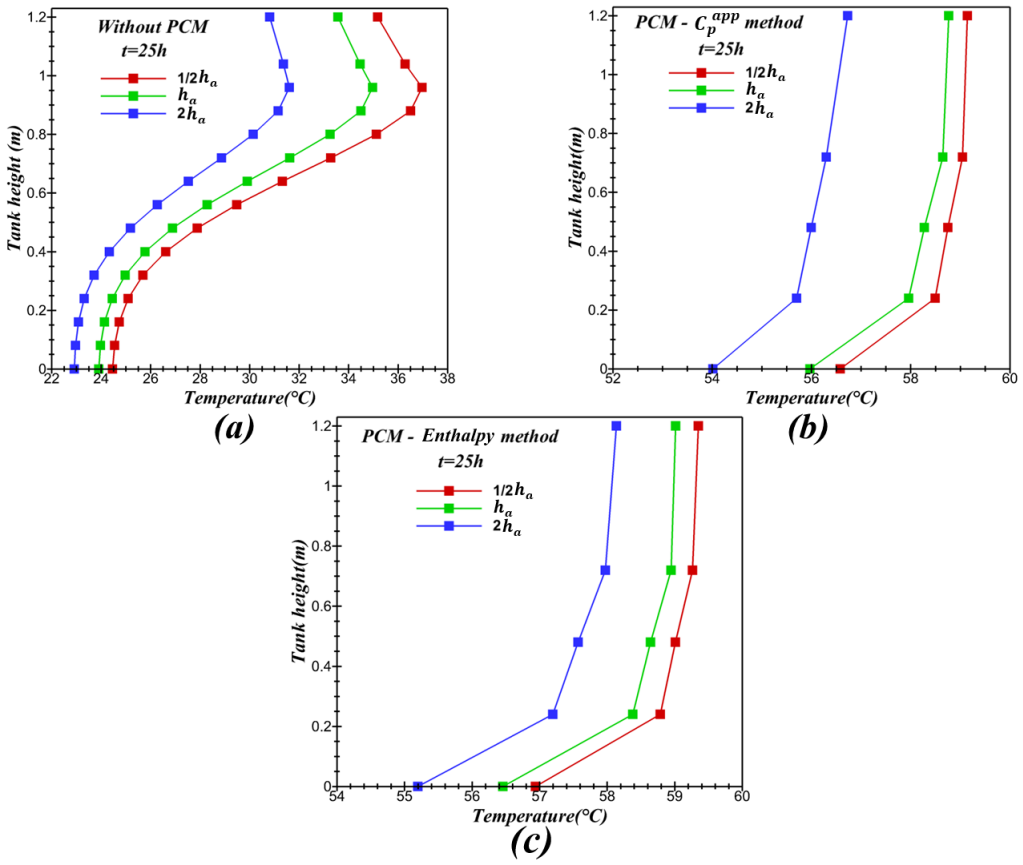

FIGURE 4.16: Temperature evolution along tank height

4.6.2 Liquid fraction

One of the main limits of the method of apparent heat capacity C_p^{app} is that doesn't allow access directly to the liquid fraction values. For this reason, we content to present only the liquid fraction curves for the case of the Enthalpy method. Figs. 4.17-(a) and (b) show, respectively, the PCM temperature and the variation of the liquid fraction (the percentage of the PCM which has been melted) and the impact of PCM portion ϵ on melting process vs time. From Fig. 4.17-(a), we can observe that at $t = 0$ min all the PCM inside the storage tank is in solid state so the melting fraction is zero. As the time passes, the PCM gets melted because of water heating from solar collector and the value of melting fraction increase with time from 16 h when the water temperature achieved 60 °C which is the PCM melting point. The value of melting fraction is 50% for the melting time of 18 h. At the end of the melting cycle i.e. after 20 h, all the PCM inside the storage tank has been melted; giving a melting fraction of 100%. As the PCM are considered as a spherical capsules, it is noticed that the rate of melting is not the same inside the capsule ($r = 0$) and in the PCM/water interface ($r = r_{ext}$). Indeed, the melting process increases for $r = r_{ext}$ faster than $r = 0$ because the PCM is in direct contact with hot water inside the storage tank (see Fig. 4.17-(a)). Tores et al., 2013 also simulated the behaviour of a packed bed latent heat thermal energy storage system connected to solar collector located in south of Spain. Their obtained results show a similar melting trend of PCM.

Fig. 4.17-(b) represents the PCM temperature (T_{pcm}) evolutions vs time (24 h) for various proportions ϵ of the tank volume occupied by PCM. In the literature,

the suggested amount of PCM in the storage tank varies greatly from about 5% to near 75% of the tank volume (Mehling et al., 2003). It is seen in Fig. 4.17-(b) that, when the temperature inside the storage tank reaches 60 °C, the PCM starts melting. Moreover, the evolution of temperature decreases when the PCM quantity (ϵ) is enhanced. Indeed, the amount of PCM (10–50%) corresponding to an increase in heat storage capacity relative to that of water alone and to an enhancement of heat losses. As expected, the increase in amount of PCM leads to a decrease in melting velocity.

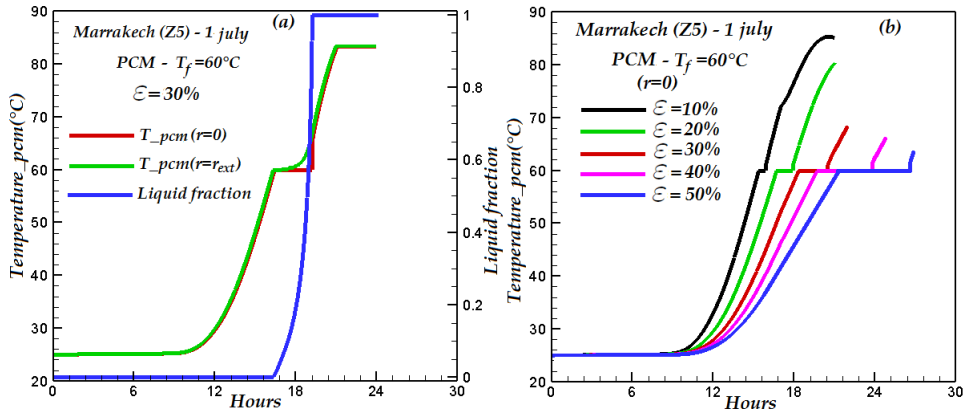

FIGURE 4.17: PCM liquid fraction and its temperature evolution for different PCM portion ϵ in the tank's middle

4.6.3 Impact of PCM proportion on storage top tank temperature

A point not to be overlooked is in the packaging of PCM. The PCM are encapsulated in spherical nodules inside the storage tank. Indeed, the spherical encapsulation is a geometric configuration, a priori, optimal insofar as it directly impacts the storage capacity of the tank, so the amount of possible heat transfer and the exchange surface between the water and the PCM.

The amount of PCM in the storage tank suggested in the literature varies greatly, from about 5% to near 75% of the tank volume (Talmatsky and Kribus, 2008). As previously mentioned, four volume proportions of PCM (20-50%) were examined inside the storage tank connected to the solar collector in order to study their effect on the latent energy storage improvement.

The evolution of the top layer temperature of the tank vs time (the first hot day of July in Marrakech city) is presented in Fig. 4.18. Four volume proportions of PCM were examined inside the storage tank connected to the solar collector in order to study their effect on the latent energy storage improvement (Lu, Zhang, and Chen, 2018). The PCM amounts used are $\epsilon = 20\%$, $\epsilon = 30\%$, $\epsilon = 40\%$ and $\epsilon = 50\%$.

As shown in Fig. 4.18, the top tank layer temperature connected to the consumer load is enhanced for a PCM fraction equal to 20% for both the investigated models, namely, the C_p^{app} method besides to the Enthalpy method.

The melting time of the PCM is important when the volume it fills inside the tank is important too (we are referring here to the used 50% of tank volume), because it requires a supplement of energy from the storage tank, which in parallel tends to decrease because of the loading demand performed by the consumer. On the other hand, an optimized volume fraction of the PCM (30%) tends to melt faster, because the hottest layer of water is located at the top according to the development of thermal stratification occurring inside thermal storage tanks subjected to charging and discharging cycles (Bouhal et al., 2017b). The optimized used PCM proportion will

work as an energy booster, hence it is going to provide its latent heat when there is no insolation. Indeed, this energy helps to heat the water during night or when solar radiation is not sufficient. The C_p^{app} method overestimates the top layer temperature of tank, where various PCM amounts are located. In fact, between midnight and 8 am the temperature is decreasing from $40°\mathrm{C}$ to $28°\mathrm{C}$, while it is maintained constant at $28°\mathrm{C}$ during the same cold time interval for the Enthalpy method. The same remark can be made regarding the other cold time interval that spans between 6pm and 12pm, where the top temperature layer of the tank decreases from $75°\mathrm{C}$ to $60°\mathrm{C}$ using the C_p^{app} , and from $75°\mathrm{C}$ to $50°\mathrm{C}$ using the Enthalpy method.

Including 40% and 50% of PCM in the storage tank have a slight effect on the performance of the solar water heating system. In addition, the cost of the PCM is high and a high PCM fraction is not practical because the heat losses will increase. The simulations in this work were carried out with 30% of the tank volume occupied by PCM. A 30% of PCM amount is considered a reasonable compromise.

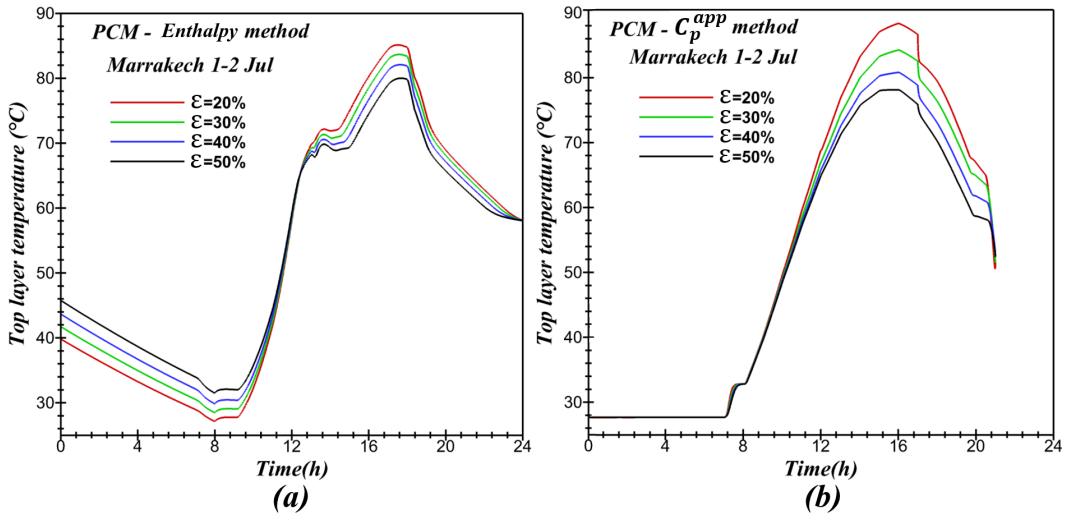

FIGURE 4.18: Effect of PCM quantity ϵ on top layer temperature evolution

4.6.4 Impact of heat losses on storage tank temperature

The effect of three values of the heat loss coefficient, namely, $1/2h_a$, h_a and $2h_a$ on the top layer temperature evolution of the storage tank is presented in Figs. 4.19, according to the first hot day of July reported in Marrakech. The heat loss coefficient ($2h_a$) induces a significant loss compared to both $1/2h_a$, h_a (see Fig. 4.19-(a)) in case of Enthalpy method is applied. For instance, at 6pm the top layer temperature difference between $1/2h_a$ and h_a is estimated equal to $15°\mathrm{C}$. On the other hand, the C_p^{app} method does not really affect the evolution of top layer temperature, as it is presented in Fig. 4.19-(b) during the interval [12pm; 2pm]. After 2pm, the difference in the top layer temperature is not very large, whatever the heat loss coefficient applied to the external circumference of the storage tank.

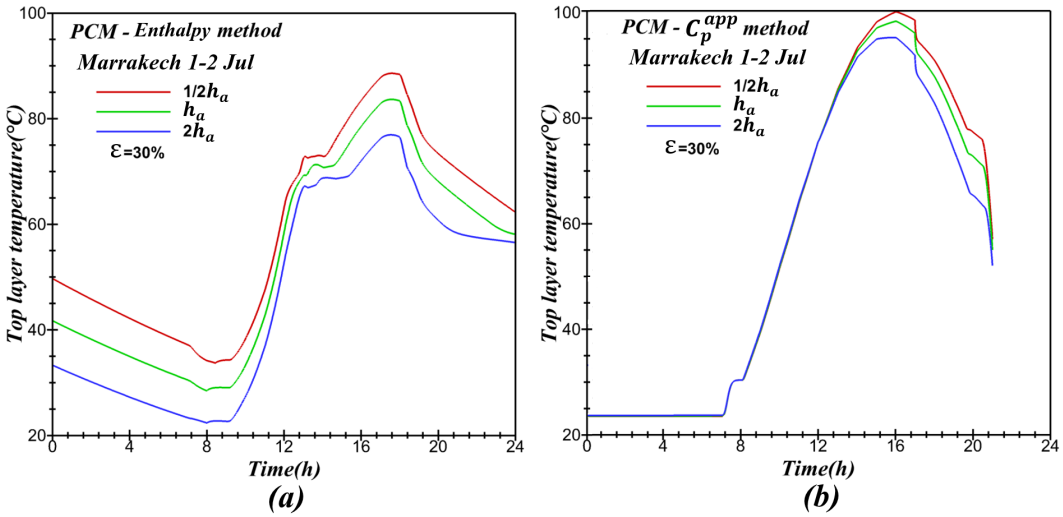

FIGURE 4.19: Effect of heat losses h_a on top layer temperature evolution

4.6.5 Impact of collector technology on its outlet temperature

The outlet temperature from the collector of the solar water heater during the first hot day in July is presented in Fig. 4.20. The weather of Marrakech (Morocco) has been used as solar boundary conditions inputs to assess the effect of the C_p^{app} and Enthalpy method on the melting of the PCM. It is noted that three collector technologies were studied, namely, FPC, CPC and ETC collectors.

It is noted from Fig. 4.20 that the Enthalpy method slightly overestimates the outlet temperature Bejarano et al., 2018 between midnight and 8am. Indeed, this temperature drops from 20 degrees to 5 degrees using the apparent specific heat method (C_p^{app}). While it drops from 30 degrees to reach 20 degrees using the Enthalpy method. When the solar irradiation becomes important (between 8am and 4pm), it is found that the outlet temperature of the heat transfer fluid from the collector becomes important independently from the collector technologies. In fact, the energy contribution of ETC collector is significantly greater than that of the FPC and CPC collectors (Bouhal et al., 2017a). In addition, the Enthalpy method compared to the apparent specific heat method (C_p^{app}) has several peaks identified during several sub-intervals. In particular, between 1pm and 2pm, 3pm and 4pm and finally between4pm and 6pm. At approximately 8pm, the outlet temperature from the collector reached 35 degrees using the Enthalpy method, while it reached 30 degrees using the C_p^{app} method. It is concluded that the C_p method overestimates the heat transfer fluid outlet temperature regardless of the collectors technology used, such as FPC, ETC or CPC.

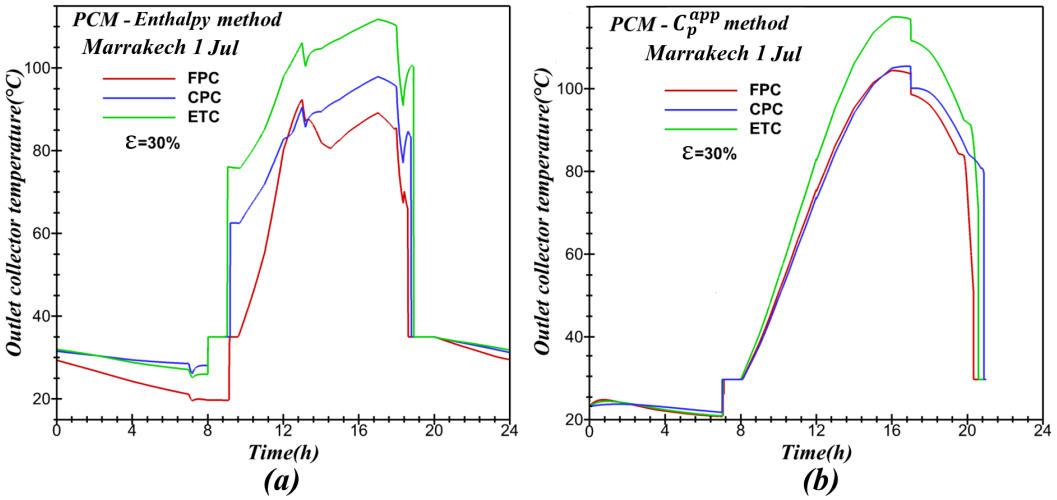

FIGURE 4.20: Effect of collector technology on its outlet temperature evolution

4.6.6 Optimization, models improvement and recommendations

Before even discussing possible ways to improve the both models, it is useful to be interested in common sense issues. It should be noted that the good functioning and the relevance of the models developed in this study depend on many conditions such as the geographical areas of implantation of such systems (rate of sunshine), the security and health standards (Hot water at 45 °C in Morocco, case of this study, but 60 °C in France for example), etc. Through this work, some possible improvements are summarized in the following points:

Improvement of the models

A set of suggestions are drawn for improving the studied numerical methods. For instance, the division of the tank in N layers is sufficient or not for a correct modeling of the whole of the tank. In addition, the both methods are based on 1D model where the water temperature depends only on the height (z) while it depends also on the radius r especially when the shape ratio D/L is high.

Physically, the apparent heat capacity C_p^{app} method is used to investigate the phenomenon of phase change. Indeed, this method is not widely used insofar as it is considered that when the phase change is not complete, the error on the C_p can be important. In fact, the C_p varies enormously over the change of state interval. Moreover, the exact melting or solidification temperature over this interval is probabilistic. Thus, a systematic error exists on the estimate phase change temperature, and this error, as small as it is, generates a not insignificant approximation at the level of the specific heat. This is why the apparent C_p method is not unanimous. We are therefore entitled to question the accuracy of this method of determination. Other techniques such as the phase change interface tracking method exist, but are they more relevant? The question is at the center of current research.

Load consumption conditions also play a major role in the efficiency of the system. To resume the model, the hot water is drawn here at 45 °C. On the one hand, the choice of PCM whose temperature of change of state occurs at 60 °C seems debatable. Thus, latent heat storage should be at a temperature close to that desired for water distributing, so a choice of a melting temperature of about 35 °C would have been preferable. On the other hand, the operation of an installation like the

one studied certainly finds its full dimension in terms of efficiency for DHW distribution temperatures rather between 60 °C and 90 °C. Indeed, the profitability of the system for a DHW load temperature of only 45 °C seems limited.

PCMs conditioning and selection

It is necessary to study the characteristics of the different PCMs that exist to evaluate the selection criteria that most suited to the operating conditions of the system. The factors that playing a major role in the profitability of the installation are:

- Moderate cost;
- Phase change temperature range suitable for use;
- PCM that does not supercool (or very little) during phase change;
- High sensible and latent heats;
- High thermal conductivities in both solid and liquid phases;
- High mass heat capacities in both solid and liquid phases.

The challenge here is to find the best suited PCMs. Melting temperatures are one of the most important parameters since they not only maximize energy storage in latent form but also regulate the temperature of the water in the tank so as to minimize the heat losses dissipation through it.

Systems operating with the simultaneous use of several PCMs in the tank appear to be more effective than when there is only one. In fact, at the level of the tank loading profile, the stack of different PCMs with different melting temperatures may stratify the storage tank and obtain better yields than in so-called "conventional" systems. Here, the gravity that causes the separation of hot and cold water. A temperature gradient is then established within the tank. The temperature variations that are established step by step are small, but in the case of small changes in temperature, the latent storage is much more interesting than the sensible storage. In addition, since the temporal evolution of temperature at the top of a stratified tank is very small, it is thus possible to "stick" to the user's temperature, thus limiting the use of the auxiliary electrical resistance.

A study on the interest of a stratified system (Cabeza et al., 2006) shows an increase in storage energy density from +20% to +45%, an increase in the duration of thermal diffusion through the tank of +50% at +200%, and the significant water heating related to the presence of PCM. It should be noted that the performance of a stratified system essentially depends on:

- Position of the inlets and outlets of the tank
- Conditions at the inlet and outlet levels
- Conduction and losses in the tank

In addition, a reflection at the level of the distribution PCM within the tank layers is to lead. In some type of systems, the entire PCM are put at the top of the tank. This technique, different from our models in which the lower and upper layers are considered lack of PCM, justifies the fact that an optimization of the system in terms of proportion and positioning of the PCM is to be expected.

Optimization and sizing of the system

Regardless of the sizing, the tank must be insulated to minimize heat losses. The loading profile of the tank should ideally be chosen so as to optimize the ratio of the volume of PCM to the volume of water contained in the tank. For a given volume of the tank, what volume proportion of optimal PCM is to put in the tank? It is the same with regard to the ratio of the volume of PCM on the exchange surface between water and the PCM which conditions the heat exchange potential and therefore the energy storage capacity. For a given volume of PCM and exchange surface, what is the best choice: put in the tank hundreds of small nodules? Dozens of nodules of average size? Some large nodules?

In order to carry out a thermo-economic study, the optimization of the quantity of PCM used is essential. This is indeed the key element of the system in terms of energy storage capacity of the tank but also in terms of cost, the price of PCM is high or very high since it's difficult to prepare. The ideal compromise is to be determined (in ratio form for example) in order to be in possession of a tool to size the best possible tank regardless of the parameters imposed. For instance, for a tank of dimensions given by the manufacturer, we multiply the volume by the calculated ratio and we obtain the volume of PCM to put in the tank. Then, we study the best possible arrangement that combines both the diameter and the number of PCM nodules.

4.7 Conclusion

In this chapter, two numerical heat transfer models were developed and compared to investigate thermal storage tank filled with encapsulated PCM connected with solar collectors for solar hot water production. These models were built to model operating cycles of the solar water heating systems under a realistic climate zone (Marrakech, Morocco). One of the methods was based on the technique of apparent heat capacity C_p^{app} while the second used the Enthalpy method which question the relevance of the use of PCM as a medium of storing energy inside storage tank for solar hot water production.

The main target was to compare both programs by studying different operating conditions. The used numerical methods indicate that a margin of progression still exists. The differences observed can be explained by the existing uncertainties in the determination of certain operating conditions and the definition of the geometry of the physical model. Therefore, we have reformulated hypotheses and selected substitution conditions by ensuring that they have an internal coherence and respect the relevance of the model. Nevertheless, additional research will be needed to overcome the inconsistencies of the model we have relied upon. The non-determinism of the phase change phenomenon gives rise to many inaccuracies, such as the evaluation of the apparent specific heat capacity C_p^{app} which needs experimental equipments and measurements to find the shape of specific heat evolution. The solution may lie in conducting dispersion studies on such phenomena.

In addition, we are indeed able to question the universality of such a system. In the context of domestic use, it seems rude to assume that everyone would stock and destock the solar hot water at the same time of the day. In this hypothesis, the efficiency of the system becomes very variable according to the consumption load profile. The introduction of automated "smart systems" to choose modes of operation or regulation, and the establishment of servo systems functions of operations

conditions and meteorological data could constitute possible avenues of improvement and technical solutions interesting to develop the system.

Based on the analyses of the results, the conclusions drawn from this numerical study can be summarized as:

- The heat transfer model using Enthalpy method needed more computing time than the apparent heat capacity C_p^{app} model.
- The C_p^{app} technique is relevant if the form of the specific heat capacity of the PCM is known during the phase change process.
- Further studies need to be conducted to improve the optimal position of PCMs inside the storage tank. In practice, some industrial companies choose the option to put the entire PCM at the top of the tank which is different from our proposed models in which the lower and upper layers are considered lack of PCM, justifies that an optimization of the system in terms of proportion and positioning of the PCM is to be expected.
- It seems that the question of the interest of PCMs in domestic hot water production systems does not admit of a trivial answer and that this will probably be depending on the system and consumer habits. This work must nevertheless be continued to address the case of solar operation and the influence of other parameters introduced in the model.

The presented models were used as a development tool for optimal selection and improving the performance of solar cooling systems integrating PCM modules under various operating conditions for thermal energy storage enhancement which is the objective the next chapter (Chapter 5).

Chapter 5

Energy analysis and thermal performance assessment of solar cooling systems integrating PCMs in Morocco

5.1 Introduction

As highlighted in Chapter 4, two numerical methods were developed and used to simulate the Phase Change Materials (PCMs) integrated in solar hot water production systems. In Chapter 5, the developed numerical models are used now to simulate the role of PCMs addition inside solar cooling process. Accordingly, Chapter 5 focuses on latent thermal energy storage and the integration of PCMs within the solar cooling systems and their thermal performance optimization. The role of PCMs addition is investigated inside solar storage tank connected to the generator of the absorption chiller in order to optimize the thermal energy storage in dynamic mode.

5.2 Background

Thermal energy storage has been shown to enhance the efficiency of solar hot water and absorption air-conditioning systems by capturing excess radiation during peak hours to meet cooling need in low insolation periods. The limited operating temperature range of solar cooling systems limits the water energy density because it is the most commonly used thermal storage medium in solar cooling applications. Conversely, Phase Change Materials (PCMs) keep a high energy density under small temperature ranges, and are perfectly appropriate for such applications (Royon, Karim, and Bontemps, 2013). Techniques to choose and size suitable thermal storage technologies in solar cooling applications vary between investigations with no standard methodology being utilized across the literature. Our literature survey outlines relevant studies dealing with the role of PCMs addition in the solar cooling process i.e. solar collectors and/or storage tank for possible enhancement of thermal energy storage efficiency. Thus, this section provides a review of recent studies related to the benefit of the thermal energy storage using PCMs for solar cooling applications.

Relevant investigations are identified dealing with predicting the expected benefit from both water and phase change materials based thermal storage for solar air-conditioning applications with limited temperature ranges. Hirmiz, Lightstone, and Cotton, 2018 examined the performance enhancement of solar absorption cooling systems using thermal energy storage with phase change materials (PCMs). They have given an engineering approach for predicting the expected benefit from both

PCMs and water based thermal storage for applications with limited temperature ranges. In addition, Kabeel and Abdelgaied, 2018 investigated a solar energy assisted desiccant air conditioning system (three types A, B and C) with PCM as a thermal storage medium. They found that the average percentage savings in the electrical energy which consumed about 20.85% for Type B and 75.82% for Type C as compared to the Type A. Accordingly, Gao et al., 2018 conduction an optimization of pre-cooling with intermittent mode using a coupled cooling method and application of latent heat thermal energy storage combined with pre-cooling of envelope. They demonstrated the significant potential of intermittent operational mode application in underground thermal energy storage systems. Wang et al., 2018 performed a thermodynamic performance analysis and comparison of a combined cooling heating and power system integrated with two types of thermal energy storage. Their results indicate that the combined cooling heating and power system integrated with the jacket water storage tank achieves a primary energy ratio of 83.8% and a ratio of cooling to electricity of 2.24.

The scope of the PCMs is wide. Indeed, recent studies are interested in integrating PCMs for solar cooling applications and possible improvement of thermal energy storage of these systems. For instance, Pan et al., 2018 conducted a cost estimation and sensitivity analysis of a latent thermal energy storage system for supplementary cooling of air cooled condensers. Research on the solar cooling systems is numerous and diversified in the literature in terms of experimental and numerical studies. Pop et al., 2018 conducted an energy efficiency of PCM integrated in fresh air cooling systems in different climatic conditions. The evaluation of PCM energy efficiency in fresh air cooling systems revealed that savings in the electric energy consumption of (7-41) % can be achieved, depending on the particular local conditions. Further, Agyenim, 2016 assessed the use of enhanced heat transfer phase change materials (PCM) to improve the coefficient of performance (COP) of solar powered LiBr/H_2O absorption cooling systems. Overall utilization efficiencies achieved for longitudinal and multitube finned systems were 82% and 83.2% respectively. Under meteorological conditions of Shanghai, Zhou et al., 2017 performed a performance assessment of a single/double hybrid effect absorption cooling system driven by linear Fresnel solar collectors with latent thermal storage. They found that the optimized solar cooling system can provide the average seasonal cooling capacity of 102kW, the seasonal solar fraction of 27.2% and the seasonal thermal COP of 0.88. Allouche et al., 2017 carried out dynamic simulation of an integrated solar-driven ejector based air conditioning system with PCM cold storage. They identified an optimal storage volume of 1000l and they found that the solar thermal ratio and maximum COP were 0.097 and 0.193, respectively. In addition, the identification and characterization of promising PCMs for solar cooling applications have been studied by Brancato et al., 2017. Their results indicate that the commercial PCMs ranging between 120 and 150 J/g, confirmed their stability which makes them ready for practical applications.

The following part focuses on latent thermal energy storage and the integration of PCMs within the solar cooling systems i.e. storage tank connected to the generator of the absorption chiller in order to optimize the thermal energy storage of the system in dynamic mode.

5.3 Physical model

5.3.1 Problem specification

The production of hot water for solar air-conditioning applications is considered as one of solar energy's favored use in the buildings sector due to the nature of the needs. For instance, the range of hot water temperature requirement for solar cooling applications is generally between 60 and 160°C depending on the requested cooling power. The solar cooling installation under investigation contains three circuits as shown in Fig. 5.1: **Circuit 1**, **Circuit 2** and **Circuit 3**. Indeed, **Circuit 1** produces the hot water at required temperature (up to 80°C) and stores it inside the thermal storage tank. In addition, **Circuit 2** includes the absorption machine and its accessories while **circuit 3** is devoted to building for indoor space heating or air-conditioning depending on the season.

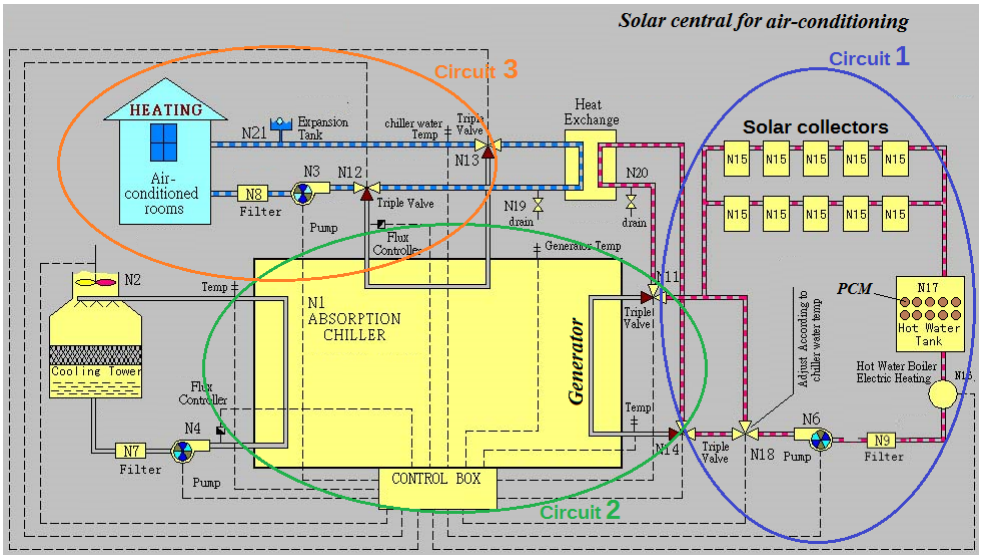

FIGURE 5.1: Schematic of integrated solar central heating and absorption cooling system for indoor space air-conditioning

In this part, we will focus on the **Circuit 1** as the aim is to produce solar hot water to feed the generator of the absorption chiller with a required temperature (in the range $80-95°C$) and a fixed flow rate ($0.77 kg\,s^{-1}$). In addition to the solar collectors, the determinant equipment of a solar hot water production system connected to a solar absorption cooling machine is the hot water storage tank. The energy stored inside the tank is increased, if the stratification is well improved. Consequently, the aim of the present study is to describe the thermal behaviour of the storage tank filled by PCM in its interior by performing a numerical parametric and comparative studies on a standard solar cooling process. Three PCMs types were selected and three typical solar collectors were considered in this work which consist of a Flat plate (FPC), Evacuated tube (ETC) and Compound parabolic (CPC), controller, a storage tank of 300l integrating layers of PCMs. The storage tank is connected to the generator of the absorption chiller and equipped with an auxiliary electric heater and a pump as shown in Fig. 5.2.

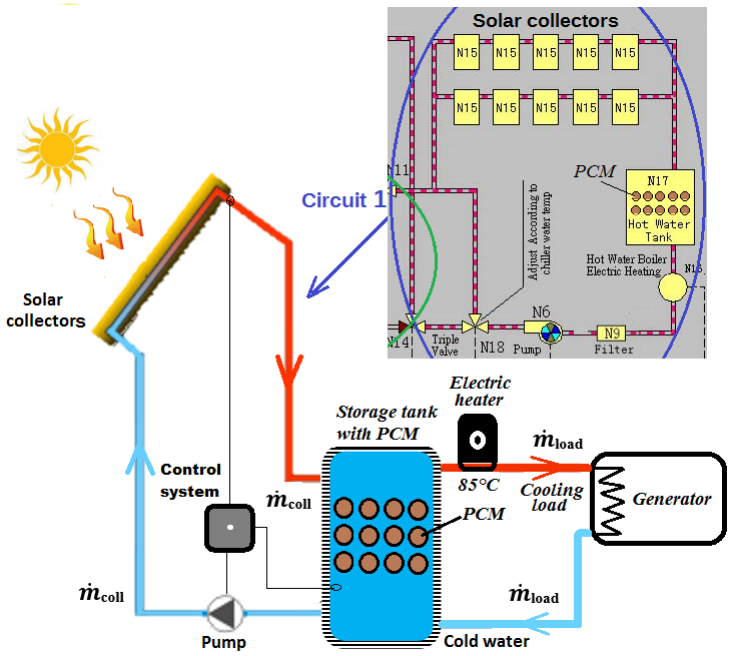

FIGURE 5.2: Layout of the solar hot water circuit integrating PCM connected to the generator of the absorption cooling process

One of the determining points in this kind of modeling lies in the management of the phase change phenomena of the PCM, with overall problems that they cause (dissymmetry of the phase change, supercooling, etc.). For several years, numerous studies have been carried out on these phenomena (Yamagishi et al., 1996; Haillot et al., 2013 and Zalba et al., 2003). Part of these studies focusing on the phase change modeling. There are now several numerical methods each having their advantages and disadvantages depending on the cases encountered. In particular, Enthalpy methods and methods of monitoring the interface of phase change. The former are free from the evaluation of the evolution of the phase change front; the heat exchanges are represented by a variation of enthalpy and more precisely simulated by an equivalent specific heat.

In this work, a numerical approach is used to compare two numerical procedures: a technique based on apparent heat capacity called in this study C_p^{app} and the second uses the enthalpy method typically used to model the PCM melting process integrated inside a storage tank. Therefore, the PCM with a reference proportion $\epsilon = 30\%$ is occupied a storage tank volume as schematically presented in Fig. 5.2.

The geometric characteristics of the studied storage tank are presented in the Table 5.1.

Volume (l)	300
Diameter (mm)	560
Length (mm)	1200
Environment temperature of the storage tank	20 [°C]
Initial temperature of the storage tank	25 [°C]
Tank heat loss coefficient	$0.57 - 1.133$ [W m^{-2} K^{-1}]
Insulation	40 mm cfc free Polyurethane

TABLE 5.1: Characteristics of the studied storage tank

The aim is to investigate the effect of the introduction of PCM on the temperature evolution and on the thermal performance of the solar hot water system operating in dynamic mode. A point not to be overlooked is in the packaging of PCM. It's a topic that has sparked a lot of research (Marongiu, Berhe, and Fallon, 2000). The latest ones seem to agree on the merits of encapsulating PCMs in cylindrical nodules which is used in the current work. Indeed, it is a geometric configuration a priori optimal insofar as it allows to maximize the ratio between the volume of PCM in the tank (which directly impacts the storage capacity of the tank, so the amount of possible heat transfer) and the exchange surface between the water and the PCM (which affects the quality of thermal transfers occurring within the storage tank). In this study, three PCMs were chosen as working fluids since they are the most efficient for our application: (PCM1: $Ba(OH)_2, 8H_2O$, PCM2: $NaOAc$, $3H_2O$ and PCM3: $Mg(NO_3)_2$, $16H_2O$) with different melting tmperatures incorporated inside the storage tank. The selection of an appropriate PCM for solar cooling application requires the PCM to have melting temperature between 50 °C and 90 °C corresponding to the set point temperature of the hot water storage tank. In Table 5.2, the main physical and thermal properties of these PCMs are given.

Properties	PCM1	PCM2	PCM3	Unit
Density (liquid)	1300	1937	1550	$[\mathrm{kg\,m^{-3}}]$
Melting tempearture	60	70	80	[°C]
Thermal conductivity	5	0.653	0.49	$[\mathrm{W\,m^{-1}\,K^{-1}}]$
Latent heat of fusion	17300	184	149.5	$[\mathrm{J\,kg^{-1}}]$
Liquidus specific heat capacity	3860	-	-	$[\mathrm{J\,kg^{-1}\,K^{-1}}]$

TABLE 5.2: Physical properties of the studied PCMs: PCM1 - $NaOAc$, $3H_2O$, PCM2 - $Na_2P_2O_7$, $10H_2O$ and PCM3 - $Mg(NO_3)_2$, $16H_2O$ (Talmatsky and Kribus, 2008, Cabeza et al., 2011, Khan, Saidur, and Al-Sulaiman, 2017)

As previously mentioned, the objective is to investigate numerically the effect of PCM integration on the water's temperature distributions inside the tank under various operating conditions. The investigation will also focus on the heat transfer during the melting process of PCM within the storage tank. A relevant consideration in such systems is the effective use of the storage tank filled by PCM in an optimal disposition, location and size. Consequently, two numerical methods were used: the Enthalpy and the C_p^{app} methods, to model the PCM's solidification and melting and compared using a set of numerical results.

5.3.2 Mathematical model

Model description of the solar water heating systems with PCM (Circuit 1)

A number of phenomena are taken into account in terms of thermal processes that take place within the system. Each phenomenon is described in the code by a physical equation. The set of equations forms a system to describe the evolution of the temperature of the system as a function of time and along the storage tank's height. 1D unsteady flow models in dynamic mode were built in the FORTRAN programming code. The numerical code was accounting for two-dimensional effects. Indeed, 2D section passing throughout the half of the tank was modeled, since the storage

tank geometry was symmetric. Working on a 2D section was adopted to optimize the computational time and it was a suitable approach to model the PCM melting process. Fig. 5.3 shows a schematic of storage tank divided into N layers. The cold water comes in through the mains to solar collector by means of a pump. The temperature of water in each node varies and it decreases gradually from the top of the tank specified as node 1 to the bottom specified as node N. In order to maximize the amount of water above 80 °C which is assumed to be the minimum water temperature for a comfortable use, it is important to control the mixing between the hot and cold water in the tank. In such modeling (see Fig. 5.3), 20 layers were used as required in the works of Kleinbach, Beckman, and Klein, 1993; Oliveski, Krenzinger, and Vielmo, 2003.

The tank storing hot water requires the stratification effect which means that there will be temperature gradient increasing from the bottom to the top. This stratification enables a better comfort for the user who will draw water from the top with a temperature higher than at the bottom. Furthermore, a low temperature will increase the coefficient of performance of the heat pump if this one is heating at the bottom of the tank. To take advantage from the stratification, the storage tank is assumed to be divided into $N = 20$ separate, thoroughly mixed and isothermal layers of equal height. The schematic diagram representing hybrid water PCM numerical model with stratified nodes of water and cylindrical PCMs capsules is depicted in Fig. 5.3.

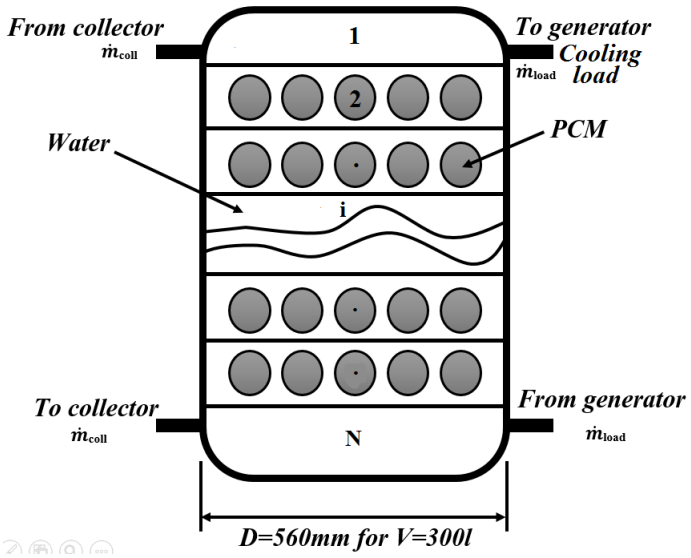

FIGURE 5.3: Schematic representing hybrid water PCM numerical model with stratified nodes of water and cylindrical PCMs capsules

Model description of solar collector

The solar collector's efficiency η_c is a determinant indicator to evaluate the thermal performance of a solar water heater. The efficiency η_c is defined as the ratio of energy transferred from the collector to the heat transfer medium to the incident solar radiation. Three typical solar collectors were used in the current study, Flat Plate (FPC), Evacuated tube (ETC) and Compound Parabolic (CPC).

In steady state for one single thermal collector, a mathematical modeling allows to express the overall energy balance based on the standard second-order collector performance Eq. 5.1:

$$\eta_c = \eta_0 - k_1 X^* - k_2 I_c X^{*2} \tag{5.1}$$

where η_c is the collector operating efficiency, X^* is the standardized temperature difference factor expressed as: $X^* = \frac{1}{I_c}(T_{avg} - T_\infty)$, $T_{avg} = \frac{1}{2}(T_N + T_{fout})$ is the average temperature within the collector, η_0 indicates the optical efficiency of the collector, and k_1 and k_2 present the first and second order heat loss coefficients, respectively, I_c is the solar incident radiation and T_∞ is the ambient temperature.

As our work involves a set of collectors connected in series, the Eq. 5.1 is valid only for a single collector. Indeed, the heated water after the first collector will go slightly higher in the second one. As a result, the thermal performance in the second module is decreasing according to Eq. 5.2. More accurate analytical formulas can be found in the literature concerning the calculation of performance of a set of collectors connected in series (Oonk, Jones, and Cole-Appel, 1979).

The technical characteristics of the selected thermal collectors are listed in Table 5.3.

Parameters	Value			Unit
	FPC	ETC	CPC	
Collector absorber area A_c	2.67	2.67	2.67	[m^2]
η_0	0.735	0.821	0.660	[-]
k_1	4.6	2.82	0.82	[$W\,m^{-2}\,K^{-1}$]
k_2	0.0164	0.0047	0.0064	[$W\,m^{-2}\,K^{-2}$]

TABLE 5.3: Solar collector's characteristics (*Viessmann - Solar thermal systems*)

The collectors constituting the solar field are connected in series (see Fig. 5.4) to increase the temperature of the HTF and also to exploit the available surface of the terrace available in *Green Energy Park*.

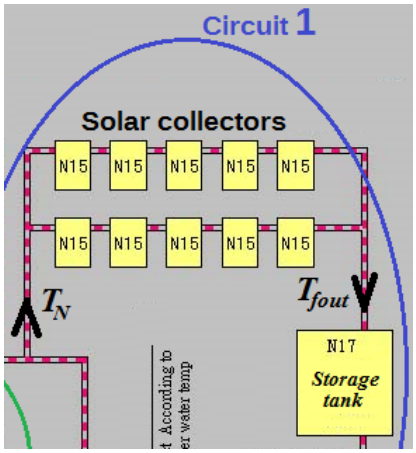

FIGURE 5.4: Solar collectors field connected to storage tank

The rate of heat extraction from the collectors may be measured by means of the amount of heat transferred to the fluid passed through it which is expressed in Eq.

5.2:

$$\eta_c I_c A_t = \dot{m}_{coll} C_w (T_{fout} - T_N) \tag{5.2}$$

A_t represents the total area of n collectors ($A_t = n \times A_c$) constituting the solar field which are connected in series. This connection between the different collectors is performed to exploit the available surface of the terrace in order to ensure their ergonomic distribution. As the generator requires a water temperature up to 80 °C, the installation with several collectors connected in series has the effect of increasing the temperature of the heat transfer fluid. Eqs. 5.1 and 5.2 were solved simultaneously to obtain the collector water outlet temperature. The pump with variable-speed sets in motion the heat transfer fluid when it is hotter than the water tank. Its operation is controlled by a regulating device acting on the temperature differences: if the temperature of storage tank is hotter than the solar collector temperature, the controller system stop the pump. Otherwise, the pump is restarted and the primary fluid heats the water inside the storage tank. In our developed code, the pump will be activated if:

- $T_{fout} > 84°\mathrm{C}$
- $T_{fout} - T_N > 4°\mathrm{C}$

In winter or during long periods with no insulation, all of the hot water can't be provided by the solar energy, an extra device (an auxiliary electrical heater) is therefore the relay and reconstructs a hot water stock. In the current study, the electric heater is placed outside the storage tank (Fig. 5.2). The electric heater integrates a thermostat that measures the water temperature delivered to the use and when this temperature decreases below $80°\mathrm{C}$, the heater is activated at an average power sufficient to bring the temperature back to $80°\mathrm{C}$. This system enables a clear separation between auxiliary heat and solar derived heat and definition of the minimum amount of backup electricity that is needed to satisfy the user's requests. Thus, the electric supplement is triggered for two cases:

- if $T_1 < 80°\mathrm{C}$, the backup electric energy is: $Q_{aux} = \dot{m}_{load} C_w (80 - T_1)$
- Otherwise, the water is cooled by water at $20°\mathrm{C}$ with a flow rate of: $\dot{m}_{load} = \dot{m}_{max} \frac{80°\mathrm{C} - 20°\mathrm{C}}{T_1 - 20°\mathrm{C}}$

The fluid motion in water is considered as laminar. Indeed, the laminar flow regimes for water is firstly checked when forming the mathematical model. Indeed, we have determined the Reynolds number of the flow using this formula: $Re = \frac{4\dot{m}_{max}}{\pi D \mu_w}$. The calculation of Re number was performed where μ_w is the dynamic viscosity of the heat transfer fluid (water) and $\dot{m}_{max}$=0.77 $kg.s^{-1}$ is the flow rate feeding the generator of the absorption machine. As a result, it was determined that the maximum value of $Re = 1.74 \times 10^3$ which indicates that the flow in the storage tank is laminar.

The same models developed in Chapter 4 were adopted (apparent capacity C_p^{app} heat tranfer model and Enthalpy method) in order to evaluate the temperature inside the storage tank and performance of solar water heating system connected to the absorption chiller with latent heat storage using phase change materials (PCMs). As climatic conditions are required in the simulations, the average values of the incident solar irradiation on the solar collector system and the ambient temperature of the six Moroccan climate zones were considered (Bouhal et al., 2018c). Meteonorm platform

(Version, 2010) was used to obtain the meteorological data which are intrinsic to the Moroccan zones in terms of ambient temperature and solar radiation flux (see Chapter 2).

The cooling demand profile depends on user's behavior and the location where the simulation is performed. Indeed, we have estimated the cooling consumption profiles for typical residence. Our estimation is based on a simple user load profile that concentrates air-conditioning consumption during three periods per day (Morning, Evening and Day) as shown in Fig. 3.5.

5.4 Physical modeling of the absorption chiller (Circuit 2)

The process of the absorption cycle and its internal operation is given by **Circuit 2** presented schematically in Fig. 5.5. The chiller works with Lithium Bromide (LiBr) as sorbent and the water (H_2O) as refrigerant. In the high pressure zone (condenser and steam generator), when the temperature is high under equivalent pressure, the refrigerant (H_2O) is separated by expelling LiBr (steam generator (boiler) using a source of motive heat necessary produced by solar hot water collectors (Agrouaz et al., 2017). In the condenser, the refrigerant liquefies with the absorption of heat. This step aims to reuse the refrigerant, namely water, in its pure form. The fluid refrigerant then passes through pressure separation lines and is brought into the low pressure zone (evaporator, absorber). It then evaporates at very low temperatures between 5 and 15 °C. In the evaporator, the refrigerant evaporates with the absorption of the ambient heat and the cold is obtained. The vapor of the refrigerant generated is absorbed into the absorber by LiBr and dissolved in the salt by the release of heat pumped to the high pressure zone (boiler/condenser) by consuming very little electrical energy. The operating cycle is maintained continuously.

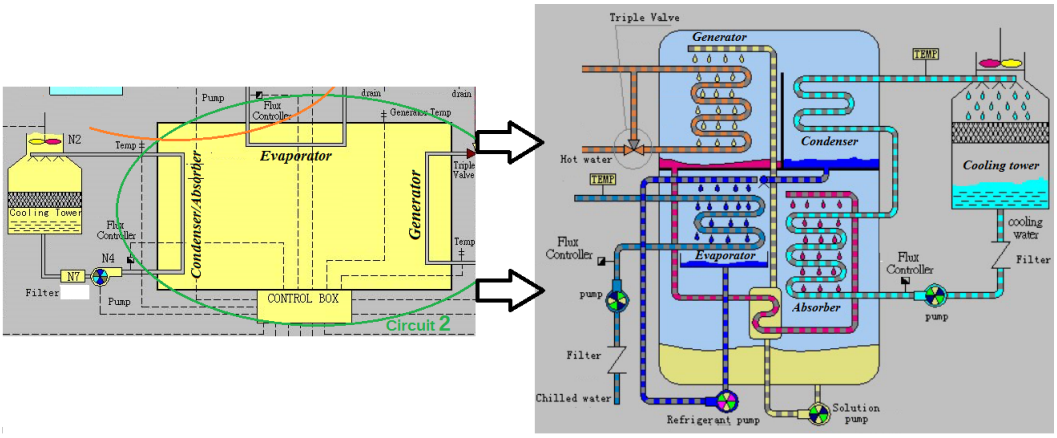

FIGURE 5.5: Model of the absorption chiller (*Shandong Lucy New Energy Technology Co., Ltd.*)

The modeling of the single effect machine working with the couple (H_2O/LiBr) was based on the thermodynamics laws for a real cycle and the following conditions and assumptions were used:

- The temperatures in the exchangers (generator, condenser, evaporator and absorber) are assumed to be uniform over the entire volume under consideration.

- The solution rich in refrigerant fluid at the outlet of the absorber is a saturated liquid at the temperature and concentration in the absorber. Likewise, the refrigerant fluid solution leaving the generator is at a concentration linked by an equilibrium relationship to the pressure and temperature of the generator.
- The refrigerant flowing out of the condenser is taken as a liquid saturated at the temperature and the corresponding pressure.
- The refrigerant, at the exit of the evaporator, is in the vapor state saturated at the temperature and low pressure of the evaporator.
- Relaxation is supposed to be isenthalpic.
- The thermal exchanges with the environment and the losses of loads are negligible.

5.4.1 Mass balance

At the absorber level, two mass balances can be performed as:

- Overall balance of the H_2O/LiBr solution:

$$\dot{m}_{cnd} + \dot{m}_r = \dot{m}_p \tag{5.3}$$

- The balance of LiBr:

$$\dot{m}_1 \times X_r - \dot{m}_p \times X_p = 0 \tag{5.4}$$

  where

  - X_p is the mass quality of the poor solution;
  - X_r is the mass quality rich solution;
  - $\dot{m}_{cnd}$ is the mass flow rate of the refrigerant (H2O);
  - $\dot{m}_p$ is the mass flow rate of poor solution (LiBr);
  - $\dot{m}_r$ is the mass flow of the rich solution (LiBr);

From the two relations i.e. Eqs. 5.3 and 5.4, the expressions of mass flow rates $\dot{m}_r$ and $\dot{m}_p$ were deduced:

$$\dot{m}_r = \dot{m}_1 \times \frac{\dot{m}_p}{X_r - X_p} \tag{5.5}$$

$$\dot{m}_p = \dot{m}_1 \times \frac{\dot{m}_r}{X_r - X_p} \tag{5.6}$$

5.4.2 Energy balance

The enthalpy balance is performed on each component exchanging heat or work with the external environment:

$$Q_{abs} + Q_{cnd} = Q_{evp} + Q_{gen} \tag{5.7}$$

- Generator power (heat exchanged from the solar hot water to the LiBr-H_2O solution in the generator):

$$\dot{Q}_{gen} = \dot{m}_{ge}.C_p(T_{ge,i} - T_{ge,o}) \tag{5.8}$$

$T_{ge,i}$ and $T_{ge,o}$ are measured at the inlet and outlet entries of the generator, respectively. It is interesting to note that the generator has a temperature range between 60°C and 80°C depending on solar sunshine (Agrouaz et al., 2017).

- Chilling power (heat exchanged from the chilling circuit to the evaporator):

$$\dot{Q}_{evp} = \dot{m}_{ch}.C_p(T_{evp,i} - T_{evp,o}) \tag{5.9}$$

$T_{ev,i}$ and $T_{ev,o}$ are measured at the inlet and outlet entries of the evaporator, respectively.

- The heat exchanged from the chilling circuit to the absorber:

$$Q_{abs} = \dot{m}_{cnd} \times (h_{evp,o} - h_{abs,i} - (h_{abs,i} - h_{abs,o}) \times \frac{X_r}{X_p - X_r}) \tag{5.10}$$

where $h_{evp,o}$, $h_{abs,i}$ and $h_{abs,o}$ are the enthalpy in the outlet of evaporator and in the inlet and outlet of absorber, respectively.

- Cooling power (heat exchanged from the absorber and the condenser to the cooling circuit):

$$\dot{Q}_{cnd} = \dot{m}_{c}.C_p(T_{ex,i} - T_{ex,o}) \tag{5.11}$$

$T_{ex,i}$ and $T_{ex,o}$ are measured at the inlet and outlet entries of the absorber and condenser loop.

- Solar power (incident solar radiation on the solar field surface of the installation):

$$\dot{Q}_{rad} = A_t.I_c \tag{5.12}$$

where A_t the total area of the solar collectors field.

- Collectors power (solar heat supplied by the solar collectors):

$$\dot{Q}_{sc} = \dot{m}_{sc}.C_{sc}(T_{sc,o} - T_{sc,i}) \tag{5.13}$$

$T_{sc,i}$ and $T_{sc,o}$ are measured at the inlet and outlet entries of the solar field collectors, respectively.

5.4.3 Generator of the absorption chiller

The generator of a LiBr-H_2O absorption chiller is a pool type heat exchanger that is capable of extracting heat from hot water available from solar water heater using an evacuated tube collectors. As previously mentioned, the solar collector's efficiency is expressed as a function of incident radiation and temperature difference. To power the generator of the absorption air-conditioning temperature required is in the range

of 85 °C to 90 °C at certain flow rate $\dot{m}_{load} = 0.77 \mathrm{kg\,s^{-1}}$. Single effect LiBr-$H_2O$ systems are ideal for air conditioning operations where the refrigerant flow normally does not exceed 10 °C under normal conditions. The generator of these systems is powered easily with a low grade energy source from solar hot water with evacuated tube collectors. The hot water heats up the refrigerant-absorbent mix in a pool boiling type heat exchanger. LiBr-H_2O solution enters the generator at a particular concentration and when heat is supplied, fraction of the water in the solution vaporizes leaving behind a strong solution of water and lithium bromide in the heat exchanger. The change in concentration of the solution affects its heat transfer coefficient. The heat transfer coefficient is found to increase as the heat flux increases (Assilzadeh et al., 2005).

5.5 Assessment of system thermal performance

In this section, the results presenting the thermal behaviour of the absorption chiller are presented. Annual simulations were carried out to simulate the PCM melting and the temperature evolutions inside the storage tank for two cases with and without PCMs. It's interesting to note that the manufacturer of the absorption machine (*Shandong Lucy New Energy Technology Co., Ltd.*) has set up a series of tests carried out by the machine during its operation mode. If these criteria are not met the machine will not start.

- 1^{st} step: check that there is a request for cold using a thermocouple placed in the building to be air conditioned.
- 2^{nd} step: each circuit must respect a minimum incoming water flow, namely:
  - 33.3 $\mathrm{l/\,min}$ for the evaporator;
  - 46.6 $\mathrm{l/\,min}$ for the generator;
  - 25 $\mathrm{l/\,min}$ for the absorber and condenser.
- 3^{rd} step: the temperature of the water entering the generator must be at least equal to 80 °C.

These steps are visible on the absorption chiller bulletin board and control panel. Indeed, two action buttons are present, an "ON/OFF" button and a "restart" button. Different indicators are present, indicating whether the motor is running or not and whether the desired temperature in the solar circuit is reached. A screen that can display codes corresponding to error messages is also present.

It's necessary to note that the pressure gauges (display) are present on each circuit in order to fill the circuits properly, the filling pressure (before starting the installation) must be between 1.5 and 2 bar.

Annual simulations of the solar storage tank with and without PCM connected to the absorption chiller via the generator were carried out. Those simulations included ambient temperatures and solar insolation as a function of time at Marrakech as it was received from *Meteonorm* data. Three different load profiles as shown in Fig. 3.5 were used. Thus, a set of important parameters such as temperature profiles, liquid fraction, solar fraction and coefficient of performance (COP) of the absorption chiller were drawn as indicators to numerically assess the predicted enhancement of the energy storage tank and the possible improvement in the system thermal performance.

5.5.1 Impact of climatic conditions and PCMs integration on temperature profiles

To examine the thermal behavior of the system, Figs. 5.6 present the temperature evolutions inside the storage tank. Indeed, Fig. 5.6-(a) represents the temperature history inside the storage tank without PCM while Figs. 5.6-(b) shows the temperature inside the storage tank filled with PCM for two summer days (July). As the cooling demand is required in summer period, two successive days of summer (July 1-2) relative to the Moroccan city Marrakech are considered. Representative numerical tank temperatures plotted in these figures show very definite stratification for the considered configurations (see Figs. 5.6-(a) and (b)). Indeed, Figs. 5.6-(a) and (b) present the 48-hours evolution of the ambient temperature, top and bottom layers temperatures of the solar tank and outlet temperature from the collector for ETC technology. During these two days, it is interesting to mention that the ambient temperature has a low annual values. During the night, the ambient temperature decreases from 42 °C to 20°C while during the morning it goes up gradually to reach its maximum daily value of 45 °C and decreases during the evening. In addition, the collector outlet temperature follows the trend of the ambient temperature and the incident solar radiation. As illustrated in Figs. 5.6-(a) and (b), it is important to note that the solar water tank temperatures, and outlet collector drop when the cooling profile loads is present at 12h (see Fig. 3.5). This phenomena is clearly apparent in the case without PCM at 12h. During the afternoon, the temperature of the top layers in the tank with PCM (Fig. 5.6-(b)) has approximately the same profile than that observed without PCM (see Fig. 5.6-(a)). A such situation is in qualitative accordance with that reported by Kleinbach, Beckman, and Klein, 1993. The, simulations were carried out with the same type of PCM whose melting temperature around 60 °C and the different behaviour is noticed. In fact, after 18h, i.e. overnight when there is no solar radiation, we observe that the top layer temperature in case without PCM decreases roughly while there is an opposite situation in the both cases with PCM as a result of heat transfer from the PCM to the water and the values of temperature in the collector in the storage tank with PCM become slightly higher than in the case without PCM. The effect of PCM is well observed, which limits the water temperature drop. It should be noted in this case that all of the PCM is melted during the heating period and then again solidified over the night period, the changes of state corresponding to the temperature step presents at the melting temperature of the PCM 60 °C. Fig. 5.6-(b) indicates a reheating of water overnight even if there is no solar radiation as a result of heat transfer from the PCM to the water and the temperatures in the storage tank with PCM become higher than in the case without PCM. As can be seen in Fig. 5.6, the top layer temperature is characterized by a higher and a quasi-constant temperature level which is apparently due to the stationary reheating of the water because of the solidification process follow up by the PCM. As the generator requires a temperature up to 80 °C, the absorption chiller generates cooling charges during the day between 11 am and 6 pm according to Figs. 5.6 for both cases with and without PCMs. During the night hours, the top temperature from the tank exceeds 80 °C for the case with PCM during the two days 30-31 of July.

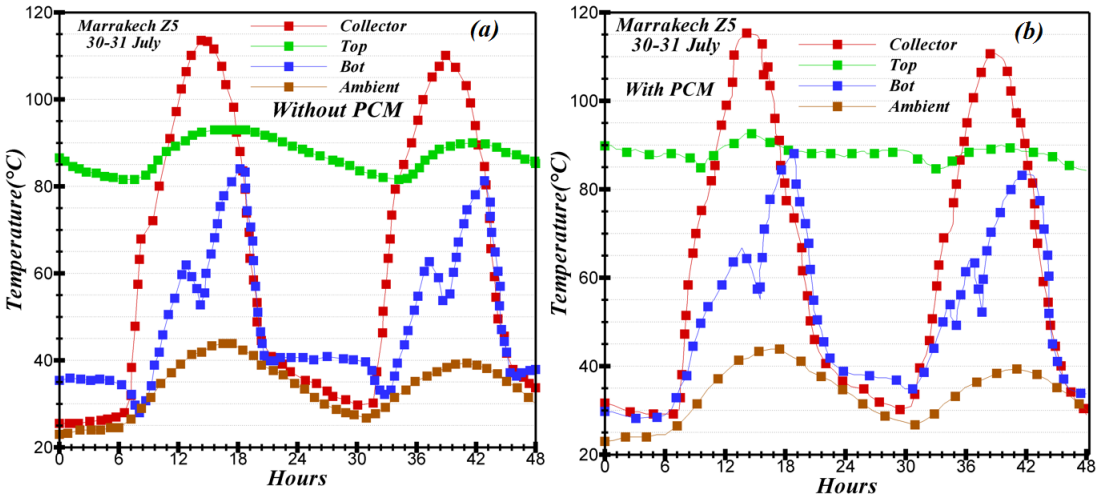

FIGURE 5.6: Temporal evolution of temperatures inside the storage tank with and without PCM

5.5.2 Impact of storage tank volume, technology of collectors and their surface on generator temperature

This part focuses on the impact of storage tank volume, technology of collectors and their surface on generator temperature. The top layer temperature from the tank intended to feed the generator during the first hot days in July (1-2) is presented in Fig. 5.7. The weather of Marrakech (Morocco) has been used as solar boundary conditions inputs to assess their effect on generator thermal performance. It is noted that two collector technologies were studied, namely, FPC and ETC collectors. Indeed, Figs. 5.7 show the evolution of the temperature intended to be loaded at the inlet of the generator as function of the first two days of July in Marrakech. Three parametric studies were carried out in order to describe the effect of the collector technologies, either by using evacuated tube collectors (ETC) or by flat plate collectors (FPC) on the temperature to the generator (see Figs. 5.7-(a) and (d)). In addition, the effect of the overall area of the solar collector panel on the temperature to the generator has been investigated using three areas, namely $S = 15m^2$, $S = 22m^2$ and $S = 25m^2$ (see Figs. 5.7-(b) and (e)). The third parametric study aimed to assess the volume effect of the hot water storage tank on the charged temperature at the inlet of the generator. In fact, three storage volumes were used: $V = 200l$, $V = 300l$ and $V = 500l$ (see Figs. 5.7-(c) and (f)). It should be noted that for each considered parametric study previously presented, two cases were distinguished according to the integration of PCMs (see Figs. 5.7-(d), (e) and (f)), or without integrating the PCMs inside the storage tank (see Figs. 5.7-(a), (b) and (c)). For instance, the ETC technology increased the temperature to the generator compared to the FPC technology from 102.5 °C to 113 °C at t= 2 pm for the storage tank with no PCMs (see Fig. 5.7-(a)). While it has increased the temperature to the generator from 100 °C to 105 °C at the same instant, but for the storage tank integrating PCMs (see Fig. 5.7-(d)). Moreover, increasing the overall area of the collector field tend to increase the temperature to the generator. In fact, for the case of the storage tank without PCMs, and at t=2 pm the temperature to the generator has been enhanced from 85 °C to 115 °C (see Fig. 5.7-(b)). While it has increased from 70 °C to 110 °C at the same instant, namely t=2 pm for the configuration of the storage tank filled with a volume fraction of 30% PCMs (see Fig. 5.7-(e)). As can be seen, changing the storage tank volume from 200 l to 500 l has not affected the temperature to load to the generator during the considered hot two days of July,

where the COP of the chiller has to be maximal in order to produce the required amount of cooling energy. This result was noticed for both configuration, namely with and without integrating the PCMs inside the storage tank (see Fig. 5.7-(c) and (f)).

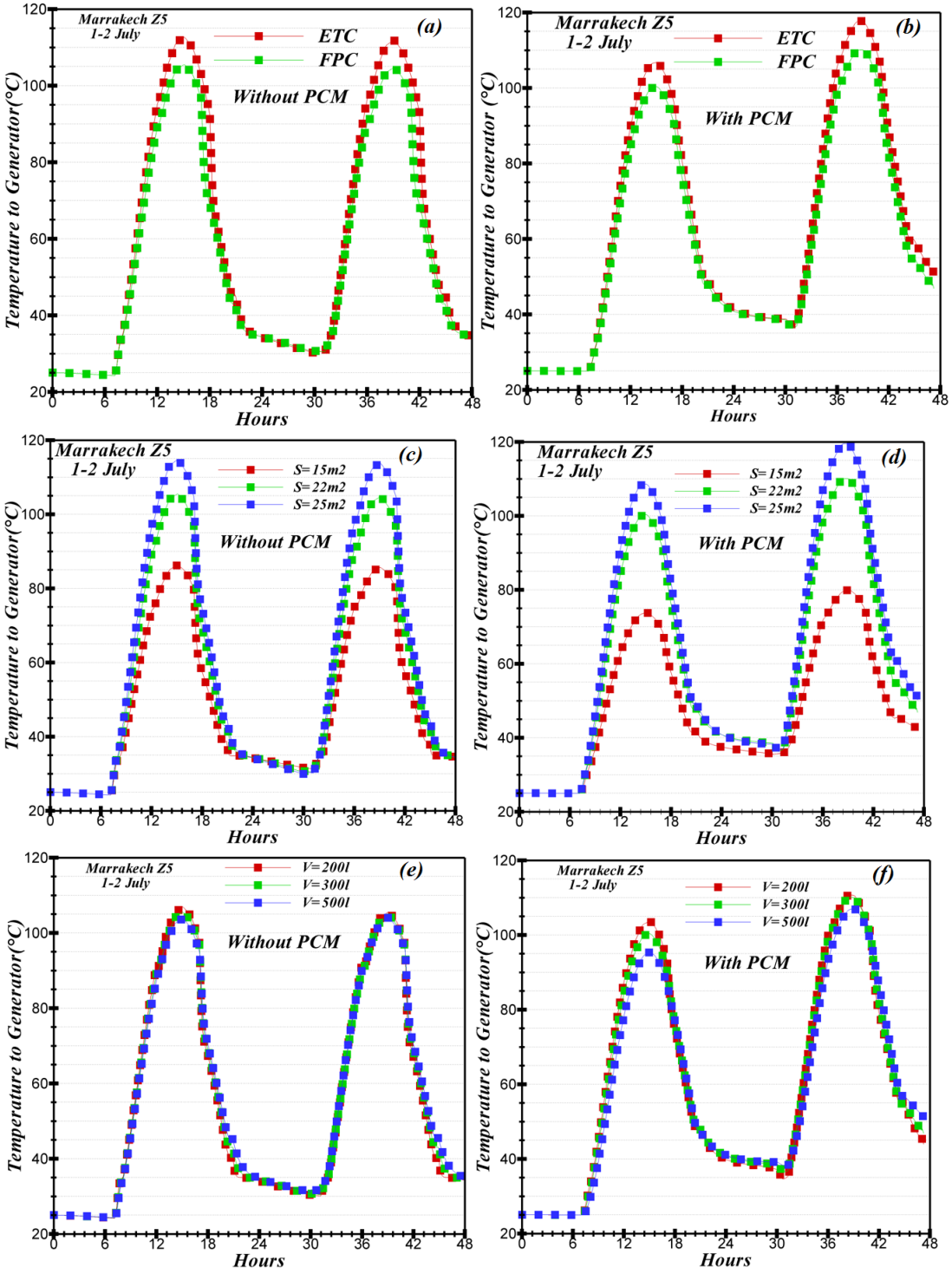

FIGURE 5.7: Effect of storage tank volume, technology of collectors and their surface on generator temperature

5.5.3 Impact of PCM types and their amount on generator temperature

The introduction of PCM in solar heating/cooling systems and their beneficial fact has to be considered with great attention (Tyagi and Buddhi, 2007). In order to evaluate the effect of PCM type on thermal performance, three types of PCMs with different melting temperatures were chosen, namely: PCM1 ($T_m = 60$ °C), PCM2 ($T_m = 70$ °C) and PCM3 ($T_m = 80$ °C). The annual simulations were carried out and the results for the case with Morning profile are shown in Figs. 5.8. Indeed, Figs. 5.8-(a), (c) and (d) depict the PCMs temperatures and liquid fractions for PCM1, PCM2 and PCM3. We notice that each time the temperature within the solid PCM reaches the melting temperature the corresponding PCM changes phase until the complete melting ($f = 100\%$). From Figs. 5.8-(a), (c) and (d)), we can observe that at $t = 0$ min all the PCM inside the storage tank is in solid state so the melting fraction is zero. As the time passes, the PCM gets melted because of water heating from solar collector and the value of melting fraction increase with time from 16 h, 20 h and 22 h when the water temperature achieved 60 °C, 70 °C and 80 °C which is the PCM melting points for PCM1, PCM2 and PCM3, respectively. For instance, the value of PCM1 melting fraction is 50% for the melting time of 18 h. At the end of the melting cycle i.e. after 20 h, all the PCM1 inside the storage tank has been melted; giving a melting fraction of 100%. As the PCM are considered as a spherical capsules, it is noticed that the rate of melting is not the same inside the capsule ($r = 0$) and in the PCM/water interface ($r = r_{ext}$). Indeed, the melting process increases for $r = r_{ext}$ faster than $r = 0$ because the PCM is in direct contact with hot water inside the storage tank (see Fig. 5.8-(a)). Tores et al., 2013 also simulated the behaviour of a packed bed latent heat thermal energy storage system connected to solar collector located in south of Spain. Their obtained results show a similar melting trend of PCM. Fig. 5.8-(e) shows the temperature history inside the storage tank, i.e. outlet collector, top layer and PCM1 temperatures. In addition, Fig. 5.8-(b) represents the PCM temperature (T_{pcm}) evolutions vs time (24 h) for various proportions ϵ of the tank volume occupied by PCMs. In the literature, the suggested amount of PCM in the storage tank varies greatly from about 5% to near 75% of the tank volume (Mehling et al., 2003). It is seen in Fig. 5.8-(e) that, when the temperature inside the storage tank reaches 60 °C, the PCM starts melting. Moreover, the evolution of temperature decreases when the PCM quantity (ϵ) is enhanced. Indeed, the amount of PCM (10%–50%) corresponding to an increase in heat storage capacity relative to that of water alone and to an enhancement of heat losses. As expected, the increase in amount of PCM leads to a decrease in melting velocity. Fig. 5.8-(f) shows the top layer temperature of the tank intended to feed the generator of the absorption chiller for different PCMs (PCM1, PCM2 and PCM3) in order to check the sensitivity of simulation results to the PCM melting temperatures. These temperatures follow the evolution of the solar radiation. During the day, they are almost up to 100 °C while during night when the insolation and ambient temperature are low, the temperatures decrease to reach 45 °C. In fact, during the day, the temperatures are often below the phase change temperature level and most of the time both systems (without and with PCM) store energy as sensible heat only. Consequently, the PCM is far from being completely utilized. It's necessary to find a suitable PCM melting point taking into account the specific weather climate of the site over the year. PCM1 provides the higher temperature during the day and night while PCM2 and PCM3 used in simulations go through phase change in a higher temperature range around 70 or 80 °C (see Fig. 5.8-(f)). The temperatures in the storage tank during the day are lower than this phase change temperature, hence most of the time both systems store energy as sensible heat only,

and the potential of the PCM is not fulfilled. It should be possible to find an optimal PCM melting temperature considering the specific climate of the site. According to our parametric study, the composite graphite H_2O-NaOAc mixture (PCM1) was found as the appropriate PCM energy storage medium for the solar water heating system for cooling applications. Since including $\varepsilon = 20\%$ of PCM1 in the storage tank did not improve the annual performance of the solar water heating system, it was decided to increase the PCM amount in the storage tank. Since the cost of the PCM is high, we assume that a high PCM fraction is not practical. The simulations in this section were carried out with $\varepsilon = 30\%$ of the tank volume occupied by PCM. This is still a relatively high fraction (leading to an expensive system). However, we expected to obtain a significant improvement in system's performances using this volume fraction. Therefore it is considered a reasonable compromise.

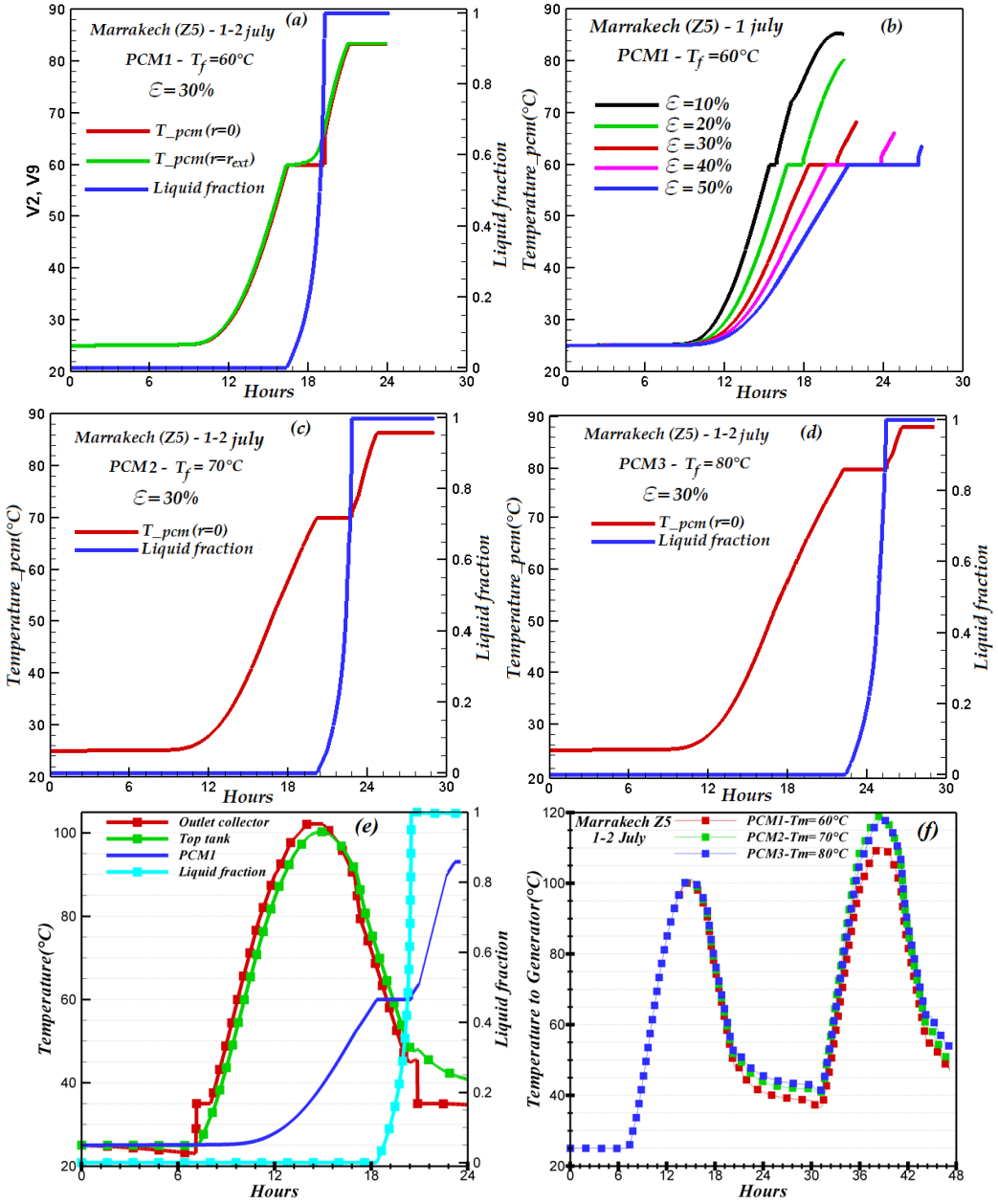

FIGURE 5.8: PCMs melting process, liquid fraction and water temperature evolutions

The evolution of the top layer temperature of the tank vs time (1-2 July in Marrakech city) is presented in Fig. 5.9. Four volume proportions of PCM were examined inside the storage tank connected to the solar collector in order to study their effect on the latent energy storage improvement (Lu, Zhang, and Chen, 2018). The PCM amounts used are $\epsilon = 20\%$, $\epsilon = 30\%$, $\epsilon = 40\%$ and $\epsilon = 50\%$. As depicted in Fig. 5.9, the top tank layer temperature connected to the consumer load is enhanced for a PCM fraction equal to 20% for both the investigated models, namely, the C_p^{app} method besides to the Enthalpy method. The melting time of the PCM is important when the volume it fills inside the tank is important too (we are referring here to the used 50% of tank volume), because it requires a supplement of energy from the storage tank, which in parallel tends to decrease because of the loading demand performed by the consumer. On the other hand, an optimized volume fraction of the PCM (20%) tends to melt faster, because the hottest layer of water is located at the top according to the development of thermal stratification occurring inside thermal storage tanks subjected to charging and discharging cycles (Bouhal et al., 2017b). The optimized used PCM proportion will work as an energy booster, hence it is going to provide its latent heat. Indeed, this energy helps to heat the water if solar irradiations are not sufficient. The Enthalpy method overestimates the top layer temperature of tank, where various PCM amounts are located. In fact, between midnight and 8 am the temperature is decreasing from 67°C to 43°C, while it is maintained constant at 42°C during the same cold time interval for the C_p^{app} method. The same remark can be made regarding the other cold time interval that spans between 6 pm and 12 pm, where the top temperature layer of the tank decreases from 115°C to 80°C using the Enthalpy, and from 120°C to 70°C using the C_p^{app} method.

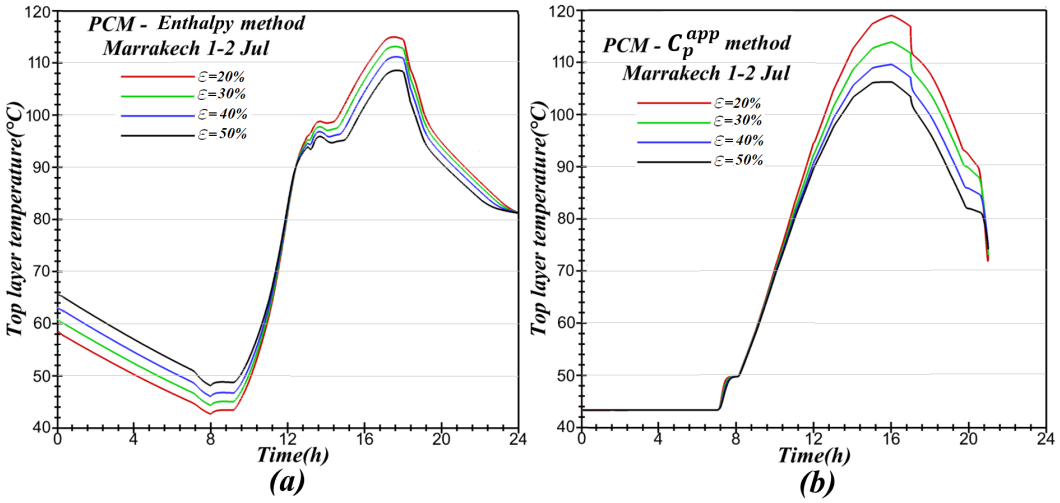

FIGURE 5.9: Effect of PCM proportion ϵ on top layer temperature evolution

5.6 Energy analysis of system performance

5.6.1 Heat losses and auxiliary heater consumption

Annual simulations using the **Morning** load profile (see Fig. 5.6) were done and the results for the two systems, with and without PCM in a solar water heating system connected to the absorption chiller via the generator are shown in Fig. 5.10. The integrals of energy transport were computed to yield the monthly and annual

amounts of energy delivered from the collectors, delivered to the absorption chiller load, lost to the surrounding, and provided by the electrical heater to compensate for insufficient stored heat. The results are shown in Fig. 5.10.

Fig. 5.10-(a) represents the electrical consumption of the auxiliary system connected the hot water storage tank of the chiller during the year. Marrakech city, which belongs to the climatic zone 5, has been considered as a case study to assess the effect of its weather conditions on the annual efficiency of the absorption machine. Moreover, "Morning" load profile has been selected to carry out this assessment and to analyze and discuss its effect on the thermal yield of the chiller, because it is the consumption profile of hot water which corresponds the most to the daily need of the Moroccan consumer (Dîn Fertahi et al., 2018a). It should be noted that two configurations were considered in this parametric study, namely a first configuration where PCMs were integrated inside the storage tank and a second configuration where no PCMs were submerged in the tank. In addition, Fig. 5.10-(b) shows the annual evolution of the energy losses from the tank by convection to the external surrounding medium for two configuration with and without PCMs also integrated in the solar storage tank.

The consumption of the electrical backup during the cold season of the year (November, December, January, February and March) is much more important than the hot season (May, June, July and August), because of the weak amplitude of the solar radiations incident on the solar collector field of the chiller (Buonomano, Calise, and Palombo, 2018b). For instance, in January, the auxiliary heater could consume up to 420 MJ for the tank's configuration without PCMs. While it is 410 MJ for the tank with PCMs during the same month. In comparison with June, the electrical backup is consuming up to 10 MJ for a tank with submerged PCMs and almost 8 MJ for a tank without PCMs. The use of PCMs decreases the consumption of the electric back up, hence the price of the total annual energy bill, because they can be considered as a free heat sources, which releases its latent heat useful for heating domestic hot water. In fact, the latent heat is released when the temperature of the tank becomes slightly lower than the melting temperature of the PCM, and conversely it stores the excess of solar energy transferred from the solar loop when the temperature of the tank becomes slightly higher than its melting temperature.

The losses from the tank are maximum during the summer period and minimum during the cold season of the year (Talmatsky, 2007). For example, the tank losses recorded during July for the storage tank with PCMs are 635 MJ. While they are nearly 615 MJ for the same storage tank which is integrating PCMs. Meanwhile, during November and December, the averaged losses from the tank without PCMs are assessed to be slightly below 160 MJ. Besides, the tank losses are evaluated at 170 MJ for the configuration with PCMs. Hence, it can be concluded that the fact of submerging PCMs inside the tank could be an alternative solution to enhance their thermal efficiency. Because, as shown in Figs. 5.10-(a) and (b) the annual consumption of the electric backup and the energy losses from the tank are reduced during the year, which lead to the enhancement of the thermal yield of the absorption machine.

The most striking observation is that the differences between the system with PCM and the one without PCM are very small even through the amount of PCM is significant. The system with PCM delivers more energy annually to the load than the system without PCM, instead of less, as was expected. As a result, the system with PCM requires less electrical power from the backup heater. The annual thermal losses from the storage tank are also higher for the system with PCM. The collector efficiency is almost the same for both systems. All the differences between

two systems are very small (less than 2%) which is well within the uncertainty of the simulation, and are therefore negligible.

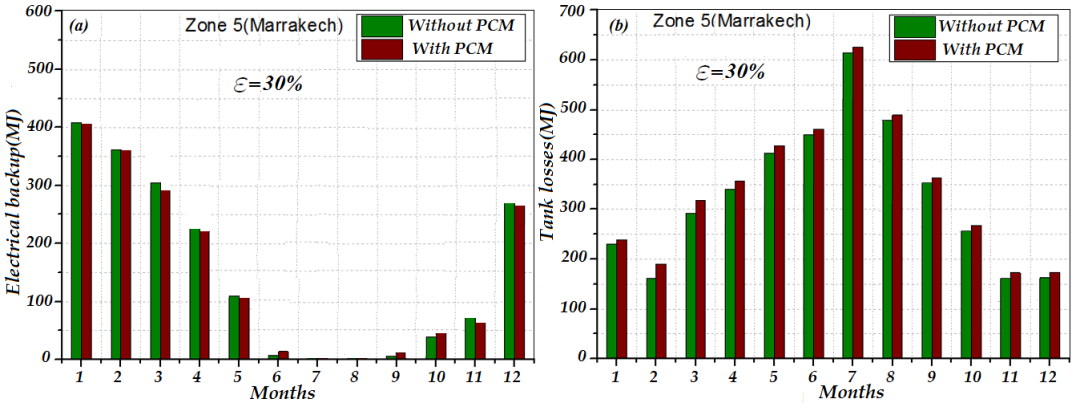

FIGURE 5.10: Annual auxiliary electrical consumption and tank heat losses in different zones for the cases with and without PCMs

Figs. 5.11 show the results of the annual simulation for $\varepsilon = 30\%$ of PCM in Marrakech and stepwise Morning load profile is considered. The gain is the difference in annual energy between the system with PCM and the system without PCM, divided by annual energy required to the load. Fig. 5.11-(a) represents the evolution of the electric backup as function of two different seasons of the year: winter and summer. The climatic Zone 5 represented by Marrakech has been considered as a case study, in order to investigate the thermal efficiency of the storage tank according to two cases: with and without submerging the PCMs. In addition, three different load profiles have been used to evaluate the contribution of the electric booster to generate the necessary energy needed to meet the requirement of the consumers in terms of the produced hot water. The selected load profiles were Morning, Evening and Day profiles. A general overview of the bar diagrams presented in Fig. 5.11-(a) show that integrating PCMs within the solar storage tank decreases the consumption of the auxiliary heater either for winter or summer periods, because they work as autonomous heating sources that release their latent heat if their temperature became slightly below the solidus temperature Kee, Munusamy, and Ong, 2018. The loading profile also affects the amount of the averaged consumed energy by the electrical backup, because each load profile is defined by a specific amount of the charged water at some specific hours and intervals during the day Bouhal et al., 2017a. For instance, during winter season and considering the Evening profile, it has been found that the electrical booster has consumed 415 MJ for the storage tank without PCMs and only 410 MJ for the same tank with PCMs. While in the month of July, the electrical backup consumed 105 MJ for the tank that is not submerging PCMs and approximately 30 MJ for the same tank with PCMs. Moreover, Fig. 5.11-(b) shows the evolution of the energy losses from the tank of the chiller located at the climatic Zone 5. The convective energy losses from the tank to the surrounding medium were assessed during two months, namely January and July. It is noted that three profiles were used to describe the pattern of consuming hot water, while two parametric studies were investigated to present the effect of PCMs addition within the storage tank of the absorption machine. In fact, the storage tank integrating PCMs tends to release less energy to the external medium compared to the storage tank without PCMs. For instance, the solar tank without PCMs releases only 600

MJ during summer for Morning loading profile, while it is 620 MJ for the tank with PCMs.

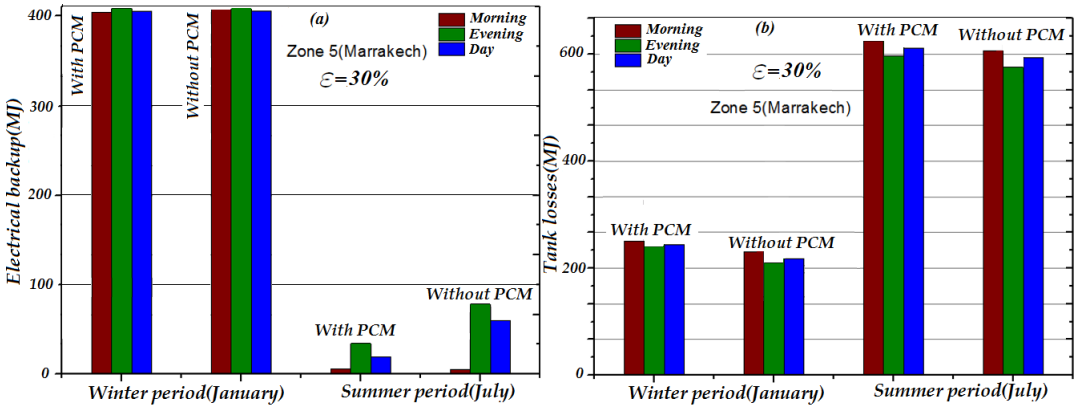

FIGURE 5.11: Auxiliary electrical backup and tank heat losses in different zones for the cases with and without PCMs

It is seen in Fig. 5.11-(a) that, unlike our expectations, most of the year there is a slight difference between the two systems. During the winter the system without PCM delivers even less solar energy to the load than the system with PCM. As a result, more electrical energy from the backup heater is required in this case. The tank losses to the surrounding are also alike for both systems during the year. Fig. 5.12-(a) shows that the annual performances of both systems which are not almost identical. The main conclusion from the results is that an addition of small amount of PCM ($\varepsilon = 30\%$ of PCM) improves the annual system performance as was expected from previous experiments with the static storage. The evolution of the annual chiller's solar fraction is presented in Fig. 5.12-(a). Two configurations were studied in order to depict the effect of filling 30% of the tank with PCMs. Besides, the Morning profile has been considered as the loading profile of reference. As described in Fig. 5.12-(a), submerging PCMs inside the tank enhances the solar fraction of the chiller, especially during the coldest season of the year. For example, the solar fraction has increased from 31% to 33% due to the uses of PCMs during February. Further, it has increased from 27% to 29% during November. In addition, Fig. 5.12-(b) shows the solar fraction evolution for two periods, namely January (winter) and July (summer). Three load profiles were tested in the fifth climatic zone of Morocco (Marrakech). Moreover, two configurations of the thermal storage tank were studied: a storage tank with and without submerged PCMs. As can be seen from the general pattern of the bar diagrams, the solar fraction of the chiller (Ge et al., 2018) is enhanced with the integration of PCMs inside the solar storage tank. For instance, during winter, and if the Morning profile is selected, solar fraction has increased from 25% to 28% due to the use of PCMs. While during the summer period, solar fraction has increased for Day profile from 50% to 52%.

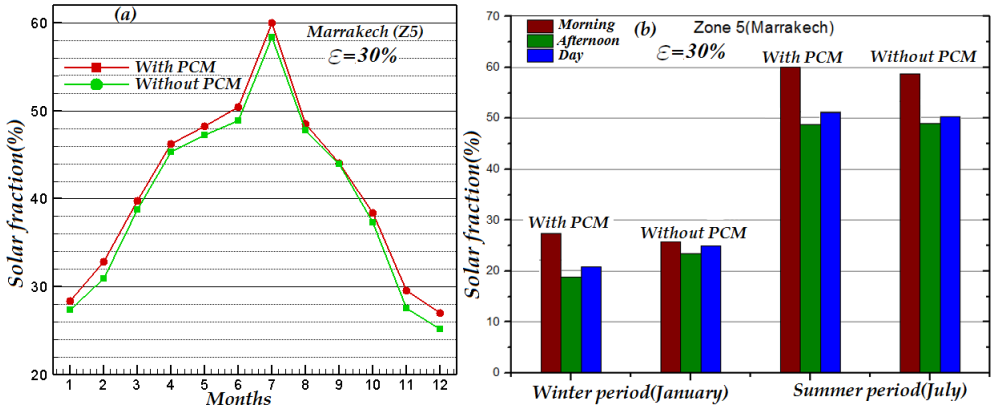

FIGURE 5.12: Effect of PCMs integration on solar fraction evolution

Results of the annual simulation for 30 % of PCM1 under Marrakech city (Z5) and morning load profile have been evaluated. Table 5.4 shows that the annual performances of both systems are not almost identical. The main conclusion from the results is that an addition of small proportion of PCM (30 % of PCM1) can improve the annual system performance as was confirmed from the gain obtained which is the difference in annual energy between the system with PCM and the system without PCM, divided by annual energy required to the load.

Energy rates [MJ]	Without PCM	With PCM	Gain [%]
Useful energy	12353	12456	0,8
Thermal losses	3910	3965	1,4
Electrical backup	1820	1705	-6,3
Collectors efficiency [%]	46,5	46,7	0,43

TABLE 5.4: Results of the annual simulation for 30 % of PCM1, in Marrakech Z5

Fig. 5.13-(a) represents the evolution of the electrical backup assessed during sumer period (July) for the six climatic zones of Morocco. The Morning load profile has been used to describe the consumption pattern of solar hot water. In fact, two configurations were studied, namely a thermal storage tank with/without PCMs. Fig. 5.13-(b) shows the evolution of the energy losses from the tank during the same month of the year (July) and for the same load profile (Morning). For instance, the auxiliary heater connected to the storage tank where no PCMs are integrated consumes up to 5 MJ per month for the climatic Zone 1, 3.8 MJ for the climatic Zone 3, 4.5 MJ for the climatic Zone 5 and 3.5 MJ for the climatic Zone 6. Meanwhile, the storage tank where PCMs are submerged tends to decrease the consumption of the electric booster. For instance, the electric energies consumed during July for the climatic Zones 2 and 4 are assessed at 4.8 MJ and 4.9 MJ, respcetively, while it is 4.4 MJ for the climatic Zone 5. The energy losses from the tank by convection to the external surrounding medium present some discrepancies for the considered two configurations (with/without submerging PCMs). These results can be explained by the fact that, during the hot season, the energy transferred to the storage tank is sufficient to heat the water and melt the PCMs generating more thermal losses inside the storage tank.

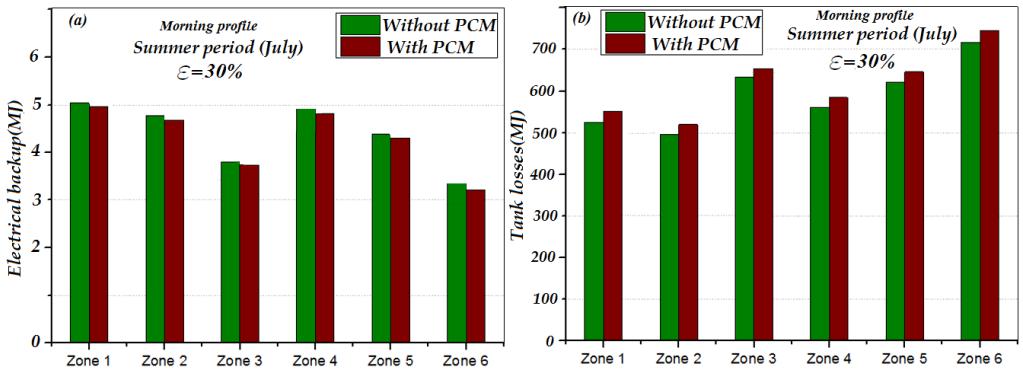

FIGURE 5.13: Auxiliary electrical backup and tank heat losses in Marrakech (Zone 5) during summer months for the cases with and without PCMs

If the amount of solar energy transferred from the solar loop to the storage tank is enough to achieve the heating requirement of the consumer during the summer period (see Fig. 5.14-(b)), then the PCMs submerged in the tank will store the supply of energy. Hence, the magnitude of the tank losses will be different from the case where PCMs are integrated and the other one without PCMs. Furthermore, Fig. 5.14-(a) represents the annual solar fraction during the summer season for six different climatic zones, with the same loading profile (Morning). The electric backup provides more energy to the storage tank, which is integrating PCMs in order to heat water, compared to the second configuration of the solar tank where PCMs are not submerged. In fact, if the climatic Zone 5 is considered as example, thus it can be noticed that the solar fraction is 30 % in winter while is has a value arround 60 % for the case with PCM in summer period. To illustrate more the positive effect of submerging PCMs inside the tank, the climatic Zone 6 can be considered as example which is the region that has the high energy potential. Indeed, the solar fraction has an approximatelly value of 70% thank to the use of PCMs while it has only 68 % for the other case (without PCM) in summer season.

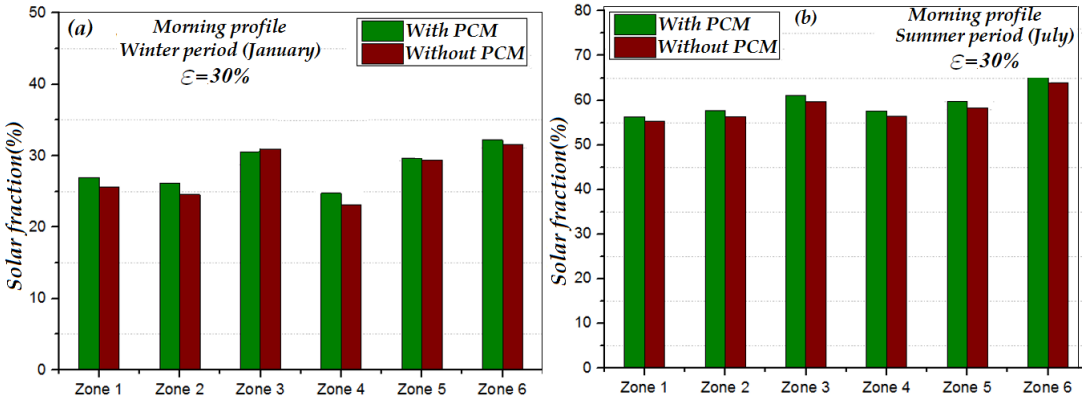

FIGURE 5.14: Solar fraction in different Moroccan regions with and without PCMs for winter and summer months

5.7 Conclusion

In Chapter 5, parametric studies were conducted dealing with the PCMs integration within solar storage tank connected to the generator of the absorption chiller.

The simulations focused on numerical approachs to assess the benefit of thermal energy storage using PCMs on the performance of solar absorption machine. The framework is used to compare thermal energy storage without and with PCMs of different types. The simulation results allow a great understanding of the dynamic discharging and charging processes of the PCMs and prescribe efficiently the operation of the storage tank filling PCMs capsules and its integration with the solar cooling systems. The overall results show that Morocco with its great solar potential is a promising field to the application of solar cooling technologies for both sensible and latent energy storage.

It should be noted that the current solar cooling absorption machine adopted in our project provides solar hot water as well as space heating which can be seen as additional economic gain and a source of energy savings. A technico-economic evaluation of the combined solar heating/cooling applications is of major importance to assess the viability of these systems which is the purpose of the Chapter 6.

Chapter 6

Potential of a combined solar DHW, heating and air-conditioning processes: Technico-economic evaluation under Moroccan conditions

6.1 Introduction

This chapter focuses on the potential of a solar installation combining heating, DHW production and air-conditioning processes intended for mass use in building sector in Morocco. The objective is to measure the relevance of the investment in such systems through a technico-economic assessment based on classic economic choice criteria. Then, a sensitivity study was conducted to analyze the impact of the major characteristics of a solar plant project (amount of investment, operation cost, solar sunshine, etc.) on the decision-making in various environments to conclude the technical feasibility and economic viability of these systems under Moroccan conditions. Parametric optimization, including the solar collectors' technology and field area in addition to the storage tank volume, was carried out to design the solar plant and to ensure its optimization during the dynamic mode operation. Several recommendations were drawn from the profitability study to identify the sensitive points and to consider avenues for improvement with a view to future industrialization of the combined solar thermal installation in Morocco.

6.2 Simulation procedure and methodology

The current work aims to derive a knowledgeable data base for the energetic performance parameters concerning the use and implementation of dynamic solar plant projects combining air-conditioning, heating and DHW systems in Morocco. Indeed, this paper aims to provide useful guidelines about the dynamic mode operation of solar air-conditioning and heating systems under Moroccan conditions based on technical and economic aspects. In this sense, the combined effects of collector's area and technology, climatic conditions and storage tank volumes on the performance of solar heating, DHW and air-conditioning systems were carried out. The novelty of the present work consists of conducting not only a techno-economic assessment but also a risk analysis study, which is less published despite its major importance especially for decision making, to evidence the effect of the operating and design parameters on the solar systems performance. On this way, dynamic

simulations were conducted for a typical modern residence located in Ben Guerir city and the energy analysis, economic viability and investment risk analysis related to the implementation of these systems were performed, and the system's optimal design and recommendations were as well addressed. The dynamic simulations were performed using Transol software which used to size thermal solar systems using the transient simulation tool TRNSYS power (*Transient System Simulation Tool (TRNSYS)*).

6.2.1 Building characteristics

The building sector accounts for 35% of Morocco's energy consumption, with an average increase of 41% over the last 8 years, as previously mentioned. Demand for electricity peaks during the summer months due to the widespread use of vapor-controlled air-conditioning systems. In addition, these systems, because of the refrigerants used can negatively influence the environment. In this vision, this section aims to outline the integration of solar air-conditioning, heating and DHW production systems in the Moroccan residential sector according to the new climate zoning established by *Moroccan Agency for Energy Efficiency (AMEE)*. It is interesting to draw the energy situation of our country. In fact, Morocco are facing increasingly significant electricity consumption (with an average rate of increase of 5.2%). Moreover, this electricity is largely of fossil origin. In addition, the kingdom suffer from a very high energy dependence rate of about 93% (Bouhal et al., 2018c). Although, Morocco has a huge potential in solar energy with more than 3000 h/year of sunshine and an average solar irradiation of 5 kWh/m^2/day (*Moroccan Agency for Sustainable Energy (MASEN)*). Therefore, this potential can be exploited to ensure the comfort needs while reducing our energy bill and respecting the environment. In this framework, this study aims to carry out a technico-economic evaluation of solar air-conditioning, heating and DHW production systems at the national level and the potential for energy saving based on the socio-economic attributes of Morocco. Accordingly, popular Moroccan residential building typologies were established based on the statistical data of *Haut Commissariat au Plan (HCP)*. It turned out that the typology most met is the category "Modern Moroccan House" which represents the majority in the country with a percentage of 61%. Therefore, our investigation is based on this category of building which is located in the research platform in the green town of Ben Guerir as shown in Fig. 2.22-(a). It was developed by the *Research Institute for Solar Energy and New Energies (IRESEN)* with the support of the *Ministry of Energy, Mines and Sustainable Development (MEMSD), Morocco* and the *Groupe Office Chérifien des Phosphates (OCP)*. Then, the air-conditioning, heating and DHW system was defined based on the metrological data of this city (Ben Guerir) and two other cities (Agadir and Tangier) representative of the new zoning established by *Moroccan Agency for Energy Efficiency (AMEE)*.

In the current study, the reference building is a one floor building with a reference area of 300 m^2 including walls and windows. The building is oriented east–west axis. Fig. **??**-(b) represents the examined building which is located in the platform Green Energy Park in the Moroccan city Ben Guerir (Latitude: 32.23°, Longitude: -7.95°, see Fig. **??**-(a)). This building is oriented along the north axis. The main building characteristics involved in the simulation procedure are given in Table 6.1.

Parameter description	Characteristics of the building
Walls	Cement mortar 2 cm, Hollow brick 10 cm, air cavity 10 cm, Hollow brick 10 cm, plaster 2 cm
U ($\mathrm{W\,m^{-2}\,K^{-1}}$)	1.25
The type of window	Clear, single
U ($\mathrm{W\,m^{-2}\,K^{-1}}$)	1.25
Floors number	1
Windows (%)	South 19, north 20, west 0 and east 0
Infiltration ($\mathrm{h^{-1}}$)	0.8
Specific gains ($\mathrm{W\,m^{-2}}$)	15
Occupation rate ($\mathrm{m^{-2}}$)	0.06
Specific lighting ($\mathrm{W\,m^{-2}}$)	10

TABLE 6.1: Parameters used for the reference building

6.2.2 Weather data

In Morocco, six climate zones were defined by *Moroccan Agency for Energy Efficiency (AMEE)* where each zone is represented by a reference city in order to establish a new thermal building regulations.

Three characteristic regions are considered in the present work which are Ben Guerir, Agadir and Tangier. The main weather data are described below:

- Ben Guerir ($31°0.37'$ N $8°0.00'$ W) representing climate zone 5, is located to the north of the foothills of the snow-capped Atlas Mountains. It enjoys a semi-arid climate with mild damp winters and hot dry summers. Its population in 2010 was 909 000 inhabitants.
- Agadir ($30°0.25'$ N $9°0.36'$ W) representing zone 1, is a city in the southwest of Morocco with a population 570 000, located on the Atlantic coast, in the region of Souss. The sunshine is more than 340 days per year. Generally, the ambient temperatures vary between 14-23 $°\mathrm{C}$.
- Tangier ($35°0.46'$ N $5°0.48'$ W) representing zone 2, is a northern Moroccan city with a population of about 850 000. It is located on the North African coast at the western entrance to the Strait of Gibraltar. Summers in Tangier are hot while winters are mild and occasionally wet.

The main meteorological data concerning the average values of the incident solar irradiation on the solar collector's field, the ambient temperature and the cold water temperature of the climate zones Ben Guerir, Agadir and Tangier are presented in Fig. 6.1 as they generated by Meteonorm Software 7.0.

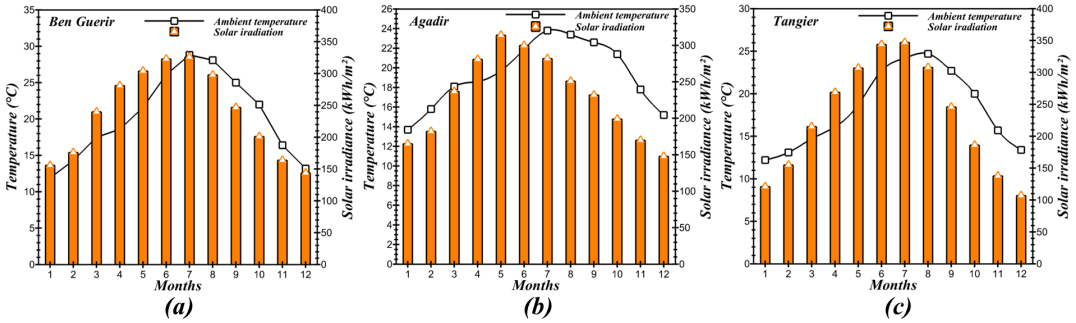

FIGURE 6.1: Meteorological data for simulations (*Moroccan Agency for Energy Efficiency (AMEE)*)

The cold water temperature depends on the location where the simulation is performed. Fig. 6.2-(a) shows the average monthly cold water temperature for Ben Guerir city. As the domestic hot water loads is required in the simulations, Figs. 6.2 ((b) and (c)) represent the daily and the annual consumption profile of domestic hot water. Indeed, a MORNING profile that represents high DHW consumption in the morning is selected as the input of our model in all cases. Indeed, the typical Moroccan load profile presented in Fig. 6.2-(b) could be described as a morning profile (*Transient System Simulation Tool (TRNSYS)*), where the daily consumption is concentrated in the morning between 7 am and 9 am, besides to the first three hours of the afternoon, namely 12 pm, 1 pm and 2 pm. The hourly coefficients of 4th-5th hours are reported to be null values, because water is not consumed during this two hours period. In fact, the hourly coefficient H_{coeff} is determined using the following equation: $H_{coeff} = \frac{V_{c,h}}{V_t} * 24$ while the multiplier coefficient M_{coeff} is calculated as follows: $M_{coeff} = \frac{V_{c,m}}{V_{t,m}} * 12$. In these equations, $V_{c,h}$ and V_t are the consumed volume per day and the total volume of DHW, $V_{c,m}$ and $V_{t,m}$ represent the consumed volume per month and the total annual volume of DHW. Moreover, the multiplier coefficient allows the calculation of the consumed amount of the DHW during the month Fig. 6.2-(c). The sum of the hourly and multiplier coefficients are equal respectively to 24 which is corresponding to the average number of hours per day while 12 referring to the number of the months of the year (*Transient System Simulation Tool (TRNSYS)*).

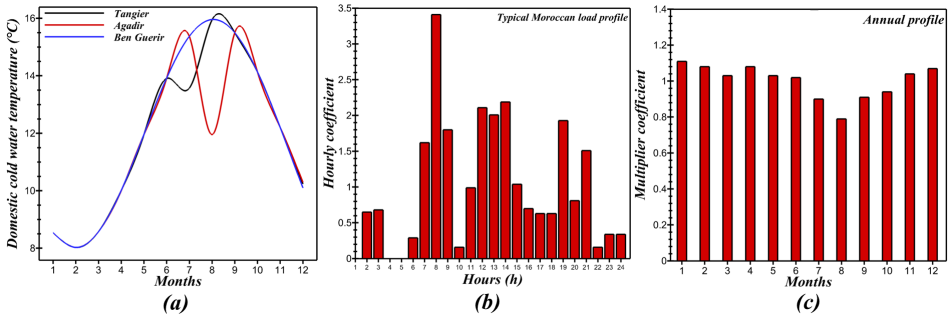

FIGURE 6.2: (a)- Average monthly cold water temperature for each Moroccan zone, (b)- Daily and annual consumption profile of domestic hot water

The valuable solar potential of each region will be exploited in order to satisfy the cooling requirements of the building. The calculation of the cooling loads Q_{load} for air conditioning aims to determine the power of the installation which will be able to meet the requested criteria. This calculation is based on real gains, i.e. when calorific

contributions reach their maximum in the local. The choice of sizing elements of solar cooling system and its design are strongly dependent on the region's climatic conditions and the thermal load of the building. The calculation of the loads must be done under the basic conditions which lead to the maximum loads and which allow to know the powers to be installed. As reported in the work of (Pedersen, Fisher, and Liesen, 1997), the building thermal loads dynamically changing with time and can be classified in 2 categories: external loads (insolation, air infiltration, outdoor ambient temperature, outdoor humidity, windblown, etc) and internal loads (occupants, lighting, office equipment, ancillary facilities, etc.).

A safety factor is generally adopted after having made the calculation of air-conditioning for the considered building. This coefficient varies between 0 and 5% depending on whether one knows more or less the elements entering during the establishment of the thermal balance (Florides et al., 2002b; Eicker, 2006).

Fig. 6.3 presents the estimated cooling loads which take into account several factors such as both external and internal gains, occupancy and climatic data as it was generated from Meteonorm database.

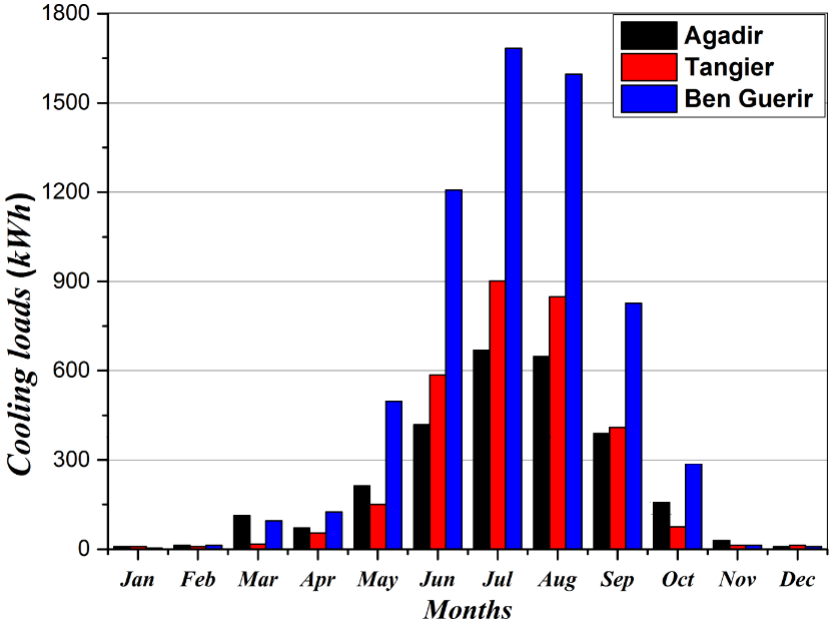

FIGURE 6.3: Cooling requirements for the three regions

It can be shown from Fig. 6.3 that the cooling loads vary according to the months of the year and the climate; the maximal cooling loads in all the climatic regions are observed during the July month. In Zone 5 (represented by Ben Guerir city characterized by extremely hot summer months), the cooling loads exceed a value of 1750 kWh. From Fig. 6.3, it is observed that the cooling demand of Tangier is higher than Agadir for most the summer. The cooling loads are generally negligible during winter months independently on the region. As we studied the heating/cooling production, it's interesting to present the estimated cooling and heating loads for Marrakech city (Z5) that are generated from Meteonorm database as shown in Fig. 6.4. The comfort temperatures T_c for the three options:

- Air-conditioning : $T_{c,con}$= 26 °C
- Heating : $T_{c,hea}$= 19 °C
- DHW : $T_{c,dhw}$= 45 °C

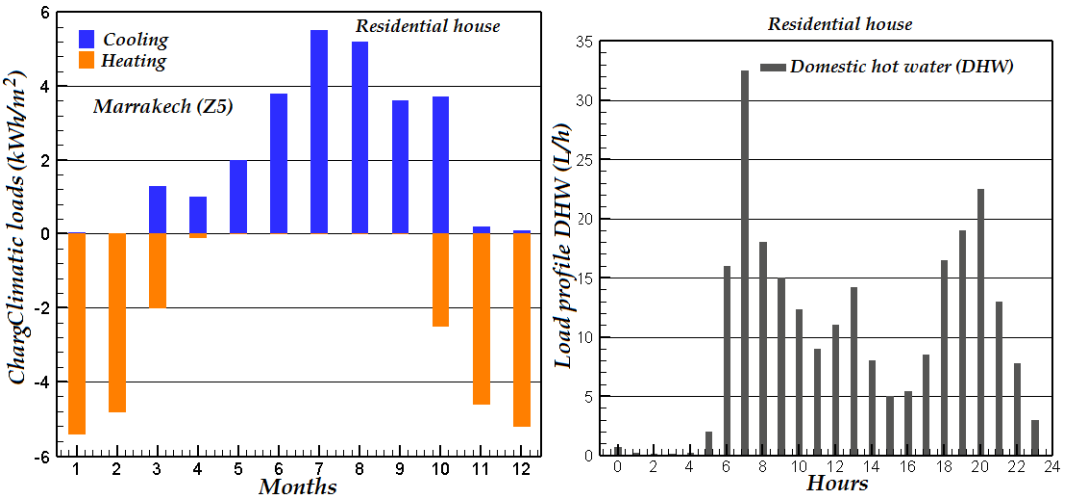

FIGURE 6.4: Cooling/heating demands and DHW profile for the studied city Marrakech (Z5)

In order evaluate the performance of the solar cooling and heating systems under Moroccan conditions, the dynamic simulation software Transol has been used. This tool is based on dynamic simulation and has been developed with the TRNSYS simulation tool which is a well-known academic and commercial software. The software includes a large library of built-in components, often validated by experimental data (*Transient System Simulation Tool (TRNSYS)*). From this study, we deduce the economic performance indicators to finally generalize it throughout the Moroccan territory.

6.3 Economic approach

An economic approach is applied to the solar installation of Fig. **??** combining air-conditioning, heating and DHW production. The solar plant consists of an absorption machine which is the most present on the solar refrigeration market. Their combination with flat plat and vacuum thermal solar collectors is fairly well known in the field of large installations. However for small systems, which is the case of this work (11.5 kW), the unsteady behavior of these machines is not yet well known due to all the transient parameters influencing the functioning of these machines, such as the solar resource, the environmental conditions and the refrigerating charge of the building. A set of economic indicators were used to assess the economic viability of the system.

6.3.1 Cost of energy saving K_{es}

The cost of energy saving K_{es} is considered as the first economic indicator. In our case, it compares economic gain when the solar absorption system replaces a conventional cooling unit (a vapor compression machine). The K_{es} is expressed as follows:

$$K_{es} = K_{cv} - K_{sol} \tag{6.1}$$

where K_{cv} is the cost of the consumed electric energy in the case of the conventional system and K_{sol} is the cost of the consumed electric energy in the case of solar

cooling system. The cost of annual electricity consumption K_{el} can vary during the lifetime, so the inflation rate of electricity must be introduced, as in Eq. 6.2:

$$K_{el} = K_0(1 + i\%)^T \tag{6.2}$$

In Eq. 6.2, K_0 is the cost of annual electricity consumption at the first operation year, $i\%$ the inflation rate (%) which is the change in energy prices relative to general inflation or energy inflation in the country and T is the lifetime period.

6.3.2 Payback period P

The payback period P that refers to the required time of recovering the cost of the initial investment paid in the whole thermal installation. P is expressed as:

$$P = \frac{log(1 + \frac{I_0.i\%}{100.K_{es}})}{log(1 + \frac{i\%}{100})} \tag{6.3}$$

In Eq. 6.3, $i\%$ is the electricity inflation rate, and K_{es} is the cost of energy saving in (e/yr). The term I_0 presents the capital cost of the investment which is the sum of the separate costs. More specifically, the solar collectors (C_{coll}, A_c), the storage tanks (C_{tank}, V), the absorption chiller (C_{ch}, $Q_{e,m}$) and the mechanical compression refrigerator (C_{mc}, Q_{ch}), are the main parts of the system that have to be taken into account in the cost analysis. The other costs are assumed to be included in these quantities. Eq. 6.4 describes the way that the investment cost is calculated in every case:

$$I_0 = C_{coll}.A_c + C_{tank}.V + C_{ch}.Q_{e,m} + C_{mc}.Q_{ch} \tag{6.4}$$

6.3.3 Net Present Value (NPV)

The Net Present Value (NPV) is the benchmark for investment choice which is an economic criteria used to evaluate the present value ($t = 0$) of a number of future cash flows at a given interest (Henry, 1974).

$$NPV = -I_0 + \sum_{t=1}^{T} \frac{CF_t}{(1+r)^t} \tag{6.5}$$

where I_0 is cost investment of installing solar cooling equipments (e), r is the market discount rate, T is the project life time (yr). CF_t is the cash flow or the net yearly benefit (e/yr) that represents the difference between the operation and maintenance cost in addition to insurance of solar cooling and conventional electric cooling system. Indeed, CF_t is calculated as the income from the cooling production minus the cost of the electrical consumption and minus the costs for operation and maintenance, according to Eq. 6.6. It is important to state that the yearly cooling production (Q_{prod}) and the yearly electrical consumption (Q_{aux}) are calculated with integration during the entire year period.

$$CF_t = C_{ref}.Q_{prod} - C_{O\&M} - I_0 - C_{el}.Q_{aux} \tag{6.6}$$

The cooling cost (C_{ref}) can be calculated as the ratio of the electricity cost (C_{el}) to the equivalent COP of the single stage mechanical compressor refrigeration system $C_{ref} = C_{el}/COP$ (Mroz, 2006).

6.3.4 Internal Rate of Return (IRR)

The Internal Rate of Return (IRR) is also an important parameter which shows the real efficiency of the investment. IRR is the discount rate for which the NPV of the project is nil as expressed in Eq. 6.7:

$$NPV = -I_0 + \sum_{t=1}^{T} \frac{CF_t}{(1+IRR)^t} = 0 \tag{6.7}$$

The review of the literature indicates a wide difference on the costs of the thermal components. In fact, these costs vary according the country, the power range and the manufacturer. Accordingly, some assumptions are considered and justified through the literature review and the market considerations (Tsoutsos et al., 2003).

In this chapter, two major optimization studies were carried out. The first study focuses on the thermal performance of the solar plant project combining air-conditioning, heating and DHW. The volume of the storage tank was varied and its impact on solar fraction as well evaluated. The effect of the collector's field was also studied. Indeed, the system performances were compared by adopting an evacuated tube collector (ETC), and a flat plate collector (FPC). The second study focuses on the cost benefit and investment risk analysis of the studied solar plant project based on classic economic indicators such as IRR and NPV. Then, a sensitivity study was performed to analyze the impact of the major characteristics of the solar plant project (amount of investment, operation cost, solar sunshine, etc.) on the decision-making in various environments to conclude the economic viability of such solar plant projects and their generalization in Morocco.

6.4 Effects of ETC collector's area and storage tank volume on the annual solar fraction

The impact of ETC ollector's technology on solar fraction for DHW, heating and cooling was studied. Fig. 6.5-(a) shows the evolution of the monthly solar fraction regarding domestic hot water production. Then, Fig. 6.5-(b) describes the evolution of the monthly solar heating fraction. Finally, Fig. 6.5-(c) presents the evolution of the monthly solar fraction of cooling. These parametric studies were conducted taking into account the evolution of the annual solar irradiation in the city of Marrakech for the solar collector technology ETC. In addition, the number of the collectors constituting the solar field has been varied to evaluate the effect of their area on the various solar fractions, whether for the hot water production, heating or air-conditioning. Indeed, the initial number of the collectors used to satisfy the need of this application is 16 m^2, and an increment step of 8 m^2 was used to constitute the new collector panels. In fact, a maximum number has been constituted in this parametric study in which the total collector's area is 40 m^2. However, it is interesting to note that the optimization objectives of a solar thermal system aren't usually linked to maximum collect of energy throughout the year but avoiding overheating to secure the solar system lifetimes as long as possible (Duffie and Beckman, 2013). The optimization of the assessed solar fractions can be ensured by increasing the number of collectors, independently of their technologies either ETC or FPC collectors. For example, for the month of January, the solar fraction for the production of domestic hot water has been improved from 82% to 100% by increasing the ETC collectors from 16 to 40 m^2. It is the same for the solar fraction of the heating which increases

up to 88% by combining an ETC collector's area of 16 m^2 (see Figs 6.5-(b)). The annual solar fraction of air-conditioning (see Figs 6.5-(c)) shows that the solar fraction is zero for a independently on the collector's area. This behavior is explained by the fact that there is no needs for the air-conditioning during winter. Otherwise, the solar fraction for cooling reaches more than 80 % in summer period for an important collector's area.

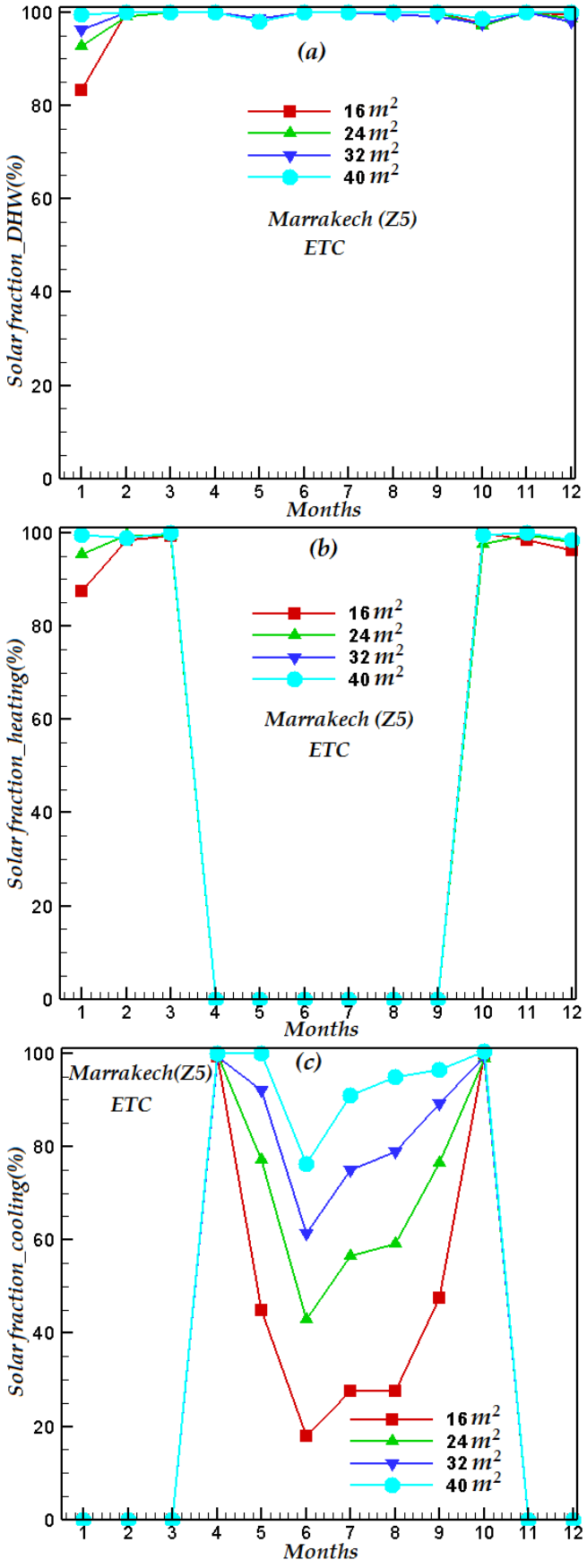

FIGURE 6.5: Effect of the ETC collector's areas on the monthly solar fraction for DHW, heating and cooling loads in Marrakech city

To assess the impact of climate zones on thermal performance of the solar plant, the meteorological data of Agadir and Tangier cities are considered. The same tendencies have been observed as those of Ben Guerir city as shown in Figs. 6.6.

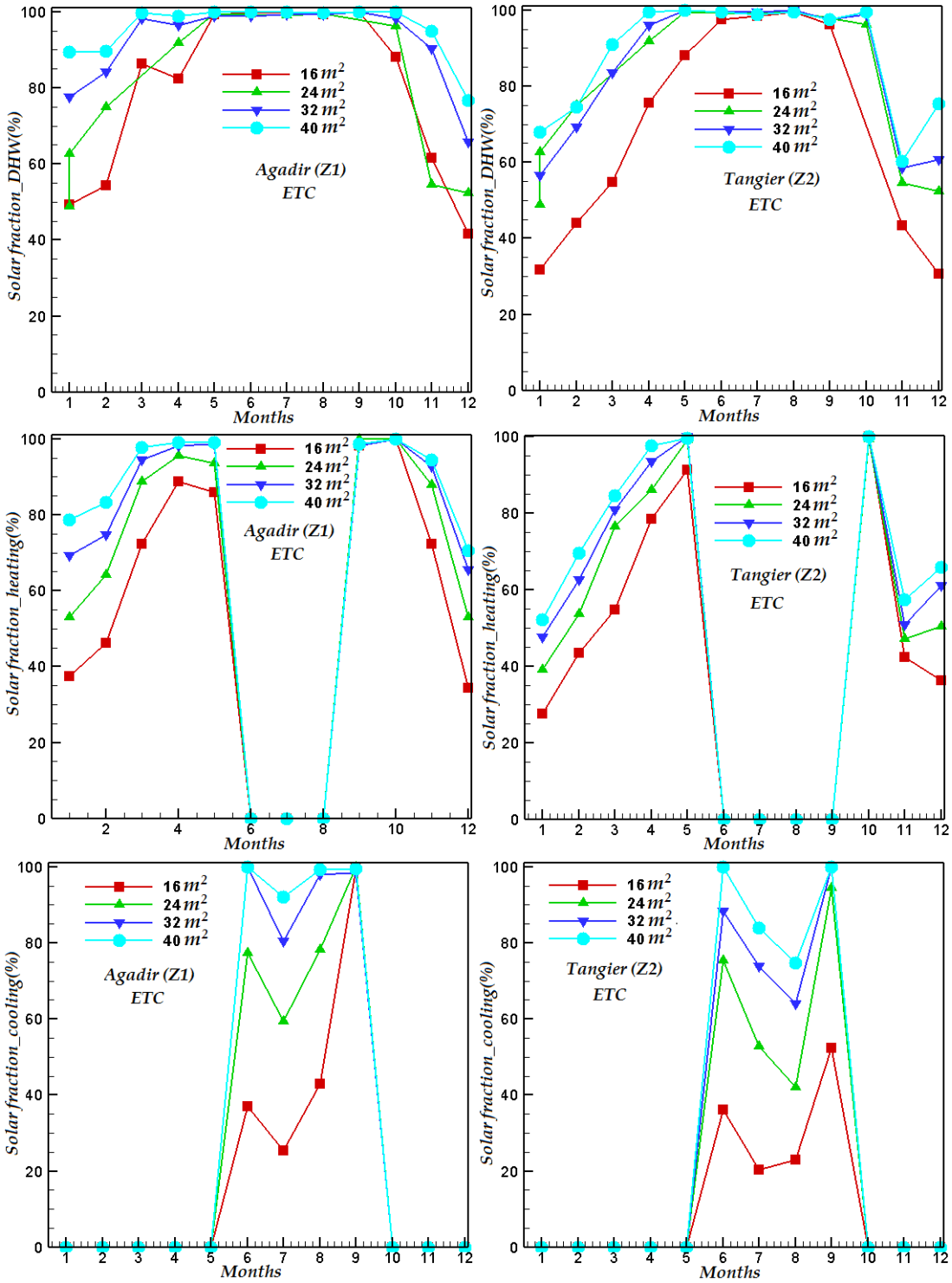

FIGURE 6.6: Effect of the ETC collector's areas and climate zones on the monthly solar fraction for DHW, heating and cooling loads in Agadir city

The effect of storage tank volumes on solar fraction for DHW, heating and cooling was studied. First, Figs. 6.7-(a) shows the evolution of the monthly solar fraction regarding hot water production. Then, Fig. 6.7-(b) describes the evolution of the monthly solar heating fraction. Finally, Fig. 6.7-(c) presents the evolution of the monthly solar fraction of cooling. These parametric studies were carried out taking into account the evolution of the annual solar irradiation in the city of Marrakech for ETC collectors. In addition, the volume of the storage tank has been varied to assess its impact on the investigated solar fractions, whether for hot water production, heating or air-conditioning. Indeed, the initial storage tank volume used to satisfy the need of this application was 500 liters, and an increment step of 500 liters was used to constitute the new vertical thermal storage tank volume. In fact, a maximum volume has been reached in this parametric study in which the total volume was 2000 liters. The volume of the storage tank does not greatly affect the solar fraction of the heating as shown in Fig. 6.7-(b). On the other hand, its effect remains notable with regard to the improvement of the solar fraction relative to the production of domestic hot water during winter and solar cooling during summer. For ETC technology, the solar domestic hot water fraction was improved from 80% to 100% by decreasing the volume of the storage from 2000 to 500 l. It should also be noted that the volume of the storage tank is inversely proportional to the improvement of the solar fraction of cooling because of the increase of thermal losses inside the storage tanks when their volume would be increased (see Fig. 6.7-(c)). A similar study under Malaysian climatic conditions can be found in the literature in which Assilzadeh et al., 2005 have performed the simulation and the optimization of a LiBr solar absorption cooling system with evacuated tube collectors.

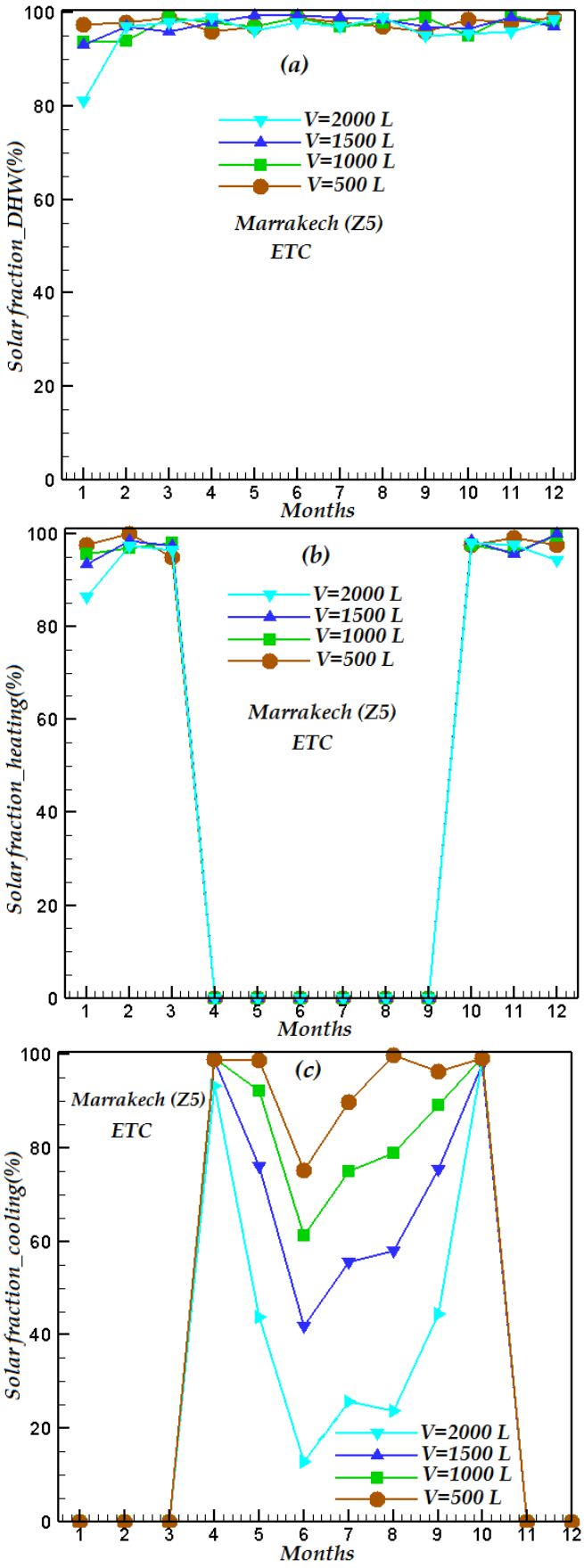

FIGURE 6.7: Effect of the tank's volume on the monthly solar fraction for DHW, heating and cooling loads in Marrakech city

To examine the impact of climate zones on thermal performance of the solar plant, the meteorological data of Agadir and Tangier cities are selected. The same tendencies have been observed as those of Marrakech city as shown in Figs. 6.8.

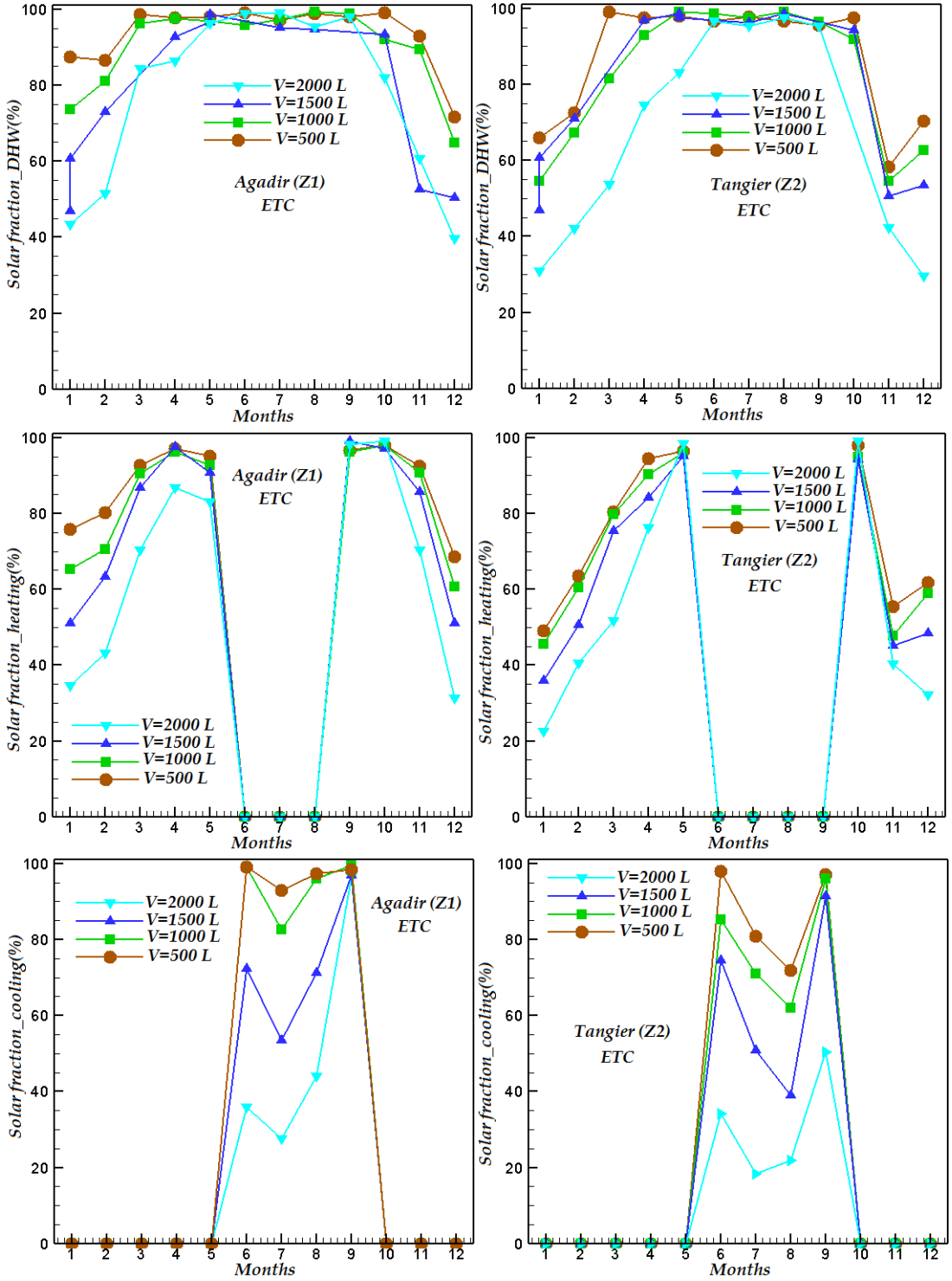

FIGURE 6.8: Effect of the storage volumes and climate zones on the monthly solar fraction for DHW, heating and cooling loads in Agadir and Tangier city

Solar fraction for DHW, heating and cooling production as function of different ETCs collecting areas and tank's volumes are presented in Figs. 6.9. Two months

were considered to describe the evolution of the solar thermal coverage, namely February defined by [M-2] and June described by [M-6] (see Fig. 6.9-(a)). Moreover, the weather effect of the previously selected cities was also taken into consideration to establish this parametric study, which investigates the effect of the collector's number on the solar coverage during the cold and the hot period of the Moroccan weather. Solar fraction for DHW remains between 65% and 90% during February, while it is between 90% and 100% during July for a solar collector field that integrates between 8 and 20 ETCs. Moreover, as shown in Fig. 6.9-(a) the fact of using 18 ETCs allow to achieve high solar thermal performances. In fact, the solar coverage for Agadir during February is 88%, also it is 82.50% for Ben Guerir and finally it is 83% for Tangier. Further, solar fraction for heating as presented in Fig. 6.9-(c) has been assessed at zero which is an obvious result (Mateus and Oliveira, 2009). In addition, the solar coverage concerning heat production is increasing with the increase of the ETCs number. Indeed, using 14 ETCs help to achieve a solar fraction of 40% for Agadir during February, while it remains 23% if 8 ETCs are used to constitute the solar collector field. Finally, the solar fraction for cooling is also affected by the number of the ETCs as illustrated on Fig. 6.9-(e). The fact of using 16 ETCs tends to increase the solar coverage intended for cooling application to 90% for Tangier, knowing that it was 8% while considering a solar panel composed of 8 ETCs. It can be concluded from this parametric study that the optimal number of ETCs is 16 evacuated tube collectors, because the solar coverage for DHW, heating and cooling is enhanced and could achieve an average value during the cold period of the year above 38%.

The effect of the storage tank volume on the solar coverage for DHW, heating and cooling production has been assessed under the weather conditions of Ben Guerir city. Five storage volumes of the vertical thermal tank were considered, namely 1000, 1500, 2000, 2500 and 3000 liters to investigate the monthly solar thermal efficiency according to two periods: February defined as [M-2] and June described as [M-6] (see Fig. 6.9-(b)). As shown in Fig. 6.9-(d) the storage tank volume do not affect the solar fraction for DHW during June, where the magnitude of solar irradiations are important Dîn Fertahi et al., 2018a. However, an additional incremental increase of 500 liters on the storage tank volume affects the solar coverage for DHW. In fact, it was 49% while using 1000 liters and it has increased to 63% by doubling the storage capacity to 2000 liters. Moreover, it can be seen that heat production is enhanced during February with the increase of the storage volume to 2000 liters, because the solar fraction for heating has achieved 46%. Indeed, slight changes were noticed above this volume (see Fig. 6.9-(d)). Furthermore, the solar coverage for heating during hot periods such as June are described with null values, as it is reported in the study of Ge et al., 2017. Concerning solar fraction for cooling, the effect of the storage tank volume does not seem to have an effect on the solar coverage intended to produce cooling during hot periods of the year such as June Fig. 6.9-(f), because solar fraction for cooling remains between 19% and 23%. However, the storage tank volume does affect the solar coverage for cooling during the coldest period of the year in Morocco such as February. Indeed, it has decreased from 100% related to a storage volume of 1000 liters to 24% related to the use of 2500 liters. Similar results were achieved in the study of Mateus and Oliveira, 2009.

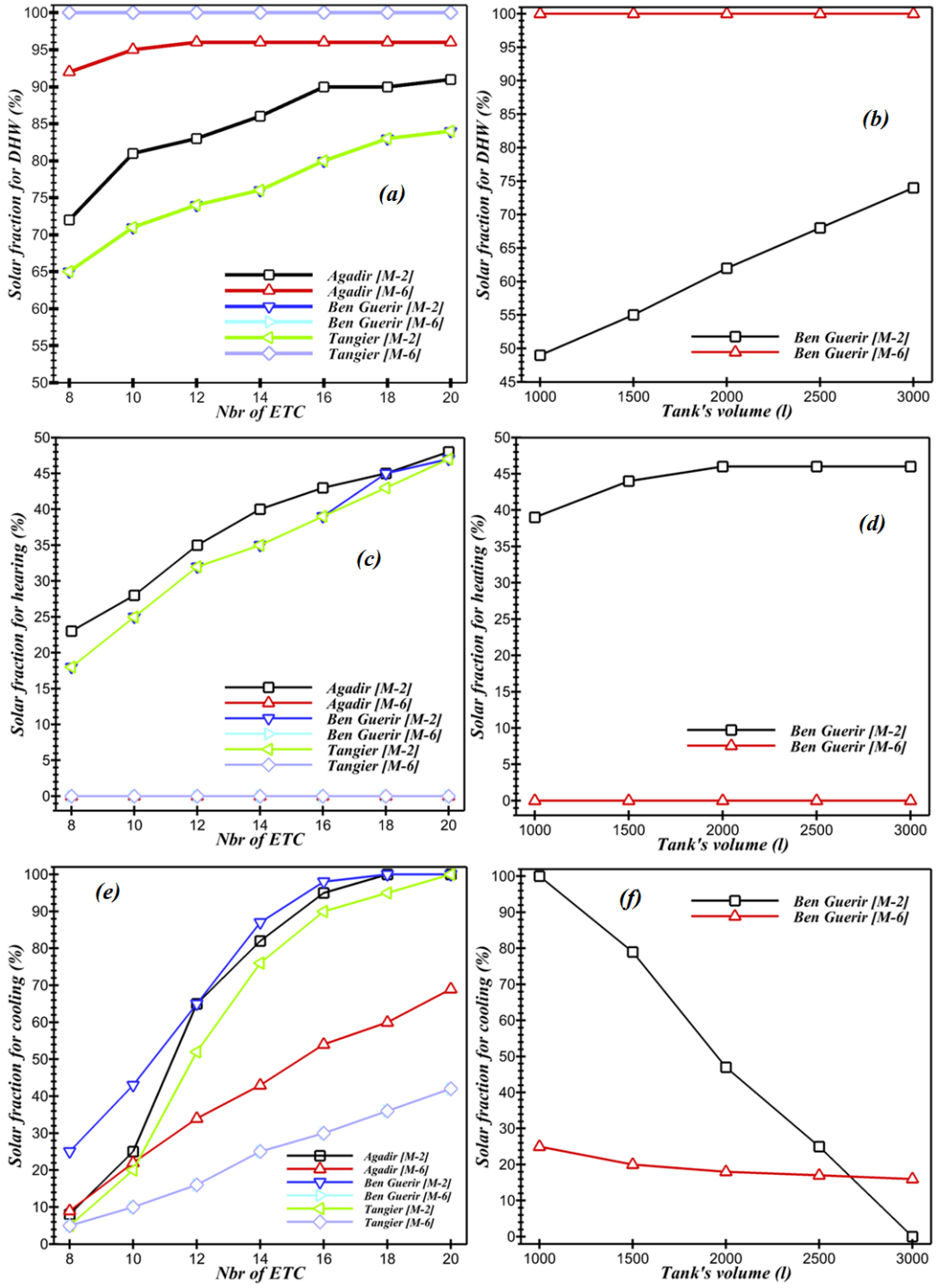

FIGURE 6.9: Impact of ETC collecting areas and tank's volumes on solar coverage during the winter and summer months for DHW, heating and cooling in different regions

The annual solar cooling production for Ben Guerir, Agadir and Tangier is presented in Fig. 6.10-(a). Regarding Fig. 6.10-(b), it helps to assess the amount of the annual booster consumption during the year. It has been found that, solar cooling production is maximized during the summer season considered as a significant sunshine period (Agrouaz et al., 2017). For instance, for July, the cold production reached 400 kWh for the city of Agadir, 620 kWh for the city of Tangier and 600 kWh for the city of Ben Guerir. An interest was brought to maximizing the production

of cold in the summer to ensure the comfort of the inhabitants, while reducing the bill for electricity/hydraulic deployed to meet the needs of the consumer when solar radiations are not sufficient (Dîn Fertahi et al., 2018a). As shown in Fig. 6.10-(b), the electric auxiliary heater does not work during the months of June, July, August and September due to significant solar irradiation. On the other hand, it is maximized during the winter season. For example for the month of January it reaches 1250 kW h for the city of Agadir, 1875 kW h for the city of Tangier and 2225 kW h for the city of Ben Guerir. Relevant studies have been done in other countries. For instance in Europe, solar cooling systems were also tested and validated. Accordingly, energy and economic aspects of an integrated solar absorption cooling and heating system in different building types were evaluated under different locations Berlin (Germany), Lisbon (Portugal), and Rome (Italy) (Mateus and Oliveira, 2009).

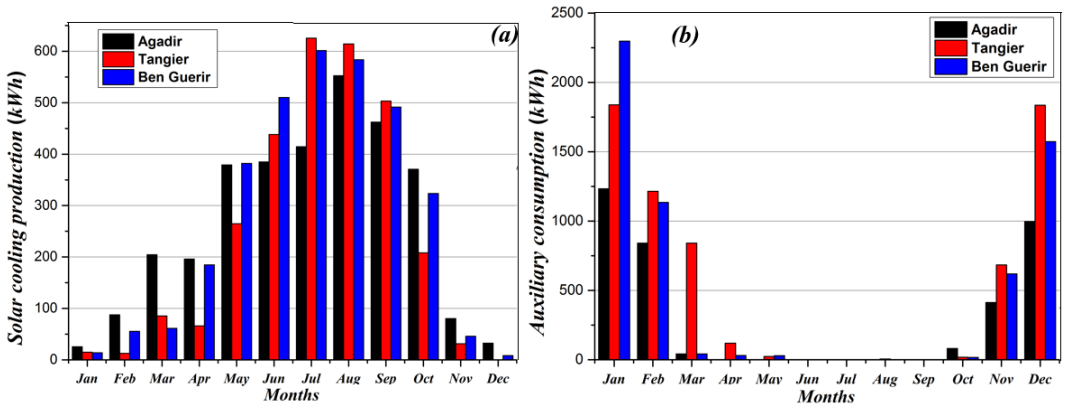

FIGURE 6.10: Solar cooling production and auxiliary energy consumption in different regions

Fig. 6.11 presents the contribution of the annual solar energy to produce hot water, heating and air conditioning for the considered cities, notably Ben Guerir presented in Fig. 6.11-(a), Agadir shown in Fig. 6.11-(b) and the city of Tangier presented in Fig. 6.11-(c). The difference in the solar contribution recorded with respect to each studied city is caused by the climate effect in terms of solar irradiation incident on the collector panel. Regarding solar air conditioning, and if June is considered to conduct the comparison study in terms of the solar contribution. Hence, it was recorded that the solar contribution reaches 950 kW h, 690 kW h and 890 kW h respectively for the three cities of Ben Guerir, Agadir and Tangier. Regarding the production of hot water, the field of solar collectors ensures a contribution, assessed during the month of June, equal to 650 kW h, 690 kW h and 650 kW h for the cities of Ben Guerir, Agadir and Tangier. Last but not least, concerning the thermal heating, the solar contribution that has been recorded for the month of January is assessed to 450 kW h, 550 kW h and 570 kW h for the cities of Ben Guerir, Agadir and Tangier. Finally, it has been concluded that the field of solar collectors have to be sized according to the amount of incident solar radiation which is available per city, besides to the consumer needs in terms of heating, cooling or daily hot water production. In addition, it has been noticed that the solar contribution of the absorption machine is zero during the summer season, but it is maximized for the production of cooling (Agrouaz et al., 2017).

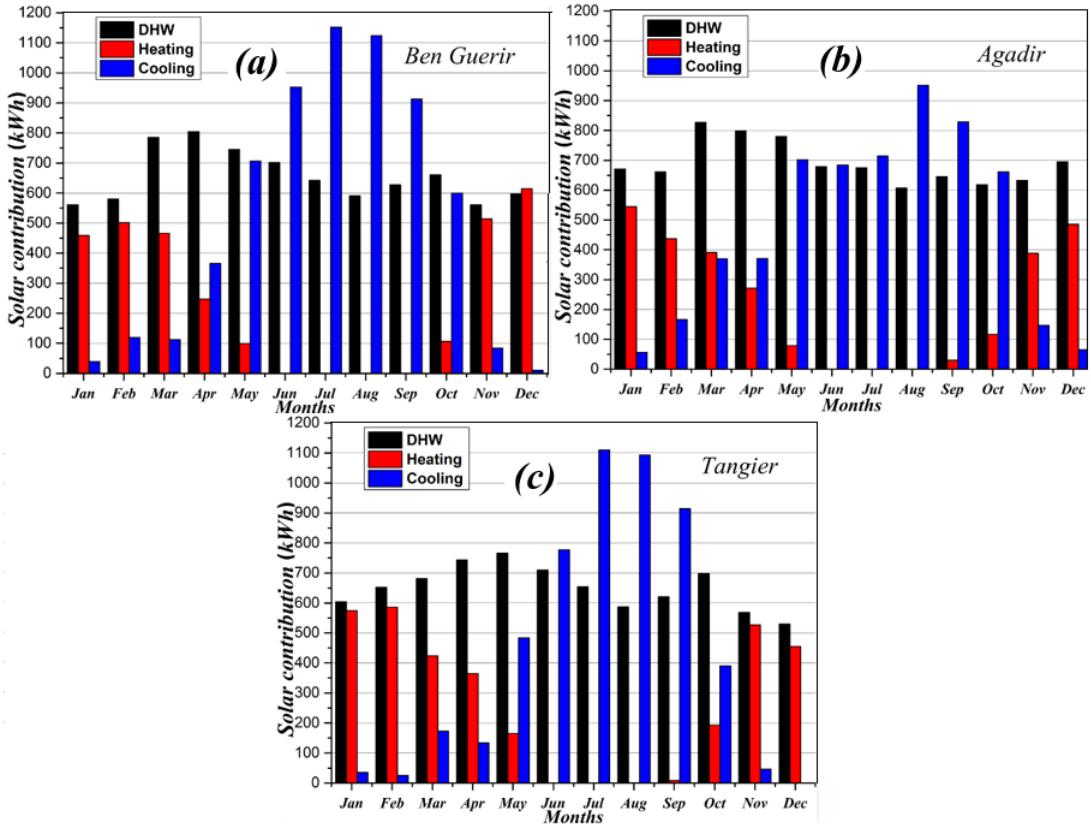

FIGURE 6.11: Solar contribution in different regions

In order to make clearer what energy flows (DHW, cooling, heating, auxiliary) are greater in the studied cities, summer and winter months were selected as shown in Fig. 6.12. Thus, the solar contribution for DHW, heating and cooling has been assessed for Ben Guerir, Agadir and Tangier as presented in Fig. 6.12. Two significate months were considered to evaluate the auxiliary consumption and the solar coverage expressed in kWh (Desideri, Proietti, and Sdringola, 2009), because the effect of higher and lower solar irradiations measured respectively for January and June were taken into account. For instance, the assessed solar contribution for Ben Guerir (see Fig. 6.12-(a)) during January achieved 48 kWh and almost 950 kWh during June. Further, according to Fig. 6.12-(c), that describes the pattern's evolution of the solar coverage for Tangier, it was reported that the solar contribution has increased from 605 kWh in January to 705 kWh in June. In addition, the heating requirements in Agadir Fig. 6.12-(b) are satisfied with a solar coverage of 540 kWh during January, which is the cold period of the year accordingly to the Moroccan weather. The booster consumption has also been assessed during January and June for the three studied cities, in order to depict the effect of the weather conditions on the thermal efficiency of the current investigated solar heating/cooling system intended to be integrated in Morocco. For example, the auxiliary consumption has achieved respectively 1450 kWh, 1875 kWh and 2300 kWh for Agadir, Tangier and Ben Guerir during January Fig. 6.12-(d). It is noted that the operating mode of the booster equipment remains off during June, because the amount of solar radiations is sufficient to meet the requirements of DHW, heating and cooling (Eicker and Pietruschka, 2009).

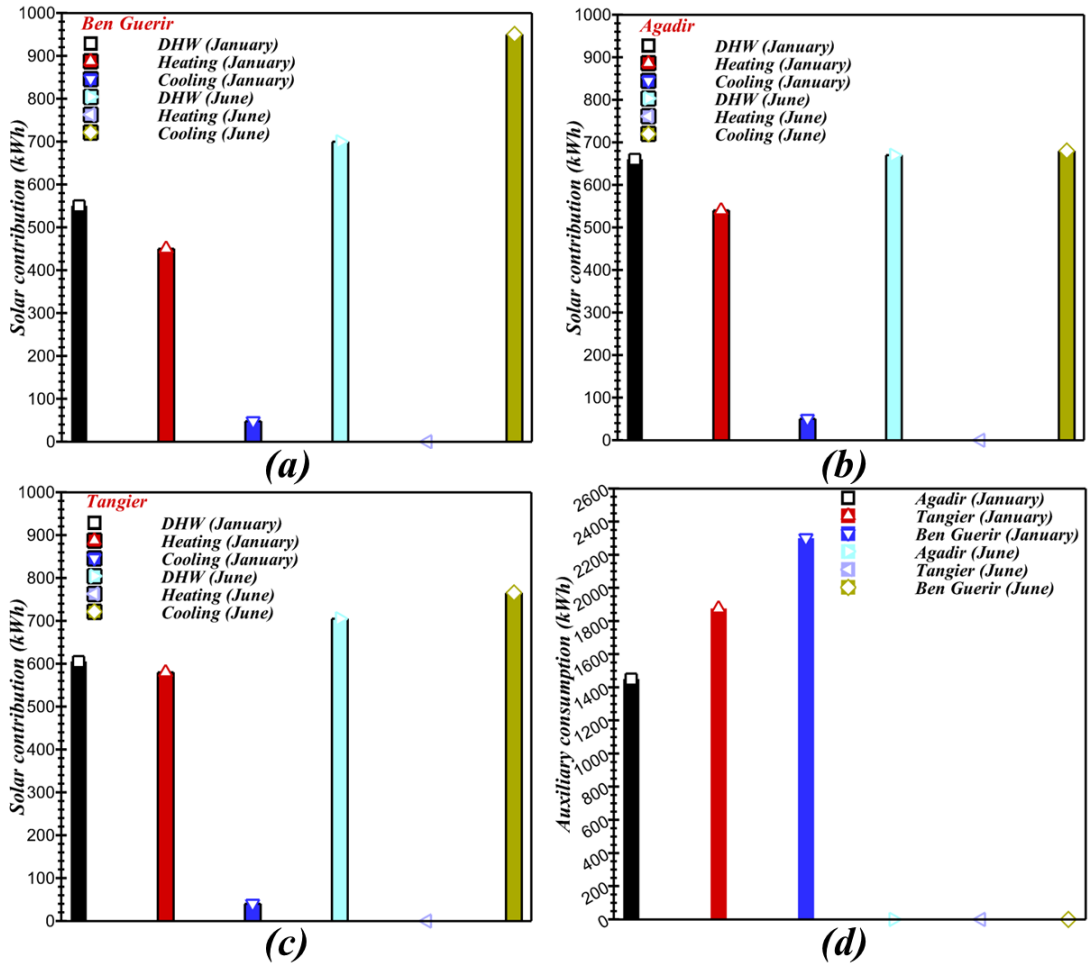

FIGURE 6.12: Energy flows of DHW, cooling, heating and auxiliary in different cities in winter and summer months

In many parts of the world, similar studies have been carried out and several researchers are interested in the technical feasibility of the solar air-conditioning and heating systems and their performance. In Jordan, the potential of utilizing solar cooling in residential sector such as universities has been assessed by Fasfous et al., 2013. Under different climates of Algeria, Bahria et al., 2016 carried out a parametric study of solar heating and cooling systems and conducted a comparison between high-energy-performance and conventional buildings. The studied countries have approximately similar geographic and cultural properties to Morocco and the trends in these countries are in qualitative accordance to our achieved results.

6.5 Economic and investment risk analysis applied to solar plant combining air-conditioning, heating and DHW production

6.5.1 Investment profitability of the solar plant project

The solar installation combining heating, air-conditioning and domestic hot water production remains one of the relevant options for the exploitation of solar energy potential in Morocco. The flow diagram for the development of such solar plant project is presented in Fig. 6.13.

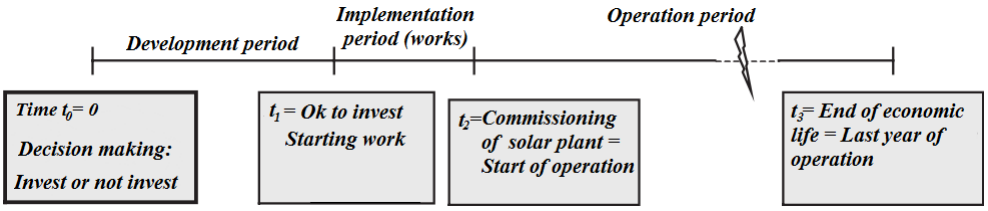

FIGURE 6.13: Tasks planing during the development of solar plant combining heating, air-conditioning and domestic hot water production

At the beginning of the development period (at time t_0 = 0), the question for the project manager is whether or not should enter the development period. As the decision is very crucial in this framework, a study of the intrinsic profitability of the project (including the development period) has been done. The Business Plan of the solar cooling, heating and DHW project provides the following information which we have considered as *certain* in this first part:

- The development phase of the project ends in t_1 = 25 months.
- We assume that the financing of the investment is made half by equity (shares paid 8%), half by bank loan (at the rate of 4%).
- The duration of the works (installation of equipment and connection to the hydraulic/electrical network) is 12 months ($t_2 = t_0 + 3$ years).
- The production of cooling, heating and DHW starts at the commissioning of the plant (t_2) and is identical each year over an economic life of 20 years ($t_3 = t_0 + 22$ years = last year of operation).
- The solar field is estimated at 3000 hours per year (more than 3000 h/year of sunshine on average in Morocco (*Moroccan Agency for Sustainable Energy (MASEN)*).
- Given the solar potential and Moroccan legislations (*Office National d'Electricité et de l'Eau Potable (ONEE)*), the price per kWh will be 0.09 e during the full years of operation.
- Operating expenses (maintenance, operation, insurance) are estimated at 1% of the initial investment cost (Allouhi et al., 2015b).

The results of financial costs of the solar plant project are listed in Table 6.2.

Parameter description	Value
Prices (€)	-
Absorption chiller	4048
Thermal collectors	6000
Cooling tower	750
Back-up chiller	300
Cold storage tank	300
Hot storage tank	720
Pumps	600
Installation costs	1526.16
Initial investment I_0	14244.16
Maintenance cost of the solar system	142
Mean cost of energy saving	405.7
Payback period	25 years

TABLE 6.2: Financial cost of the solar plant project

We aim to determine the classic economic indicators such as gross return time (i.e. undiscounted), the Net Present Value (NPV) and the Intern Rate of Return (IRR). Financial and net cash flows CF_t are determined using Eq. 6.6 for each year of the solar plant project. In this case, the cumulative cash flows CF_t become positive after 10 years and then the gross return time is 10 years. In the Project Financing approach, the discount rate to be considered is the weighted average cost of the capital raised for the investment $r = 1/2 \times 8\% + 1/2 \times 4\% = 6\%$. The IRR for this case is 10.48%. Indeed, if the shareholders, like the bank, asked for a return on capital invested of 11%, the project would not be retained because it would take a discount rate of 11%. Therefore, the discount rate would be higher than the IRR, the NPV would be negative and the project would not be profitable. Then, the NPV of this reference project NPV is 3.16 ke (its IRR is 10.48%). These results are good. This is partly explained by the important solar energy contribution and then the cash flow generated. Also, it is mainly due to the fact that this result is based on a simplified model that does not take into account the corporation tax.

6.5.2 Sensitivity analysis applied to solar plant for air-conditioning, heating and DHW production

It is clear from the views of the planning uncertainties that the developer has a vague idea of the profitability of a solar plant project at the beginning of its development. Thus, the classic indicators related to investment choice, the net present value (NPV), the internal rate of return (IRR), the payback period (P) and the cost of energy saving, are determined to examine the project profitability which depends on the project environment. In particular, there is a risk on the amount of investment, the solar sunshine, the operating expenses and the rate of inflation.

The annual cost of energy saving was defined as a monetary indicator to evaluate the effect of the three cities, namely Agadir, Tangier and Ben Guerir. In addition, its evolution has been presented using a diagram in a stick as shown in Fig. 6.14. Cost of energy saving has been assessed using Eq. 6.1, and the curve of energy cost saving was highest during the summer period of the year, because the efficiency of the absorption machine to generate cold was important (see Fig. 6.14). For July, cost of energy saving recorded the following values: 312.5, 320 and 310 euros respectively for the cities of Agadir, Tangier and Ben Guerir. However, for the month of January,

cost of energy saving recorded the following values: 25, 30 and 22.50 euros respectively for the cities of Agadir, Tangier and Ben Guerir. Thus, I can be concluded that the solar contribution in the efficiency of the absorption machine, as well as the hours of operation of the electric/hydraulic booster affect the total balance sheet that has been quantified in euro of the monetary indicator cost of energy savings. In other words, the higher the annual solar fraction of the absorption machine, the lower the consumption of non-renewable energies, which generates a significant annual optimization of Cost of energy saving are recorded, especially since the demand for air conditioning is increased during the summer period to ensure consumer comfort (Wu et al., 2014).

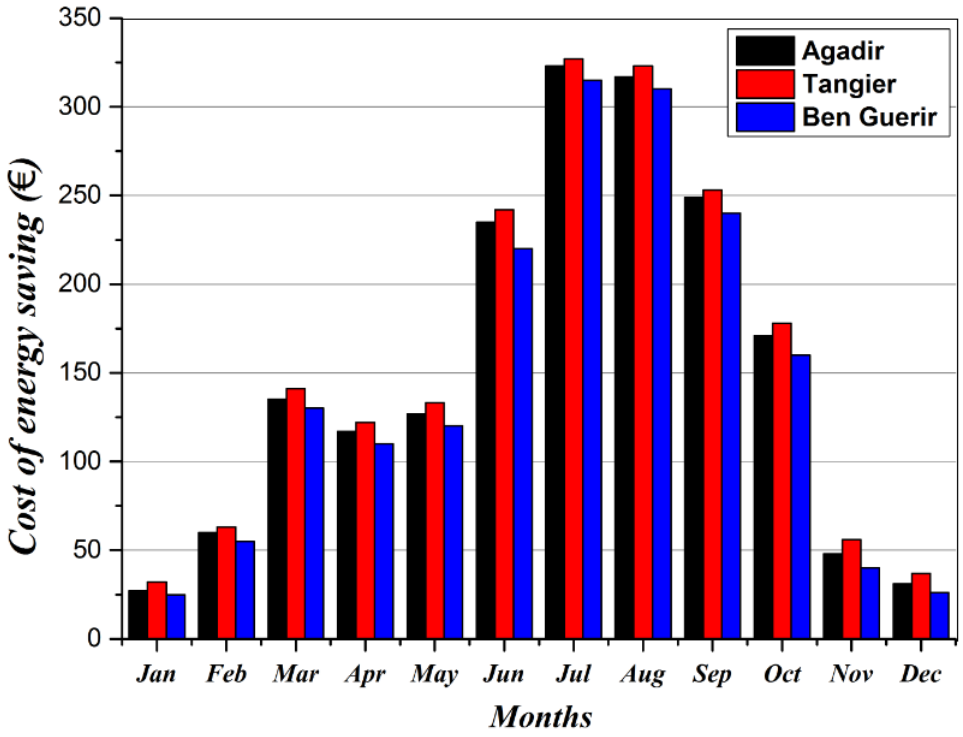

FIGURE 6.14: Monthly cost of energy saving in different cities

The effect of inflation rate and reduction of initial investment on the payback period have been assessed and presented respectively in Figs. 6.15-(a), (b). Indeed, these indicators (Orioli and Gangi, 2017; Jung, 2017) are of extreme importance when carrying out feasibility studies, as well as economic studies, especially on projects that give a major interest to the integration of solar thermal energy technologies in countries that are in economic emergence phase such as Morocco (Lybbert et al., 2010). As presented in Fig. 6.15-(a), the payback period expressed in years is a decreasing function of the inflation rate. For example, for an annual inflation rate of 2%, the payback period is equal to 26.25, while it is equated to 18.75 for 7% inflation rate. Thus, an increase of 5% in the inflation rate generates a 7.5 years reduction in the payback period. With respect to the discount effect of initial investment which is presented in Fig. 6.15-(b). Moreover, it is noted that the payback period remains a descending function of this indicator. For instance, the lack of a reduction in the initial investment make the payback period evaluated at 25 years, while it is equal to 20 years for 30% reduction of initial investment. Consequently, a reduction of 5 years can be recorded, if a reduction on the initial investment of 30 % is ensured.

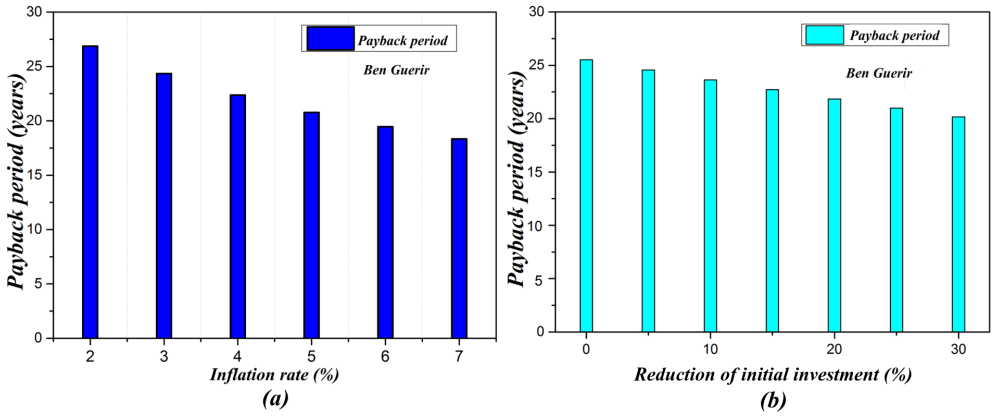

FIGURE 6.15: Effect of energy inflation rate ($i\%$, (a)) and the reduction of the initial investment (I_0, (b)) on the payback period

As previously mentioned, a sensitivity study is conducted to evaluate the effects of the solar project environment on its profitability. The study is based on the assessment of the risk in the amount of investment, the solar sunshine, the operating expenses and the rate of inflation. Fig. 6.16-(a) shows the result of the sensitivity study according to the amount of investment regarding the implementation of the solar plant project combining solar air-conditioning, heating and DHW production. The average total investment amount for this project was about 20 ke. Regarding the equipment themselves, their price varies according to constraints identified during the technical evaluation (see Table 6.2). As expected, we note that changes in the amount of the investment have a considerable impact. The gain of 10% of initial investment earn almost 2 ke on the NPV. The impact of solar sunshine on the profitability of a solar plant project is presented in Fig. 6.16-(b). For this study, we considered values between 2000 and 3500 hours/yr. The threshold of 2000 hours corresponds to the low performance and then it is practically impossible to build a solar plant project because it is not profitable (negative NPV). Regarding the value of 3500 hours, it corresponds to particularly sunshine sites. We logically observe that the solar potential has a high effect on the economic profitability of the solar plant project. The difference between the NPVs for the two extreme cases was more than 14 ke (see Fig. 6.16-(b)).

Fig. 6.16-(c) shows that the cost variations including operation, maintenance and insurance have a slight impact on the profitability of a solar plant project. The NPV varying from 300 e from one extreme to another.

Fig. 6.16-(d) represents the effect of discount rate on the profitability of the studied solar plant project. A discount a rate higher than 10% makes the project unprofitable because the NPV becomes negative. The IRR of the reference project was 10.48% and when it's higher than the company's discount rate, the investment must be realized, the profitability of the committed funds being greater than their opportunity cost. It's interesting to note that the classification between several projects is carried out in descending order of the IRR with as the lower limit the discount rate of the company.

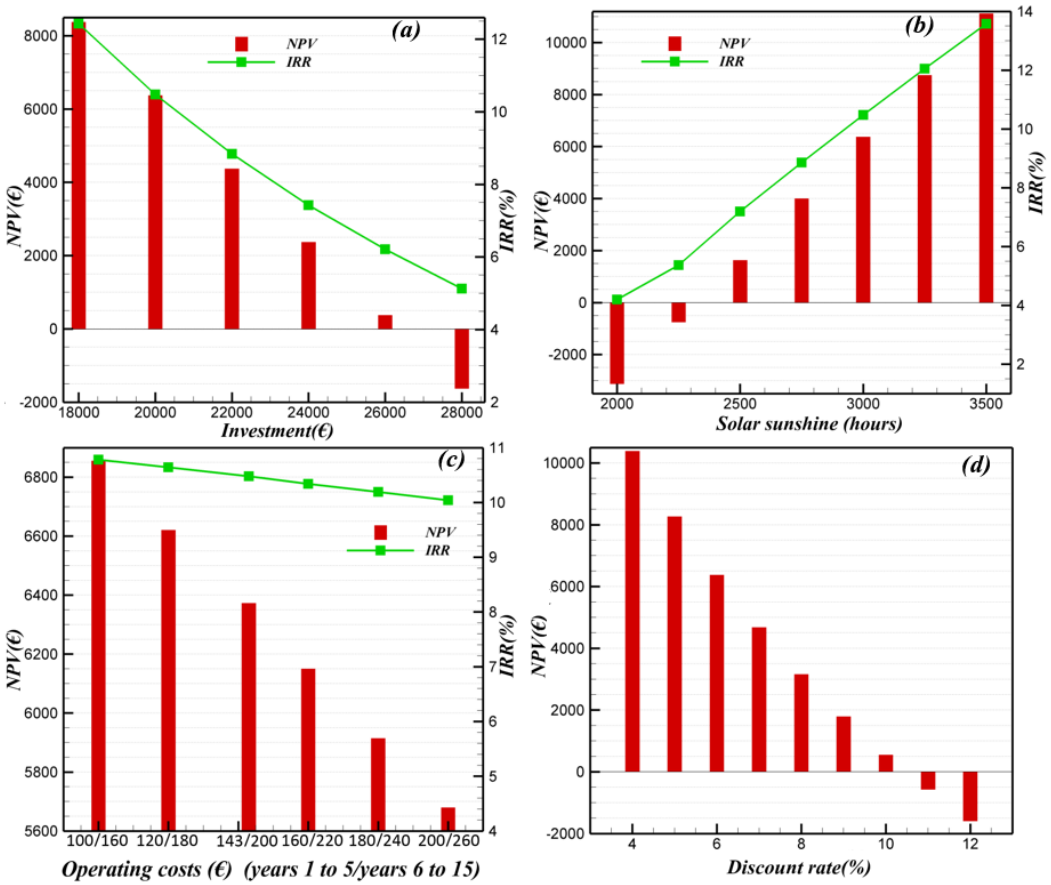

FIGURE 6.16: Sensitivity study of the profitability of the solar plant project: (a)- Effect of the amount of investment, (b)- Effect of the solar sunshine, (c)- Effect of the operating expenses and (d)- Effect of the discount rate

6.6 Conclusion

This chapter investigated through a parametric study the thermal performance of a combined solar air-conditioning, heating and DHW production systems and outlines their economic viability and risk analysis under Moroccan conditions. The combination of heating/cooling configurations is considered as additional economic gain and energy savings. Indeed, the classic investment choice criteria (NPV and IRR) are used for measuring the relevance of an investment in such integrated solar plant project in Morocco. Then, a sensitivity analysis is performed to analyze the impact of the major characteristics of the studied solar plant project on the decision-making in various environments. The major finding of this work is that incrementing the collector's field area to 30 m^2 optimizes the thermal efficiency of the solar plant, and the electric booster consumption is reduced. Furthermore, it would be advantageous to use a number of collectors of 14 (a total surface of 22 m^2) to satisfy the cooling, heating and hot water needs over the year since the overall system solar fraction remain above 55% when the optimum parameters are considered. The results indicated also that solar cooling systems in hot climates are an attractive option to increase energy savings and to mitigate CO_2 emissions. In addition, the solar contribution has increased from 605 kWh to 705 kWh in winter and summer periods, respectively, while the auxiliary consumption has achieved 1450 kWh, 1875 kWh

and 2300 kWh for Agadir, Tangier and Ben Guerir, respectively. However, according to the economic assessment, the high solar plant cost is a main barrier facing their implementation in Morocco. It is found also that the investment could be feasible if the Moroccan government enacts a new law for renewable energy that grants exemptions, incentives and subsidizes projects that invest in solar energy applications in building by about 20% of initial investment cost of the system, as various countries in the world are acting nowadays.

Through this work, we recommend the following policy measures to enhance the integration of the studied solar plant projects in Morocco. Government has to encourage the implementation of solar plants on buildings and to introduce various financing tools supported by commercial banks to decrease the initial central cost of the solar installations. Also, the industries engaged in the manufacturing of such solar technologies must be motivated to decrease the sale prices, taxes. Further, conferences, electronic and print media must be used to promote the utility of this solar innovative technology among masses and to encourage their involvement as a national energy policy. Moreover, extraneous investors, manufacturers and experts should be invited to transfer the technology and knowledge to Moroccan homologues for the efficient manufacturing and economic competitiveness of solar plant combining air-conditioning, heating and DHW production and accessories on local scale. In addition, particular financial resources have to be afforded to the prototypes development projects for education, practical training and the technology transfer of solar thermal systems. These points are highly suggested to be executed to bring the commercial, industrial companies and citizens to have a foothold in such solar innovative technologies.

Several suggestions and relevant policy directions are recommended in order to improve the adoption of solar heating/cooling technologies in the last chapter (Chapter 7).

Chapter 7

Conclusions and recommendations for future work

7.1 Conclusions

The main aim of this thesis was to analyze the thermal performance of solar cooling systems and their feasibility under Moroccan conditions. Thermal performance of the solar thermal systems are estimated using numerical methods and software since the solar processes are transient in nature been driven by time dependent forcing functions and loads. The system components are defined with mathematical relationships that describe how components function. They are based on first principles (energy balances, mass balances, rate equations and equilibrium relationships) at one extreme or empirical curve fits to operating data from specific machines such as solar thermal collectors and absorption chillers. Through numerical simulations are determined the long-term system performance i.e. data are obtained for the energy consumption, solar fraction, collector efficiency also it is performed parametric analysis to determine the influence of specific parameters like collector area, storage tank capacity, mass flow rate, etc.

Solar absorption air-conditioning machine are a promising and an innovative alternative to reduce the peak energy consumption generated by excessive use of vapor compression systems, especially during summer months. The attractiveness of utilizing solar energy is mainly due to the demand and supply of energy coincides. In fact, cooling is required when the solar radiation is abundantly available. Moreover, great majority of solar techniques employs harmless working fluids. In this thesis, the topic of solar air-conditioning was treated from four aspects:

- The first is general, in which the objectives were: providing a clear picture of the different solar DHW, heating/cooling options, reporting the most relevant cycles, describing the market status, presenting the recent developments of the most promising technologies and discussing the main performance indicators figuring in the literature (Chapter 2). Chapter 2 describes also the experimental aspect of the solar air-conditioning installation adopted in the project of **Solar Cooling Process in Morocco (SCPM)** funded by *Research Institute for Solar Energy and New Energies (IRESEN)*. The aim of this section is to identify the important technical characteristics of the installation, the sensitive points and to consider avenues for improvement with a view to future implementation and industrialization of the solar absorption cooling process in Morocco. Further, the difficulties encountered during the realization of the project are as well discussed.
- The second dimension concerns The second dimension concerns the technical feasibility of solar air-conditioning system and its integration in Moroccan

building sector. Therefore, Chapter 3 focuses on the modeling, design and performance optimization of solar absorption cooling systems using energy and economic indicators taking into account the combined effects of climates, building categories and cooling demands under Moroccan conditions.

- The third aspect presents the latent thermal energy storage using Phase Change Materials (PCMs). In this way, Chapter 4 concerns the investigation of numerical methods used in the modeling of phase change phenomena. To this end, a numerical comparative approach and optimization of thermal energy storage by means of PCM integration within solar hot water production system operating in dynamic mode is presented. Besides, Chapter 5 focuses on PCMs addition in the solar cooling process integrated inside solar storage tank connected to the generator of the absorption chiller to evaluate the possible enhancement in the system efficiency.

- The fourth dimension of this thesis outlines the technico-economic and risk analysis applied to the development of a combined processes of solar DHW, heating and air-conditioning in Morocco. In fact, the economic aspect is a determinant parameter deciding on the adoption of solar cooling technologies for air-conditioning requirements in residential buildings (Chapter 6). A technico-economic assessment of a complete solar DHW, heating and air-conditioning plant using an absorption chiller and operating under Moroccan climates was carried out based on adequate indicators. Thus, annual dynamic simulations of the optimal configuration were lunched for various Moroccan climatic regions. A scenario evaluation was conducted based on economic, social and Moroccan policy attributes. The overall analysis via a generalization of the results to the national level was carried out in addition to a risk analysis related to the investment in these systems in order to assess the potential of replacing traditional technologies with the solar systems and the possible risks related to their implementation in Morocco.

7.2 Recommendations and policy directions

Despite the benefits of the combined solar air-conditioning, heating and DHW production systems, several barriers (technological, financial) hamper the development of these systems. According to our works performed through this thesis, the implementation of such systems is not directly feasible in the present investment climate in Morocco. The investment could be feasible if the Moroccan government enacts a new law for renewable energy that grants exemptions, incentives and subsidizes projects that invest in solar energy applications in building by about 20% of initial investment cost of the system, like that done by various countries in the world to encourage investors and citizens to use renewable energy resources and attract investment in such fields. Through this contribution, we recommend the following policy measures to enhance the adoption of solar plant projects combining air-conditioning, heating and DHW production in Morocco:

- Government is obliged to encourage the implementation of solar plants combining air-conditioning, heating and DHW production on residential and public buildings;

- Electronic and print media must be exploited to promote the utility of this solar innovative technology among masses;

- Government must introduce various financing tools supported by commercial banks to make the initial central cost of the solar installation more accessible to the citizens;
- Conferences and workshops in remote zones may also help the request of promotion of this specified technology;
- Government is also required to encourage entrepreneurs through policy actions taking into account the enormous earnings of solar air-conditioning, heating and DHW production. For instance, the industries engaged in the manufacturing of such solar technologies must be motivated for their activities through exemptions/reduction in the sales taxes and import duties;
- Afford particular financial resources to the prototypes development projects for education, practical training and the technology transfer of solar thermal systems;
- Public authorities should implement clear actions to provide financial supports and incentives for the practical prototypes of solar air-conditioning, heating and DHW applications to sensitize and ensure the public;
- To seize the potential earnings of solar air-conditioning, heating and DHW production, long term initiatives must be established to integrate these solar technologies in the national energy strategy;
- R&D institutes and laboratories with main activity on sustainable energy technologies must be implemented in school of engineering at all higher national educational centers and students must be motivated to perform research projects on innovative renewable technologies;
- Public authorities must provide suitable financial forms to all R&D institutes to transform lab-scale solar prototypes into industrial products;
- Loans/grants must be offered to the public users of solar installations combining air-conditioning, heating and DHW production;
- Professionals should take advantages from program sharp internship through extern cooperation, because the implementation of such solar plant at a special site belongs to various parameters and that's quasi-impossible unless the pertinent overview of experts;
- Extraneous investors, manufacturers and experts should be invited to transfer the technology and knowledge to Moroccan homologues for the efficient manufacturing and economic competitiveness of solar plant combining air-conditioning, heating and DHW production and accessories on local scale.

These points are highly suggested to be executed to bring the commercial, industrial companies and citizens to have a foothold in such solar innovative technologies.

7.3 Suggestions for future work

Although, the present thesis has given worthy contributions in the solar DHW, heating and cooling issue. It has been pointed out that more effort should be paid in future research works. In order to extend the knowledge in this field, suggested perspectives appropriates are listed below:

- Experimental realization of the prototype of solar cooling system by absorption in order to validate the numerical simulations.
- Elaborate a more systematic comparative analysis of the available solar DHW, heating and cooling alternatives based on relevant exergetic, economic and environmental indicators.
- The integration of thermal storage technologies (sensible and latent options using PCMs) in order to provide DHW, heating and air-conditioning continuously.
- Further research is also required into the simulation and modeling of PCM's solidification and melting processes integrated in solar systems (storage tank) especially numerical models including supercooling and expansion contraction problems.
- The study of the other solar cooling options particularly solar adsorption and desiccant cooling technologies (liquid and solid systems) as they have recently gained particular attention due to their growing market potential in the building sector.
- it is interesting to develop systems with a supplementary energy source such as biomass in order to maximize the service availability.
- Concerning the absorption technology, several types of research works can be proposed: the performance improvement throughout the innovation of efficient working pairs, enhancement of the heat transfer inside the absorber, the research of optimal designs (technologically and economically) and the development of novel high-efficient options eventually based on hybrid configurations.
- At the Moroccan level, a demonstration pilot of solar DHW, heating and cooling system has been implemented under the project of Solar Cooling Process in Morocco funded by *Research Institute for Solar Energy and New Energies (IRESEN)*. This solar heating/cooling process requires experimental assessment and needs more dynamic analysis of its performances based on real Moroccan weather data in order to encourage a future national industrialization of this mature technology.

Bibliography

Abdulateef, JM et al. (2009). "Review on solar-driven ejector refrigeration technologies". In: *Renewable and Sustainable Energy Reviews* 13.6-7, pp. 1338–1349.

Adeff, Jay A and Thomas J Hofler (2000). "Design and construction of a solar-powdered, thermoacoustically driven, thermoacoustic refrigerator". In: *The Journal of the Acoustical Society of America* 107.6, pp. L37–L42.

Agrouaz, Y. et al. (2017). "Energy and parametric analysis of solar absorption cooling systems in various Moroccan climates". In: *Case Studies in Thermal Engineering* 9, pp. 28 –39. ISSN: 2214-157X. DOI: https://doi.org/10.1016/j.csite.2016.11.002. URL: http://www.sciencedirect.com/science/article/pii/S2214157X16300454.

Agyenim, Francis (2016). "The use of enhanced heat transfer phase change materials (PCM) to improve the coefficient of performance (COP) of solar powered LiBr/H2O absorption cooling systems". In: *Renewable Energy* 87, pp. 229 –239. ISSN: 0960-1481. DOI: https://doi.org/10.1016/j.renene.2015.10.012. URL: http://www.sciencedirect.com/science/article/pii/S0960148115303670.

Agyenim, Francis, Ian Knight, and Michael Rhodes (2010). "Design and experimental testing of the performance of an outdoor LiBr/H2O solar thermal absorption cooling system with a cold store". In: *Solar Energy* 84.5, pp. 735 –744. ISSN: 0038-092X. DOI: https://doi.org/10.1016/j.solener.2010.01.013. URL: http://www.sciencedirect.com/science/article/pii/S0038092X10000265.

Agyenim, Francis et al. (2010). "A review of materials, heat transfer and phase change problem formulation for latent heat thermal energy storage systems (LHTESS)". In: *Renewable and sustainable energy reviews* 14.2, pp. 615–628.

Ali, Ahmed Hamza H., Peter Noeres, and Clemens Pollerberg (2008). "Performance assessment of an integrated free cooling and solar powered single-effect lithium bromide-water absorption chiller". In: *Solar Energy* 82.11, pp. 1021 –1030. ISSN: 0038-092X. DOI: https://doi.org/10.1016/j.solener.2008.04.011. URL: http://www.sciencedirect.com/science/article/pii/S0038092X08001059.

Allouche, Yosr et al. (2017). "Dynamic simulation of an integrated solar-driven ejector based air conditioning system with PCM cold storage". In: *Applied Energy* 190, pp. 600 –611. ISSN: 0306-2619. DOI: https://doi.org/10.1016/j.apenergy.2017.01.001. URL: http://www.sciencedirect.com/science/article/pii/S0306261917300016.

Allouhi, Amine et al. (2015a). "Economic and environmental assessment of solar air-conditioning systems in Morocco". In: *Renewable and Sustainable Energy Reviews* 50, pp. 770 –781. ISSN: 1364-0321. DOI: http://dx.doi.org/10.1016/j.rser.2015.05.044. URL: http://www.sciencedirect.com/science/article/pii/S1364032115005043.

Allouhi, Amine et al. (2015b). "Solar driven cooling systems: an updated review". In: *Renewable and Sustainable Energy Reviews* 44, pp. 159–181.

Almohammadi, K.M. et al. (2013). "Computational fluid dynamics (CFD) mesh independency techniques for a straight blade vertical axis wind turbine". In: *Energy* 58, pp. 483 –493. ISSN: 0360-5442. DOI: http://dx.doi.org/10.1016/j.energy.2013.06.012. URL: http://www.sciencedirect.com/science/article/pii/S0360544213005100.

Alves, Carolina A, Denise HS Duarte, and Fábio LT Gonçalves (2016). "Residential buildings' thermal performance and comfort for the elderly under climate changes context in the city of São Paulo, Brazil". In: *Energy and Buildings* 114, pp. 62–71.

Assilzadeh, F et al. (2005). "Simulation and optimization of a LiBr solar absorption cooling system with evacuated tube collectors". In: *Renewable Energy* 30.8, pp. 1143–1159.

Atmaca, Ibrahim and Abdulvahap Yigit (2003). "Simulation of solar-powered absorption cooling system". In: *Renewable Energy* 28.8, pp. 1277 –1293. ISSN: 0960-1481. DOI: https://doi.org/10.1016/S0960-1481(02)00252-5. URL: http://www.sciencedirect.com/science/article/pii/S0960148102002525.

Ayala, R, CL Heard, and FA Holland (1998). "Ammonia/lithium nitrate absorption/compression refrigeration cycle. Part II. Experimental". In: *Applied Thermal Engineering* 18.8, pp. 661–670.

Bahria, Sofiane et al. (2016). "Parametric study of solar heating and cooling systems in different climates of Algeria–A comparison between conventional and high-energy-performance buildings". In: *Energy* 113, pp. 521–535.

Balaras, Constantinos A et al. (2007). "Solar air conditioning in Europe—an overview". In: *Renewable and sustainable energy reviews* 11.2, pp. 299–314.

Balduzzi, Francesco et al. (2016). "Critical issues in the CFD simulation of Darrieus wind turbines". In: *Renewable Energy* 85, pp. 419 –435. ISSN: 0960-1481. DOI: http://dx.doi.org/10.1016/j.renene.2015.06.048. URL: http://www.sciencedirect.com/science/article/pii/S0960148115300719.

Balghouthi, M., M.H. Chahbani, and A. Guizani (2008). "Feasibility of solar absorption air conditioning in Tunisia". In: *Building and Environment* 43.9, pp. 1459 –1470. ISSN: 0360-1323. DOI: https://doi.org/10.1016/j.buildenv.2007.08.003. URL: http://www.sciencedirect.com/science/article/pii/S0360132307001497.

Barreneche, Camila et al. (2014). "New database on phase change materials for thermal energy storage in buildings to help PCM selection". In: *Energy Procedia* 57, pp. 2408–2415.

Battisti, Riccardo and Annalisa Corrado (2005a). "Environmental assessment of solar thermal collectors with integrated water storage". In: *Journal of Cleaner Production* 13.13, pp. 1295–1300.

— (2005b). "Environmental assessment of solar thermal collectors with integrated water storage". In: *Journal of Cleaner Production* 13.13. Life Cycle Assessment, pp. 1295 –1300. ISSN: 0959-6526. DOI: https://doi.org/10.1016/j.jclepro.2005.05.007. URL: http://www.sciencedirect.com/science/article/pii/S0959652605001204.

Beek, John (1962). "Design of packed catalytic reactors". In: *Advances in Chemical Engineering* 3, pp. 203–271.

Behi, Hamidreza, Morteza Ghanbarpour, and Mohammadreza Behi (2017). "Investigation of PCM-assisted heat pipe for electronic cooling". In: *Applied Thermal Engineering* 127.Supplement C, pp. 1132 –1142. ISSN: 1359-4311. DOI: https://doi.org/10.1016/j.applthermaleng.2017.08.109. URL: http://www.sciencedirect.com/science/article/pii/S1359431116322748.

Bejarano, Guillermo et al. (2018). "Novel scheme for a PCM-based cold energy storage system. Design, modelling, and simulation". In: *Applied Thermal Engineering* 132, pp. 256 –274. ISSN: 1359-4311. DOI: https://doi.org/10.1016/j.applthermaleng.2017.12.088. URL: https://www.sciencedirect.com/science/article/pii/S1359431117350809.

Bellos, Evangelos, Christos Tzivanidis, and Kimon A Antonopoulos (2016). "Exergetic, energetic and financial evaluation of a solar driven absorption cooling system with various collector types". In: *Applied Thermal Engineering* 102, pp. 749–759.

Bennouna, Amin and Charaf El Hebil (2016). "Energy needs for Morocco 2030, as obtained from GDP-energy and GDP-energy intensity correlations". In: *Energy Policy* 88, pp. 45–55.

Bergman, Theodore L and Frank P Incropera (2011). *Fundamentals of heat and mass transfer*. John Wiley & Sons.

Bermejo, Pablo, Francisco Javier Pino, and Felipe Rosa (2010). "Solar absorption cooling plant in Seville". In: *Solar Energy* 84.8, pp. 1503 –1512. ISSN: 0038-092X. DOI: https://doi.org/10.1016/j.solener.2010.05.012. URL: http://www.sciencedirect.com/science/article/pii/S0038092X10002033.

Book, Buildings Energy Data (2010). *US Department of Energy, 2011*.

Bouhal, T. et al. (2017a). "Impact of load profile and collector technology on the fractional savings of solar domestic water heaters under various climatic conditions". In: *International Journal of Hydrogen Energy* 42.18, pp. 13245 –13258. ISSN: 0360-3199. DOI: http://dx.doi.org/10.1016/j.ijhydene.2017.03.226. URL: http://www.sciencedirect.com/science/article/pii/S0360319917312776.

Bouhal, T. et al. (2017b). "Numerical modeling and optimization of thermal stratification in solar hot water storage tanks for domestic applications: CFD study". In: *Solar Energy* 157.Supplement C, pp. 441 –455. ISSN: 0038-092X. DOI: https://doi.org/10.1016/j.solener.2017.08.061. URL: http://www.sciencedirect.com/science/article/pii/S0038092X17307429.

Bouhal, T. et al. (2017c). "Towards an energy efficiency optimization of solar horizontal storage tanks and circulation pipes integrating evacuated tube collectors through CFD parametric studies". In: *Sustainable Energy Technologies and Assessments*. ISSN: 2213-1388. DOI: https://doi.org/10.1016/j.seta.2017.10.004. URL: http://www.sciencedirect.com/science/article/pii/S2213138817303909.

Bouhal, T. et al. (2018a). "PCM addition inside solar water heaters: Numerical comparative approach". In: *Journal of Energy Storage* 19, pp. 232 –246. ISSN: 2352-152X. DOI: https://doi.org/10.1016/j.est.2018.08.005. URL: http://www.sciencedirect.com/science/article/pii/S2352152X18304134.

Bouhal, T. et al. (2018b). "Technical assessment, economic viability and investment risk analysis of solar heating/cooling systems in residential buildings in Morocco". In: *Solar Energy* 170, pp. 1043 –1062. ISSN: 0038-092X. DOI: https://doi.org/10.1016/j.solener.2018.06.032. URL: https://www.sciencedirect.com/science/article/pii/S0038092X18305838.

Bouhal, T. et al. (2018c). "Technical feasibility of a sustainable Concentrated Solar Power in Morocco through an energy analysis". In: *Renewable and Sustainable Energy Reviews* 81, Part 1, pp. 1087 –1095. ISSN: 1364-0321. DOI: https://doi.org/10.1016/j.rser.2017.08.056. URL: http://www.sciencedirect.com/science/article/pii/S1364032117312017.

Brancato, Vincenza et al. (2017). "Identification and characterization of promising phase change materials for solar cooling applications". In: *Solar Energy Materials and Solar Cells* 160, pp. 225 –232. ISSN: 0927-0248. DOI: https://doi.org/10.1016/j.solmat.2016.10.026. URL: http://www.sciencedirect.com/science/article/pii/S0927024816304354.

Brand, Bernhard and Jonas Zingerle (2011). "The renewable energy targets of the Maghreb countries: Impact on electricity supply and conventional power markets". In: *Energy Policy* 39.8, pp. 4411–4419.

Buckles, WE and SA Klein (1980). "Analysis of solar domestic hot water heaters". In: *Solar Energy* 25.5, pp. 417–424.

Buker, Mahmut Sami and Saffa B Riffat (2016). "Solar assisted heat pump systems for low temperature water heating applications: A systematic review". In: *Renewable and Sustainable Energy Reviews* 55, pp. 399–413.

Buonomano, Annamaria, Francesco Calise, and Adolfo Palombo (2018a). "Solar heating and cooling systems by absorption and adsorption chillers driven by stationary and concentrating photovoltaic/thermal solar collectors: Modelling and simulation". In: *Renewable and Sustainable Energy Reviews* 82, pp. 1874–1908.

— (2018b). "Solar heating and cooling systems by absorption and adsorption chillers driven by stationary and concentrating photovoltaic/thermal solar collectors: Modelling and simulation". In: *Renewable and Sustainable Energy Reviews* 82, pp. 1874 –1908. ISSN: 1364-0321. DOI: https://doi.org/10.1016/j.rser.2017.10.059. URL: http://www.sciencedirect.com/science/article/pii/S1364032117314326.

Cabeza, Luisa F et al. (2006). "Experimentation with a water tank including a PCM module". In: *Solar Energy Materials and Solar Cells* 90.9, pp. 1273–1282.

Cabeza, Luisa F et al. (2011). "Materials used as PCM in thermal energy storage in buildings: a review". In: *Renewable and Sustainable Energy Reviews* 15.3, pp. 1675–1695.

Cascales, J.R. García et al. (2011). "Modelling an absorption system assisted by solar energy". In: *Applied Thermal Engineering* 31.1, pp. 112 –118. ISSN: 1359-4311. DOI: https://doi.org/10.1016/j.applthermaleng.2010.08.025. URL: http://www.sciencedirect.com/science/article/pii/S1359431110003649.

Chunnanond, Kanjanapon and Satha Aphornratana (2004). "Ejectors: applications in refrigeration technology". In: *Renewable and sustainable energy reviews* 8.2, pp. 129–155.

Climate Change, Intergovernmental Panel on (2015). *Climate change 2014: mitigation of climate change*. Vol. 3. Cambridge University Press.

Conti, John et al. (2016). *International Energy Outlook 2016 With Projections to 2040*. Tech. rep. USDOE Energy Information Administration (EIA), Washington, DC (United States). Office of Energy Analysis.

Critoph, RE (1999). "Rapid cycling solar/biomass powered adsorption refrigeration system". In: *Renewable Energy* 16.1-4, pp. 673–678.

Darkwa, J., S. Fraser, and D.H.C. Chow (2012). "Theoretical and practical analysis of an integrated solar hot water-powered absorption cooling system". In: *Energy* 39.1. Sustainable Energy and Environmental Protection 2010, pp. 395 –402. ISSN: 0360-5442. DOI: https://doi.org/10.1016/j.energy.2011.12.045. URL: http://www.sciencedirect.com/science/article/pii/S0360544211008711.

Desideri, Umberto, Stefania Proietti, and Paolo Sdringola (2009). "Solar-powered cooling systems: Technical and economic analysis on industrial refrigeration and

air-conditioning applications". In: *Applied Energy* 86.9, pp. 1376 –1386. ISSN: 0306-2619. DOI: https://doi.org/10.1016/j.apenergy.2009.01.011. URL: http://www.sciencedirect.com/science/article/pii/S0306261909000087.

Dieng, AO and RZ Wang (2001). "Literature review on solar adsorption technologies for ice-making and air-conditioning purposes and recent developments in solar technology". In: *Renewable and sustainable energy reviews* 5.4, pp. 313–342.

Duffie, John A and William A Beckman (2013). *Solar engineering of thermal processes*. John Wiley & Sons.

Dîn Fertahi, Saïf ed et al. (2017). "Thermo-mechanical strength analysis for energy storage improvement of horizontal storage tanks integrating evacuated tube collectors". In: *International Journal of Hydrogen Energy* 42.49, pp. 29370 –29383. ISSN: 0360-3199. DOI: https://doi.org/10.1016/j.ijhydene.2017.10.016. URL: http://www.sciencedirect.com/science/article/pii/S0360319917339137.

Dîn Fertahi, Saïf ed et al. (2018a). "Design and thermal performance optimization of a forced collective solar hot water production system in Morocco for energy saving in residential buildings". In: *Solar Energy* 160, pp. 260 –274. ISSN: 0038-092X. DOI: https://doi.org/10.1016/j.solener.2017.12.015. URL: http://www.sciencedirect.com/science/article/pii/S0038092X17310873.

Dîn Fertahi, Saïf ed et al. (2018b). "Performance optimization of a two-phase closed thermosyphon through CFD numerical simulations". In: *Applied Thermal Engineering* 128.Supplement C, pp. 551 –563. ISSN: 1359-4311. DOI: https://doi.org/10.1016/j.applthermaleng.2017.09.049. URL: http://www.sciencedirect.com/science/article/pii/S1359431117339558.

Eames, PC and PW Griffiths (2006). "Thermal behaviour of integrated solar collector/storage unit with 65 C phase change material". In: *Energy conversion and management* 47.20, pp. 3611–3618.

Eicker, Ursula (2006). *Solar technologies for buildings*. John Wiley & Sons.

Eicker, Ursula and Dirk Pietruschka (2009). "Design and performance of solar powered absorption cooling systems in office buildings". In: *Energy and Buildings* 41.1, pp. 81 –91. ISSN: 0378-7788. DOI: https://doi.org/10.1016/j.enbuild.2008.07.015. URL: http://www.sciencedirect.com/science/article/pii/S0378778808001734.

El-Wakil, Mohamed Mohamed (1971). "NUCLEAR HEAT TRANSPORT." In:
Energypoles company SA, Rabat, Morocco. URL: http://www.energypoles.com.

Esen, Mehmet, Aydin Durmuş, and Ayla Durmuş (1998). "Geometric design of solar-aided latent heat store depending on various parameters and phase change materials". In: *Solar energy* 62.1, pp. 19–28.

Etat des lieux de la climatisation solaire, INES, 2013. URL: {http://www.ines-solaire.org/}.

Fan, Z., C.A. Infante Ferreira, and A.H. Mosaffa (2014). "Numerical modelling of high temperature latent heat thermal storage for solar application combining with double-effect H2O/LiBr absorption refrigeration system". In: *Solar Energy* 110, pp. 398 –409. ISSN: 0038-092X. DOI: https://doi.org/10.1016/j.solener.2014.09.036. URL: http://www.sciencedirect.com/science/article/pii/S0038092X14004769.

Farid, Mohammed M et al. (2004). "A review on phase change energy storage: materials and applications". In: *Energy conversion and management* 45.9-10, pp. 1597–1615.

Farshi, L Garousi, SM Seyed Mahmoudi, and MA Rosen (2011). "Analysis of crystallization risk in double effect absorption refrigeration systems". In: *Applied Thermal Engineering* 31.10, pp. 1712–1717.

Fasfous, A et al. (2013). "Potential of utilizing solar cooling in The University of Jordan". In: *Energy conversion and management* 65, pp. 729–735.

Florides, G.A. et al. (2002a). "Modelling, simulation and warming impact assessment of a domestic-size absorption solar cooling system". In: *Applied Thermal Engineering* 22.12, pp. 1313 –1325. ISSN: 1359-4311. DOI: https://doi.org/10.1016/S1359-4311(02)00054-6. URL: http://www.sciencedirect.com/science/article/pii/S1359431102000546.

Florides, Georgios A et al. (2002b). "Modelling and simulation of an absorption solar cooling system for Cyprus". In: *Solar Energy* 72.1, pp. 43–51.

Fong, KF et al. (2010). "Comparative study of different solar cooling systems for buildings in subtropical city". In: *Solar Energy* 84.2, pp. 227–244.

francophonie, Institut de l'énergie et de l'environnement de la and Koassi d'Almeida (2001). *Cadre institutionnel législatif et réglementaire de l'évaluation environnementale dans les pays francophones d'Afrique et de l'océan Indien: les indicateurs de fonctionnalité, les écarts fondamentaux et les besoins prioritaires: essai de typologie*. IÉPF.

Gao, Xiangkui et al. (2018). "Coupled cooling method and application of latent heat thermal energy storage combined with pre-cooling of envelope: Optimization of pre-cooling with intermittent mode". In: *Sustainable Cities and Society* 38, pp. 370 –381. ISSN: 2210-6707. DOI: https://doi.org/10.1016/j.scs.2018.01.014. URL: http://www.sciencedirect.com/science/article/pii/S221067071731051X.

Ge, T.S. et al. (2017). "Solar heating and cooling: Present and future development". In: *Renewable Energy*. ISSN: 0960-1481. DOI: https://doi.org/10.1016/j.renene.2017.06.081. URL: http://www.sciencedirect.com/science/article/pii/S0960148117305852.

— (2018). "Solar heating and cooling: Present and future development". In: *Renewable Energy* 126, pp. 1126 –1140. ISSN: 0960-1481. DOI: https://doi.org/10.1016/j.renene.2017.06.081. URL: http://www.sciencedirect.com/science/article/pii/S0960148117305852.

Ghritlahre, Harish Kumar and Radha Krishna Prasad (2018). "Application of ANN technique to predict the performance of solar collector systems-A review". In: *Renewable and Sustainable Energy Reviews* 84, pp. 75–88.

Global Energy Statistical Yearbook 2018 (GESY). URL: https://yearbook.enerdata.net/total-energy/world-energy-production.html.

Green Energy Park. URL: http://www.greenenergypark.ma.

Groupe Office Chérifien des Phosphates (OCP). URL: http://www.ocpgroup.ma.

Haillot, Didier et al. (2013). "Optimization of solar DHW system including PCM media". In: *Applied energy* 109, pp. 470–475.

Haut Commissariat au Plan (HCP). URL: http://www.hcp.ma.

Henning, Hans-Martin (2007). "Solar assisted air conditioning of buildings–an overview". In: *Applied thermal engineering* 27.10, pp. 1734–1749.

Henning, HM et al. (2001). "The potential of solar energy use in desiccant cooling cycles". In: *International journal of refrigeration* 24.3, pp. 220–229.

Henry, Claude (1974). "Investment decisions under uncertainty: the" irreversibility effect"". In: *The American Economic Review* 64.6, pp. 1006–1012.

Hidalgo, M.C. Rodríguez et al. (2008). "Energy and carbon emission savings in Spanish housing air-conditioning using solar driven absorption system". In: *Applied Thermal Engineering* 28.14, pp. 1734 –1744. ISSN: 1359-4311. DOI: https://doi.

org/10.1016/j.applthermaleng.2007.11.013. URL: http://www.sciencedirect.com/science/article/pii/S135943110700381X.

Hirmiz, R., M.F. Lightstone, and J.S. Cotton (2018). "Performance enhancement of solar absorption cooling systems using thermal energy storage with phase change materials". In: *Applied Energy* 223, pp. 11 –29. ISSN: 0306-2619. DOI: https://doi.org/10.1016/j.apenergy.2018.04.029. URL: http://www.sciencedirect.com/science/article/pii/S0306261918305713.

Institut international du froid (IIF). URL: www.iifiir.org.

IUT/GTE des Pays de l'Adour, Pau, France. URL: http://iutpa.univ-pau.fr/fr/index.html.

Izquierdo, M. et al. (2008). "Air conditioning using an air-cooled single effect lithium bromide absorption chiller: Results of a trial conducted in Madrid in August 2005". In: *Applied Thermal Engineering* 28.8, pp. 1074 –1081. ISSN: 1359-4311. DOI: https://doi.org/10.1016/j.applthermaleng.2007.06.009. URL: http://www.sciencedirect.com/science/article/pii/S1359431107002098.

Jamekhorshid, A, SM Sadrameli, and Mohammed Farid (2014). "A review of microencapsulation methods of phase change materials (PCMs) as a thermal energy storage (TES) medium". In: *Renewable and Sustainable Energy Reviews* 31, pp. 531–542.

Jin, Xing et al. (2018). "Comparison of two numerical heat transfer models for phase change material board". In: *Applied Thermal Engineering* 128.Supplement C, pp. 1331 –1339. ISSN: 1359-4311. DOI: https://doi.org/10.1016/j.applthermaleng.2017.09.015. URL: http://www.sciencedirect.com/science/article/pii/S1359431117324754.

JOFFRE, André (2005). "Énergie solaire thermique dans le bâtiment. Chauffage. Climatisation". In: *Techniques de l'ingénieur. Génie énergétique* BE9165.

Joudi, Khalid A. and Qussai J. Abdul-Ghafour (2003). "Development of design charts for solar cooling systems. Part I: computer simulation for a solar cooling system and development of solar cooling design charts". In: *Energy Conversion and Management* 44.2, pp. 313 –339. ISSN: 0196-8904. DOI: https://doi.org/10.1016/S0196-8904(02)00045-6. URL: http://www.sciencedirect.com/science/article/pii/S0196890402000456.

Jung, Kuk Mo (2017). "Uncertainty-induced dynamic inefficiency and the optimal inflation rate". In: *International Review of Economics & Finance*. ISSN: 1059-0560. DOI: https://doi.org/10.1016/j.iref.2017.12.006. URL: http://www.sciencedirect.com/science/article/pii/S1059056017307815.

Kabeel, A.E. and Mohamed Abdelgaied (2018). "Solar energy assisted desiccant air conditioning system with PCM as a thermal storage medium". In: *Renewable Energy* 122, pp. 632 –642. ISSN: 0960-1481. DOI: https://doi.org/10.1016/j.renene.2018.02.020. URL: http://www.sciencedirect.com/science/article/pii/S0960148118301630.

Kalkan, Naci, EA Young, and Ahmet Celiktas (2012). "Solar thermal air conditioning technology reducing the footprint of solar thermal air conditioning". In: *Renewable and Sustainable Energy Reviews* 16.8, pp. 6352–6383.

Kalogirou, Soteris (2009). "Thermal performance, economic and environmental life cycle analysis of thermosiphon solar water heaters". In: *Solar energy* 83.1, pp. 39–48.

Kee, Shin Yiing, Yamuna Munusamy, and Kok Seng Ong (2018). "Review of solar water heaters incorporating solid-liquid organic phase change materials as thermal storage". In: *Applied Thermal Engineering* 131, pp. 455 –471. ISSN: 1359-4311. DOI: https://doi.org/10.1016/j.applthermaleng.2017.12.

032. URL: http://www.sciencedirect.com/science/article/pii/S1359431117347804.

Khalifa, Abdul-Jabbar N and Salman S Al-Mutawalli (1998). "Effect of two-axis sun tracking on the performance of compound parabolic concentrators". In: *Energy Conversion and Management* 39.10, pp. 1073–1079.

Khan, Mohammed Mumtaz A., R. Saidur, and Fahad A. Al-Sulaiman (2017). "A review for phase change materials (PCMs) in solar absorption refrigeration systems". In: *Renewable and Sustainable Energy Reviews* 76, pp. 105 –137. ISSN: 1364-0321. DOI: https://doi.org/10.1016/j.rser.2017.03.070. URL: http://www.sciencedirect.com/science/article/pii/S1364032117303854.

Khudhair, Amar M and Mohammed M Farid (2004). "A review on energy conservation in building applications with thermal storage by latent heat using phase change materials". In: *Energy conversion and management* 45.2, pp. 263–275.

Kim, DS and CA Infante Ferreira (2008). "Solar refrigeration options–a state-of-the-art review". In: *International Journal of refrigeration* 31.1, pp. 3–15.

Kleinbach, Eberhard Markus, WA Beckman, and SA Klein (1993). "Performance study of one-dimensional models for stratified thermal storage tanks". In: *Solar energy* 50.2, pp. 155–166.

Kousksou, T and P Bruel (2010). "Encapsulated phase change material under cyclic pulsed heat load". In: *International Journal of Refrigeration* 33.8, pp. 1648–1656.

Kousksou, T et al. (2011). "PCM storage for solar DHW: From an unfulfilled promise to a real benefit". In: *Solar Energy* 85.9, pp. 2033–2040.

Kousksou, T et al. (2015). "Renewable energy potential and national policy directions for sustainable development in Morocco". In: *Renewable and Sustainable Energy Reviews* 47, pp. 46–57.

Kylili, Angeliki et al. (2018). "Environmental assessment of solar thermal systems for the industrial sector". In: *Journal of Cleaner Production* 176, pp. 99 –109. ISSN: 0959-6526. DOI: https://doi.org/10.1016/j.jclepro.2017.12.150. URL: https://www.sciencedirect.com/science/article/pii/S0959652617331098.

Lee, H-R et al. (2000). "Thermodynamic design data and performance evaluation of the water+ lithium bromide+ lithium iodide+ lithium nitrate+ lithium chloride system for absorption chiller". In: *Applied Thermal Engineering* 20.8, pp. 707–720.

Li, YQ et al. (2013). "Numerical analysis and parameters optimization of shell-and-tube heat storage unit using three phase change materials". In: *Renewable Energy* 59, pp. 92–99.

Li, Z.F and K Sumathy (2001). "Experimental studies on a solar powered air conditioning system with partitioned hot water storage tank". In: *Solar Energy* 71.5, pp. 285 –297. ISSN: 0038-092X. DOI: https://doi.org/10.1016/S0038-092X(01)00064-0. URL: http://www.sciencedirect.com/science/article/pii/S0038092X01000640.

Liao, Xiaohong and Reinhard Radermacher (2007). "Absorption chiller crystallization control strategies for integrated cooling heating and power systems". In: *International journal of Refrigeration* 30.5, pp. 904–911.

Lu, Shilei, Tianshuai Zhang, and Yafei Chen (2018). "Study on the performance of heat storage and heat release of water storage tank with PCMs". In: *Energy and Buildings* 158.Supplement C, pp. 1770 –1780. ISSN: 0378-7788. DOI: https://doi.org/10.1016/j.enbuild.2017.10.059. URL: http://www.sciencedirect.com/science/article/pii/S0378778817320339.

Lybbert, Travis J et al. (2010). "Dynamic field experiments in development economics: Risk valuation in Morocco, Kenya, and Peru". In: *Agricultural and Resource Economics Review* 39.2, pp. 176–192.

Mammoli, Andrea et al. (2010). "Energetic, economic and environmental performance of a solar-thermal-assisted HVAC system". In: *Energy and Buildings* 42.9, pp. 1524 –1535. ISSN: 0378-7788. DOI: https://doi.org/10.1016/j.enbuild.2010.03.023. URL: http://www.sciencedirect.com/science/article/pii/S0378778810001155.

Marongiu, Maurice J, MK Berhe, and GS Fallon (2000). "Thermal management of IC's using heat sinks incorporating phase change materials (PCM)". In: *SPIE proceedings series*. Society of Photo-Optical Instrumentation Engineers, pp. 60–65.

Mateus, Tiago and Armando C. Oliveira (2009). "Energy and economic analysis of an integrated solar absorption cooling and heating system in different building types and climates". In: *Applied Energy* 86.6, pp. 949 –957. ISSN: 0306-2619. DOI: https://doi.org/10.1016/j.apenergy.2008.09.005. URL: http://www.sciencedirect.com/science/article/pii/S0306261908002249.

Mazloumi, M., M. Naghashzadegan, and K. Javaherdeh (2008). "Simulation of solar lithium bromide–water absorption cooling system with parabolic trough collector". In: *Energy Conversion and Management* 49.10, pp. 2820 –2832. ISSN: 0196-8904. DOI: https://doi.org/10.1016/j.enconman.2008.03.014. URL: http://www.sciencedirect.com/science/article/pii/S0196890408001143.

Mazman, Muhsin et al. (2009). "Utilization of phase change materials in solar domestic hot water systems". In: *Renewable Energy* 34.6, pp. 1639–1643.

McGlade, Christophe and Paul Ekins (2015). "The geographical distribution of fossil fuels unused when limiting global warming to 2 C". In: *Nature* 517.7533, p. 187.

Mehling, H et al. (2003). "PCM-module to improve hot water heat stores with stratification". In: *Renewable energy* 28.5, pp. 699–711.

Meteonorm. URL: http://www.meteonorm.com.

Ministry of Energy, Mines and Sustainable Development (MEMSD), Morocco. URL: http://www.mem.gov.ma.

Miranville, Frédéric (2002). "Contribution à l'étude des parois complexes en physique du bâtiment: modélisation, expérimentation et validation expérimentale de complexes de toitures incluant des produits minces réfléchissants en climat tropical humide". PhD thesis. Université de la Réunion.

Monghasemi, Nima and Amir Vadiee (2017). "A review of solar chimney integrated systems for space heating and cooling application". In: *Renewable and Sustainable Energy Reviews*.

Montagnino, Fabio Maria (2017). "Solar cooling technologies. Design, application and performance of existing projects". In: *Solar Energy* 154. Solar Thermal Heating and Cooling, pp. 144 –157. ISSN: 0038-092X. DOI: https://doi.org/10.1016/j.solener.2017.01.033. URL: http://www.sciencedirect.com/science/article/pii/S0038092X1730052X.

Moroccan Agency for Energy Efficiency (AMEE). URL: http://www.amee.ma.

Moroccan Agency for Sustainable Energy (MASEN). URL: http://www.masen.ma.

Mroz, Tomasz M (2006). "Thermodynamic and economic performance of the LiBr–H2O single stage absorption water chiller". In: *Applied thermal engineering* 26.17-18, pp. 2103–2109.

Najeh, Ghilen et al. (2016). "Performance of silica gel-water solar adsorption cooling system". In: *Case Studies in Thermal Engineering* 8, pp. 337–345.

Office National d'Electricité et de l'Eau Potable (ONEE). URL: http://www.one.org.ma/.

Oliveira, Armando C et al. (2000). "Thermal performance of a novel air conditioning system using a liquid desiccant". In: *Applied Thermal Engineering* 20.13, pp. 1213–1223.

Oliveski, Rejane De Césaro, Arno Krenzinger, and Horácio A Vielmo (2003). "Comparison between models for the simulation of hot water storage tanks". In: *Solar Energy* 75.2, pp. 121–134.

Oonk, Rodney L, Dennis E Jones, and Bruce E Cole-Appel (1979). "Calculation of performance of N collectors in series from test data on a single collector". In: *Solar Energy* 23.6, pp. 535–536.

Orioli, Aldo and Alessandra Di Gangi (2017). "Six-years-long effects of the Italian policies for photovoltaics on the pay-back period of grid-connected PV systems installed in urban contexts". In: *Energy* 122, pp. 458 –470. ISSN: 0360-5442. DOI: https://doi.org/10.1016/j.energy.2017.01.110. URL: http://www.sciencedirect.com/science/article/pii/S0360544217301184.

Ortiz, M. et al. (2010). "Modeling of a solar-assisted HVAC system with thermal storage". In: *Energy and Buildings* 42.4, pp. 500 –509. ISSN: 0378-7788. DOI: https://doi.org/10.1016/j.enbuild.2009.10.019. URL: http://www.sciencedirect.com/science/article/pii/S0378778809002576.

Pan, Chunjian et al. (2018). "Cost estimation and sensitivity analysis of a latent thermal energy storage system for supplementary cooling of air cooled condensers". In: *Applied Energy* 224, pp. 52 –68. ISSN: 0306-2619. DOI: https://doi.org/10.1016/j.apenergy.2018.04.080. URL: http://www.sciencedirect.com/science/article/pii/S030626191830638X.

Papadopoulos, AM, S Oxizidis, and Nikolaos Kyriakis (2003). "Perspectives of solar cooling in view of the developments in the air-conditioning sector". In: *Renewable and Sustainable Energy Reviews* 7.5, pp. 419–438.

Pedersen, Curtis O, Daniel E Fisher, and Richard J Liesen (1997). *Development of a heat balance procedure for calculating cooling loads*. Tech. rep. American Society of Heating, Refrigerating and Air-Conditioning Engineers, Inc., Atlanta, GA (United States).

Perez, Richard and Marc Perez (2009). "A fundamental look at energy reserves for the planet". In: *The IEA SHC Solar Update* 50.2.

Pérez-Lombard, Luis, José Ortiz, and Christine Pout (2008). "A review on buildings energy consumption information". In: *Energy and buildings* 40.3, pp. 394–398.

PERIER-MUZET, Maxime et al. (2011). *Modélisation et simulation transitoire d'un réfrigérateur thermo-acoustique solaire.*

Petroleum, British (2014). "BP energy outlook 2035". In: *BP stats, Jan*.

Pintaldi, Sergio et al. (2017). "Energetic evaluation of thermal energy storage options for high efficiency solar cooling systems". In: *Applied Energy* 188, pp. 160 –177. ISSN: 0306-2619. DOI: https://doi.org/10.1016/j.apenergy.2016.11.123. URL: http://www.sciencedirect.com/science/article/pii/S0306261916317548.

Pongtornkulpanich, A. et al. (2008). "Experience with fully operational solar-driven 10-ton LiBr/H2O single-effect absorption cooling system in Thailand". In: *Renewable Energy* 33.5, pp. 943 –949. ISSN: 0960-1481. DOI: https://doi.org/10.1016/j.renene.2007.09.022. URL: http://www.sciencedirect.com/science/article/pii/S0960148107002960.

Pons, M et al. (1999). "Thermodynamic based comparison of sorption systems for cooling and heat pumping: Comparaison des performances thermodynamique des systèmes de pompes à chaleur à sorption dans des applications de refroidissement et de chauffage". In: *International Journal of Refrigeration* 22.1, pp. 5–17.

Pop, Octavian G. et al. (2018). "Energy efficiency of PCM integrated in fresh air cooling systems in different climatic conditions". In: *Applied Energy* 212, pp. 976 –996. ISSN: 0306-2619. DOI: https://doi.org/10.1016/j.apenergy.2017.12.122. URL: http://www.sciencedirect.com/science/article/pii/S0306261917318469.

Praene, Jean Philippe et al. (2011). "Simulation and experimental investigation of solar absorption cooling system in Reunion Island". In: *Applied Energy* 88.3, pp. 831 –839. ISSN: 0306-2619. DOI: https://doi.org/10.1016/j.apenergy.2010.09.016. URL: http://www.sciencedirect.com/science/article/pii/S0306261910003818.

Qu, Ming, Hongxi Yin, and David H. Archer (2010). "A solar thermal cooling and heating system for a building: Experimental and model based performance analysis and design". In: *Solar Energy* 84.2, pp. 166 –182. ISSN: 0038-092X. DOI: https://doi.org/10.1016/j.solener.2009.10.010. URL: http://www.sciencedirect.com/science/article/pii/S0038092X09002424.

Reddy, T Agami et al. (2016). *Heating and Cooling of Buildings: Principles and Practice of Energy Efficient Design*. CRC Press.

Research Institute for Solar Energy and New Energies (IRESEN). URL: http://www.iresen.org.

Rossetti, Andrea, Emanuele Paci, and Gianluca Alimonti (2017). "Experimental analysis of the performance of a medium temperature solar cooling plant". In: *International Journal of Refrigeration* 80, pp. 264 –273. ISSN: 0140-7007. DOI: https://doi.org/10.1016/j.ijrefrig.2017.05.002. URL: http://www.sciencedirect.com/science/article/pii/S0140700717301913.

Royon, Laurent, Laurie Karim, and André Bontemps (2013). "Thermal energy storage and release of a new component with PCM for integration in floors for thermal management of buildings". In: *Energy and Buildings* 63, pp. 29 –35. ISSN: 0378-7788. DOI: https://doi.org/10.1016/j.enbuild.2013.03.042. URL: http://www.sciencedirect.com/science/article/pii/S0378778813002107.

Russek, Steven L and Carl B Zimm (2006). "Potential for cost effective magnetocaloric air conditioning systems". In: *International Journal of Refrigeration* 29.8, pp. 1366–1373.

Santamouris, Mat et al. (2007). "Recent progress on passive cooling techniques: Advanced technological developments to improve survivability levels in low-income households". In: *Energy and Buildings* 39.7, pp. 859–866.

Sarbu, Ioan and Calin Sebarchievici (2013). "Review of solar refrigeration and cooling systems". In: *Energy and Buildings* 67, pp. 286–297.

Sattari, H. et al. (2017). "CFD simulation of melting process of phase change materials (PCMs) in a spherical capsule". In: *International Journal of Refrigeration* 73.Supplement C, pp. 209 –218. ISSN: 0140-7007. DOI: https://doi.org/10.1016/j.ijrefrig.2016.09.007. URL: http://www.sciencedirect.com/science/article/pii/S0140700716302870.

Şencan, Arzu (2007). "Modeling of thermodynamic properties of refrigerant/absorbent couples using data mining process". In: *Energy Conversion and Management* 48.2, pp. 470–480.

Senhagi, F (2003). "Financing the development of the renewable energy in the Mediterranean region-Baseline study for Morocco". In: *United Nations Environment Programme (UNEP), Division of Technology, Industry and Economics, 65p*.

Shafiee, Shahriar and Erkan Topal (2009). "When will fossil fuel reserves be diminished?" In: *Energy policy* 37.1, pp. 181–189.

Shandong Lucy New Energy Technology Co., Ltd. URL: https://lucysolar.en.made-in-china.com/.

Sharif, MK Anuar et al. (2015). "Review of the application of phase change material for heating and domestic hot water systems". In: *Renewable and Sustainable Energy Reviews* 42, pp. 557–568.

Sharma, Atul et al. (2009). "Review on thermal energy storage with phase change materials and applications". In: *Renewable and Sustainable energy reviews* 13.2, pp. 318–345.

Shirazi, Ali et al. (2016a). "A systematic parametric study and feasibility assessment of solar-assisted single-effect, double-effect, and triple-effect absorption chillers for heating and cooling applications". In: *Energy Conversion and Management* 114, pp. 258 –277. ISSN: 0196-8904. DOI: https://doi.org/10.1016/j.enconman.2016.01.070. URL: http://www.sciencedirect.com/science/article/pii/S0196890416300140.

Shirazi, Ali et al. (2016b). "Solar-assisted absorption air-conditioning systems in buildings: Control strategies and operational modes". In: *Applied Thermal Engineering* 92, pp. 246 –260. ISSN: 1359-4311. DOI: https://doi.org/10.1016/j.applthermaleng.2015.09.081. URL: http://www.sciencedirect.com/science/article/pii/S1359431115010066.

Shirinbakhsh, Mehrdad, Nima Mirkhani, and Behrang Sajadi (2018). "A comprehensive study on the effect of hot water demand and PCM integration on the performance of SDHW system". In: *Solar Energy* 159, pp. 405–414.

Sumathy, K, Z.C Huang, and Z.F Li (2002). "Solar absorption cooling with low grade heat source — a strategy of development in South China". In: *Solar Energy* 72.2, pp. 155 –165. ISSN: 0038-092X. DOI: https://doi.org/10.1016/S0038-092X(01)00098-6. URL: http://www.sciencedirect.com/science/article/pii/S0038092X01000986.

Summers, Edward K, Mohammed A Antar, and John H Lienhard (2012). "Design and optimization of an air heating solar collector with integrated phase change material energy storage for use in humidification–dehumidification desalination". In: *Solar Energy* 86.11, pp. 3417–3429.

Sun, Da-Wen (1998). "Comparison of the performances of NH3-H2O, NH3-LiNO3 and NH3-NaSCN absorption refrigeration systems". In: *Energy Conversion and Management* 39.5-6, pp. 357–368.

Swift, Gregory W (2002). "A unifying perspective for some engines and refrigerators". In: *Acoustical Society of America*, pp. 16–20.

Syed, A et al. (2005). "A novel experimental investigation of a solar cooling system in Madrid". In: *International Journal of refrigeration* 28.6, pp. 859–871.

Talmatsky, Ella (2007). *PCM Storage for Domestic Solar Hot Water Systems*. Tel Aviv University.

Talmatsky, Ella and Abraham Kribus (2008). "PCM storage for solar DHW: An unfulfilled promise?" In: *Solar Energy* 82.10, pp. 861–869.

Tarsitano, Anna, Virgilio Ciancio, and Massimo Coppi (2017). "Air-conditioning in residential buildings through absorption systems powered by solar collectors". In: *Energy Procedia* 126. ATI 2017 - 72nd Conference of the Italian Thermal Machines Engineering Association, pp. 147 –154. ISSN: 1876-6102. DOI: https://doi.org/10.1016/j.egypro.2017.08.134. URL: http://www.sciencedirect.com/science/article/pii/S1876610217336202.

Thür, Alexander, Simon Furbo, and Louise Jivan Shah (2006). "Energy savings for solar heating systems". In: *Solar Energy* 80.11, pp. 1463–1474.

Tian, Yuan and Chang-Ying Zhao (2013). "A review of solar collectors and thermal energy storage in solar thermal applications". In: *Applied energy* 104, pp. 538–553.

Tores, Ledesma Juan et al. (2013). "Numerical simulation of the solar thermal energy storage system for domestic hot water supply located in south Spain". In: *Thermal Science* 17.2, pp. 431–442.

Transient System Simulation Tool (TRNSYS). URL: http://www.trnsys.com.

Transol. URL: http://boutique.cstb.fr/fr/transol-3-0.html.

Tsoutsos, Theocharis et al. (2003). "Solar cooling technologies in Greece. An economic viability analysis". In: *Applied Thermal Engineering* 23.11, pp. 1427–1439.

Tyagi, Vineet Veer and D Buddhi (2007). "PCM thermal storage in buildings: a state of art". In: *Renewable and Sustainable Energy Reviews* 11.6, pp. 1146–1166.

Tyagi, VV, SC Kaushik, and SK Tyagi (2012). "Advancement in solar photovoltaic/thermal (PV/T) hybrid collector technology". In: *Renewable and Sustainable Energy Reviews* 16.3, pp. 1383–1398.

Version, Meteonorm (2010). "6, software version 6.1. 0.20 of April 2010". In: *Meteotest, Switzerland*.

Viessmann - Solar thermal systems. URL: https://www.viessmann-us.com/en/commercial/solar-systems.html.

Villa, E et al. (2009). *SOLAIR–Increasing the market implementation of solar air conditioning systems for small and medium applications in residential and commercial buildings CLIMAMED2009 Lisbon*.

Voller, VR (1990). "Fast implicit finite-difference method for the analysis of phase change problems". In: *Numerical Heat Transfer* 17.2, pp. 155–169.

Vujić, Jasmina, Dragoljub P Antić, and Zorka Vukmirović (2012). "Environmental impact and cost analysis of coal versus nuclear power: the US case". In: *Energy* 45.1, pp. 31–42.

Wang, Jiangjiang et al. (2018). "Thermodynamic performance analysis and comparison of a combined cooling heating and power system integrated with two types of thermal energy storage". In: *Applied Energy* 219, pp. 114 –122. ISSN: 0306-2619. DOI: https://doi.org/10.1016/j.apenergy.2018.03.029. URL: http://www.sciencedirect.com/science/article/pii/S0306261918303593.

Wang, LW, RZ Wang, and RG Oliveira (2009). "A review on adsorption working pairs for refrigeration". In: *Renewable and Sustainable Energy Reviews* 13.3, pp. 518–534.

Wang, RZ et al. (2009). "Solar sorption cooling systems for residential applications: options and guidelines". In: *International journal of refrigeration* 32.4, pp. 638–660.

Wang, R.Z. et al. (2016). "Solar driven air conditioning and refrigeration systems corresponding to various heating source temperatures". In: *Applied Energy* 169, pp. 846 –856. ISSN: 0306-2619. DOI: http://dx.doi.org/10.1016/j.apenergy.2016.02.049. URL: http://www.sciencedirect.com/science/article/pii/S0306261916301726.

Wei, Gaosheng et al. (2018). "Selection principles and thermophysical properties of high temperature phase change materials for thermal energy storage: A review". In: *Renewable and Sustainable Energy Reviews* 81.Part 2, pp. 1771 –1786. ISSN: 1364-0321. DOI: https://doi.org/10.1016/j.rser.2017.05.271. URL: http://www.sciencedirect.com/science/article/pii/S1364032117309188.

Weiss, Werner W (2003). *Solar heating systems for houses: a design handbook for solar combisystems*. Earthscan.

Wu, Wei et al. (2014). "Absorption heating technologies: A review and perspective". In: *Applied Energy* 130, pp. 51 –71. ISSN: 0306-2619. DOI: https://doi.org/10.1016/j.apenergy.2014.05.027. URL: http://www.sciencedirect.com/science/article/pii/S0306261914005224.

Xu, Z.Y. and R.Z. Wang (2017). "Simulation of solar cooling system based on variable effect LiBr-water absorption chiller". In: *Renewable Energy* 113, pp. 907 –914. ISSN: 0960-1481. DOI: https://doi.org/10.1016/j.renene.2017.06.069. URL: http://www.sciencedirect.com/science/article/pii/S0960148117305748.

Yamagishi, Yasushi et al. (1996). "An evaluation of microencapsulated PCM for use in cold energy transportation medium". In: *Energy Conversion Engineering Conference, 1996. IECEC 96., Proceedings of the 31st Intersociety*. Vol. 3. IEEE, pp. 2077–2083.

Yaïci, Wahiba et al. (2013). "Three-dimensional unsteady {CFD} simulations of a thermal storage tank performance for optimum design". In: *Applied Thermal Engineering* 60.1–2, pp. 152 –163. ISSN: 1359-4311. DOI: http://dx.doi.org/10.1016/j.applthermaleng.2013.07.001. URL: http://www.sciencedirect.com/science/article/pii/S1359431113004894.

Yeung, M.R. et al. (1992). "Performance of a solar-powered air conditioning system in Hong Kong". In: *Solar Energy* 48.5, pp. 309 –319. ISSN: 0038-092X. DOI: https://doi.org/10.1016/0038-092X(92)90059-J. URL: http://www.sciencedirect.com/science/article/pii/0038092X9290059J.

Youssef, W., Y.T. Ge, and S.A. Tassou (2018). "{CFD} modelling development and experimental validation of a phase change material (PCM) heat exchanger with spiral-wired tubes". In: *Energy Conversion and Management* 157, pp. 498 –510. ISSN: 0196-8904. DOI: https://doi.org/10.1016/j.enconman.2017.12.036. URL: https://www.sciencedirect.com/science/article/pii/S0196890417311871.

Zachár, A., I. Farkas, and F. Szlivka (2003). "Numerical analyses of the impact of plates for thermal stratification inside a storage tank with upper and lower inlet flows". In: *Solar Energy* 74.4, pp. 287 –302. ISSN: 0038-092X. DOI: http://dx.doi.org/10.1016/S0038-092X(03)00188-9. URL: http://www.sciencedirect.com/science/article/pii/S0038092X03001889.

Zalba, Belen et al. (2003). "Review on thermal energy storage with phase change: materials, heat transfer analysis and applications". In: *Applied thermal engineering* 23.3, pp. 251–283.

Zhai, X.Q. et al. (2008). "Design and performance of a solar-powered air-conditioning system in a green building". In: *Applied Energy* 85.5, pp. 297 –311. ISSN: 0306-2619. DOI: https://doi.org/10.1016/j.apenergy.2007.07.016. URL: http://www.sciencedirect.com/science/article/pii/S0306261907001225.

Zhou, Dao, Chang-Ying Zhao, and Yuan Tian (2012). "Review on thermal energy storage with phase change materials (PCMs) in building applications". In: *Applied energy* 92, pp. 593–605.

Zhou, Lingyu et al. (2017). "Performance assessment of a single/double hybrid effect absorption cooling system driven by linear Fresnel solar collectors with latent thermal storage". In: *Solar Energy* 151, pp. 82 –94. ISSN: 0038-092X. DOI: https://doi.org/10.1016/j.solener.2017.05.031. URL: http://www.sciencedirect.com/science/article/pii/S0038092X17304061.